PV Adoption Enabled By Low-Carbon Technologies: Trade-Offs Between Prosumer Benefits And Grid Impacts

Pena Bello, Alejandro

UNIVERSITÉ DE GENÈVE FACULTÉ DES SCIENCES

Département F.-A. Forel des sciences de
l'environnement et de l'eau Professeur M.K. Patel

PV Adoption Enabled By Low-Carbon Technologies:

Trade-Offs Between Prosumer Benefits And Grid Impacts

THÈSE

Présentée à la Faculté des sciences de l'Université de Genève
Pour obtenir le grade de Docteur ès sciences, mention sciences de l'environnement

Par

Alejandro Peña-Bello

de

Bogota (Colombie)

Thèse N°5663

GENÈVE

2022

UNIVERSITÉ DE GENÈVE

FACULTÉ DES SCIENCES

DOCTORAT ÈS SCIENCES, MENTION SCIENCES DE L'ENVIRONNEMENT

Thèse de Monsieur Alejandro PENA BELLO

intitulée :

«PV Adoption Enabled By Low-Carbon Technologies: Trade-Offs Between Prosumer Benefits And Grid Impacts»

La Faculté des sciences, sur le préavis de Monsieur M.K. PATEL, professeur ordinaire et directeur de thèse (Département F.-A. Forel des sciences de l'environnement et de l'eau), Monsieur D. PARRA MENDOZA, docteur et codirecteur de thèse (Institut des sciences de l'environnement), Monsieur W. VAN SARK, professeur (Copernicus Institute of Sustainable Development, Utrecht University, Utrecht, The Netherlands), Madame C. CORCHERO GARCIA, professeure (Department of Statistics and Operations Research, Universitat Politécnica de Catalunya, Barcelona, Spain), autorise l'impression de la présente thèse, sans exprimer d'opinion sur les propositions qui y sont énoncées.

Genève, le 30 juin 2022

Thèse - 5663 -

Le Doyen

N.B. - La thèse doit porter la déclaration précédente et remplir les conditions énumérées dans les "Informations relatives aux thèses de doctorat à l'Université de Genève".

To my family

"It is not knowledge, but the act of learning, not possession but the act of getting there, which grants the greatest enjoyment." C.F. Gauss

Acknowledgements

I would like to firstly thank my supervisors, Prof. Martin K. Patel and Dr. David Parra for their support, guidance, and precise feedback during this Ph.D. I am grateful to you for all your help. Secondly, I would like to thank the Swiss Innovation Agency Innosuisse and the Swiss Competence Center for Heat and Electricity Storage (SCCER-HaE), for funding this study.

Further thanks go to Pablo, Pierre, Charlotte, Adolfo, Natalia, Sandra, Juan, Elodie, Arthur and all my friends in Geneva, without whom, I would have finished sooner. I would also like to thank my colleagues from the Energy Efficiency Group, as well as Emmanuel and Hélène from the LEBA, and more recently to my colleagues from the PV energy systems group at PV-lab, for the fruitful discussions.

I wish also to thank the jury Prof. Wilfried van Sark and Prof. Cristina Corchero for their input and critical review. I am very grateful with all my co-authors, Dr. Edward Barbour, Dr. Selin Yilmaz, Ruchi Gupta, Dr. Kai Streicher, Prof. Tobias Schmidt, Prof. Bjarne Steffen, Dr. Martin Beuse, Prof. Philipp Schuetz, Prof. Jörg Worlitschek, Dr. Mathias Berger, Dr. Ulf Hahnel, Mario Herberz, Prof. Verena Tiefenbeck, Dr. Mokhtar Bozorg, Prof. Mario Paolone, Prof. Marta C. Gonzalez, Prof. Solomon Brown, Dr. Siyuan Dong, Timothy Hutty, and all the members of the GO-P2P task 1, for the exchanges and their help across the collaborations that make part of this thesis in one way or another. Finally, I would like to thank me, for doing all this work.

PV Adoption Enabled By Low-Carbon Technologies:

Trade-offs between prosumer benefits and grid impacts

Alejandro Peña-Bello

Abstract

Solar rooftop photovoltaic (PV) systems are playing a key role in decarbonizing the energy sector due to their modularity, cost reductions, high levels of social acceptance, and policy support schemes. However, the stochastic nature of the solar resource prevents PV systems from supplying electricity on demand, limiting its final value as well as posing substantial challenges for their integration on the electricity mix. This thesis focuses on technologies and strategies which can enable PV to supply electricity on-demand at the distribution level, therefore increasing its value, and final penetration into the energy system. We study which additional currently unexploited economic benefit can be reaped by combining applications that allow to maximize the consumer revenue (e.g., PV self-consumption), by minimizing grid impacts (e.g., demand peak shaving, demand load shifting, and avoidance of PV curtailment), and/or by accessing markets, at both local (e.g., peer-to-peer), and national levels (e.g., frequency regulation).

Using technology assessment, energy system models at high temporal resolution ($\leq$ 1 hour) at the residential scale, statistical analysis, cluster analysis, optimization and simulation as research methods, this project assesses the trade-offs between consumers benefits (e.g., bill minimization) and grid impacts (e.g., maximum grid relief) depending on the type of consumer, building characteristics, technologies, control strategies, and business model. We analyze three levels that represent different business models, an individual household minimizing their bill, a local peer-to-peer community, and a national aggregator providing frequency control. In general, we find that electricity tariffs can effectively increase residential PV system flexibility by enabling energy storage to perform different applications. In particular, capacity-based tariffs can effectively mitigate distribution grid impacts by promoting a reasonable exchange with the grid. In P2P communities, a fairer distribution of community costs is needed to avoid distributional energy justice problems, since pure consumers reap the highest financial benefits under the proposed market mechanism. Finally, we find the provision of frequency control by means of an aggregator to be a profitable service for the prosumer reaching positive net present values.

Adoption du PV rendue possible par les technologies à faible émission de carbone:

Compromis entre les avantages pour les prosommateurs et les impacts sur le réseau

Alejandro Peña-Bello

Résumé

Les systèmes solaires photovoltaïques (PV) sur les toits jouent un rôle clé dans la décarbonation du secteur de l'énergie en raison de leur modularité, des réductions de coûts, des niveaux élevés d'acceptation sociale et des programmes de soutien politique. Cependant, la nature stochastique de la ressource solaire empêche les systèmes PV de fournir de l'électricité à la demande, limitant sa valeur finale et posant des défis importants pour leur intégration dans le mix électrique. Cette thèse se concentre sur les technologies et les stratégies qui peuvent permettre au PV de fournir de l'électricité à la demande au niveau de la distribution, augmentant ainsi sa valeur et sa pénétration finale dans le système énergétique. Nous étudions quel avantage économique supplémentaire actuellement inexploité peut être récolté en combinant des applications qui permettent de maximiser les revenus des consommateurs (par exemple, l'autoconsommation PV), en minimisant les impacts sur le réseau (par exemple, l'écrêtement des pics de demande, le déplacement de la charge de la demande et le contournement de la réduction du PV) , et/ou en accédant aux marchés, aux niveaux locale (par exemple, peer-to-peer) et nationale (par exemple, régulation de fréquence).

En utilisant l'évaluation des technologies, des modèles de systèmes énergétiques à haute résolution temporelle (≤ 1 heure) à l'échelle résidentielle, l'analyse statistique, l'analyse de cluster, l'optimisation et la simulation comme méthodes de recherche, ce projet évalue les compromis entre les avantages pour les consommateurs (par exemple, minimisation de la facture) et les impacts sur le réseau (par exemple, le soulagement maximal du réseau) en fonction du type de consommateur, des caractéristiques du bâtiment, des technologies, des stratégies de contrôle et du modèle commercial. Nous analysons trois niveaux qui représentent différents modèles économiques, un ménage individuel minimisant sa facture, une communauté P2P locale et un agrégateur national assurant le contrôle de la fréquence. En général, nous constatons que les tarifs de l'électricité peuvent effectivement augmenter la flexibilité du système PV résidentiel en permettant au milieu de stockage de l'énergie d'effectuer différentes applications. En particulier, les tarifs capacitifs peuvent atténuer efficacement les impacts sur le réseau de distribution en favorisant un échange raisonnable avec le réseau. Dans les communautés P2P, une répartition plus équitable des coûts communautaires est nécessaire pour éviter les problèmes de justice énergétique distributive, puisque les consommateurs purs récoltent les avantages financiers les plus élevés dans le cadre du mécanisme de marché proposé. Enfin, nous trouvons que la fourniture d'un contrôle de fréquence au moyen d'un agrégateur est un service rentable pour le prosommateur atteignant des valeurs actuelles nettes positives.

List of appended papers

I **Pena-Bello, A.**, Barbour, E., Gonzalez, M. C., Patel, M. K., & Parra, D. (2019). Optimized PV-coupled battery systems for combining applications: Impact of battery technology and geography. Renewable and Sustainable Energy Reviews, 112, 978-990. https://doi.org/10.1016/j.rser.2019.06.003.

II **Pena-Bello, A.**, Barbour, E., Gonzalez, M. C., Yilmaz, S., Patel, M. K., & Parra, D. (2020). How does the electricity demand profile impact the attractiveness of PV-coupled battery systems combining applications?. Energies, 13(15), 4038. https://doi.org/10.3390/en13154038.

III **Pena-Bello, A.**; Schuetz, P.; Berger, M.; Worlitschek, J.; Patel, M. K.; Parra, D,. (2021) Decarbonizing heat with PV-coupled heat pumps supported by electricity and heat storage: impacts and trade-offs for prosumers and the grid, Energy conversion and management, 240, 114220, https://doi.org/10.1016/j.enconman.2021.114220.

IV **Pena-Bello, A.**, Parra, D., Herberz, M., Tiefenbeck, V., Patel, M. K., & Hahnel, U. J. J. (2022) Integration of prosumer peer-to-peer trading decisions into energy community modeling. Nature Energy, 7, 74–82. https://doi.org/10.1038/s41560-021-00950-2.

V **Pena-Bello, A.**, Bozorg, M., Paolone, M., Patel, M. K., & Parra, D. Value added for prosumers and the power sector by residential batteries aggregated for frequency control. Manuscript in preparation.

Author's contributions:

Alejandro Pena-Bello is the principal author of all five papers and conducted the modeling, validation and analyses. David Parra and Martin K. Patel have contributed with discussions, editing and supervision of all five papers. David Parra conceptualized and contributed to the method development of **Papers I, III,IV and V**. Edward Barbour helped with the modeling and validation of **Paper I and II**. Selin Yilmaz did the clustering analysis and contributed with the discussion for **Paper II**. Philipp Schuetz contributed to the method development and discussion of **Paper III**. Mathias Berger and Jörg Worlitschek supervised **Paper III**. Ulf Hahnel contributed with the conceptualization, data curation, discussion and writing of **Paper IV**. Mario Herberz contributed to the edition, data curation and analyses of **Paper IV**. Verena Tiefenbeck contributed with the edition, discussion and supervision of **Paper IV**. Mokhtar Bozorg contributed to the method development, validation and supervision of **Paper V**. Mario Paolone supervised **Paper V**.

Other publications by the author not included in this thesis:

I Hutty, T. D., **Pena-Bello, A.**, Dong, S., Parra, D., Rothman, R., & Brown, S. (2021). Peer-to-peer electricity trading as an enabler of increased PV and EV ownership. Energy Conversion and Management, 245, 114634. https://doi.org/10.1016/j.enconman.2021.114634.

II Dudjak, V., Neves, D., Alskaif, T., Khadem, S., **Pena-Bello, A.**, Saggese, P., ... & Papaemmanouil, A. (2021). Impact of local energy markets integration in power systems layer: A comprehensive review. Applied Energy, 301, 117434. https://doi.org/10.1016/j.apenergy.2021.117434.

III Gupta, R., **Pena-Bello, A.**, Streicher, K. N., Roduner, C., Thöni, D., Patel, M. K., & Parra, D. (2021). Spatial analysis of distribution grid capacity and costs to enable massive deployment of PV, electric mobility and electric heating. Applied Energy, 287, 116504. https://doi.org/10.1016/j.apenergy.2021.116504.

IV Hahnel, U. J. J., Herberz, M., **Pena-Bello, A.**, Parra, D., & Brosch, T. (2020). Becoming prosumer: Revealing trading preferences and decision-making strategies in peer-to-peer energy communities. Energy Policy, 137, 111098. https://doi.org/10.1016/j.enpol.2019.111098.

V Schmidt, T. S., Beuse, M., Zhang, X., Steffen, B., Schneider, S. F., **Pena-Bello, A.**, ... & Parra, D. (2019). Additional emissions and cost from storing electricity in stationary battery systems. Environmental Science & Technology, 53(7), 3379-3390. https://doi.org/10.1021/acs.est.8b05313.

VI **Pena-Bello, A.**, Burer, M., Patel, M. K., & Parra, D. (2017). Optimizing PV and grid charging in combined applications to improve the profitability of residential batteries. Journal of Energy Storage, 13, 58-72. https://doi.org/10.1016/j.est.2017.06.002.

Abbreviations and terminology

PV	Photovoltaics	SH	Space heating
FiT	Feed-in Tariff	DHW	Domestic hot water
PVSC	PV self-consumption	SFH	Single-family house
PVCT	Avoidance of PV curtailment	COP	Coefficient of performance
DLS	Demand load shifting	CAPEX	Capital expenditure
DPS	Demand peak-shaving	OPEX	Operational expenditure
NMC	Lithium nickel manganese cobalt oxide	HP	Heat Pump
NCA	Lithium nickel cobalt aluminum oxide	EV	Electric vehicle
LFP	Lithium iron phosphate	P2P	Peer-to-peer
LTO	Lithium titanium oxide	MILP	Mixed Integer Linear Programming
ALA	Advanced lead-acid	ILR	Inverter load ratio
VRLA	Valve-regulated lead-acid	CF	Cash flow
FT	Flat tariff	ToU	Time of Use
DT	Double tariff	NPV	Net present value
LCOES	Levelized cost of energy storage	SOC	State of charge
LVOES	Levelized value of energy storage	DoD	Depth of discharge
LCOE	Levelized cost of of meeting the electricity consumption	TSO	Transmission system operator
DER	Distributed energy resources	DSO	Distribution system operator
aFRR	automatic Frequency Restoration Reserve	mFRR	manual Frequency Restoration Reserve

Description of terms used in this thesis:

Prosumer: In this work, households that are equipped with photovoltaic (PV) systems and, therefore can both produce and consume electricity.

Low-carbon technologies: The term given to technologies that emit low levels of CO_2 emissions.

Self-consumption: The share of on-site generation that is auto-consumed.

Self-sufficiency or autarky: The share of local demand that is covered by the on-site PV generation.

Demand load shifting: A load management technique that aims to move demand from peak hours to off-peak hours of the day, with the idea of reducing the total energy cost. It requires a differential tariff (e.g., double tariff, time-of-use tariff).

Demand peak-shaving: It involves proactively managing overall demand to eliminate demand spikes. This process lowers and smooths out peak loads, which reduces the overall cost of electricity tariffs.

Capacity-based tariff: Also called demand charges, bill the peak electricity demand (i.e., in \$/kW) during a billing period (e.g., annual, monthly...). In this study we use electricity tariffs with a mixed nature, with two components, one volumetric and one capacity-based.

Curtailment: The deliberate reduction in output below what could have been injected into the grid.

Hosting capacity: The amount of distributed generation for which distribution network constraints are violated.

TSO: The transmission system operator is an entity entrusted with transporting energy in the form of electrical power on a national or regional level, using fixed infrastructure.

DSO: The distribution system operators are the entities responsible for distributing and managing energy from the generation sources to the final consumers.

BRP: Balance Responsible Parties are private legal entities that overlook the balance of one or multiple access points to the transmission grid.

Reserve capacity: It refers to the remaining available power capacity [MW] of a generator (e.g., in the upward direction, it is the difference between the power generation operating point and the maximum power capacity of the generator) that is 'booked' to be used, in case the TSO needs this power to provide ancillary services.

Regulating power: It refers to the energy [MWh] that is produced by a generator by deploying the above booked reserve capacity, following a request from the TSO.

Upwards regulation: The increase of generation (or decrease of consumption) provided by actors participating in the frequency market in the case that frequency deviates below 50 Hz (in Europe).

Downwards regulation: The decrease of generation (or increase of consumption) provided by actors participating in the frequency market in the case that frequency deviates above 50 Hz (in Europe).

Contents

List of Figures

List of Tables

Chapter 1

General introduction

In order to limit global warming to 1.5°C, a threshold the Intergovernmental Panel for Climate Change (IPCC) suggests carbon neutrality by mid-21st century is essential. This target is also laid down in the Paris agreement signed by 195 countries. Since the energy system (including electricity, heat and transport) is responsible for three quarters of the global greenhouse gas emissions (Ritchie and Roser 2020), the massive integration of renewable energy resources is crucial for the energy system decarbonization.

Solar photovoltaics (PV) is the renewable energy technology with the highest growth rate, more than 33% per annum over the past decade (IRENA 2019), and the steepest learning curve, above 20% reduction in module price for each doubling in cumulative production capacity over the last 40 years (Equipment 2018). The main reasons for such an unprecedented development lie on its simplicity and reliability, requiring almost no maintenance, its scalability due to the modularity, and its low cost, recently reaching a global weighted-average levelized cost of 0.057 USD/kWh at the utility scale (IRENA 2021), and an all time low cost of 0.0104 USD/kWh in Saudi Arabia in April 2021, for an utility-scale solar PV plant. This cost makes PV competitive with the cheapest new fossil fuel-fired power generation capacity (between 0.055-0.148 USD/kWh for coal-fired Chinese plants) (IRENA 2021).

PV modularity, cost reductions, high levels of social acceptance, and policy support schemes have enabled the installation of substantial amounts of generation capacity embedded within the distribution network and close to domestic electricity demand. The levelized cost of residential PV systems have declined between 49% and 82% between 2010 and 2020, in countries such as Australia, Germany, Italy, Japan and the United States (U.S.), reaching levelized cost range between 0.236-0.055 USD/kWh in 2020 (IRENA 2021). Additionally, renewable energy policy instruments such as the Feed-in Tariff (FiT) scheme, net metering and investment-tax credits have made PV systems widely available in the residential sector. For instance, at the end of 2020, countries with high residential PV penetration such as Australia, Germany and the U.S. counted more than two million of residential PV systems. However, the unexploited potential on single and two-family houses is still of about 89% and 97% in Germany and the U.S., respectively (EUPD 2020; Feldman, K. Wu, and Margolis 2021). Therefore, there is an enormous expansion potential for distributed generation in the residential sector. Additionally, other drivers of residential PV systems are their acceptance among the population, and the (perception of) high retail electricity prices.

While being relatively cheap, clean and widely available, the massive integration of PV systems challenges the existing grid, in particular when PV is highly dis-

tributed. This is mainly because the distribution grid infrastructure was designed exclusively to transfer electricity downstream from large power plants. Distribution system operators (DSOs) must guarantee grid stability and power quality, however, since PV injection was not considered in the planning of distribution grids, the local PV feed-in affects the voltage of the distribution grid, as well as the operation of critical devices such as transformers and lines (Gupta, Pena-Bello, et al. 2021). Moreover, PV stochastic nature result into instantaneous variations of PV power generation which leads to load shedding, and makes the management of grid frequency more challenging (Abdoulaye et al. 2020). Another stability issue related to high amounts of PV penetration is the temporal imbalance between peak demand (usually after sunset) and PV generation, due to the large amount of dispatchable power required to cover peak demand, a phenomenom known as the duck-curve (Barbour, Parra, et al. 2018).

Unlike conventional centralized generation, PV production cannot be supplied on-demand without incurring in additional costs and devices. To mitigate the problems posed by residential PV while supporting its further penetration, different means are used. One common solution is demand side management, however, it has a limited impact on the demand and is less appealing for households (Yilmaz, Rinaldi, and Patel 2020). The main solution is the promotion of self-consumption. Increased PV self-consumption results in lower PV feed-in, while the share of renewable energy continues to increase. The coupling of residential PV with other low-carbon technologies allows to increase the share of on-site generation that is auto-consumed. For instance, batteries can increase PV self-consumption by 10-24% (Luthander, Widén, Munkhammar, et al. 2016). Further low-carbon technologies can help decarbonizing other energy services, such as heating (heat pumps and thermal storage) or transport (electric vehicles). In this study, we analyze the potential of low-carbon technologies which enable the penetration of residential PV systems, while reducing their burden on the distributed system. **The main focus is on energy storage, and in particular on residential batteries.**

1.1 Aim and scope

The overall aim of this thesis is to analyze the potential of low-carbon technologies which may enable the increased supply of PV-generated electricity on-demand at the distributed level. As shown in Figure 1.1, we study PV integration at the residential level and the way how low-carbon technologies, and business models, can make investments more attractive for prosumers while minimizing grid impacts. The main focus is on single-family houses (SFH) with existing PV systems (and heat pumps, in Chapter 4), and the willingness to invest in energy storage. Moreover, we analyze two new business models, namely, peer-to-peer communities and aggregators. We use various techno-economic indicators (e.g., annual bill, self-consumption rate, NPV) to understand the impact of these technologies on prosumers. Additionally, we use the maximum power exchanged with the grid (import and export power, and referred to as power flow) as an indicator of grid impacts.

Next, we formulate the specific research questions which motivate this thesis. Contrary to PV systems, batteries are not yet cost-effective. In addition, PV systems have to be combined with other technologies to provide electricity on-demand (Gupta, Soini, et al. 2020). Therefore, the combination of applications of energy storage are considered to increase the financial revenue, while providing residential

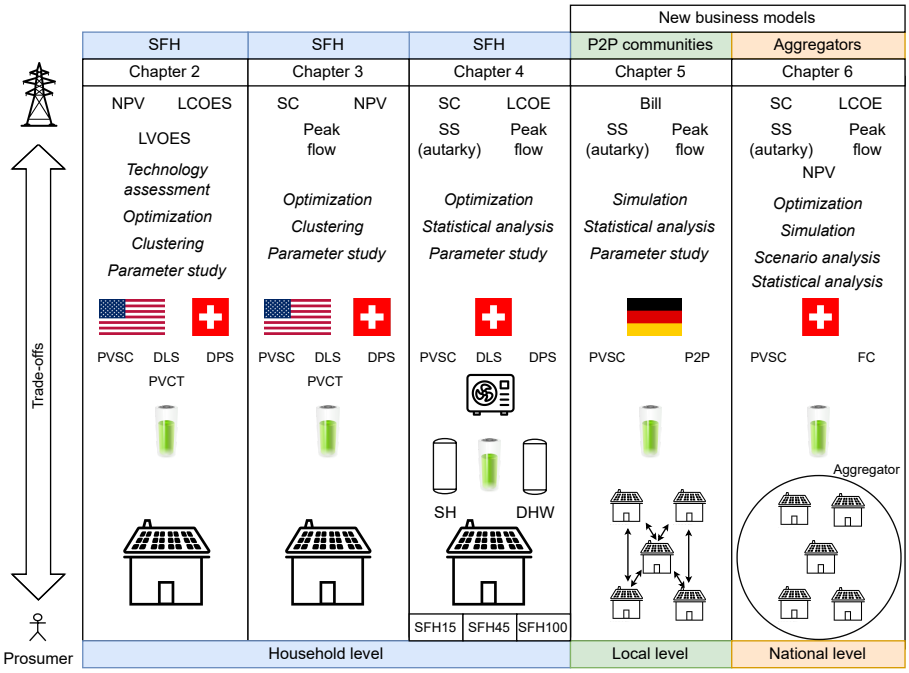

Figure 1.1: Schematic representation of this thesis with the key performance indicators, methods, geography scope, applications, and devices per chapter.

PV installations with a certain level of flexibility. This can be expected to motivate households to have a private energy storage system and to then tap into several revenue streams. Therefore, the first research question is formulated as:

Research question A

To which extent can the combination of applications help to increase the financial revenue of energy storage in the residential sector?

This thesis contributes to the field by proposing an open-source 24-h optimization framework for battery dispatching (i.e., Battery Schedule OPtimizer for Residential Applications, BASOPRA), subsequently expanded to optimize heat pumps and thermal storage operation, for space heating and domestic hot water (DHW). This tool allows us to combine different energy storage applications and assess their added value. In particular, we explore the combination of the main residential application: PV self-consumption, with secondary residential applications such as avoidance of PV curtailment, demand load shifting, demand peak-shaving, electricity trading, and frequency control. The combination of applications, also referred to as benefit stacking, can be incentivized by the design of electricity tariffs and/or policy, and therefore, different tariff structures are analyzed across this thesis. Since the same energy storage technology is used for several applications, this implies trade-offs for the prosumer and/or for the grid, not only in financial terms, but also in terms of self-consumption, self-sufficiency and grid impact. In this sense, we formulate the second research question as:

Research question B

What are the trade-offs between prosumer benefits and grid impacts in single-family houses with PV and energy storage with access to multiple revenue streams?

Finally, with the deployment of distributed energy resources (DERs), new business models are emerging (IRENA 2020). In this thesis, we analyze two new types of electricity market participants encompassing a set of households and their DERs, namely Peer-to-peer (P2P) communities and aggregators.

For P2P communities, previous research focused on the techno-economic perspective. However, factors other than financial incentives influence homeowners' P2P trading decisions (Ecker, Spada, and Hahnel 2018; Hahnel, Herberz, et al. 2020). Therefore, there is still an open question about the influence of trading preferences in P2P communities, which is formulated as:

Research question C

How does a P2P community based on actual trading preferences performs at the individual, collective and grid level?

This thesis contributes new insights to the existing body of literature by extending the so-far socio-economic focus of P2P communities, integrating citizen preferences and decision-making strategies. By means of interdisciplinary research, we were able to translate findings from psychology into performance indicators, which are relevant for policy makers and other decision-makers, helping to the development of human-centered energy systems.

1.2 Outline

Chapter 2 contributes to answering Research Questions A and B by proposing an open-source 24-h optimization framework for energy storage dispatching (i.e., BASOPRA). The optimization framework is used to determine the best-suited battery technology depending on its size and the combination of applications (i.e., PV self-consumption, avoidance of PV curtailment, demand load shifting and demand peak-shaving), for individual households in Geneva, Switzerland and Austin, U.S.

Chapter 3 contributes to answering Research Questions A and B using a 1:1:1 sizing ratio for the design of the residential energy system, where for instance, an annual electricity consumption of 5 MWh is assumed to be served by a nominal PV capacity of 5 kWp and a battery capacity of 5 kWh. Additionally, we expand the previous contribution by analysing the impact of the load profile and the annual consumption for a PV-coupled battery system combining applications.

Chapter 4 extends the developed optimization framework to include heat pumps and thermal storage operation (including space heating and domestic hot water), contributing to answer Research Question A and B by comparing electric and thermal storage performing several applications in single-family houses with different thermal envelope quality in Geneva, Switzerland.

Chapter 5 studies the impacts of trading strategies in P2P communities, using German data, directly answering Research Question C while addressing the social dimension. Additionally, this chapter contributes to answer Research Question A

and B by combining PV self-consumption with energy trading.

Chapter 6 explores, through the pooling of residential batteries, a sixth battery application: frequency control. This chapter contributes to answering Research Question A and B, using four models allowing to calculate: i) the Swiss wholesale prices (GRIMSEL); ii) the cost of regulating power (LM); iii) the amount of dispatched-by-design distribution system penetration, where batteries are deployed in the distribution grid to dispatch the operation of traditionally stochastic prosumption peak flows; and iv) the revenue and grid impact of the combination of frequency control and PV self-consumption at the household level (extended BASOPRA) in the Swiss context. A future-oriented scenario analysis is undertaken to consider different stages of the Swiss energy transition, namely 2030 and 2050.

Chapter 7 summarizes the research work and provides overall conclusion, proposing critical insights about the energy transition at the distribution level, as well as recommendations for DSOs and policy makers. Recommendations for future research are also made in this chapter.

It should be noted that each chapter of this thesis (excluding Chapter 1 and 7) represents an article which is either published or to be submitted for peer-review in a scientific journal. Therefore, some chapter sections may contain similar information (e.g., input data), resulting in some redundancy, in particular, Chapters 2, 3 and 4. Additionally, some general premises across this work are i) perfect forecast of load and generation within the 24-h optimization framework is assumed; ii) the PV investment is not considered, iii) the FiTs are abolished and replaced by the wholesale price, and iv) capacity-based tariffs are implemented for the residential sector. Finally, beyond the scope of this thesis are the device size optimization, and power flow analysis of the distribution network, although these topics are being covered in current projects where the author is involved. Finally, electric vehicles are not covered in this thesis, while they were included in related works in which the author was involved (Gupta, Pena-Bello, et al. 2021; Hutty et al. 2021).

Chapter 2

Household level - Electrochemical storage Part A

Interest in residential batteries to supply photovoltaic (PV) electricity on demand is increasing, however they are not profitable yet. Combining applications has been suggested as a way to increase their attractiveness, but the extent to which this can be achieved, as well as how the different value propositions may affect the optimal battery technology, remain unclear. In this study, we develop an open-source optimization framework to determine the best-suited battery technology depending on the size and the applications combined, including PV self-consumption, demand load-shifting, demand peak-shaving and avoidance of PV curtailment. Moreover, we evaluate the impact of the annual demand and electricity prices by applying our method to representative dwellings in Geneva, Switzerland and Austin, Texas in the United States. Our results indicate that the combination of applications helps batteries to approach to break-even by improving the net present value by up to 66% when compared with batteries performing PV self-consumption only. Interestingly, we find that the best-suited battery technology in Austin is lithium nickel cobalt aluminum oxide (NCA) as for Geneva lithium nickel manganese cobalt oxide (NMC) batteries reach in average a higher net present value than NCA-based batteries. However, NCA-based batteries could be a more promising alternative in the future.

2.1 Introduction

The modularity of solar photovoltaics (PV) is enabling the installation of substantial amounts of generation capacity embedded in the distribution network close to domestic electricity demand. In 2016, new installations in the residential sector of the United States (U.S.) represented 67% of the PV installations with a nominal power lower than 2 MW (Fu et al. 2017), while in Germany for the same year, new PV installations in the residential sector accounted for 50% of the total number of installations (Bundesnetzagentur 2017). This PV development has been facilitated by the rapid decrease in cost of PV modules during the last decade, (e.g., in Germany and the U.S. the price of installed rooftop systems has declined by 60% and 55% respectively since 2009) (Fu et al. 2017; Wirth and K. Schneider 2018). In parallel with these cost declines, retail electricity prices have risen steadily for the last decade across many countries (e.g., by 78% in Spain, 52% in Germany, and 48% in the U.K. since 2007) (Eurostat 2018), while the subsidies for PV electricity

fed to the grid, referred to as feed-in tariffs (FiT), have markedly declined (e.g., by 71% in Germany since 2009) (Pyrgou, Kylili, and Fokaides 2016). Additionally, FiT are being restricted, for example, there is a cap on the installed capacity that can profit of the FiT in Australia and Switzerland (Husser, Pius 2017). Furthermore, the stochastic nature of the solar energy resource prevents PV systems from supplying electricity on demand as is possible with many other conventional technologies such as fossil plants and hydro storage. All of these factors are significantly increasing residential consumers' interest in increasing the amount of self-generated PV that they consume in-home (this is referred to as PV self-consumption) by using battery systems (Husser, Pius 2017). Typical rates of PV self-consumption which ranges between 20 and 40% for residential consumers can be increased by 13 to 24% when battery storage is included in the system, using an elementary charging approach (Luthander, Widén, D. Nilsson, et al. 2015).

In parallel with this increased consumer interest, battery costs, especially lithium-ion technologies, are following a similar trend as experienced by PV systems and the International Renewable Energy Agency (IRENA) reported a cost reduction of 65% since 2010 for lithium-ion batteries (IRENA 2017b). To encourage battery development, dedicated subsidies have been implemented (CPUC 2017; Figgener, Habershusz, et al. 2017). In Germany, more than 30000 new residential PV-coupled battery systems have benefited from the federal program since 2013 and in 2017, half of every small PV system was installed with a coupled battery as a result of government economic incentives (Figgener, Habershusz, et al. 2017). Home battery storage is still an emerging market but some projections estimate that households and businesses may account for nearly 60% of installed storage capacity worldwide by 2040 (Finance Bloomberg New Energy 2018).

Due to its great potential, many authors have investigated key factors impacting on PV-coupled battery systems' profitability. Previous studies have focused on capital and operational expenditures associated with the design (Hesse, Martins, et al. 2017) and operation (Pena-Bello, Burer, et al. 2017; Nyholm et al. 2016; Magnor and Sauer 2016; Barbour and González 2018) of PV-coupled battery systems. In addition to cost improvement, the simultaneous provision of various applications has been presented as an alternative strategy to increase the economic attractiveness of energy storage technologies thereby enabling accelerated deployment (Stephan et al. 2016; Parra and Patel 2019). The combination of different storage applications has already been investigated at the distribution and transmission networks (Stephan et al. 2016; Muller et al. 2017; Böcker et al. 2017) and for different battery technologies (Battke et al. 2013). However, despite the fact that behind-the-meter systems are anticipated to represent major business for stationary storage, previous research on the simultaneous provision of various applications applied to these systems is scant.

The influence of solar resource, demand profiles, jurisdiction and electricity prices across locations has been evaluated for PV self-consumption individually (Kazhamiaka et al. 2017; Barbour and González 2018). Other authors investigated either various types of applications or geographical dependence and/or using a technology-agnostic approach (von Appen et al. 2015; Parra and Patel 2016; Magnor and Sauer 2016; Sani Hassan, Cipcigan, and N. Jenkins 2017; Fares and Webber 2017; Pena-Bello, Burer, et al. 2017; Zheng, Meinrenken, and Lackner 2014; Barbour and González 2018; Nyholm et al. 2016; Tant et al. 2013; Santos, Moura, and Almeida 2014; Hesse, Martins, et al. 2017; Parra and Patel 2019; Hoppmann et al. 2014; O'Shaughnessy et al. 2018b). Therefore, various battery technologies available in the market have not been evaluated with the same method and for the full combi-

nation of consumer applications.

The main aim of this work is to determine the best-suited battery technology for various combinations of applications. For this, we develop an open-source optimization framework using linear programming to solve the management problem of a PV-coupled battery system. The model is robust and can consider different combinations of applications (e.g., PV self-consumption and demand load shifting), tariff structures, export prices and battery characteristics such as aging, efficiency, lifespan and cycles. Moreover, we evaluate which additional, currently unexploited economic benefit can be reaped by combining applications and compare different battery sizes. Our model can be used by consumers and utility companies to explore different batteries and electricity tariffs for a given demand, PV generation and combination of applications. Importantly, the comparison of our results for Geneva (Switzerland) and Austin (U.S.) allow us to understand whether or not the optimal technology and break-even point for the various combinations of applications is geographically dependent in view of the different pricing structures, annual electricity demand and irradiance of the two locations.

Considering the relevance of these research questions and in order to promote the use of our model by other peers, we also make our model and data open. With this, we contribute towards openness in energy research, which is lagging behind other fields (Pfenninger, DeCarolis, et al. 2017). Open-source energy models permit more meaningful collaboration among academics, allow to engage the public and are important for energy policy communication and benefit not only academics but the public in general (Pfenninger 2017; Pfenninger, DeCarolis, et al. 2017). In the interest of transparency, and to boost collaboration and science reproducibility in the energy field, this work joins other open-source efforts such as openmod, renewables-ninja (Pfenninger and Staffell 2016) and the Linux Foundation Energy.

The remainder of this paper is structured as follows. The materials and methods are presented in the next section. Section 2.3 gives the optimization results as a function of the combination of applications, battery technology and geography. Section 2.4 presents the implications of our results and finally the main conclusions are presented.

2.2 Material and methods

Figure 2.1 is a schematic representation of our method. In first place, we specify the input data for electricity demand and PV generation (Section 2.2.1). The applications and their combinations are subsequently defined along with the respective electricity tariff structure (Section 2.2.2). Then, the battery technologies, system topology, components and techno-economic indicators are presented (Sections 2.2.3, 2.2.4 and 2.2.5). Finally, the schedule optimization is described (Section 2.2.6). Across the study we use USD as common currency for both locations[a].

2.2.1 Demand and PV generation

We use electricity consumption data with 15-minute temporal resolution monitored in single dwellings in Western Switzerland (636 dwellings) and Austin, Texas (308 dwellings) during the year 2015. Considering this amount of data, we opt to form representative consumer groups in order to reduce the computational time required.

[a]Exchange rates used: 1 USD/CHF and 1.18 USD/EUR.

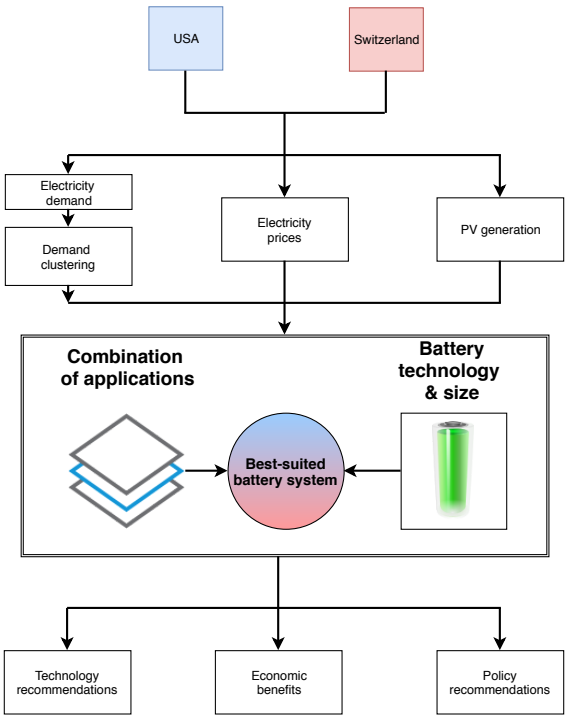

Figure 2.1: Schematic representation of the modeling approach proposed

To generate these representative consumer groups, we employ clustering to produce groups of consumers with similar behaviors. We split the consumers according to their annual consumption into three separate groups, i.e., a low, medium and high consumption group in both locations. Finally, within these three groups we cluster based on the average daily load profile. We opt to produce four clusters in each consumption bracket, noting that selecting the number of clusters in highly dimensional data is a difficult task. From each cluster we select the household that is closer to the centroid which is subsequently optimized. The results presented in this study are the average of the four representative households of each cluster per consumption bracket. For further information see Section A.1.1.

Environmental variables including outdoor temperature and horizontal solar irradiance monitored across both locations are used to model PV generation. We focus on the median PV size of the empirical distribution across Switzerland (i.e., 4.8 kW_p) (BFE 2018) and Texas (i.e., 5 kW_p) (NREL 2018) for our baseline results (i.e., unchanged PV size), while alternative scenarios including the 25th (i.e., 3.2 and 3.15 kW_p for Geneva and Austin respectively) and 75th percentiles (i.e., 6.9 and 6.4 kW_p for Geneva and Austin respectively) are shown in Section A.7.

2.2.2 Electricity tariff and battery applications

The operation of a residential battery as well as the number of applications it can deliver depends on the tariff structure. Since there is not a market mechanism incentivizing the export of electricity from residential batteries to the main grid, this case is not considered either.

Electricity prices used in this study are based on available tariffs which are offered by the local utility companies in the two locations. Both, single tariffs and double tariffs (also called Time-of-Use tariffs, which have a peak and off-peak periods) are considered in the analysis. In Geneva, double tariffs are applied all-year-round, while in Austin, they are applied only in summertime. The export price is assumed to

Table 2.1: Various electricity tariffs components depending on the bill structure and for the two locations used in this study to test various battery applications.

Name		Units	Austin	Geneva	Based on
Flat Tariff		USD/kWh	0.073	0.22	Energy
Double Tariff[a]	On-peak[b]	USD/kWh	0.183	0.24	Energy
	Off-peak	USD/kWh	0.056	0.152	Energy
Export price		USD/kWh	0.027[c]	0.047[b]	Energy
Capacity-based tariff		USD/kW/month	10.14	9.39	Power
Feed-in limit		$\%kW_{p-PV}$	50%	50%	Regulation

[a] When the capacity-based tariff is applied, the Double tariff is reduced by 20% in Geneva and 30% in Austin.
[b] In the U.S. on-peak time is only from June to September from 1 p.m. to 7 p.m. on weekdays. In Switzerland, on-peak time is all year-round from 7 a.m. to 10 p.m. on weekdays and from 5 p.m. to 10 p.m. on weekends.
[c] We use real hourly wholesale price for ERCOT and EPEXSPOT markets. The price shown in the table is the average wholesale price.

be the wholesale electricity price as is the case for traditional electricity generators. This is already the case in Switzerland for installations which are on the waiting list to be granted a one-off subsidy for the capital investment in PV (Husser, Pius 2017) and this is expected to become a widespread policy as a consequence of falling cost of PV technology. We use 2015 wholesale electricity prices from the Electric Reliability Council of Texas day-ahead market (ERCOT southern load zone) and from the European Power Exchange day-ahead market for Switzerland (EPEXSPOT). It is important to note that, apart from the electricity price, electricity bills include other fixed costs as well, such as taxes and grid usage.

Capacity-based tariffs, which bill the peak electricity demand (i.e., in USD/kW) during a billing period, have been widely applied for large consumers, typically belonging to the secondary and tertiary economic sectors. For residential customers capacity-based tariffs have only being marginally applied (e.g., by the Arizona Public Services in the U.S.), although their implementation is being suggested following the penetration of air conditioning, heat pumps and electric vehicles (AEMC 2014). As a first attempt to include them we assume low capacity-based tariffs applied to large consumers by the local utilities in the two locations (i.e., around 10 USD/kW/month), taking a more conservative approach than other studies (e.g., see (O'Shaughnessy et al. 2018b)). In order to ensure that the tariffs are revenue neutral in average for all the households evaluated (i.e., the consumer bill remains similar), the per-kWh rates are reduced by 20% in Geneva and 30% in Austin whenever the capacity-based tariff is used. Finally, following the example in Germany, a (physical) feed-in limit of 50% of the nameplate PV-system capacity for both countries is assumed as a preventive measure to keep the power system stable during periods of high PV production (Hesse, Martins, et al. 2017). Table 2.1 provides the input data for every battery application depending on the tariff structure.

On-grid batteries can perform up to 15 applications depending on the discharge duration, scale and stakeholder (IRENA 2017a). Consumer applications refer to

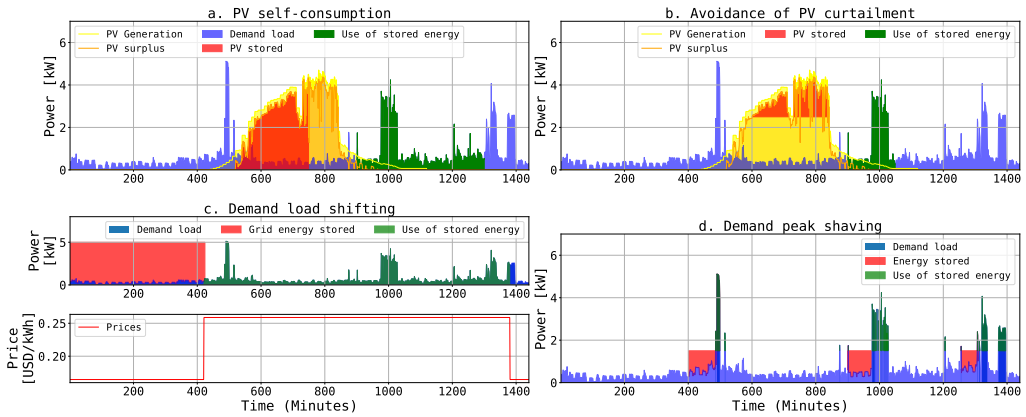

Figure 2.2: Schematic representation of the four applications analyzed in this study. a. PV self-consumption, b. Avoidance of PV curtailment, c. Demand load shifting and d. Demand peak-shaving. This figure is explanatory and does not fully represent the model constraints or approach, which are suitably explained in the Section 2.2.6.

those which help consumer to minimize the electricity bill, with the number of relevant applications depending on the bill structure. Considering the various components of a household electricity bill, a residential battery can perform the following applications (see Figure 2.2):

PV self-consumption (PVSC): PV surplus electricity is stored in a battery and used later on to meet local demand when it is higher than PV generation (see Figure 2.2 a.). The main driver is the price difference between the electricity imported from the grid (i.e., retail price) and the electricity exported to the grid (i.e., FiT or wholesale price as in this study).

Avoidance of PV curtailment (PVCT): In some regions with substantial PV penetration, a feed-in limit is set above which PV power cannot be injected to the grid to keep grid stability (see Figure 2.2 b.). Electricity dissipation is typically done using the PV inverter (Hesse, Martins, et al. 2017). Batteries can prevent this PV curtailment by storing this electricity and meeting local demand later on. The implementation of PV curtailment is determined by regulation.

Demand load-shifting (DLS): A battery is used to exploit varying tariff differentials (see Figure 2.2 c.). The battery charges from the grid when prices are low (off-peak periods) and it discharges when they are high (peak periods). The existence of varying-price tariffs is a prerequisite for demand load-shifting.

Demand peak-shaving (DPS): The discharge of a battery is used to reduce the maximum power drained from the grid (in kW) used during a specified period. Demand-peak-shaving can be used to mitigate demand electricity peaks which can result in distribution network upgrading as well as expensive electricity supply (see Figure 2.2 d.). The main driver is therefore the presence of a capacity-based component in the electricity tariff.

Back-up power is excluded from this study since we focus on distribution areas with a high level of grid stability (for both utilities referred in this study, the number of minutes of power failure experienced by a typical customer in a year was below 100 minutes in 2016) (Lim and Yurukoglu 2018). However, we acknowledge that in some locations back-up power is the main motivation for battery installation (e.g., Hawaii).

Table 2.2: Battery specifications for the six technologies compared in this study. SOC denotes the state of charge.

Technology	Cathode Material	Cycles @ DoD	Maximum lifetime [years]	Roundtrip Efficiency	Energy Costs [USD/nominal kWh]	Maximum charge/ discharge rate [kW]	ΔSOC	Maximum SOC	Minimum SOC	Cycle & calendar aging factor per year[a]	Reference
Li-ion	NMC	5000 @ 100%	15	91.8%	410	0.4*C	1	1	0	0.059 & 0.07	ITP Renewables 2016; ITP Renewables 2017; Tesla 2015
	NCA	8000 @ 100%	20	92.5%	650	1*C	1	1	0	0.047 & 0.05	Trina BESS 2017
	LFP	6000 @ 100%	20	94%	980	2*C	1	1	0	0.024 & 0.05	ITP Renewables 2016; ITP Renewables 2017; Sony 2017
	LTO	15000 @ 100%	25	96.7%	1630	4*C	1	1	0	0.003 & 0.04	Leclanche 2015, personal communication
Lead-acid	VRLA	1500 @ 50%	10	85%	330	0.1*C	0.5	1	0.5	0.236 & 0.1	Hesse, Martins, et al. 2017; Sonnenschein 2013
	ALA	4500 @ 70%	15	91%	750	1*C	0.7	0.9	0.2	0.06 & 0.07	ITP Renewables 2016; ITP Renewables 2017; Ecoult 2017

[a] The cycle aging factor is given for a 50% depth-of-discharge. For further information please refer to Section A.1.2.

2.2.3 Battery technologies

Battery technologies widely differ in cost, aging, lifetime and round trip efficiency (IRENA 2017a), and we compare here six representative products of different technologies within both the lithium and lead-acid families. Within lithium-ion technologies, we include the most common technologies in grid applications, namely lithium nickel manganese cobalt oxide (NMC) and lithium iron phosphate (LFP). Additionally, we include lithium nickel cobalt aluminum oxide (NCA) which have relative competitive installation costs, and lithium titanium oxide (LTO) that is the more thermally stable technology and has extremely high cycle lifetime (IRENA 2017b). As for lead-acid we include traditional valve-regulated lead-acid (VRLA) and advanced lead-acid (ALA). The latter incorporates an ultra-capacitor into a conventional lead-acid cell, increasing efficiency and cycle life. Advanced lead-acid batteries are currently in the demonstration phase and hence costs are currently higher than for conventional lead-acid batteries. The selected representative products are compared with the most likely values found in the market according to Schmidt et al. (2019) (the values are presented in the Section A.1.2).

The technical and economic battery input data required by the model were collected from publicly available data-sheets and personal communication with representative manufacturers. Table 2.2 presents the key specifications for the six battery technologies defined by the type of cathode material. Other relevant values for the techno-economic assessment of PV-coupled battery systems, such as the inverter and converter efficiencies, discount rate and costs are given in Table 2.3. Three currently available battery sizes were assessed, small (3 kWh), medium (7 kWh) and large (14 kWh). Moreover, battery aging is modeled on a daily basis for the first year using the maximum among the daily calendar factor and the daily cyclic factor. The former is calculated as the multiplicative inverse of the calendar lifetime, whereas the cyclic aging factors are based on Woehler curves[b] for every technology. The cyclic aging is then given by the number of cycles per day at the given depth of discharge (depth-of-discharge), divided by the maximum number of cycles at a given depth-of-discharge (Sauer et al. 2009). Further details and a detailed example of the aging model utilised for this study are presented in Section A.3.

2.2.4 PV-coupled battery system

This study focuses on the combined investment in a PV-coupled battery system; more specifically, we analyze the techno-economic implications of adding a battery

[b] The Woehler curves show the number of remaining cycles of a battery as a function of depth of discharge until the end of lifetime. This curve is given by some battery manufacturers in data sheets.

Table 2.3: Values selected for the technical and economic assessment of PV-coupled battery systems.

Component	Units	Value	Reference
Charge controller efficiency	%	98	Energy 2017
Inverter efficiency	%	94	Energy 2017
Bi-directional inverter cost	[USD/kW]	600	Ardani et al. 2017
Bi-directional inverter lifetime	years	15	Fu et al. 2017
Balance of plant cost	[USD/kW]	100	Pena-Bello, Burer, et al. 2017
Installation costs	[USD]	2000	Baumann and Baumgartner 2017
Operation and maintenance costs	[USD/kW]	0	Tesla 2015; Sonnenschein 2013
Discount rate	%/a	4	Stephan et al. 2016
End of life (EoL)	%	70	Käbitz et al. 2013
Inverter load ratio (ILR)	p.u.	1.2	Burger and Rüther 2006

system when purchasing a new PV system that would otherwise be installed on its own. We consider a DC-coupled topology (i.e., coupled on the direct current side) since a lower investment is required and the overall efficiency of stored PV electricity is higher than in AC-coupled topologies (i.e., coupled on the alternating current side) (Ardani et al. 2017). Moreover, the prevention of PV curtailment is possible (for further information see Section A.1.3). Since manufacturers claim no operational costs required for residential PV and battery technologies, we set them to zero (Tesla 2015; Sonnenschein 2013). Installation costs are considered for the inverter and battery and are assumed to be high for both countries (i.e., USD 2000).

2.2.5 Techno-economic indicators

Three complimentary indicators are used to analyze the techno-economic performance of batteries coupled with PV systems, i.e., the PV system is excluded in the analysis since we are interested in the decision of adding a battery. The levelized cost of energy storage, LCOES (USD/kWh) quantifies the cost associated with the total electricity supplied by the battery throughout the life of the system (see Eq. 2.1). The second indicator is the levelized value of energy storage, LVOES (USD/kWh). It quantifies the revenue associated with the battery discharge throughout the life of the system (see Eqs. 2.2 and 2.3). Finally, the net present value (NPV) calculated as the sum of the discounted cash flows over the lifetime of the battery system (Eq. 2.4) is used to appraise the overall impact of the system configuration and operation for each combination (geography, technology, consumer type and combination of applications) on the economic profitability of residential batteries.

$$LCOES = \frac{\sum_{i=0}^{N} \frac{CAPEX}{(1+r)^i} + \sum_{i=1}^{N} \frac{OPEX}{(1+r)^i}}{\sum_{i=1}^{N} \frac{E_{dis}}{(1+r)^i}} \tag{2.1}$$

$$LVOES = \frac{\sum_{i=1}^{N} \frac{CF_{Batt_i}}{(1+r)^i}}{\sum_{i=1}^{N} \frac{E_{dis}}{(1+r)^i}} \tag{2.2}$$

$$CF_{Batt_i} = CF_{PV-Batt_i} - CF_{PV_i} \tag{2.3}$$

$$NPV = \sum_{i=1}^{N} \frac{CF_{Batt_i}}{(1+r)^i} - \sum_{i=0}^{N} \frac{CAPEX}{(1+r)^i} \tag{2.4}$$

Where CAPEX are the capital expenditures (in USD), OPEX are the operational expenditures (in USD), r is the discount factor, E_{dis} is the energy discharged from the battery and N is the lifetime of the project (i.e., the same as the inverter which in this study is considered to be 15 years). The cash flows of the PV-coupled battery system are represented as $CF_{PV-Batt}$, CF_{Batt} are the cash flows due to the battery only, and CF_{PV} are the cash flows due to the PV system.

2.2.6 Optimization of the battery schedule

The management problem of a PV-coupled battery system is solved by Mixed Integer Linear Programming, using Pyomo, an open-source tool for modeling optimization applications in Python (Hart et al. 2012) and solved with CPLEX. The battery schedule is optimized for every day (i.e., 24 h optimization framework) and we assume perfect day-ahead forecast of the electricity demand load, solar PV generation and wholesale prices in order to determine the maximum economic potential regardless of the forecast strategy used. Battery aging was treated as an exogenous parameter, calculated on daily basis and was not subject to optimization (for further information we invite the reader to see section A.3). The temporal resolution of the input data and simulation is 15 minutes, with this value providing a reasonable compromise between the modeling real performance and computational speed (Beck et al. 2016). The model objective function has two components, namely the energy and power components of the electricity bill. As the tariff structure depends on the applications considered, a boolean parameter activates the power-based factor of the bill when is necessary.

Every optimization was run for one year and then the results are linearly-extrapolated to reach the battery end of life. We assume 30% of capacity depletion as the end of life (Käbitz et al. 2013) and when the battery lifetime exceeds the inverter lifetime, the residual value of the battery is considered using straight-line depreciation (Moore et al. 2015). Replacement is considered when the battery cannot match the inverter lifetime which is taken as the project lifetime, we take a conservative approach maintaining the same cost in the future discounted to the present, due to the high uncertainty linked to future battery costs for different battery technologies. The analysis is done with same electricity prices for all years across battery lifetime. The model objective function, constraints, variables and parameters are presented below. The validation of the model can be found in Section A.5. The model and the U.S. data (the Swiss data is confidential) are publicly available in `https://github.com/alefunxo/Basopra`.

$$Min(\overbrace{\sum_{i=0}^{t}(E_{grid_i} * \pi_{import_i} - E_{PV-grid_i} * \pi_{export_i})}^{\text{Energy-based tariff}} + \underbrace{(P_{max-day} * \pi_{capacity} * PS)}_{\text{Power-based tariff}}) \tag{2.5}$$

Where the energy-based tariff is given by E_{grid_i} which is the electricity drawn from the grid, π_{import_i} is the import price (i.e., retail price), $E_{PV-grid_i}$ is the PV-electricity exported to the grid, π_{export_i} is the export price (i.e., the wholesale price in this study), all these variables have the sub-index i representing every time step from

0 to t (i.e., 15-minutes step for this study). As for the power-based tariff, it is given by $P_{max-day}$, which is the maximum power required from the grid for the day, $\pi_{capacity}$ which is the capacity-based tariff (i.e., in USD/kW/day) and PS is a boolean variable which indicate the use of demand peak-shaving in the combination of applications. The objective function is subject to the constraints introduced below.

Subject to:

Battery constraints:

$$SOC_{min} \leq SOC_i \leq SOC_{max} \tag{2.6}$$

$$E_{char_i} = E_{PV-batt_i} + E_{grid-batt_i} \tag{2.7}$$

$$E_{dis_i} \leq (SOC_{i-1} - SOC_{min}) * C_{batt}^{nom} \tag{2.8}$$

Where, SOC_{min} and SOC_{max} are the minimum and maximum states of charge and SOC_i is the state of charge at the instant i, below and above which the battery is never discharged and charged. E_{char_i} the energy charged into the battery, $E_{PV-batt_i}$ is the PV energy flow to the battery and $E_{grid-batt_i}$ is the grid energy flow to the battery. E_{dis} is the electricity discharged from the battery and C_{batt}^{nom} is the nominal capacity of the battery.

Energy balance constraints:

$$E_{grid_i} = E_{grid-load_i} + E_{grid-batt_i} + E_{loss-inv-grid_i} \tag{2.9}$$

$$E_{PV_i} = E_{PV-load_i} + E_{PV-batt_i} + E_{PV-grid_i} + E_{PV-curt_i} + E_{loss-conv_i} + E_{loss-inv-PV_i} \tag{2.10}$$

$$E_{load_i} = E_{PV-load_i} + E_{grid-load_i} + E_{dis_i} * \eta_{inv} \tag{2.11}$$

$$SOC_i = \frac{(SOC_{i-1} * C_{batt}^{nom} + E_{char_i} - E_{dis_i} - E_{loss-batt_i})}{C_{batt}^{nom}} \tag{2.12}$$

$$E_{dis_i} = E_{batt-load_i} + E_{loss-inv-batt_i} \tag{2.13}$$

Energy balance constraints verify that all the energy flows sum up to the total energy provided by the grid (E_{grid_i}), the PV system (E_{PV_i}) and to cover the household demand (E_{load_i}), as well as to define the state of charge and the energy discharged from the battery. The energy flows are represented using the convention $E_{from-to}$, for instance, $E_{PV-grid}$ is the energy from the PV system injected into the grid. The losses are represented using the convention $E_{loss-device-dueto}$, for instance, $E_{loss-inv-PV}$ represents the losses in the inverter due to PV electricity flows. The efficiencies are represented using the convention η_{device}, where the device can be the converter (η_{conv}), the inverter (η_{inv}) or the battery (η_{batt}).

Efficiency losses constraints:

$$E_{loss-conv_i} = (E_{PV-load_i} + E_{PV-batt_i} + E_{PV-grid_i} + E_{loss-inv-PV_i}) * (1 - \eta_{conv}) \tag{2.14}$$

$$E_{loss-biinv_i} = E_{loss-inv-PV_i} + E_{loss-inv-grid_i} + E_{loss-inv-batt_i} \tag{2.15}$$

$$E_{loss-inv-PV_i} = (E_{PV-load_i} + E_{PV-grid_i}) * (1 - \eta_{inv})/\eta_{inv} \tag{2.16}$$

$$E_{loss-inv-grid_i} = E_{grid-batt_i} * (1 - \eta_{inv})/\eta_{inv} \tag{2.17}$$

$$E_{loss-inv-batt_i} = E_{dis_i} * (1 - \eta_{inv}) \tag{2.18}$$

$$E_{loss-batt_i} = E_{char_i} * (1 - \eta_{batt}) \tag{2.19}$$

Efficiency losses constraints account for the losses of the converter (Eq. 2.14), of all the losses in the inverter (Eq. 2.15), of the losses in the inverter due only to the PV (Eq. 2.16), of the losses in the inverter due to grid charging (Eq. 2.17), of the losses in the inverter due to the energy discharged from the battery (Eq. 2.18), and the losses in the battery (Eq. 2.19). Energy flows are, for convention, considered after the inverter, to calculate the converter losses, the inverter efficiency has to be considered (see Figure A.3). The PV curtailed is not taken into account as losses and it is assumed to be curtailed at the converter.

Power constraints:

$$P_{char_i} \leq P_{max-char} \tag{2.20}$$

$$P_{dis_i} \leq P_{max-dis} \tag{2.21}$$

$$P_{PV_i} \leq P_{conv} \tag{2.22}$$

$$P_{PV-grid_i} + P_{PV-load_i} + P_{dis_i} + P_{loss-inv-PV_i} + P_{loss-inv-batt_i} \leq P_{inv} \tag{2.23}$$

$$P_{grid-batt_i} + P_{loss-inv-grid_i} \leq P_{inv} \tag{2.24}$$

Power variables are designated using P and follow the same conventions previously presented. The battery maximum charging and discharging power are represented by $P_{max-char}$ and $P_{max-dis}$. P_{conv} and P_{inv} represent the converter and inverter rating.

Application selection:

$$P_{PV-grid_i} \leq P_{limit} \quad \forall \quad i \quad if \quad PVCT = 1 \tag{2.25}$$

$$E_{grid-batt_i} = 0 \quad \forall \quad i \quad if \quad DLS = 0 \tag{2.26}$$

$$P_{grid_i} \leq P_{max-day} \quad \forall \quad i \quad if \quad DPS = 1 \tag{2.27}$$

Since the model allows to select from a pool of applications (i.e., PV self-consumption, avoidance of PV curtailment, demand load shifting and demand peak-shaving), when one of the applications is selected the corresponding constraint is applied (except for PVSC which is applied by default and includes all the constraints mentioned above). Thus, when PVCT is selected, a constraint to the power feed-in $P_{PV-grid_i}$ is applied (Eq. 2.25), when demand load shifting is not applied (i.e., DLS=0), the battery cannot charge from the grid. Finally, when demand peak-shaving is applied (i.e., DPS=1), a constraint on the maximum power drawn from the grid P_{grid_i} is applied (Eq. 2.27) and limited to the minimum possible power ($P_{max-day}$), which is a result from the optimization.

2.3 Results

Since we aim to determine the best-suited battery technology for various combination of applications and analyze the impact of geography and size, we present first the results for a typical battery size of 7 kWh depending on the battery technology, location and for different combinations of applications and tariff structures (see Table 2.5). PV self-consumption is common across all combinations since this application is the baseline for residential batteries. Depending on the combination of applications, different tariff structures are needed, thus combinations of tariffs are done (e.g., if demand peak-shaving is combined with PV self-consumption, then a combination of flat tariff with capacity-based tariff is made - combination 2 in Table 2.5). Afterward, we evaluate the impact of the battery size. All results are based

Table 2.4: List of model parameters and variables.

Modeling parameters	Name	Units	Modeling variables	Name	Units
Converter efficiency	η_{conv}	%	PV generation fed to the load	$E_{PV-load}$	kWh
Inverter efficiency	η_{inv}	%	PV generation exported to the grid	$E_{PV-grid}$	kWh
Inverter rating	P_{inv}	kW	PV generation injected to the battery	$E_{PV-batt}$	kWh
Battery Efficiency	η_{batt}	%	PV generation curtailed	$E_{PV-curt}$	kWh
Maximum discharge power	$P_{max-dis}$	kW	Energy lost due to converter efficiency	$E_{loss-conv}$	kWh
Maximum charge power	$P_{max-char}$	kW	Total energy lost due to bi-directional inverter efficiency	$E_{loss-binv}$	kWh
Battery nominal capacity	C_{batt}^{nom}	kWh	PV energy lost due to bi-directional inverter efficiency	$E_{loss-PVinv}$	kWh
Battery lifetime	N	years	Grid energy lost due to bi-directional inverter efficiency	$E_{loss-gridinv}$	kWh
Battery maximum state of charge	SOC_{max}	%	Battery energy lost due to bi-directional inverter efficiency	$E_{loss-battinv}$	kWh
Battery minimum state of charge	SOC_{min}	%	Energy lost due to battery efficiency	$E_{loss-batt}$	kWh
Retail prices	π_{import}	USD/kWh	Energy drained from the battery	E_{dis}	kWh
Export prices	π_{export}	USD/kWh	Energy injected to the battery	E_{char}	kWh
Capacity-based tariff	$\pi_{capacity}$	USD/kW	Energy delivered from the battery to the load	$E_{batt-load}$	kWh
Feed-in limit	P_{limit}	%	Energy imported from the grid to the battery	$E_{grid-batt}$	kWh
Combination of applications	[PVCT, PVSC, DLS, DPS]	Boolean array	Energy imported from the grid to the load	$E_{grid-load}$	kWh
Load demand	E_{load}	kWh	Energy drained from the grid	E_{grid}	kWh
PV generation	E_{PV}	kWh	Maximum power drained from the grid	$P_{max-day}$	kW
Optimization time framework	t	minutes	Power related to any energy parameter	$P_x = E_x/\Delta t$	kW
Temporal resolution	Δt	fraction of hour	State of charge	SOC_i	%

on a representative (median of the distribution) fixed PV size in each geographical region (4.8 kW_p for Geneva and 5 kW_p for Austin). Results for other PV sizes and alternative combinations of applications are given in Sections A.6 and A.7.

Table 2.5: Various combination of applications and the respective electricity tariff structure compared in this study. If the application indicator is ON, it means that the referred application is included in the combination, same is valid for the electricity tariff structure indicators.

Combination name	Applications				Electricity tariff structure			
	PV Self-consumption (PVSC)	Avoidance of PV curtailment (PVCT)	demand load shifting (DLS)	Demand peak-shaving (DPS)	Flat tariff (FT)	Double tariff (DT)	Capacity-based tariff	Feed-in limit
Combination 1 (Baseline scenario)	ON	OFF	OFF	OFF	ON	OFF	OFF	OFF
Combination 2	ON	OFF	OFF	ON	ON	OFF	ON	OFF
Combination 3	ON	OFF	ON	OFF	OFF	ON	OFF	OFF
Combination 4	ON	ON	OFF	OFF	ON	OFF	OFF	ON
Combination 5	ON	ON	ON	ON	OFF	ON	ON	ON

2.3.1 Levelized cost

Figure 2.3 displays the levelized cost of energy storage for six battery technologies and five combinations of applications in Geneva and Austin. Three major observations can be made. First, NCA and NMC-based batteries offer lower levelized cost for all combinations, the former due to an elevated lifespan and a high number of cycles, while for the latter the reason is a combination of low cost (technology with the lowest cost after VRLA) and a reasonable compromise between number of cycles and lifespan. Secondly, batteries performing in Austin offer lower cost per kWh since they are heavily cycled, (i.e., the average battery in Austin supplies 62% more

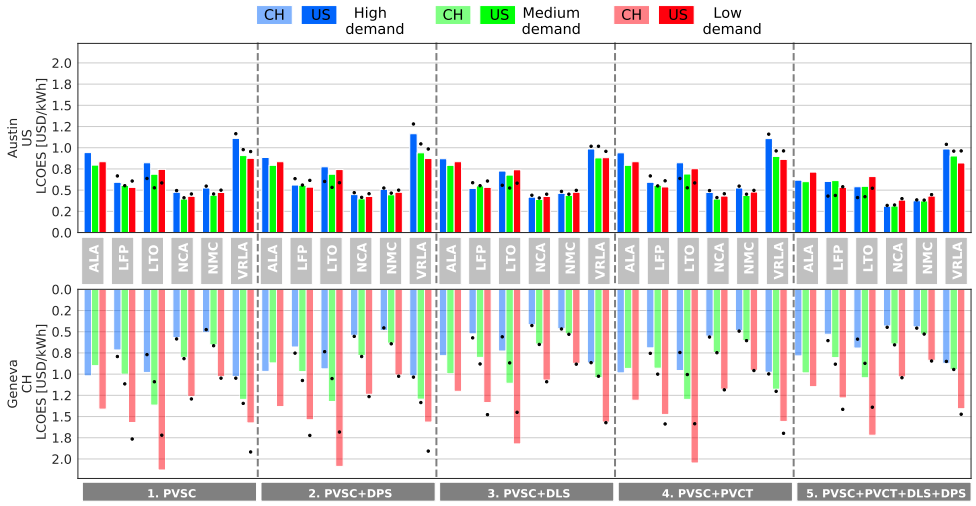

Figure 2.3: Levelized cost of energy storage of a 7 kWh battery for all battery technologies depending on the type of combination of applications for Austin, U.S. (top) and Geneva, Switzerland (bottom). The size of the PV system correspond to the median installed capacity across both locations (i.e., 4.8 for Geneva and 5 kW_p for Austin). The black point in the graph corresponds to the optimization results for the most likely values for every technology in terms of battery pack cost, calendric and cycle lifetime, depth of discharge and round-trip efficiency according to Schmidt et al. (2019) (except for advanced lead-acid, for which there is no public data available beyond the proposed manufacturer). Note that for the LCOES the lower is the bar the better are the results.

electricity throughout its lifetime than in Geneva). As for Geneva, the LCOES also clearly decreases as household electricity consumption increases (demand data for both countries is analyzed in Section A.2.1). These results have important implications for the energy transition since residential batteries cycle more for consumers with large electricity consumption and consumers with low consumption could group themselves under communities battery schemes in order to reach lower costs.

Finally, in terms of combination of applications, demand load-shifting increases the use of the battery, reducing the levelized cost, particularly in Geneva where battery use increases on average by 23% when demand load-shifting is included. This is mainly due to the double tariff structure which is applied all year-round and low PV surplus in winter, in contrast to Austin where there is a relatively high PV surplus in winter and the double tariff is applied only during summertime. Accordingly, demand load-shifting reduces the LCOES in average by 14% in Geneva and by 9% in Austin.

Additionally, Figure 2.3 shows the optimization results for the most likely values for every technology in terms of battery pack cost, calendric and cycle lifetime, depth of discharge and round-trip efficiency according to Schmidt et al. (2019) (except for ALA, for which there is no public data available beyond the proposed manufacturer, for further information see Section A.1.2). These values are very close to the chosen manufacturer. The greater difference corresponds to LTO chemistry, mainly due to the great cost's deviation (i.e., 1650 USD/kWh in this study vs. 1060 USD/kWh in Schmidt et al. (2019)).

2.3.2 Levelized value

Figure 2.4 displays the levelized value for all battery technologies depending on the combination of applications. The differences among technologies regarding added

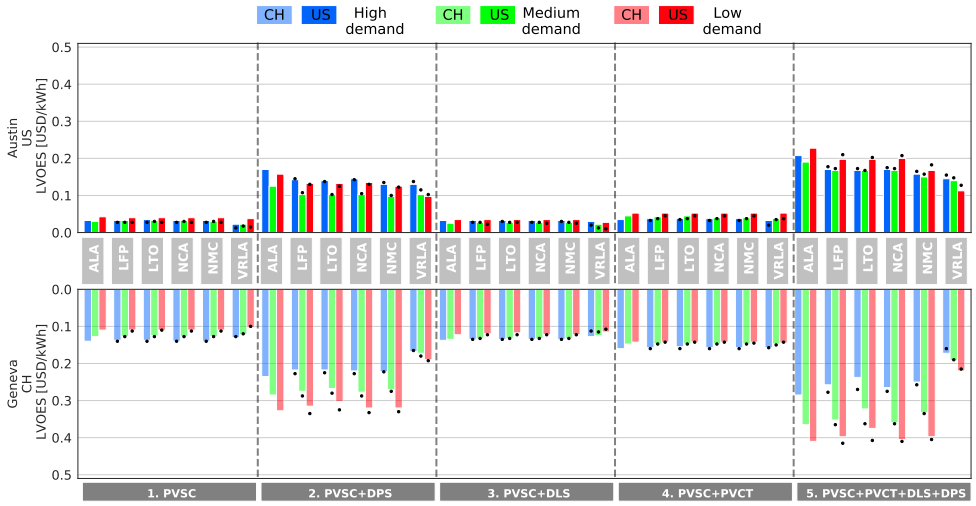

Figure 2.4: Levelized value of energy storage of a 7 kWh battery for all battery technologies depending on the type of combination of applications for Austin, U.S. (top) and Geneva, Switzerland (bottom). The size of the PV system correspond to the median installed capacity across both locations (i.e., 4.8 for Geneva and 5 kW_p for Austin). The black point in the graph corresponds to the optimization results for the most likely values for every technology in terms of battery pack cost, calendric and cycle lifetime, depth of discharge and round-trip efficiency according to Schmidt et al. (2019) (except for advanced lead-acid, for which there is no public data available beyond the proposed manufacturer). Note that for the LVOES the higher is the bar the better are the results.

value per-kWh for combinations that do not include demand peak-shaving is relatively small (i.e., less than 9% for both countries). Conversely, ALA-based and VRLA-based batteries add more and less value per-kWh respectively than other battery chemistries when demand peak-shaving is included (on average 25% and 15%, respectively) because in both cases, less electricity is supplied by the battery due to a shallower depth-of-discharge. However, in the case of ALA-based batteries, the battery is used mostly for demand-peak-shaving since it is the application that adds most value and this technology offers significant discharge rating (see Section 2.3.4). On the other hand, the cash flow is significantly lower for VRLA-based batteries due to low depth-of-discharge (50%), efficiency (85%) and crucially the limited power characteristics (i.e., maximum charge and discharge power of 0.1*C) leading to lower levelized value. In terms of geography, more value per-kWh is added in Geneva (i.e., in average 0.21 USD/kWh), compared to Austin. (i.e., in average 0.09 USD/kWh), due to higher electricity prices. Furthermore, when excluding demand peak-shaving, batteries in households with higher demand create slightly more value per-kWh due to a higher self-consumption. On the other hand, when demand peak-shaving is included, batteries in Geneva households with lower demand create more value per-kWh, due to a higher relative influence of the capacity-based tariff, i.e., the battery is primarily used for demand peak-shaving.

The addition of applications such as demand load shifting (combination 3) or avoidance of PV curtailment (combination 4) to the baseline scenario (PV self-consumption referred to as combination 1) adds only marginal value, however, when the four applications are combined, the results are significantly better than the combination of PV self-consumption and demand peak-shaving (i.e., value per-kWh is on average 27% higher). This improvement is due to the synergies between demand load shifting and demand peak-shaving (see Section A.6). Demand peak-shaving is

the application adding most value per-kWh (i.e., 0.11 and 0.15 USD/kWh in the U.S. and Switzerland, respectively), owing to the importance of the capacity-based tariff in the final bill even if the bill is revenue neutral when it is added. The LVOES obtained When the optimization is run using the most likely values for every technology remains very similar (see the black points in Figure 2.4).

2.3.3 NPV

Figure 2.5 displays the net present value for all battery technologies depending on the type of combination of applications for Geneva and Austin. It can be seen that due to high costs (as well as reduced cycle life, depth-of-discharge and lifespan in the case of VRLA) there is no positive economic case. However, we can see that the profitability is markedly improved for most technologies by combining applications. Since the battery operation adds more value in Geneva than in Austin, the NPV is higher as a result. In the U.S., similar NPV across the consumption brackets is present, with the clear exception of medium demand households using LFP-based batteries. This exception is due to a replacement battery for consumers 3 months before the project lifetime in this consumption bracket, which includes a supplementary investment to replace the battery and therefore further reduces the net present value (the same applies to high demand households for full combination of applications in Austin). In terms of applications, the combination of PV self-consumption with demand peak-shaving increases the NPV on average by 15%, which can be improved 6% more when demand load-shifting is included. The NPV obtained When the optimization is run using the most likely values for every technology remains very similar (see the black points in Figure 2.4). The greater difference corresponds to LTO chemistry, mainly due to the great cost's deviation (i.e., 1650 USD/kWh in this study vs. 1060 USD/kWh in Schmidt et al. (2019)).

2.3.4 Impact of battery size

Figure 2.6 displays the average levelized cost, levelized value and net present value across the three groups of consumers (see Material and methods Section and Section A.1.1), for small (i.e., 3 kWh), medium (i.e., 7 kWh) and large (i.e., 14 kWh) batteries performing simultaneously all consumer applications depending on the battery technology. Since batteries are heavily cycled in Austin, lower levelized cost is reached. The per-kWh cost difference between the two countries increases when the battery size increases. In Geneva, a large battery incurs higher per-kWh cost due to relatively low number of cycles and higher capital expenditure. In contrast, in Austin, large batteries reduce further the levelized cost.

VRLA and NMC-based batteries increase their added value when the battery size increases. This is due to their lower charge and discharge rates (0.1*C and 0.4*C, respectively) which means that they need a large energy capacity to provide significant power, while added value decreases with battery size for other chemistries with larger charge and discharge rates. For small size batteries, NCA-based batteries have better results in both countries, whereas VRLA batteries reach worst results for the full combination of applications. NCA-based batteries are preferred in Austin and very competitive with NMC-based batteries in Geneva for medium-sized batteries, while for large-sized batteries NMC chemistry get the better net present value. Overall, the net present value results of Figure 2.6 indicate that batteries in Geneva are on average 13% (10% for small sizes, 16% for medium sizes and 12% for large

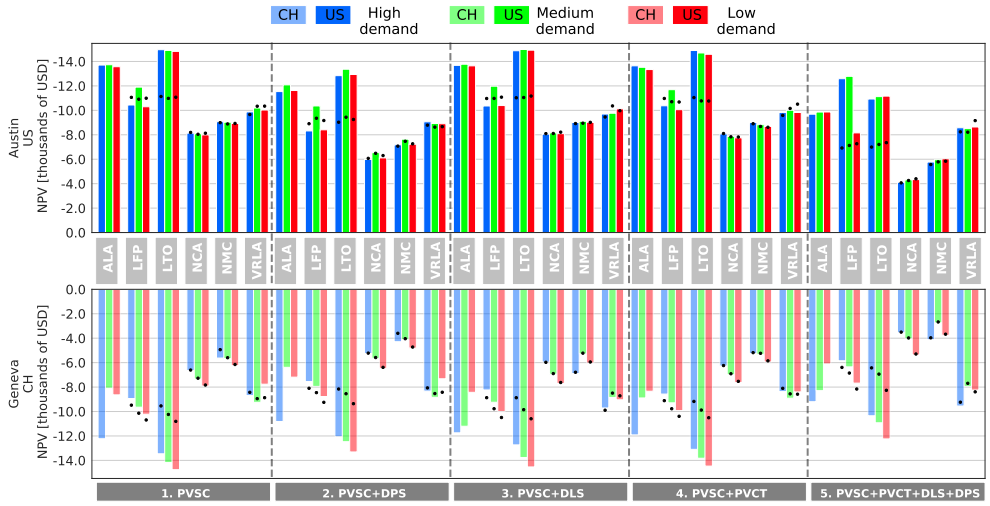

Figure 2.5: Net present value of a 7 kWh battery for all battery technologies depending on the type of combination of applications for Austin, U.S. (top) and Geneva, Switzerland (bottom). The size of the PV system correspond to the median installed capacity across both locations (i.e., 4.8 for Geneva and 5 kW_p for Austin). The black point in the graph corresponds to the optimization results for the most likely values for every technology in terms of battery pack cost, calendric and cycle lifetime, depth of discharge and round-trip efficiency according to Schmidt et al. (2019) (except for advanced lead-acid, for which there is no public data available beyond the proposed manufacturer). Note that the y-axis presents negative NPV for both countries, thus the lower is the bar the better are the results.

sizes) more attractive than in Austin, due to higher value added as a result of higher electricity electricity prices.

2.4 Discussion

Based on our experiments for Geneva and Austin, we find that NCA and NMC are the best-suited battery technologies for various combinations of applications (i.e., PV self-consumption, avoidance of PV curtailment, demand load shifting and demand peak-shaving). When all the applications are combined NCA is the best-suited battery technology in Austin, which represent a place with high irradiance, in general high electricity consumption, low electricity prices and where the use of air conditioning is extended. On the other hand, NMC-based batteries reach in average a net present value 7% higher than NCA-based batteries (i.e., NPV is very similar) in Geneva, where electricity consumption and irradiance are lower, electricity prices higher and where there is no air conditioning in summer. The household demand marginally affects the profitability of PV-coupled battery systems and we find the NPV difference among the three consumption brackets for all technologies and combinations of applications is less than 10% (2% in the U.S. and 8% in Switzerland, on average). On the other hand, geography impacts the battery's economic viability and the net present value of battery systems in Geneva are on average 16% more attractive than in Austin, mainly due to higher electricity prices.

Despite significantly increasing the NPV, batteries simultaneously performing several applications are not yet profitable under existing market conditions. However, further (expected) reductions in battery costs, together with combining battery applications may hold the key towards household battery profitability. In particular,

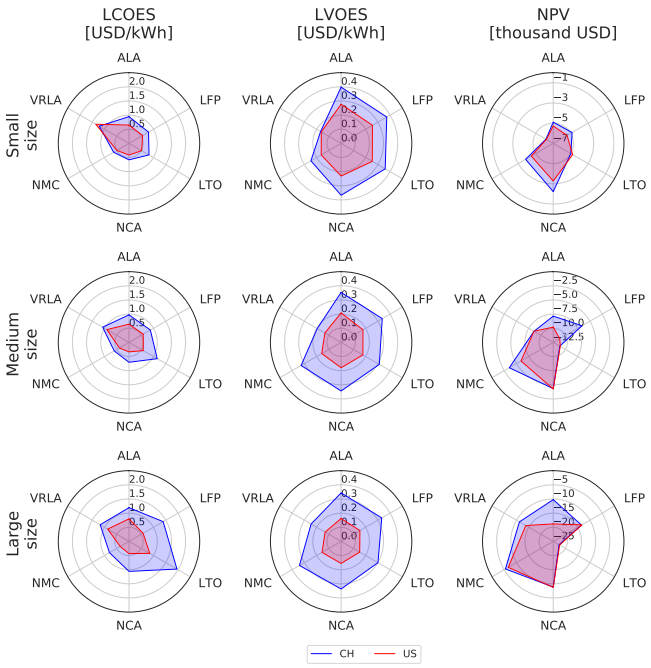

Figure 2.6: Comparison of the average LCOES (left), LVOES (middle) and NPV (right) for various battery technologies performing simultaneously all consumer applications in Austin, U.S. (red) and Geneva, Switzerland (blue) depending on the type of annual electricity demand, namely small (top), medium (middle) and large (bottom).

adding demand peak-shaving to PV self-consumption brings clear benefits compared to the baseline scenario (PV self-consumption only), especially for NCA and NMC-based batteries (up to 66% higher NPV). It is expected that demand peak-shaving would also introduce other benefits for the wider energy system, since electricity peaks are typically met by more costly or carbon-intense generators across many countries (this is not however the case of Switzerland where hydropower is used for this purpose). Moreover, distribution system operators could also defer or even save investment in infrastructure. Thus, demand peak-shaving is an application which provides synergies for the consumer, utility companies and distribution system operators. Demand load-shifting increases battery use but when demand peak-shaving is not included in the combination, it barely increases the net present value, even in Switzerland where double tariff is applied all year-round. Being a regulation-based application, the avoidance of PV curtailment is more interesting from the grid perspective than from the consumer perspective.

In the residential electricity market, small battery sizes offer the best economic case. Despite a higher annual electricity demand in Texas compared to Geneva, larger battery capacities are not economically justified and a small size battery (3 kWh in this study) obtains the best results in both locations. However, with (installed) cost reductions of 55%, medium size batteries will get more economically attractive than small size batteries in both countries. From a market perspective, further cost reduction of lithium-ion technologies may result in more market competition for NMC-based batteries which have the strongest position in the market at the moment. For instance, NCA-based batteries are more suitable than NMC-based ones when combining applications mainly due to higher charge and discharge rates, cycles and extended lifespan, even if the price is higher, thus a cost reduction of NCA-based batteries can compromise the leader position of NMC-based batteries

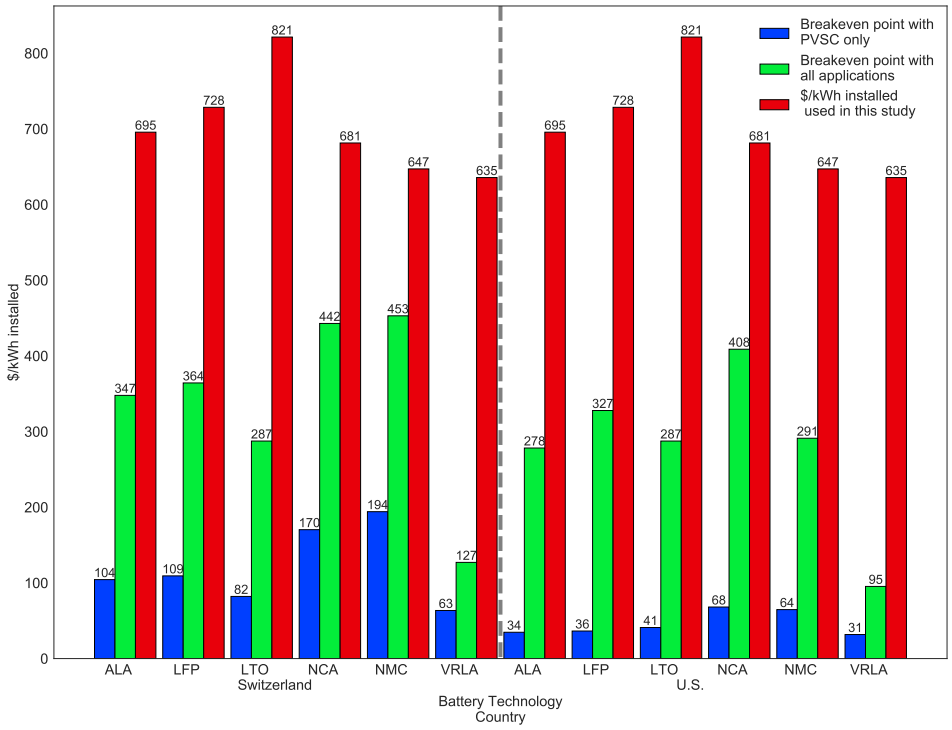

Figure 2.7: Break-even point of a 7 kWh battery for all battery technologies depending on the type of combination of applications, PV self-consumption only (blue), the full combination of applications (green) and for comparison, the installed cost per kWh used in this study (red), for the U.S. (right) and Switzerland (left). The size the PV system correspond to the median installed capacity across both locations.

in the residential market.

In order to reach economic profitability, battery systems require further cost reductions regardless of battery technology. Installation costs (including permitting, inspection, interconnection, overhead, profit and installation labor) in Geneva and Austin are assumed to be $ 2000 in this study (Baumann and Baumgartner 2017; Ardani et al. 2017) but may reduce with increasing installation experience (learning by doing) and market competition. Figure 2.7 displays the break-even point of a 7 kWh battery performing only PV self-consumption as well as all four applications depending on the battery technology and location. The current installation cost per kWh considering battery, inverter and installation are also given for reference purposes. When all applications are combined, NCA-based batteries are closest to profitability. They require only 35% reduction in installed costs to be profitable in Switzerland and 40% in the U.S. NMC-based batteries in Switzerland require a 30% reduction on installed costs, however, in the U.S. this increases up to 55%. Due to higher electricity prices, profitability may be reached first in Switzerland even if PV self-consumption is the only application, however, on average a reduction of 83% in the cost per-kWh-installed, compared to today's cost, is required. On the other hand, when all applications are combined, a reduction of 52% is required. In the case of the U.S., further reductions are needed (93% if only PV self-consumption is addressed and 60% if all applications are combined). According to IRENA lithium-ion batteries', installation costs will be reduced by 60% on current levels by 2030

(IRENA 2017a), thus residential batteries may reach profitability (without subsidies) in both countries in the next decade if all applications are combined. This break-even period may be however shorter if electricity prices increase.

NCA-based batteries already have the appropriate characteristics to combine applications and expand their deployment. LFP-based batteries have suitable technical characteristics but a high number of cycles must be ensured. On the other hand, LTO-based batteries can be considered as over-designed for household needs which leads to higher cost, and if they are over-sized, entail a higher cost than other battery types. NMC-based batteries are expected to lead the cost decline due to their leader position in the market, however, technical specifications, mainly calendar life, will need further development if manufacturers want to keep their dominant position in a near future with residential batteries performing several applications simultaneously. Advanced lead-acid batteries have competitive characteristics and performance, however, shallow depth-of-discharge and high costs, penalize them when compared with lithium-ion technologies. Therefore, only aggressive cost reductions and significant technical improvements could lead to increase their market share. The environmental dimension can be an important asset for this technology since its recycling process has been already established and other criteria such as their material criticality is far lower compared to lithium-ion batteries (Moss et al. 2013). Finally, already-mature traditional lead-acid batteries, which have limited margin for improvement, are clearly less attractive for exploiting additional applications which appears to be a strategy that cannot be ignored.

2.5 Conclusions

The aim of this study was to determine the best-suited battery technology for various combination of applications (i.e., PV self-consumption, avoidance of PV curtailment, demand load shifting and demand peak-shaving) for two locations with different irradiance profiles, electricity prices and average demand consumption (i.e., Austin, U.S. and Geneva, Switzerland) and taking into account three battery sizes (i.e., 3, 7 and 14 kWh). We found that NCA and NMC are the best-suited batteries in both locations and for all the combinations of applications, being NCA slightly better in the U.S. example than NMC-based batteries.

Moreover, emerging from the present study, we contribute with four factors that influence the economic profitability of a PV-coupled battery system: (a) The low influence of annual household demand, which in this study varies from 4.9% in Austin to 2.2% in Geneva; (b) the rather high impact of location (i.e., 18% higher NPV in Geneva than in Austin), whose uncertainty is rather low since the electricity bill structure and environmental factors are widely known; (c) the medium impact of battery technology which depends not only on the technical characteristics, which are already good for residential applications, but as well on battery costs which are still high for the same niche and whose uncertainty is rather high; (d) the impact of the combination of applications, which can be marked, especially with demand peak-shaving, but there is rather high uncertainty since the number of applications depends on local regulation by utility companies and policy makers.

Although our study proposes a robust framework to quantify the attractiveness of batteries and the proposed models are rich in technology details, it is not without limitations, which in turn call for future research. Other forecast strategies different to perfect forecast could be introduced in the optimization framework, with this

reducing the revenue. In addition, the design of future electricity tariffs including time-of-use and capacity components is still a topic under investigation. In particular, capacity-based tariffs are expected to become more widespread since they offer great cost reflectivity as well as revenue variability for network businesses in the face of current and expected disruptions and conduct to flexibility (ACCC 2018). Additionally, while the scope of the research presented in this paper is limited to electricity demand in dwellings, future research should also incorporate heat and transport demand and the trade-offs of different low carbon technologies such as residential batteries, heat pumps and electric vehicles. Finally, the proposed optimization framework could be extended to more geographies.

The open-source model used in this study is publicly available in `https://github.com/alefunxo/Basopra`, and could be used for different PV generation profiles and demand profiles, as well as different tariff structures and batteries with user-defined characteristics.

Chapter 3

Household level - Electrochemical storage Part B

Energy storage is a key solution to supply renewable electricity on demand and in particular batteries are becoming attractive for consumers who install PV panels. In order to minimize their electricity bill and keep the grid stable, batteries can combine applications. The daily match between PV supply and the electricity load profile is often considered as a determinant for the attractiveness of residential PV-coupled battery systems, however, the previous literature has so far mainly focused on the annual energy balance. In this paper, we analyze the techno-economic impact of adding a battery system to a new PV system that would otherwise be installed on its own, for different residential electricity load profiles in Geneva (Switzerland) and Austin (U.S.) using lithium-ion batteries performing various consumer applications, namely PV self-consumption, demand load-shifting, avoidance of PV curtailment, and demand peak-shaving, individually and jointly. We employ clustering of the household's load profile (with 15-minute resolution) for households with low, medium, and high annual electricity consumption in the two locations using a 1:1:1 sizing ratio. Our results show that with this simple sizing rule-of-thumb, the shape of the load profile has a small impact on the net present value of batteries. Overall, our analysis suggests that the effect of the load profile is small and differs across locations, whereas the combination of applications significantly increases profitability while marginally decreasing the share of self-consumption. Moreover, without the combination of applications, batteries are far from being economically viable.

3.1 Introduction

Rooftop photovoltaic (PV) systems have played a critical role in deploying solar energy owing to dramatic PV panel cost reductions (60% since 2010) driven by market-stimulating policies such as feed-in tariffs (FiT), as well as ease of building integration and low maintenance (IRENA 2017a; Kavlak, McNerney, and Trancik 2018). The progressive reduction of FiTs and the increase in electricity prices have called for maximizing PV self-consumption, i.e., maximizing self-consumption of auto-produced PV electricity. As a result, batteries are increasingly being coupled to residential PV systems. The cost of batteries has also decreased by 65% since 2010 (IRENA 2017a), with dedicated incentives in several locations (CPUC 2017).

Factors such as system size, location, electricity tariff structure, applications performed by the battery (also called services), PV generation and battery degradation

impact the profitability of PV-coupled batteries. Most of these factors have already been addressed in the literature (Weniger, Tjaden, and Quaschning 2014; Luthander, Widén, Munkhammar, et al. 2016; Pena-Bello, Burer, et al. 2017; Truong et al. 2016; Hesse, Martins, et al. 2017; Magnor and Sauer 2016). Overall, there is still a large variation in the value which a battery can offer to consumers, across regions (Barbour and González 2018). This variation can be partly explained by the household's electricity load profile (Schopfer, Tiefenbeck, and Staake 2018), but this factor has received rather limited attention so far, in particular for batteries combining applications. Only for PV self-consumption, several authors have studied the impact of the household's load profiles. For example, Linssen et al. concluded that the profile has a significant impact on the optimal PV-coupled battery configuration after comparing three synthetic load profiles, different in terms of relation between peak and base load and load fluctuations, that were scaled to a single annual electricity consumption (Linssen, Stenzel, and Fleer 2017). Schopfer et al. also highlighted that load profile is a key predictor of self-sufficiency and PV self-consumption ratios according to the different machine learning models, and therefore key for taking PV-coupled battery investment decisions (Schopfer, Tiefenbeck, and Staake 2018).

In the same way that the balance between PV generation and electricity demand influences self-consumption, it should influence the value of a PV-coupled battery performing other applications beyond PV self-consumption. However, earlier research on batteries performing multiple applications at the household level has not explored this yet. The review of O'Shaughnessy et al. found that apart from the total amount of electricity demand, the household's electricity load profiles determine the susceptibility to incentives for demand load shifting (using control of deferrable loads) but this review addresses exclusively studies with PV electricity as the sole input to the battery (O'Shaughnessy et al. 2018a). Among the literature focusing on the combination of applications, Ratnam et al. assessed the benefit of demand load-shifting for several households in Australia (Ratnam, Weller, and Kellett 2015). They found that in most of the cases, but not in all, batteries performing demand load-shifting help to reduce the electricity bill.

Against this background, the present paper aims to contribute to an improved understanding of the impact of electricity load profile on PV-coupled batteries combining applications. To do so, we optimize the schedule of battery operation depending on considered applications, thereby including PV self-consumption, demand load-shifting, demand peak-shaving and avoidance of PV curtailment, depending on the tariff structure. We focus on the impact of the load profile, annual consumption and combination of applications in two regions with very different climates, load profiles and electricity consumption, namely, Geneva (Switzerland) and Austin (US). We use a sizing ratio of 1:1:1 (e.g., an annual electricity consumption of 5 MWh leads to a nominal PV capacity of 5 kWp and a battery capacity of 5 kWh) which is commonly found in the literature (e.g., Litjens, Worrell, and van Sark (2018b) and Weniger, Tjaden, and Quaschning (2014)).

The paper is structured as follows. The materials and methods are presented in Section 3.2 which describes the input data, the system configuration, electricity tariff design as well as the optimization setup and the techno-economic indicators. Section 3.3 gives the clustering and optimization results as a function of the combination of applications, clusters and location. Section 3.4 presents a discussion of the implications of our results and finally, Section 3.5 presents the main conclusions.

3.2 Materials and methods

3.2.1 Demand data

Two datasets of measured electricity demand from 305 dwellings in Austin (U.S., from the Pecan Street project) and 636 in Geneva (Switzerland) are used in this study, both with a temporal resolution of 15-minute throughout the year 2015. This temporal resolution provides a reasonable compromise between modeling technology performance and computational speed (Beck et al. 2016). Figure 3.1 presents a normalized histogram (it shows the proportion of cases that fall into each of several categories, with the sum of the heights equaling 1) of the electricity demand data from Austin and Geneva. Households in Austin have a median electricity consumption of 10.4 MWh p.a. (within a range of 2.9-23.9 MWh p.a.), while households in Geneva have a median electricity consumption of 2.5 MWh p.a. (within a range of 0.2-7.4 MWh p.a. In terms of average yearly electricity consumption the American households use 4.2 times more electricity than Swiss households from the datasets.

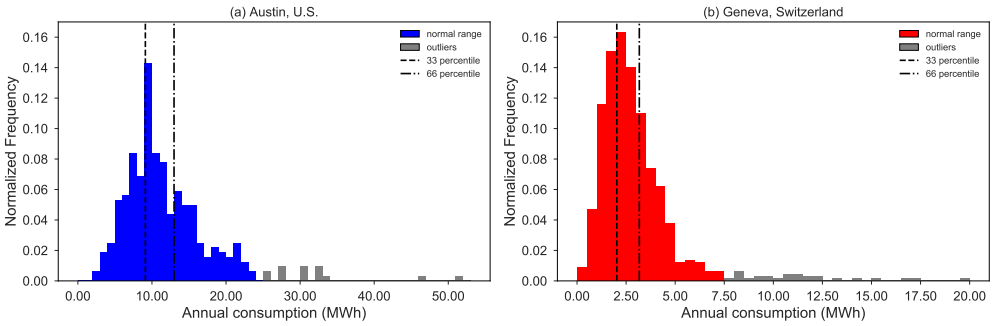

Figure 3.1: Normalized distributions of annual household electricity consumption for our data from (a) Austin, U.S. and (b) Geneva, Switzerland. Note that the scale of the horizontal axis differs for Geneva and Austin

3.2.2 Load profile clustering

To generate representative consumer groups, we employ a clustering method. A range of clustering methods has been employed to form consumer segments in the previous literature (for a review of the clustering techniques applied to electricity load data see Chicco (2012)). The k-means clustering method is one of the most widely used due to its versatility and applicability to large datasets (Kwac, Flora, and Rajagopal 2014; Xu, Barbour, and González 2017; Benítez et al. 2014; Al-Wakeel, J. Wu, and N. Jenkins 2017). Furthermore, it is important to normalize the smart meter data to identify time series with equivalent consumption patterns, instead of identical annual consumption (Tureczek, Nielsen, and Madsen 2018; Yilmaz, Chambers, and Patel 2019). While this approach is successful for forming groups of load profiles with similar shapes independent of consumption magnitudes, in this work we also need to study the effect of differing levels of overall consumption. Additionally, averaging the data suppresses the diversity of the electricity use patterns within the individual household. Therefore, it is important to find a robust analysis to identify clusters that explain the daily load profiles. Figure 3.2 shows the methodology used in this study to cluster and characterise the households in Geneva and Austin separately depending on the load patterns they exhibit, divided into four steps: segmentation by consumption level, normalization, clustering daily profiles and household classification.

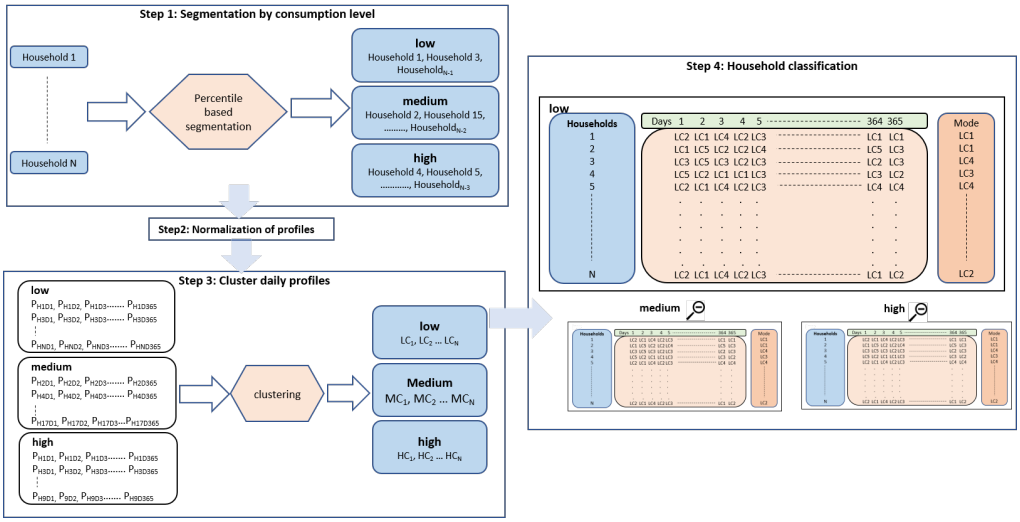

Figure 3.2: Methodological approach to electricity load profile characterisation through k-means clustering: Steps 1, 2, 3 and 4 are described.

Table 3.1: Consumption brackets per location

Consumption bracket	Austin [kWh p.a.]	Geneva [kWh p.a.]
Low	[2900,9052]	[150, 2025]
Medium	[9052, 12365]	[2025,3170]
High	[12365,24000]	[3170,7400]

Step 1 (segmentation by consumption levels): We first compare the distributions of annual consumption across both locations and form groups with similar consumption levels. Figure 3.1 shows that there are several non-representative consumers with abnormally high annual consumption which are excluded from the analysis. In particular, an annual consumption above 7500 kWh and 25000 kWh is considered as an outlier in Switzerland and Texas respectively. We then split the remaining consumers into three separate groups - a low annual consumption group (0th-33rd percentile), a medium annual consumption group (34th-66th percentile) and a high annual consumption group in both locations (67th-100th percentile). Table 3.1 shows the boundaries of the categorization of yearly consumption levels for both Geneva and Austin.

Step 2 (normalization): We normalize the electricity load profiles in each sub-group (low, medium and high) in order to cluster the load profiles of the daily curves as described by Eq. 3.1.

$$e_c(t) = \frac{l_c(t)}{\sum_{t=1}^{24} l_c(t)} \tag{3.1}$$

$e_c(t)$ is the normalized load at time t and $l_c(t)$ is the load of consumer c at time t before normalization.

Step 3 (clustering of daily profiles): We then cluster each daily profile within each sub-category of consumption levels (i.e., low, medium, high) as shown in Figure 3.2, where P_{HNDM} represents the daily profile of the household N at the

day M. For example, if there are 50 households within the low consumption bracket in Geneva, the total number of profiles used for clustering corresponds to 18250 (equivalent to 50 households x 365 days).

For clustering the normalized load profiles, we use the feature-based clustering, since it improves cluster quality relative to using raw profile data (Yilmaz, Chambers, and Patel 2019; Räsänen and Kolehmainen 2009). The principle of this approach is to extract few features to explain the shape of the load profile, thereby reducing the dimensionality of the time series (originally 15-minute data points) to avoid "curse of dimensionality", which refers to the fact that many algorithms become intractable when the input is high-dimensional (Bellman 2015). Here, we focus on three key periods to analyze PV-coupled battery systems. First, we divide the daily profiles into three time periods based on the value of the mean load profile throughout the day: night-time (12 am-10 am), daytime (10 am-6 pm) and evening time (6 pm-12 am). It is important to note that cluster outcomes do not change if the periods are shifted by ±1 h based on the work of Yilmaz, Chambers, and Patel (2019) and Haben, Singleton, and Grindrod (2015). The average values of the normalized profiles are calculated for each period, and they constitute the first three features to be included in the cluster analysis. The fourth feature corresponds to the mean standard deviation over the three periods, expressing variability in electricity demand throughout the day. By using the k-means clustering method, we randomly assign an initial set of centroids, and then move them in iterations to minimize the objective function given in Eq. 3.2, which allows to identify the clusters. Here, j indexes the clusters from 1 to K and i indexes the load profiles assigned to the cluster j, where n_j is the total number of shapes in the cluster j. $e_{i,j}$ is the i-th load profile assigned to the cluster j and ζ_j is the centroid of the cluster j. Therefore, the Euclidean distance metric between centroids and the normalized load profiles (J) is minimized. Finally, f is the feature index.

$$J = \sum_{j=1}^{K} \sum_{i=1}^{n_j} \sqrt{\sum_{f=1}^{f=4} (e_{i,j}(f) - \zeta_j(f))^2} \tag{3.2}$$

The silhouette score (s) presented by Rousseeuw (1987), defined in Eq. 3.3, is used to determine the optimal value for the number of clusters (k), where a is the average intra-cluster distance, and b is the average shortest distance to another cluster. Consequently, the silhouette score has a range of [-1, 1], where a score close to +1 indicates a better performance of the clustering algorithm. The algorithm that produces clusters with low intra-cluster distances (i.e., high intra-cluster similarity) and high inter-cluster distances (i.e., low inter-cluster similarity) has a high silhouette score. The k with the highest silhouette score corresponds to the optimum number of clusters for each consumption group.

$$s = \frac{b - a}{max(a, b)} \tag{3.3}$$

Step 4 (household classification): We then list the cluster IDs that each household exhibit on a particular day for the whole year. As households use electricity differently on a daily basis, there are multiple cluster IDs over a period. We, therefore, used the statistical mode of the cluster outcome to determine the most common cluster ID for each household throughout the year, and classify that household with the corresponding ID.

3.2.3 PV generation

Outdoor temperature and horizontal solar irradiance monitored in both locations for the year 2017 are used to model PV generation. Hourly solar irradiation and temperature data from Austin, Texas was obtained from the National Solar Radiation Database provided by NREL (`https://nsrdb.nrel.gov/`, accessed the 20.07.2020), as for Geneva, the data was collected by the UNIGE (`http://www.cuepe.ch/html/meteo/archives-numeriques.html`, accessed the 20.07.2020). We simulate PV generation using a standard one-diode model (Parra, Walker, and Gillott 2014) and PV technology with a nominal efficiency of 18.6% (*HIT photovoltaic module HIT-N2XXSE10 datasheet* n.d.), representative of the current state. The model also includes a maximum power point tracker system, as is the case of most PV systems in order to maximize the output regardless of the environmental conditions (temperature and solar irradiance). The installed capacity of the PV system is modeled based on the annual demand of each household with 1 kWp installed per 1 MWh of annual demand (i.e., 1000 full-load hours) (Litjens, Worrell, and van Sark 2018b).

3.2.4 PV-coupled battery system

We analyze the techno-economic implications of adding a battery system to a new PV system that would otherwise be installed on its own (we hereby disregard all costs related to the PV system). We assume a DC-coupled configuration illustrated in Figure 3.3, including an integrated inverter with a buck-boost charge controller (i.e., a step-up and step-down converter combined), a maximum power point tracking system and a bi-directional inverter (required to charge a battery from the main grid). An inverter loading ratio (i.e., the ratio between the inverter rating and the PV rating, referred to as ILR) of 1.2 is considered for this study (Burger and Rüther 2006). We simulate Lithium Nickel Manganese Cobalt Oxide (NMC) batteries since this technology is currently dominating the residential market. The battery capacity is coupled to the PV system in a one-to-one ratio, i.e., 1 kWh battery capacity per 1 kWp of PV installed. Following a conservative approach, we consider relatively high installation costs for the battery and inverter, equal to 2000 USD in both countries, regardless their nominal capacity (Baumann and Baumgartner 2017). We assume that NMC batteries can use 100% of depth of discharge (DoD) (ITP Renewables 2016) and can be charged or discharged in 2.5 h (i.e., a C-rate of 0.4*C, where C is the nominal capacity of the battery). Moreover, we consider the battery to reach the end-of-life (EoL) when 30% of the nominal capacity is depleted (Pena-Bello, Barbour, Gonzalez, Patel, et al. 2019). The techno-economic values for the PV-coupled battery system used in this study are displayed in Table 3.2.

3.2.5 Electricity tariff design and battery applications

In this study, we consider all battery applications which help consumers to reduce their bill, namely PV self-consumption, avoidance of PV curtailment, demand load-shifting and demand peak-shaving, except for back-up power. Back-up power is excluded since we focus on distribution areas with a high level of grid stability. These consumer applications can be described as follows (see also Parra and Patel (2019)): PV self-consumption, the predominant application for residential batteries, uses the battery to store PV surplus electricity for later consumption. Avoidance of PV-curtailment applies where grid regulators seek to maintain grid stability through feed-in limitations, prohibiting injection of PV power into the grid above a threshold

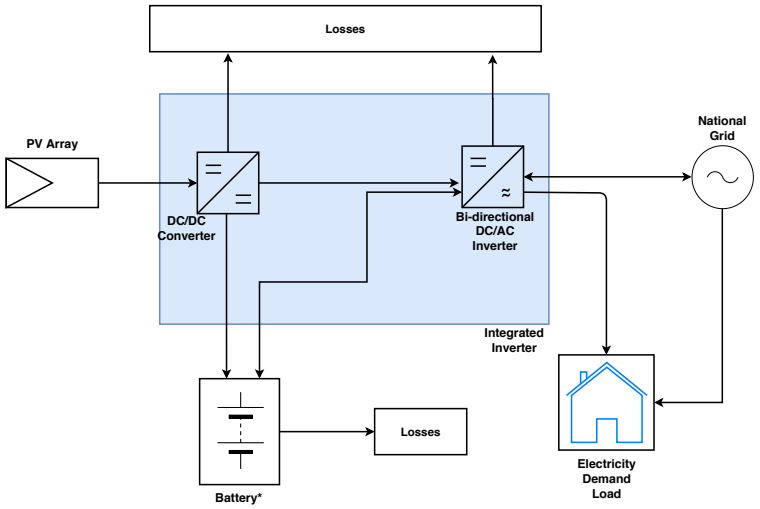

Figure 3.3: DC-coupled PV-battery system with integrated inverter used in this study. Arrows indicate the direction of possible energy flows between the individual components.

Table 3.2: Values selected for the technical and economic assessment of PV-coupled battery systems. The cycle aging factor is given for a 100% depth-of-discharge.

Component	Units	Value	Reference
Charge controller efficiency	%	98	Energy 2017
Inverter efficiency	%	94	Energy 2017
Bi-directional inverter cost	USD/kW	600	Ardani et al. 2017
Bi-directional inverter lifetime	years	15	Fu et al. 2017
Balance of plant cost	USD/kW	100	Pena-Bello, Burer, et al. 2017
Installation costs	USD	2000	Baumann and Baumgartner 2017
O&M	USD/kW	0	Tesla 2015
Discount factor	% p.a.	4	Stephan et al. 2016
End of life (EoL)	%	70	Käbitz et al. 2013
ILR	p.u.	1.2	Burger and Rüther 2006
Cycles at a given depth of discharge	-	5000 @ 100%	Tesla 2015
Battery lifetime	Years	15	Tesla 2015
Battery roundtrip efficiency	%	91.8	Tesla 2015
Battery Energy costs	USD/nominal kWh	410	Tesla 2015
Maximum charge/discharge rate	kW	0.4*C	Tesla 2015
ΔSOC	%	100	ITP Renewables 2016
Maximum SOC	%	100	ITP Renewables 2016
Minimum SOC	%	0	ITP Renewables 2016
Cycle aging factor	per cycle	0.00042	Based on Truong et al. 2016
Calendar aging factor	per day	0.00038	Based on Truong et al. 2016

level. The PV excess is stored in the battery and can be used at a later time, thereby allowing to increase the share of renewable energy used. Demand load-shifting uses the battery to exploit varying tariff differentials, shifting electricity consumption to times with low price. Finally, demand peak-shaving uses energy stored in the battery to reduce the maximum power drained from the grid (in kW) in order to mitigate demand electricity peaks. These various applications are enabled by different retail electricity tariff structures.

Demand-peak-shaving is performed if, in addition to a a volumetric component (USD/kWh), the retail tariff also includes a capacity-based tariff (USD/kW) to bill the peak demand. Capacity tariffs are being widely suggested following the penetration of air conditioning, heat pumps and electric vehicles (AEMC 2014). In order to ensure that the tariffs are on average revenue neutral for all the households evaluated (i.e., the utility company does not charge more money for the same service and the consumer bill remains in a similar range), the per-kWh rates are reduced by 20% and 30% in Geneva and Austin respectively, whenever the capacity-based tariff is assumed. Additionally, currently where capacity tariffs are in place (typically for higher voltage consumers) volumetric charges are lower.

For the volumetric component, we also compare a flat tariff, for which the battery only performs PV self-consumption, and a double tariff (also referred to as a Time-of-use tariff), for which demand load-shifting is also performed. Based on the current offer from local utilities, the double tariff is applied throughout the year in Geneva, but only in summer-time in Austin. Finally, a (physical) feed-in limit of 50% of the PV nominal capacity (i.e., a user cannot inject PV electric power beyond 50% of its PV rated power into the grid) is assumed in order to prevent instability on the power system, which is a main concern during periods with large PV production periods, following the example of Germany (Hesse, Martins, et al. 2017). This allows a PV-coupled battery to get some value by avoiding PV curtailment.

Based on the sharp decline of FiT across many countries, the PV export price is assumed to correspond to the wholesale electricity price, as is the case for traditional electricity generators. Wholesale electricity prices from the day-ahead market for Texas (from ERCOT southern load zone, average price of 0.027 USD/kWh) and Switzerland (from EPEXSPOT, average price of 0.047 USD/kWh) are used. Table 3.3 displays the values of the electricity tariff used in this study. It is important to highlight that electricity bills include also other fixed costs, such as taxes and grid usage.

3.2.6 Optimization of the battery schedule

The management problem of a PV-coupled battery system is solved using the open-source model presented in Pena-Bello, Barbour, Gonzalez, Patel, et al. (2019), which relies on Pyomo, an open-source tool for modeling optimization applications in Python (Hart et al. 2012) and is solved with CPLEX. The battery schedule is optimized on a daily basis (i.e., 24 h optimization framework, with a resolution of 15-minute) and we assume perfect day-ahead forecast of the electricity load profile, solar PV generation and wholesale prices in order to determine the maximum economic potential regardless of the forecast strategy used. Aging of the battery was treated as an exogenous parameter, calculated on a daily basis, and therefore not subject to optimization (for further information see Pena-Bello, Barbour, Gonzalez, Patel, et al. (2019)).

The objective function, Eq. 3.4, minimizes the costs C incurred by the house-

Table 3.3: Electricity tariff components depending on the bill structure used in this study. The peak time in Geneva occurs from 7:00 to 22:00 on weekdays and from 17:00 to 22:00 for the weekends, whereas it is from 13:00 to 19:00 for the weekends between June and September in Austin. The PV export price corresponds to the wholesale price, with the given value corresponding to the average wholesale price.

Name		Units	U.S.	Switzerland	Based on
Flat Tariff		USD/kWh	0.07	0.22	Energy
Double Tariff	On-peak	USD/kWh	0.18	0.24	Energy
	Off-peak	USD/kWh	0.06	0.15	Energy
Export price		USD/kWh	0.03	0.05	Energy
capacity-based tariff		USD/kW/month	10.14	9.39	Power
Feed-in limit		$\%kW_{p-PV}$	50%	50%	Power

holds, thereby considering two components, namely the energy and power components of the electricity bill. The energy component is composed of the costs of electricity imports and the reward for the electricity exports. The power component relates to the maximum power used by the household. Here, i is the time of the day, E_{grid} is the energy drained from the grid, $E_{PV-grid}$ is the energy exported to the grid, π_{import_i} is the import price, π_{export_i} is the export price, $P_{max-day}$ is the maximum power at each day, $\pi_{capacity}$ is the capacity price (USD/kW/day) and PS is a Boolean parameter to activate the power-based factor of the bill when necessary.

$$C = min(\overbrace{\sum_{i=0}^{t}(E_{grid_i} \cdot \pi_{import_i} - E_{PV-grid_i} \cdot \pi_{export_i})}^{\text{Energy-based tariff}} + \underbrace{(P_{max-day} \cdot \pi_{capacity} \cdot PS)}_{\text{Power-based tariff}}) \tag{3.4}$$

For further information on the constraints, parameters and validation of the model please see (Pena-Bello, Barbour, Gonzalez, Patel, et al. 2019). The model and the U.S. data (the Swiss data is confidential) are publicly available in `https://github.com/alefunxo/Basopra` (Accessed on 20.07.2020).

Every optimization is run for one year and then the results are linearly extrapolated to cover the PV's entire lifetime (i.e., 30 years). We assume 30% of capacity depletion as the battery's end-of-life (Parra, Norman, et al. 2016) and assume replacements of inverter and battery, in the case that the (replacement) battery lifetime exceeds the project lifetime, the residual value of the battery is considered using straight-line depreciation (Moore et al. 2015). We take a conservative approach maintaining the same battery cost for the future (discounted to the present), due to the high uncertainty linked to future battery costs. The analysis is conducted with identical electricity prices for all years across battery lifetime.

3.2.7 Techno-economic indicators

We use three indicators to compare the impact of the household's load profile on the attractiveness of the PV-coupled battery systems. As technical indicators, we use (i)

the PV self-consumption (SC), which is the share of on-site generation that is auto-consumed (Eq. 3.5), which is the most relevant indicator for prosumers who pursue autarky. Although in this study all the applications provided by the battery deliver power exclusively to the household, it is noteworthy to mention that in the case that the battery is used to provide electricity to the grid for additional applications (e.g., frequency control), this energy should not be accounted for self-consumption. (ii) The maximum peak flow shaved (PS) in the electricity exchange with the grid (Eq. 3.6), taking into account both import and export power flow, is a very relevant for distribution grid planning. In addition, we use (iii) the Net Present Value (NPV) to quantify the battery investment attractiveness, which is relevant for prosumers from a financial point of view (see Eqs. 3.7 and 3.8). The NPV is calculated using annual project cash flows (CF) taking into account the difference between the cash flows from a PV-coupled battery system and a system with only PV.

$$SC = \frac{\sum_{i=0}^{N} \left(E_{PV-total-demand} + E_{PV-batt-demand}\right)}{\sum_{i=0}^{N} E_{PV}} \tag{3.5}$$

$$PS = \frac{P_{grid-batt} - P_{grid-nobatt}}{P_{grid-nobatt}} \tag{3.6}$$

$$CF_{Batt_i} = CF_{PV-Batt_i} - CF_{PV_i} \tag{3.7}$$

$$NPV = \sum_{i=1}^{N} \frac{CF_{Batt_i}}{(1+r)^i} - \sum_{i=0}^{N} \frac{CAPEX}{(1+r)^i} \tag{3.8}$$

In Eq. 3.5, $E_{PV-total-demand}$ is the PV generation used to meet the household demand, $E_{PV-batt-demand}$ is the energy from the PV that is charged into the battery and delivered to the household demand and E_{PV} is the total PV generation. In Eq. 3.6, $P_{grid-batt}$ is the peak flow exchanged with the grid with a battery and $P_{grid-nobatt}$ is the peak flow without a battery (i.e., only with a PV system). $CF_{PV-Batt_i}$ is the cash flow of the PV-coupled battery system, CF_{PV_i} is the cash flow of the PV system alone and CF_{Batt_i} is the cash flow due to the installation of the battery system in Eq. 3.7. Finally, $CAPEX$ represents the total capital expenditures (excluding the PV system), r is the discount factor (a weighting term that multiplies value to discount it back to the present value), i is the year and N is the lifetime of the project in Eq. 3.8.

3.3 Results

We firstly present the clustering results, then the technical results and finally, the NPV for PV-coupled systems as a function of the load profile, the electricity consumption bracket (i.e., low, medium or high electricity consumption) and the location (namely Austin and Geneva). We assess three combinations of applications. First, a baseline scenario, where PV self-consumption is analyzed individually (using a flat tariff). Secondly, PV self-consumption is combined with demand peak-shaving (using a flat tariff and a capacity-based tariff), since it is reported to be the next most attractive application for residential consumers (see Käbitz et al. (2013) and AEMC (2014)). Finally, the combination of PV self-consumption, demand peak-shaving (using a capacity-based tariff), demand load-shifting (using a Time of Use -ToU- tariff, structured according to peak and off-peak times of day) and avoidance

Table 3.4: Cluster nomenclature by consumption bracket and location. The assignation of every household depends on the statistical mode of the cluster outcome to determine the most common cluster ID throughout the year.

Consumption bracket	Geneva		Austin	
	Cluster id	Number of households (%)	Cluster id	Number of households (%)
Low	LC1	177 (27.8%)	LC1	14 (4.6%)
	LC2	43 (6.8%)	LC2	86 (28.2%)
Medium	MC1	14 (2.2%)	MC1	24 (7.9%)
	MC2	63 (9.9%)	MC2	16 (5.2%)
	MC3	57 (9.0%)	MC3	60 (19.7%)
	MC4	86 (13.5%)	-	-
High	HC1	54 (8.5%)	HC1	16 (5.2%)
	HC2	71 (11.2%)	HC2	26 (8.5%)
	HC3	71 (11.2%)	HC3	63 (20.7%)

of PV curtailment (using a physical feed-in limit). To highlight the statistically significant differences across the results, a Shapiro-Wilk test is used to prove non-normality of the results, followed by a paired Wilcoxon test with Holm procedure to control the family-wise error rate. We report the p-values that indicate the probability of obtaining test results at least as extreme as the results actually observed, assuming that the null hypothesis is correct.

3.3.1 Clustering results

Table 3.4 presents the distribution of cluster IDs (i.e., the statistical mode of daily profiles) for each consumption level and location, including number and percentage of households. Figure 3.4 shows the cluster centroids for daily electricity load profiles with their average silhouette score for each sub-group and location. In Geneva two clusters with similar shape are present across the three consumption brackets, one with a high peak in the evening and one that is mostly flat. In Austin, there are as well two similar clusters across the three consumption brackets with one high peak around 16 h, the second one presents a high peak around 20 h. The optimal number of clusters k for each approach was determined based on the highest silhouette score. The silhouette analysis, displayed in Figure 3.5, shows the optimum number of clusters for each combination of location and consumption bracket: k=2 for Texas-low; k=3 for Texas-medium; k=3 for Texas-high; and k=2 for Geneva-low; k=4 for Geneva-medium; k=3 for Geneva-high).). The silhouette scores improve as more aggregation/averaging of profiles is applied, with the best scores resulting from aggregating each day across all households and the worst scores for the approach without aggregation (here in this paper we cluster one profile per household per day hence silhouette scores are slightly lower than those published in literature for average profiles).

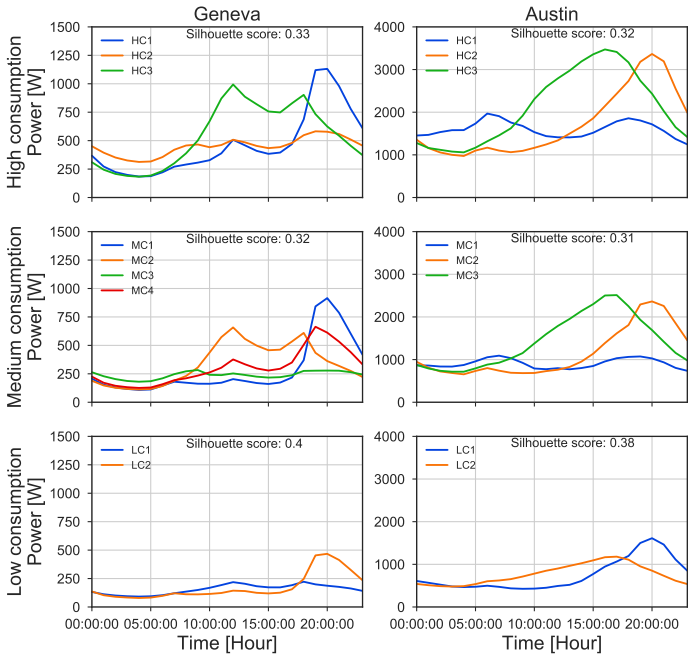

Figure 3.4: Centroids of the various clusters found for daily electricity profiles with their average silhouette score for each sub-group and location. Note that the scale of the vertical axis differs for Geneva and Austin.

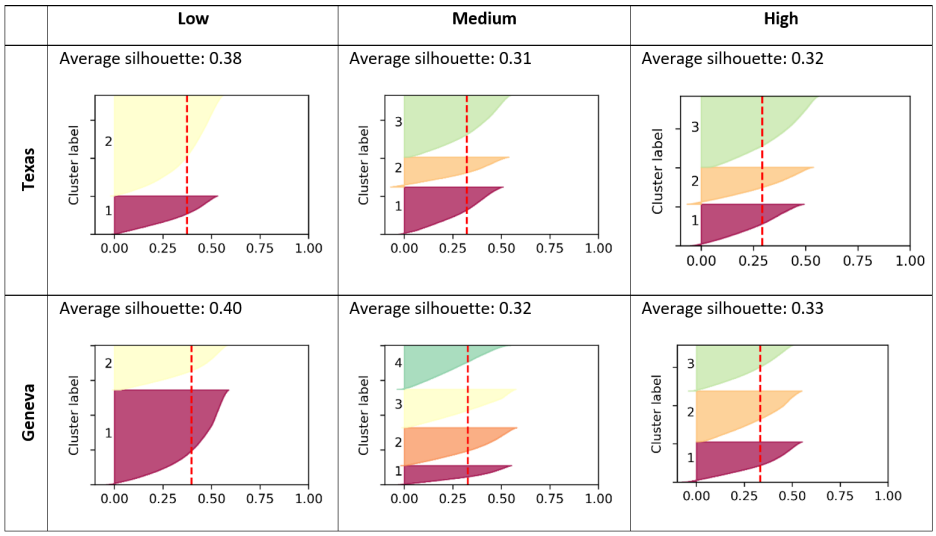

Figure 3.5: Silhouette analysis for k-means clustering using the daily profile features (optimum number of clusters, k=2 for Texas low ; k=3 for Texas-medium; k=3 for Texas-high and k=2 for Geneva low ; k=4 for Geneva-medium; k=3 for Geneva-high).

3.3.2 PV Self-consumption

The increase of PV self-consumption share due to addition of a battery to the PV system ranges between 14-22% in Austin and 6-24% in Geneva, with median values of 19% and 18%, respectively as shown in Figure 3.6 a. Regarding the combination of applications, there is a slight reduction (2.6%) of the total PV self-consumption in the households in Austin when other applications are performed together with PV self-consumption (p-value<0.05). However, this is not the case for the households in Geneva, which may suggest that there is no competition among applications as is the case in Austin.

Regardless the combination of applications, the PV self-consumption increases with electricity consumption in both countries (p-value<0.05). However, this increase is small, with median differences between the low and high consumption brackets of only 2% and 3% for Austin and Geneva, respectively (see Figure 3.6 b). The load profile influences PV self-consumption (p-value<0.05) and it can differ by up to 5% (e.g., LC1 vs. LC2 in Austin, see Figure 3.6 c), while it is more limited when comparing households with a peak during daytime (dashed boxplots in Figure 3.6 c and d, e.g., MC2 and HC3 in Geneva) with those without a daytime peak, with maximum median differences of 4% and 2.5% for Austin and Geneva, respectively. Overall, the addition of a battery significantly increases the self-consumption, especially for households with a peak during daytime; the low penalty related to combining all applications suggests that it is a smart strategy to follow.

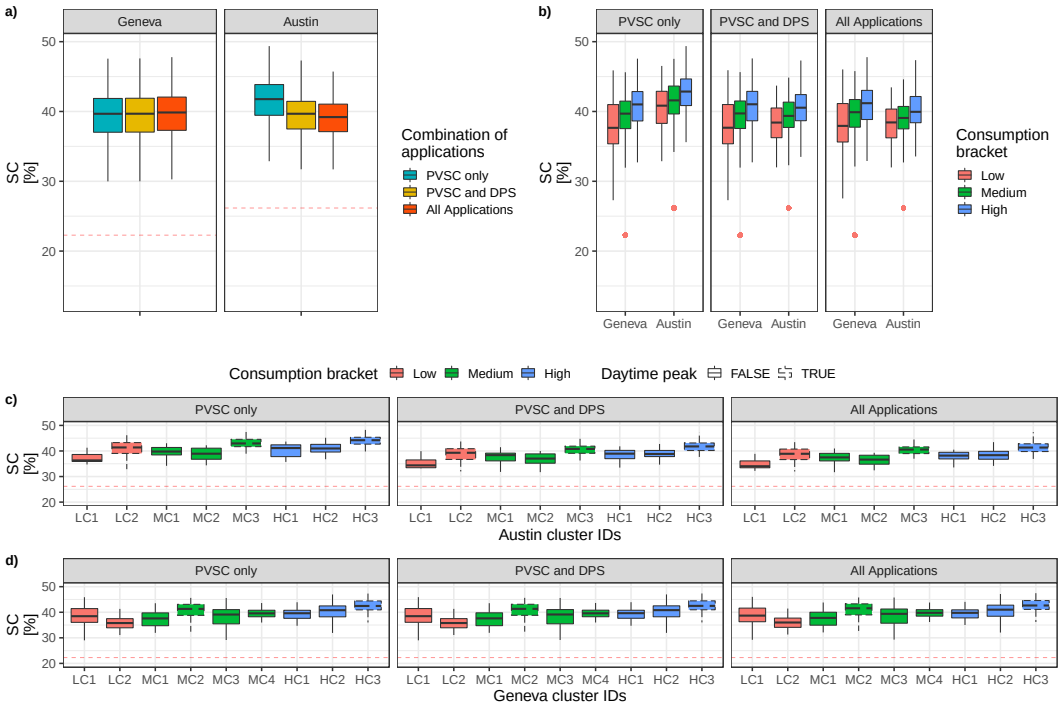

Figure 3.6: PV self-consumption (SC) of PV-coupled batteries. a) Comparing the impact of the combination of applications per country; b) Comparing the consumption bracket impact per country and per combination of applications; c) Comparing the impact of the load profile (cluster) per consumption bracket and per combination of applications for Austin and; d) Comparing the impact of the load profile (cluster) per consumption bracket and per combination of applications for Geneva. Dashed boxplots represent households with peaks during daytime (i.e., from 10 am to 6 pm). The number of observation per cluster is indicated on top of the boxplots. The red dashed lines and red points represent the median SC of the same PV system without battery support. PVSC stands for PV self-consumption and DPS for demand peak-shaving.

3.3.3 Peak-shaving

Figure 3.7 shows the results of peak flow reduction in absolute terms for PV-coupled battery systems, for the three combination of applications we analyze. In the case of PV self-consumption only, there is not incentives to reduce the peak (i.e., no capacity-based tariff) and therefore, the peak in some cases can be even higher than the case where PV systems are installed without a battery (i.e., 0 kW of peak shaved). The combination of PV self-consumption and demand peak-shaving reduces the median peak flow by 1.9 kW and 1.1 kW in Austin and Geneva, respectively, when compared to the cases where the battery is used exclusively for PV self-consumption (see Figure 3.7 a, p-values$<$0.05). Additionally, when demand load-shifting (allowance to charge from the grid) and avoidance of PV curtailment are included on top of the above mentioned applications (i.e., when all applications are combined), the median peak flow is reduced further by 1.5 kW in Austin and 0.1 kW in Geneva, compared to the PV self-consumption and demand peak-shaving combination (p-values$<$0.05). In total, peak flow reduction by up to 3.4 kW and 1.2 kW can be achieved in Austin and Geneva, respectively, which compared to the median value of the maximum power demand across both datasets (7.9 kW and 3.8 kW), represents a substantial reduction of peak flow.

The peak flow reduction when there are incentives to reduce it, is moderately affected by the annual consumption of the household (see Figure 3.7 b). For instance, the median values of the peak flow are reduced more in households with high electricity consumption than in households with low electricity consumption when all applications are combined; for high electricity consumption households, it is reduced by up to 5.1 kW in Austin and up to 1.6 kW in Geneva, whereas the maximum reduction for low electricity consumption households amounts to 2.5 kW and 0.6 kW in Austin and Geneva, respectively.

The impact of the load profile on the peak flow reduction achieved by batteries in Austin is in general not statistically significant. The only case where there is a statistically significant difference is when all applications are combined (i.e., right panel in Figure 3.7 c), and the median values between households with peaks in the evening (HC2) and with a peak during daytime (HC3) are compared, with a median difference of 2.2 kW. For Geneva (Figure 3.7 d), when PV self-consumption is combined with demand peak-shaving, the peak flow reduction in households with medium annual demand and a flat load profile (MC3) is slightly lower (0.1 kW of difference, p-value$<$0.05) than in households with a demand peak during daytime (MC2) or with double demand peak (one during the day and one in the evening, MC4). Similarly, in houses with high annual electricity demand, the differences between the households with a flat load profile (HC2) and other households is small in power terms (0.3 kW, p-value$<$0.05). When all applications are combined, the differences between the households presenting a flat load profile and those with a peak in the evening (HC1) are no longer statistically different. The absence of statistically significant differences among the different clusters (but within consumption brackets) suggest a low impact of the load profile on the peak flow.

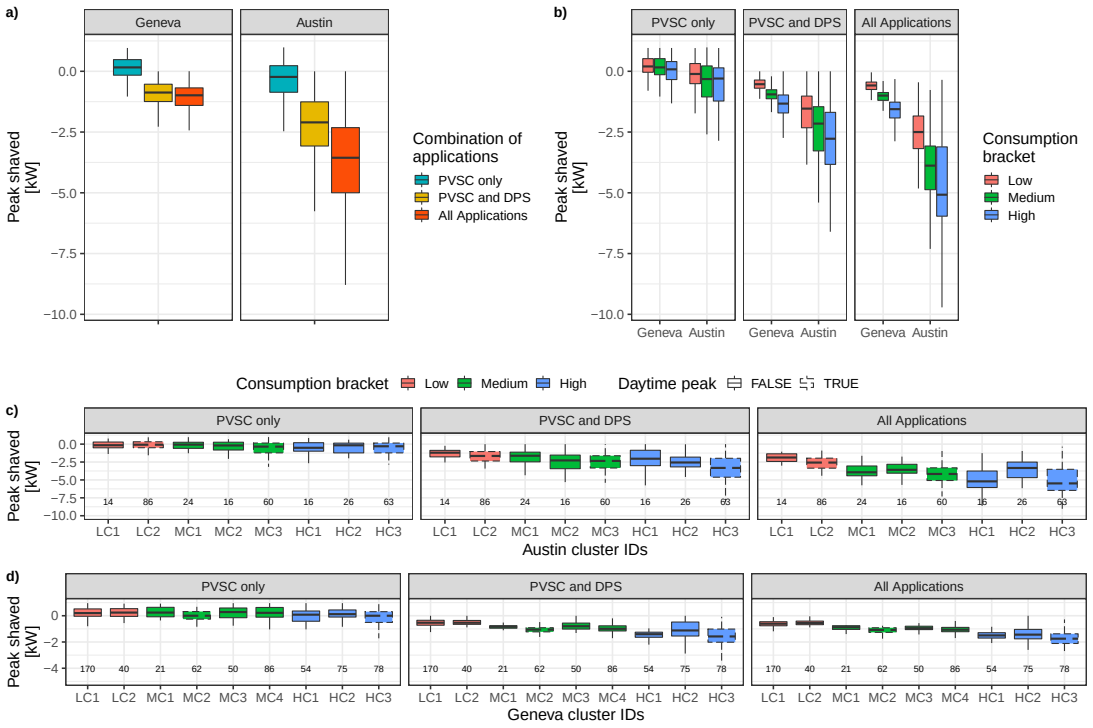

Figure 3.7: Peak flow shaved by PV-coupled batteries. a) Comparing the impact of the combination of applications per country; b) Comparing the consumption bracket impact per country and per combination of applications; c) Comparing the impact of the load profile (cluster) per consumption bracket and per combination of applications for Austin and; d) Comparing the impact of the load profile (cluster) per consumption bracket and per combination of applications for Geneva. Dashed boxplots represent households with peaks during daytime (i.e., from 10 am to 6 pm). The number of observation per cluster is indicated on top of the boxplots. PVSC stands for PV self-consumption and DPS for demand peak-shaving.

3.3.4 NPV

Figure 3.8 shows that NPVs remain negative (i.e., no profitability) in by far most cases. To put the results into perspective, the NPVs can be compared to the total investment costs of the battery system (i.e., including inverter, balance of plant, installation costs and replacements to match the PV lifetime of 30 years): In Austin, in average households lose 0.83 USD per dollar invested in a battery, while in Geneva, households lose 0.67 USD per dollar invested. However, the combination of two or more applications helps batteries to improve the economic case in both locations (see Figure 3.8 a).

The NPV is negatively affected by and strongly dependent on the annual electricity consumption as shown in Figure 3.8 b. The differences of the median NPV among the three consumption brackets are as high as 9200 USD in Austin, decreasing to 1400 USD in Geneva, being statistically significant in both cases (p-values$<$0.05). Interestingly, the combination of all applications in Geneva is able reverse the negative influence of the annual electricity consumption that can be seen when PV self-consumption is the only application (see Figure 3.8 b, right panel).

In Austin, the differences within consumption bracket and across the clusters are not statistically significant (see Figure 3.8 c). On the other hand, batteries performing PV self-consumption only in the households with medium annual consumption in Geneva (i.e., in the range of 2025-3170 kWh) with a peak in the evening (MC1) offer higher NPV (up to 230 USD, i.e., 5%) (p-values$<$0.05). Batteries in households with flat load profiles (LC1, MC3 and HC2), generally achieve lower NPV (differ-

ences up to 250 USD, i.e., 6%), in particular when PV self-consumption is combined with other applications. Finally, the combination of applications increases the economic viability of the batteries up to 8400 USD in Austin and 2250 USD in Geneva (p-values<0.05).

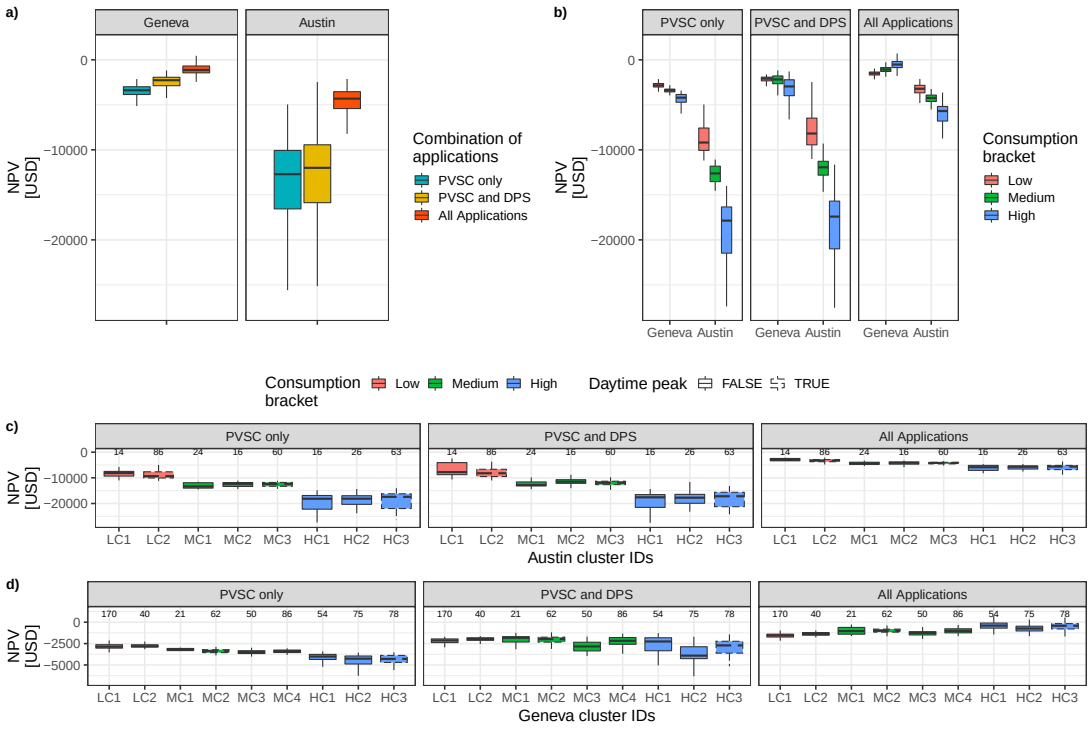

Figure 3.8: NPV achieved by PV-coupled batteries. a) Comparing the impact of the combination of applications per country; b) Comparing the consumption bracket impact per country and per combination of applications; c) Comparing the impact of the load profile (cluster) per consumption bracket and per combination of applications for Austin and; d) Comparing the impact of the load profile (cluster) per consumption bracket and per combination of applications for Geneva. All values presented in this graph refer only to the investment in the battery, i.e., the cost of the PV panel is excluded. Dashed boxplots represent households with peaks during daytime (i.e., from 10 am to 6 pm). The number of observation per cluster is indicated on top of the boxplots. PVSC stands for PV self-consumption and DPS for demand peak-shaving.

3.4 Discussion

Our results highlight the interest on the combination of applications (also called services) at the residential level and the impact of the household electricity consumption on the economic viability of installing a battery in an otherwise stand-alone PV system. They show as well the limited impact of the load profile on the performance and economic attractiveness of PV-coupled battery systems. The results of this study are based on a 1:1:1 sizing ratio (e.g., an annual electricity consumption of 5 MWh leads to a nominal PV capacity of 5 kWp and a battery capacity of 5 kWh) (Litjens, Worrell, and van Sark 2018b; Weniger, Tjaden, and Quaschning 2014).

3.4.1 Impact of combination of applications

Overall, batteries significantly increase self-consumption (ranging from 6-24%). According to our results, the combination of applications does not compromise total PV self-consumption shares or only hardly does so. We find that there are not

statistically significant differences in Geneva for batteries combining applications with respect to the case of batteries performing PV self-consumption only, and in Austin we find a limited decrease of total PV self-consumption (2.6%). In turn, peak-shaving is positively affected by the combination of applications when PV self-consumption is combined with demand peak-shaving (by up to around 20%). Interestingly, charging the battery from the grid contributes to reduce the peak flow with the grid by an additional 1.5 kW in Austin and a more modest 0.1 kW in Geneva, when compared to the combination of PV self-consumption and demand peak-shaving. The combination of applications boosts the economic attractiveness of batteries, with increases by up to 8500 USD and 2250 USD in Austin and Geneva, respectively. Combining applications leads to some positive NPV (up to 1342 USD) in households with high electricity consumption in Geneva, reversing in this way the negative impact of annual electricity consumption observed in all the other cases. Additionally, battery applications such as demand peak-shaving and avoidance of PV curtailment provide indirect benefits to the grid operation and stability that are not captured in the NPV indicator but cannot be neglected.

A rule-of-thumb such as the 1:1:1 ratio is not reasonable for today's households with large annual consumption (e.g., Austin households) and in particular if the battery is used only for PV self-consumption. Instead, batteries should be able to combine applications to justify their large capacity and the related investment, which call for a faster deployment of policies in this direction around the globe. Further applications not included in this study should be considered, such as frequency control (e.g., within a pool of batteries controlled by a centralized organization). In households with more modest annual consumption, e.g., Swiss and other European households, the above-mentioned ratio together with the combination of applications can lead to positive economic cases, even with the current high costs of batteries (350 USD/kWh and 2000 USD for the installation). We find as well that the exclusive use of the batteries for PV self-consumption is currently not profitable without subsidies. The combination of applications and in particular the use of demand peak-shaving (enabled by a capacity-based tariff) not only helps to reduce the stress on the grid but helps as well to improve battery profitability for all household types, regardless the consumption bracket or the load profile.

3.4.2 Impact of electricity annual consumption and load profile

Under the sizing ratio of 1:1:1, the impact of the annual electricity demand on total PV self-consumption is small, but statistically significant (i.e., 2% in Austin and 3% in Geneva). This is also the case for the maximum peak flow exchanged with the main grid (i.e., accounting for import and export power), since higher annual electricity consumption leads to higher battery sizes and higher reductions of the peak (compared to the peak without the PV-coupled battery system) of 2.6 kW (1 kW) in Austin (Geneva). Additionally, the impact of annual consumption on profitability is remarkable, with differences in NPV larger than 9000 USD in Austin and 1400 USD in Geneva, with large consumers being negatively affected due to the installation of larger batteries (but not when all applications are combined). Thus, small (or even no) battery systems should be preferred to maximize NPV in the absence of the combination of applications, due to still high costs (Barbour and González 2018; Pena-Bello, Barbour, Gonzalez, Patel, et al. 2019). However, larger batteries will become more affordable as battery costs progressively decline,

enabling further reduction of the peak flow exchanged with the main grid.

Finally, there is a limited impact of the load profile on the performance and economic attractiveness of PV-coupled batteries combining applications. In the Swiss case, the NPVs are slightly lower in households with mostly flat load profiles compared to other load profiles (6% lower NPVs for clusters LC1, MC3 and HC2, see Figure 3.8 d). Additionally, households with load peaks at the evening (e.g., MC2 in Geneva) achieve NPVs 5% higher than when the battery is used only for PV self-consumption. On the other hand, in Austin, the load profile does not have an impact on battery profitability, which suggest that the effect of load profile differs across locations with different retail tariff values and electricity consumption thresholds.

3.4.3 Limitations and future research

Future research can apply the proposed method to analyze other locations with different electricity load profiles and retail tariff values. The grid may benefit from distributed storage in several ways, however, in this study we look at the problem from a consumer perspective. Further research regarding the potential benefits to the grid and extra remuneration mechanisms should be explored. The effect of future load profiles (e.g., by better insulation of buildings in the U.S.) could also be studied. Furthermore, alternative choices of battery sizing can be explored, which may lead to different findings. In the same way, we acknowledge that a smaller value of the DoD would lead to reduced aging, however, the amount of cycles per year would also decrease and therefore the economic benefits steaming from the battery and its economic viability. Alternative values of DoD should be investigated to precisely quantify their effects on different performance indicators. Other alternatives to physical storage such as virtual storage, as applied in some countries where the grid may be used to store PV excess and may be taken back by the prosumer within a certain period of time without charge should be explored, which may reduce the prosumer investment while maintaining similar or higher shares of self-consumption. Additionally, we suggest the use of larger datasets (the Austin dataset only includes 305 households), as is the case for Geneva (with 636 households), to increase the number of observations which helps to produce results with statistically significant differences.

3.5 Conclusions

In this study, we analyze the impact of the electricity load profile, the annual electricity consumption and the combination of applications, namely photovoltaic (PV) self-consumption, avoidance of PV curtailment, demand peak-shaving, as well as demand load-shifting (with grid-charging) for PV-coupled battery systems which are sized with a 1:1:1 ratio (e.g., an annual electricity consumption of 5 MWh leads to a nominal PV capacity of 5 kWp and a battery capacity of 5 kWh). The analysis is carried out for Austin (U.S.) and Geneva (Switzerland), which have very different climates, load profiles and electricity consumption levels. Our findings rely on tests of statistical significance using 305 and 636 electricity load profiles with 15-minute resolution monitored in Austin and Geneva.

Our results indicate that the type of load profile (established by clustering) has a limited impact on the net present value (NPV) of PV-coupled batteries in Geneva, Switzerland. For households with mostly flat profiles, the NPV is slightly lower when combining applications compared to households with other types of load

profile. Furthermore, batteries performing only PV self-consumption in households with peaks in the evening have marginally higher NPV than other households. The effect of the load profile is even less marked in Austin, Texas, U.S. where we found practically no impact on peak-shaving and NPV in Austin, while total PV self-consumption is positively affected in households with daytime peaks. In conclusion, some slight differences in the effect of the load profiles were found for the two locations indicating a relatively small influence which should be tested also for other locations. If confirmed, the value of PV-coupled battery systems is not increased by tariffs which are customized to the load profile of consumers based on our results.

Furthermore, we find that the NPV of batteries benefits most combining applications regardless of the annual electricity consumption level, load profile and location. Interestingly, the total PV self-consumption rate of PV-coupled batteries is not compromised by the inclusion of other applications beyond PV self-consumption. This finding confirms that batteries should be used for multiple applications, which in turn needs regulatory changes. For instance, the inclusion of capacity-based tariffs sends a signal to reduce peak demand. This offers synergies for consumers who increase the value of their batteries and distribution system operators who reduce grid stress. This conclusion is important for the economic viability of batteries, which are crucial to support further decentralized PV penetration.

Chapter 4

Household level - Thermal and Electrochemical storage

Heat pumps play an important role in decarbonizing the heating supply of buildings and they allow to increase the self-consumption of PV electricity, especially when supported by electricity or heat storage. In this study, we develop an open-source model to optimize PV-coupled heat pump systems with and without electricity and heat storage and we compare their performance for three types of single-family houses with different thermal envelope quality paired with 549 electricity profiles. We analyze trade-offs between prosumer benefits and grid impacts, namely bill minimization, and maximum grid relief, depending on the type of storage and incentives for grid peak reduction (i.e., a capacity-based tariff). We conclude that the use of heat storage reduces the levelized cost of meeting the electricity demand between 13-26%, in particular when heat pumps are used for both space heating and domestic hot water (DHW). Regarding total self-consumption rates, both storage technologies, namely batteries and hot water tanks (which supply both space heating and DHW) achieve similar rates between (30-39%). In contrast, batteries are found to be very effective in reducing the peak demand (14-17% compared to the baseline scenario), but only if the retail tariff has a capacity-based component. Interestingly, the quality of the envelope plays a key role and heat pumps can double the power peak demand in poorly insulated houses, with thermal storage increasing the power peak demand further up to 8%, compared to the baseline, regardless of the storage technology. Thus, we conclude that thermal retrofitting of the building stock is advisable to avoid the upgrading of the distribution grid.

4.1 Introduction

Heat supply is dominated by fossil fuels and in 2019, only 11% of the heat was supplied by renewable energy sources worldwide (IEA 2020). This fossil dependency is equivalent to a contribution of 40% to global CO2 emissions (equal to 13.3 gigatonnes) in the same year. In Switzerland, space heating demand needs to be significantly reduced as it represents more than two thirds of the total final energy demand in the built environment (Streicher, Padey, Parra, Bürer, S. Schneider, et al. 2019). Energy retrofitting programs together with heat pumps are crucial elements of the Swiss Energy Strategy 2050. Heat pumps operate with much higher efficiency, referred to as coefficient of performance (COP), than condensing boilers or furnaces, allowing to reduce the energy consumption in buildings by 15-70% (Staffell

et al. 2012). The Swiss Federal Office of Energy anticipates that the number of heat pumps sold per year will double by 2030, reaching 40.000 units p.a. (Dott, Ackerman, et al. 2019). However, most heat pumps are installed in new buildings while the retrofit rate in existing buildings is very low (less than 1% per year (Castelazzi et al. 2019)) representing the main challenge for heat pump diffusion.

Solar photovoltaics (PV), which so far has mainly be used to decarbonize electricity supply, can be key to further decarbonize heat (IEA 2020; Rinaldi et al. 2020). PV modularity and cost-reduction empower consumers that can now generate their own electricity, becoming prosumers, thereby directly contributing towards the energy transition. However, the expansion of decentralized rooftop PV systems poses a challenge to the power sector. Unlike conventional centralized generation, PV production cannot be supplied on demand without incurring into additional costs and devices. Moreover, for high distributed PV penetration levels, grid operators may be forced to use rapid and expensive ramp-up of centralized power to match the demand (this is referred to as the duck-curve problem (Barbour and González 2018)), to shut-down baseload plants and/or to curtail PV electricity to avoid voltage issues at the low and medium voltage grid levels (Wang 2018; Gupta, Pena-Bello, et al. 2021; Sichilalu and Xia 2015).

In order to supply PV electricity on demand and minimize grid impacts, there are a number of flexibility strategies that allow to increase PV self-consumption (Lund et al. 2015; Salpakari and Lund 2016). In this article, we focus on demand-side management with heat pumps supported with electricity (batteries) and heat (hot water tanks) storage. Heat pumps can increase PV self-consumption and simultaneously decarbonize space heating and domestic hot water (DHW) supply, which so far mainly relies on fossil fuels (IEA 2019). When using local PV generation, heat pumps can perform with high COP values (i.e., above 3) due to relatively high ambient temperature at midday. Regarding storage, in addition to shift PV generation, storage can also be used to exploit time-varying electricity prices, charging at low prices and discharging at high prices (prices in USD/kWh_{el}), referred to as demand load shifting (DLS) (Parra, Walker, and Gillott 2016; Luthander, Widén, Munkhammar, et al. 2016). Furthermore, storage can be used to perform demand peak-shaving (DPS), which consists of discharging for a short period of time, e.g., 15 min, to reduce the maximum power exchanged with the grid (in kW terms). DPS requires that the retail tariffs include a capacity-based component (USD/kW_{el}) in addition to the volumetric component (USD/kWh_{el})(Campana et al. 2021; Pena-Bello, Barbour, Gonzalez, Yilmaz, et al. 2020).

Considering the high interest in both PV self-consumption and heat decarbonization, we focus on PV-coupled heat pumps assisted with electricity and heat storage to meet both electricity and heat demand in single houses. This is an important topic because the diffusion of PV and heat pumps is crucial for the energy transition but influences the nationwide electricity peak demand, distribution grid stability, and electricity infrastructure upgrade cost (Heymann et al. 2019). Thus, in this study we aim to combine three storage applications for electric and heat storage, namely, PV self-consumption, DLS and DPS.

Low carbon technologies such as PV, heat pumps, batteries and hot water tanks have been a focal topic of the previous literature, however, control strategies of all the above-mentioned technologies combined in smart houses has been rather limited. When analyzing control strategies for heat pump integration, a smart response to prices was considered (Patteeuw, Henze, and Helsen 2016; Verhelst et al. 2012; Sweetnam et al. 2019). Studies focusing on PV-coupled heat pumps give

priority to the increase of PV self-consumption (Franco and Fantozzi 2016; Thygesen and Karlsson 2013; Prada et al. 2017), and combinations of applications have been hardly considered, except for PV self-consumption and demand peak-shaving (Williams, Binder, and Kelm 2012). However, these studies did not consider the added flexibility of electricity or heat storage.

Only very few studies addressing heat pumps have so far analyzed combinations of applications using energy storage. Liu et al., evaluated time-of-Use (ToU) tariffs but only assessed the impact of heat pumps on the battery schedule (X. Liu et al. 2019). They recommended to conduct a whole-system analysis to maximize PV self-consumption while reducing battery capacity, which is achieved by directly using more PV electricity in the heat pump. Terlouw et al. (2019) also considered ToU tariffs when comparing electricity and heat storage to minimize the electricity bill and CO_2 emissions at the individual household and community levels . Large hot water tanks shared by the community and small individual batteries help to minimize the bill for communities and individual houses respectively. Another recent study by Pimm et al. found that coupling heat pumps and small batteries can help to keep the peak flow at the same levels as before installation of the heat pump (Pimm, Cockerill, and Taylor 2018). However, the authors did not consider economic aspects of the systems nor economic incentives for peak demand reduction.

Since the space heating demand of a residential building largely depends on its insulation, some authors have compared different reference buildings (Tjaden, Schnorr, et al. 2015) and assessed underfloor heating and radiators (Schuetz, Gwerder, et al. 2017). However, PV-coupled heat pumps assisted with electricity and heat storage and their trade-offs for prosumers and distribution grids, in terms of PV self-consumption and demand peak-shaving, have not yet been studied as a function of the envelope quality.

To our knowledge, this is the first paper proposing a method to evaluate PV-coupled heat pump systems, and to compare their lifetime performance when assisted with electricity and heat storage, both individually and combined, for houses with different envelope quality. The proposed open-source model optimizes the energy storage, and heat pump operation for a whole year and the results are then scaled over a time period of 30 years (i.e., PV lifetime). Importantly, we analyze the trade-offs between prosumer benefits, and the impacts on the grid, using three types of houses with different thermal insulation, coupled with 549 electricity profiles which allows us to provide robust results backed by statistical tests. Our open-source model is applied to houses in Geneva, Switzerland, however, it can be adjusted to locations with temperate climate and fast diffusion of PV and heat pumps. We conclude that the quality of the envelope plays a key role and that the use of a heat pump can result in doubling the power peak demand in poorly insulated houses even when storage is present.

The remainder of this paper is structured as follows. The Input data and methods are presented in Section 4.2 which describes the input data, the system configuration, as well as the optimization setup and the techno-economic indicators. Section 4.3 presents the optimization results as a function of the system configuration, building type and electricity tariff. Section 4.4 is a discussion of the implications of our results and finally, Section 4.5 presents the main conclusions.

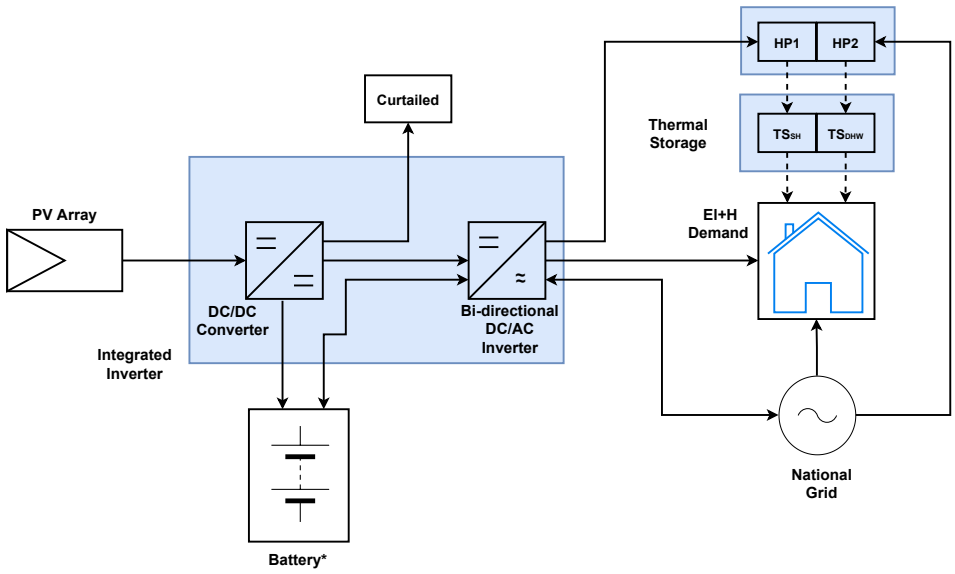

Figure 4.1: Schematic representation of a PV-coupled heat pump system supported by electricity and/or heat storage used in this study. The arrows indicate the direction of possible electricity and heat flows between the individual components. The supply of domestic hot water (DHW) and space heat (SH) is modelled with two different heat pumps (HP) whereas, in reality a single heat pump is used. TS stands for thermal storage.

4.2 Material and methods

First, we define the input data for the model in Section 4.2.1, including various types of houses, electricity and heat demand data, as well as the PV generation and the electricity tariff structure. Secondly, the optimization is described in detail in Section 4.2.2, as well as the PV-coupled heat pump configurations including storage. Finally, we present the techno-economic performance indicators in Section 4.2.4. Figure 4.1 is a schematic representation of a PV-coupled heat pump as considered in this study. We use data from 2017 across this study.

4.2.1 Input data

Thermal characteristics of the houses

Based on the reference framework for buildings and space heating simulations of the International Energy Agency (Dott, Haller, et al. 2013), we compare PV-coupled heat pump systems in three archetypical single-family houses (SFH) with identical living area (a two story SFH with 140 m^2 of heated floor area) but different heat demand, corresponding to 15, 45 and 100 kWh_{th} $/m^2$ p.a., referred to as SFH15, SFH45 and SFH100 respectively. These values represent a very well insulated recent building (i.e., Minergie-P in Switzerland or Passivhaus in Germany), a modern building from 2000-2010 (i.e., with a jagood thermal insulation of the building envelop) and a renovated old building (before 1980) or equivalently, a building from around 1980-1990 (i.e., poorly insulated) respectively (Streicher, Padey, Parra, Bürer, S. Schneider, et al. 2019). The SFH15 and SFH45 are assumed to have underfloor heating running at up to 35°C, which serves as heat storage directly coupled to the heating system. As for the SFH100, modern low-temperature radiators operated at around 50°C are assumed (Dott, Haller, et al. 2013; Arteconi, Hewitt, and Polonara 2013; Vivian et al. 2020), i.e., without storage capacity. Space heat demand and DHW demand are presented in Section B.1.

Electricity, heat demand and PV generation

In order to model the mismatch between PV generation and total electricity demand (including the consumption from appliances and the heat pump), we use data of 549 houses with 15-minute temporal resolution monitored in SFH in Western Switzerland (Pena-Bello, Barbour, Gonzalez, Patel, et al. 2019). Since only electricity consumption was monitored, we link each electricity profile to SFH15, SFH45 and SFH100 heat demands, in order to analyze all possible combinations of electricity and heat consumption, thereby considering that electricity and heat demand are not directly correlated (if the heating system is not electric).

The space heating and DHW demands for the three types of houses are calculated using a calibrated dynamic simulation tool (Schuetz, Scoccia, et al. 2018). The simulation tool calculates the dynamics of the building and energy system by solving the coupled differential equations of the individual components using a Runge-Kutta integrator. The DHW draft profile is calculated using the DHWcalc tool (Jordan and Vajen 2001) simulating the draft profile of a family with two adults and two children. The simulation framework is implemented in C++ with Visual Studio Community 2017 from Microsoft and the coupled differential equations models are solved in a program implemented using the same programming language. Further information can be found in Section B.1 and in Schuetz, Scoccia, et al. (2018).

We simulate PV generation using a standard one-diode model (Villalva, Gazoli, and Ruppert Filho 2009; Y. Zhang et al. 2017) and PV technology with a nominal efficiency of 18.6% (*HIT photovoltaic module HIT-N2XXSE10 datasheet* n.d.), representative of the current technology state. A sky model is used to transform satellite data of horizontal solar irradiance into irradiance with a tilt angle of 30° and facing south, which corresponds to the PV system orientation (Duffie and Beckman 2013). Outdoor temperature was collected locally in Geneva by the University of Geneva (Ineichen 2013). The model also includes a maximum power point tracker system, as is the case of most PV systems to maximize the output regardless of the environmental conditions (temperature and solar irradiance). Finally, we consider PV systems with a nominal capacity equal to the median size of the empirical PV distribution across Switzerland, corresponding to 4.8 kWp (BFE 2018). The capacity factor of the modelled PV system is 16.1%, which is in line with other results for the same location (e.g., 15.7% in renewables.ninja for 2019) (Pfenninger and Staffell 2016).

Electricity tariffs

Electricity prices used in this study are based on available tariffs offered by the local utility company in Geneva. We consider a ToU tariff, normally offered for heat pumps. The export PV price is assumed to be equal to the wholesale electricity price (based on the prices from the day-ahead European Power Exchange) as is the case for traditional electricity generators.

Importantly, we also test the impact of adding a capacity-based tariff (also referred to as demand charges) to today's tariff which is typically only volumetric. A capacity-based tariff (in USD/kW_{el}) represents a charge that is proportional to the maximum peak power, considering import from and export to the grid. To reduce the grid impacts of PV, heat pumps and electric vehicles and enabled by the deployment of smart meters, capacity-based tariffs are already being tested in some countries, e.g., France, Belgium, Austria and Sweden (Oualmakran et al. 2017; Azarova et al. 2018). In this study, a capacity-based tariff is modelled as 9.39 $USD/kW_{el}/month$,

Table 4.1: Electricity tariff components depending on the bill structure used in this study. The peak time occurs from 7 a.m. to 10 p.m. on weekdays and from 5 p.m. to 10 p.m. on weekends. The export value corresponds to the wholesale price in the EPEXSPOT market. The price shown corresponds to the average wholesale price.

Name		Units	Geneva	Based on
ToU tariff	On-peak	USD/kWh_{el}	0.259	Energy
	Off-peak	USD/kWh_{el}	0.165	Energy
Export price		USD/kWh_{el}	0.047	Energy
Capacity-based tariff		$USD/kW_{el}/month$	9.39	Power

while ensuring that the original overall electricity bill remains unchanged. This is achieved after reducing the volumetric component of the double tariff by 20%. Table 4.1 provides all the relevant tariff data depending on the bill structure.

4.2.2 Optimization modeling

We propose a daily schedule optimization (starting at midnight) of the PV-coupled heat pump system (see Figure 4.1). Every optimization was run for one year and then the results are scaled over a time period of 30 years, corresponding to the lifetime of the PV system (Bauer et al. 2017). We consider replacements for all the components of the system (see Section B.5 for more information). The open-source Linear Programming model developed by Pena-Bello, Barbour, Gonzalez, Patel, et al. (2019) is extended in this study to couple heating with heat pumps in combination with heat storage and electricity storage. We model eight PV-coupled heat pump systems with and without thermal and electricity storage (see subsection *System configurations*) using the open-source programming language Python. To formulate the optimization problem, we use the Pyomo package (Hart et al. 2012), a Python-based optimization modeling language and to solve the scheduling optimization problem we use CPLEX, an optimization software package developed by IBM. The model can be found in github `https://github.com/alefunxo/BASOPRA_HP`. Perfect forecast is assumed for electricity and heat demand, PV generation and wholesale prices in order to determine the maximum economic potential regardless of the chosen forecast strategy. The objective function is the minimization of the electricity bill which also includes a power-based component if a capacity-based is included, as is indicated in Eq. 4.1.

$$C = min(\overbrace{\sum_{i=0}^{t}(E_{grid_i} \cdot \pi_{import_i} - E_{PV-grid_i} \cdot \pi_{export_i})}^{\text{Energy-based tariff}} + (\underbrace{P_{max-day} \cdot \pi_{capacity} \cdot PS}_{\text{Power-based tariff}})) \tag{4.1}$$

Here, the energy-based tariff is given by E_{grid_i} $[kWh_{el}]$ which is the electricity drawn from the grid; π_{import_i} is the import price (i.e., retail price, in USD/$[kWh_{el}]$); $E_{PV-grid_i}$ $[kWh_{el}$ $]$ is the PV-electricity exported to the grid; and π_{export_i} is the export price (in USD/$[kWh_{el}]$, assumed to be the wholesale price in this study).

All these variables have the sub-index i representing every time step (corresponding to 15-minute) from 0 up to 96 per day (represented by t). The capacity-based tariff is given by $P_{max-day}$ [kW], which is the maximum power required from the grid throughout the day; $\pi_{capacity}$ is the capacity-based tariff (in USD/kW_{el}/day); and PS is a boolean variable which indicates the presence of the capacity-based tariff (to enable demand peak-shaving). The objective function is subject to various technical and energy system-related constraints which are presented hereafter. The model validation can be found in Section B.6.

Heat pump modeling

We model a bivalent heat pump system, comprising an air to water heat pump and an electric backup heater connected in series to meet all heating requirements when the heat pump cannot meet them due, for instance, to under-sizing or to extremely low temperatures. The characteristics of the heating system as a function of the type of house are presented in Table 4.2. The sizing of the heat pump as well as the specification of the supply and return temperatures follow the methodology presented by the IEA (Dott, Haller, et al. 2013) and are presented in the Table B.3.

From a modeling perspective, the heat pump is virtually split into two parts which separately provide space heat and DHW. By analogy with real heat pumps, the two virtual parts cannot work at the same time and operate at different outlet temperatures. Eqs. 2-5 describe the heat pump constraints. The constraint of electricity demand is shown in Eq. 4.2, where E_{hp_i} is the electricity required by the heat pump, while E_{PV-hp_i} [kWh_{el}], $E_{batt-hp_i}$ [kWh_{el}] and $E_{grid-hp_i}$ [kWh_{el}] are the PV electricity supplied to the heat pump, the battery and the grid, respectively.

$$E_{hp_i} = E_{PV-hp_i} + E_{batt-hp_i} + E_{grid-hp_i} \tag{4.2}$$

The thermal power of the heat pump (P_{hp_i}, in kW_{th}) (to meet the demand load or store heat) must be lower or equal to the maximum thermal power output ($P_{hp-max-th_i}$ [kW_{th}]) at each time step (Eq. 4.3)

$$P_{hp_i} \leq P_{hp-max-th_i} \tag{4.3}$$

Eq. 4.4 defines the relationship between the electricity supply and heat generation, where E_{bu_i} [kWh_{el}] is the electricity consumption of the backup heater; $\dot{Q}_{hp-hs_i}$ [kWh_{th}] and $\dot{Q}_{hp-sh_i}$ [kWh_{th}] are the heat provided by the heat pump to the heat storage and directly to the space heating load, respectively. The COP, defined as the relationship between the heat flow (kW_{th}) provided by the heat pump, and its electrical power consumption (kW_{el}) (the COP is therefore dimensionless), is calculated at each time-step as a function of the outdoor temperature and the supply temperature using a lookup table from a recognized heat pump manufacturer (see Section B.3 (Hoval 2017; Gwerder and Schuetz 2019)).

$$E_{hp_i} \cdot COP_i + E_{bu_i} = \begin{cases} \dot{Q}_{hp-hs_i} & if \quad heat \quad storage \\ \dot{Q}_{hp-sh_i} & otherwise \end{cases} \tag{4.4}$$

Thermal mass and inertia of buildings can be substantial, e.g., allowing to keep the indoor temperature at comfort level for up to 6 hr out of 24 hr (Berger and Worlitschek 2018; Vivian et al. 2020). Thus, there is a delay between the thermal supply and demand as a function of outdoor temperature and thermal resistance (Berger and Worlitschek 2018). Making use of the thermal inertia of buildings, the

heat pump does not need to be perfectly aligned to heat demand as long as the total heat supplied within two hours matches the total demand within the same period (Yao et al. 2018). Eq. 4.5 mathematically expresses the thermal inertia (or flexibility) of 2 hr (8 blocks of 2 hr represented by the sub-index j), where $\dot{Q}_{load_i}$ $[kWh_{th}]$, $\dot{Q}_{hp-sh_i}$ $[kWh_{th}]$ and $\dot{Q}_{ts-sh_i}$ $[kWh_{th}]$] are the space heating demand, the heat supplied by the heat pump for space heating and the heat supplied by the heat storage for space heating, respectively.

$$\sum_{i=8\cdot j}^{8\cdot(j+1)} \dot{Q}_{load_i} = \begin{cases} \sum_{i=8\cdot j}^{8\cdot(j+1)} \dot{Q}_{ts-sh_i} & if \quad heat \quad storage \\ \sum_{i=8\cdot j}^{8\cdot(j+1)} \dot{Q}_{hp-sh_i} & otherwise \end{cases} \tag{4.5}$$

$$where\, j \in [0,7]\, and\, i \;\in\; [0,95]$$

Modeling of heat storage

Hot water tanks for space heating and DHW are modeled as perfectly mixed with a homogeneous temperature (T_{ts} [K]). Eqs. 4.6 and 4.7 present the change of heat content in the tanks as a function of time ($\Delta\dot{Q}_{ts_i}$ $[kWh_{th}]$) depending on the heat balance determined by the inlet flow from the heat pump ($\dot{Q}_{hp-hs}$), the heat flow delivered to the demand load ($\dot{Q}_{load}$ $[kWh_{th}]$), including both space heating and DHW, and the heat losses through the surface area to the surroundings ($\dot{Q}_{ts-loss}$ $[kWh_{th}]$). The amount of thermal energy charged into the heat storage (Q_{ts_i} $[kWh_{th}]$) is given in Eq. 4.8 by the difference between the temperature of the heat storage at time i (T_{ts_i} [K]) and the supply temperature (T_{supply_i} [K]), multiplied by the mass and the specific heat of water.

$$\Delta\dot{Q}_{ts_i} = \dot{Q}_{hp-hs_i} - \dot{Q}_{ts-sh_i} - \dot{Q}_{loss-ts_i} \tag{4.6}$$

$$\Delta\dot{Q}_{ts_i} = (T_{ts_i} - T_{ts_{i-1}}) \cdot m_{ts} \cdot c_{p_{ts}} \tag{4.7}$$

$$Q_{ts_i} = (T_{ts_i} - T_{supply_i}) \cdot m_{ts} \cdot c_{p_{ts}} \tag{4.8}$$

Moreover, hot water tanks for DHW and space heating operate between minimum (T_{supply_i} [K]) and maximum ($T_{supply_i} + T_{offset}$ [K]) temperature levels and they are characterized by losses ($Q_{loss-ts_i}$ $[kWh_{th}]$), as presented in Eqs. 4.9 and 4.10. Here, U_{ts} $[kW * m^{-2} * K^{-1}$], A_{ts} $[m^{-2}]$ and ΔT_{ts_i} [K] are the heat storage's U-value, surface, and the difference of temperature (between the heat storage and the set-point temperature), respectively. The minimum temperature of the hot water tanks is constrained by the supply temperature (T_{supply} [K]; see Table 4.2). Furthermore, the maximum temperature is given by the supply temperature plus the offset temperature (i.e., ΔT [K]; see Table 4.2). It is assumed that the heat storage for space heating provides heat at the supply temperature (T_{supply} [K]), while the DHW tank, provides hot water at 50°C.

$$T_{supply_i} \leq T_{ts} \leq T_{supply_i} + T_{offset} \tag{4.9}$$

$$\dot{Q}_{ts-loss_i} = U_{ts} \cdot A_{ts} \cdot \Delta T_{ts_i} \tag{4.10}$$

For DHW, the same equations as above apply, assuming a dedicated heat pump and a water tank of 200 l, according to the standard consumption of 50 l per person and per day for a single-family house, as defined in the Swiss norm SIA 385/2

Table 4.2: Heating system characteristics depending on the building type with identical heated floor area of 140 m^2 for a two stories single-family house.

Heat Pump	SFH15	SFH45	SFH100
Required heat at the design point (kW_{th})	2.4	4.9	10.6
Supply temperature at the design point (°C)	35	35	50
Temperature difference at the design point (K)[a]	46	46	61
Generated heat demand at the design point (kW_{th})	4	4.8	9.7
HP Thermal capacity (kW_{th})	4	6	16
Working fluid	410a	410a	410a
Maximum electric demand at the design point(kW_{el})	1.7	2	6.6
Backup heater[b](kW_{th})	2	4	4
Space heating storage system	**SFH15**	**SFH45**	**SFH100**
Type of storage	Existing[c]	Existing[c]	New[d]
Specific capacity of the heat release of storage (kJ/K)	40000	40000	6300
Maximum ΔT (K)	1.5	1.5	10
Active building storage capacity based on possible temperature difference (kJ)	60000	60000	63000
Equivalent water capacity @ 10 K ΔT (l)	$\approx$ 1500	$\approx$ 1500	1500
DHW storage system	**SFH15**	**SFH45**	**SFH100**
Maximum ΔT (K)	20	20	20
Storage capacity based on temperature difference (kJ)	16800	16800	16800
Water capacity (l)	200	200	200

[a] The design point was used to size the heat pump, using IEA methodology (IEA 2019).
[b] An electric backup heater with a COP of 1 is used to meet the peak heat demand, especially when there is simultaneous DHW and space heating demands.
[c] An existing space heating storage refers to an active heat building storage, which is directly coupled to the heating system, i.e., the thermal capacity of the heating system (radiator or underfloor heating), contrary to the passive building storage which refers to the heat storage capacity of the activatable building mass (which is not considered in this study) (Gwerder and Schuetz 2019).
[d] A new storage refers to a technical storage, which is the name given to a heat storage unit that is installed in the building as an additional device (Gwerder and Schuetz 2019).

(Swiss Society of Engineers and Architects 2011). For space heating, a 1500 l hot water tank is assumed for the SFH100. As for the SFH15 and SFH45, underfloor heating allows to use the concrete of the floors and the heating water content as heat storage (i.e., existing building storage), thus, we do not consider any additional cost, since this feature is inherent to well insulated and retrofitted houses. This building storage is modeled as a tank of 1500 l with 10 K of ΔT (equivalent to a 9520 l water

tank with 1.5 K of ΔT). The cost of the hot water tank for space heating is 66 USD/kWh (with a ΔT of 10 K) while for the DHW hot water tank the cost is 132 USD/kWh (with a ΔT of 20 K) (Fischer et al. 2016). Since the optimal storage size is mainly determined by the PV size (Fischer et al. 2016), and since we pre-define the nominal PV capacity with the Swiss median for all scenarios and for all houses, no other tank sizes are considered. Furthermore, specific heat and U-values of 0.36 $W*m^{-2}*K^{-1}$ and 1.16 $Wh*l^{-1}*K^{-1}$ respectively are assumed for the tanks. The characteristics of the heat storage are shown in Table 4.2. In the cases where heat storage for space heating is not considered, a small buffer for space heating (100 l) is included regardless of the building type to ensure provision of both DHW and space heating (see Figure 4.2b and 4.2d).

Electricity storage modeling and other constraints

Electricity storage with batteries is assumed to be integrated with the PV-coupled heat pump system using a DC-coupled topology since it is more affordable and efficient than AC-coupled topologies (Ardani et al. 2017). We use a 7 kWh_{el} NMC-based battery, which is the benchmark lithium-ion technology at the moment, with a pack cost of 335 USD/kWh_{el} of nominal capacity, 5000 cycles at 93% depth-of-discharge and a round-trip efficiency of 89% (Schmidt et al. 2019). A maximum charge and discharge rates of 0.4*C are assumed (i.e., the battery can be completely charged or discharged in 2.5 hr). A bi-directional inverter is used to charge the battery from the grid and to exploit ToU tariffs and its cost is assumed to be 600 USD/kW_{el} (Ardani et al. 2017). In the cases without electricity storage, we consider a PV-inverter with a cost of 190 USD/kW_{el} (Ardani et al. 2017).

The battery model, which includes ageing, and accounts for the electricity balance, the efficiency losses in the bi-directional inverter and power constraints for the battery, as well as the characteristics of the converter and the inverter, has been derived from a previous publication and presented in Section B.4 (Pena-Bello, Barbour, Gonzalez, Patel, et al. 2019). Eq. 4.11 presents the constraint for demand peak-shaving, where P_{grid_i} [kWh_{el}] is the power drawn from or injected to the grid at any timestep and $P_{max-day}$ [USD/kWh_{el}] is the daily maximum power required from the grid. PS is the boolean flag indicating the presence of a capacity-based tariff (as in Eq. 4.1).

$$P_{grid_i} \leq P_{max-day} \quad \forall \quad i \quad if \quad PS = True \tag{4.11}$$

System configurations

Eight PV-coupled heat pump configurations are compared in this study. In the baseline scenario, electricity and heat are provided using a PV-coupled heat pump without electricity or heat storage (see Figure 4.2a). In this scenario, the existing storage of the SFH15 and SFH45 (i.e., the underfloor heating inherent to the house heating system), is disregarded to allow a direct comparison with the SFH100 (where the existing storage is very small, since it only consists of the radiators with a capacity below 100 l). In the configuration "Tank DHW" (see Figure2b), DHW is provided by the heat pump through a directly coupled tank while a small buffer for space heating is also considered (i.e., 100 l), in order to avoid the simultaneous use of the two virtual heat pumps (i.e., modeling purposes). For DHW provision without heat pumps, we assume another (non-electric) device, such as a gas boiler which is, however, not included in this analysis. In the configuration "Tank SH",

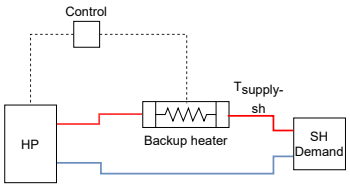

(a) No heat storage. Configuration "No storage"

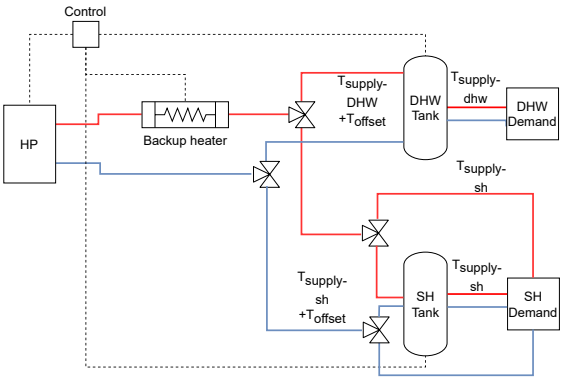

(b) heat storage for DHW (200 l) and buffer (100 l) for heat storage. Configuration "Tank DHW"

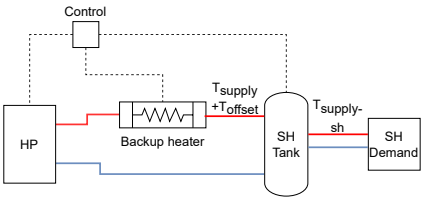

(c) heat storage for space heating (1500 l). Configuration "Tank SH"

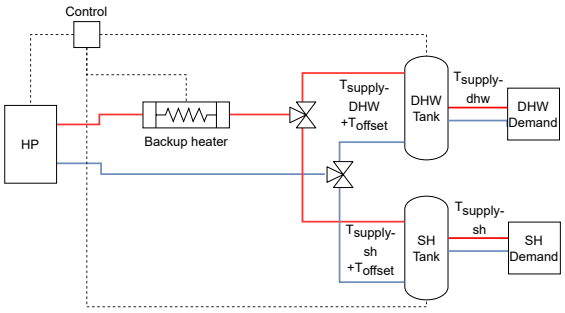

(d) heat storage for DHW (200 l) and for space heating (1500 l). Configuration "Tank SH and DHW"

Figure 4.2: A schematic representation of the four heating system configurations used in this study, regardless of the use of battery storage.

heat storage for space heating is considered; for the SFH15 and SFH45 the underfloor heating is used as storage, whereas for the SFH100 a water tank with similar capacity is assumed (equivalent to 1500 l with 10 K ΔT, see Figure 4.2c). A fourth configuration referred to as "Tank SH and DHW" includes DHW provision and heat storage for both space heating and DHW (see Figure 4.2d). Furthermore, the same configurations including a battery are considered (see Table 4.3). In all cases, the space heating demand is provided in rather conservative blocks of 2 hr (contrary to cases where higher blocks of flexibility are considered, e.g., *Yao et al.* (2018); Toradmal, Kemmler, and Thomas (2018); Schuetz, Gwerder, et al. (2017) and Waser et al. (2019)), giving an additional degree of flexibility to the system without compromising the thermal comfort. On the contrary, DHW is provided on-demand.

4.2.3 Distribution grid upgrading

The hosting capacity of distribution grids is being challenged by the addition of PV and heat pumps, together with electric vehicles. When this limit is reached, the distribution system needs to be upgraded. PV technology creates reverse power flow, potentially resulting in voltage violations and overloading of the distribution lines, while heat pumps increase the peak electricity demand (Gupta, Pena-Bello, et al. 2021). The cost of distribution grid reinforcement depends on the location, e.g., the type of urban setting, for Switzerland, a recent study finds costs between 51-213 USD/kW_p for PV additions, and between 46-1385 USD/kW for heat pumps additions by 2035 (Gupta, Pena-Bello, et al. 2021). Therefore, important investments

Table 4.3: Various PV-coupled heat pump and storage configurations assessed in this study. Note that in all cases a 4.8 kW_p PV system is included and a heat pump of 4 kW_{th}, 6 kW_{th} or 16 kW_{th} provides space heating (and in some cases DHW) for the SFH15, SFH45 and SFH100, respectively. In the cases where DHW is not provided with a heat pump, an external fuel-based boiler is assumed (outside the scope of the model presented in this study).

Configuration	DHW provision with HP	Space heating tank size (l)	DHW tank size (l)	Corresponding heating system
No storage (Baseline scenario)	No	-	-	Figure 4.2a
Tank DHW	Yes	100[a]	200	Figure 4.2b
Tank SH	No	1500[b]	-	Figure 4.2c
Tank SH and DHW	Yes	1500[b]	200	Figure 4.2d
Battery	No	-	-	Figure 4.2a
Battery and Tank DHW	Yes	100[a]	200	Figure 4.2b
Battery and Tank SH	No	1500[b]	-	Figure 4.2c
Battery, Tank SH and DHW	Yes	1500[b]	200	Figure 4.2d

[a] Values for SFH15/SFH45/SFH100 respectively.
[b] SFH15 and SFH45 use the existing building storage (underfloor heating) which is considered equivalent to this size of water reservoir with a ΔT of 10 K. SFH100 uses a tank of the stated size for space heating.

are needed into distribution grids to enable the penetration of these technologies, which could be passed on to the consumers (Horowitz et al. 2018). At high PV penetration, additional flexibility is required to supply PV electricity on demand and keep the grid stability (Horowitz et al. 2018), with energy storage being a key flexibility provider as discussed in this study.

4.2.4 Techno-economic indicators

We use four important indicators to analyze trade-offs between prosumer benefits and grid impacts for the various system configurations: levelized cost, electricity peak flow, self-consumption rate and self-sufficiency rate. The levelized cost of meeting the electricity consumption, including the various energy services of the house, namely space heating, hot water (if indicated) and all appliances, LCOE (USD/kWh_{el}). It is calculated as shown in Eq. 4.12, as the sum of the CAPEX (including replacements) and operational expenditures (OPEX) considering the lifetime of the different technologies (PV, heat pump, tanks and battery), and divided by the total electricity demand $E_{total-demand}$, which encompasses the original electricity demand for appliances and lighting plus the heat pump electricity consumption (Blok and Nieuwlaar 2016). A discount factor, r, is used to account for the time value of money, the risk associated with the project and the inflation.

$$LCOE = \frac{\sum_{i=0}^{N} \frac{CAPEX}{(1+r)^i} + \sum_{i=1}^{N} \frac{OPEX}{(1+r)^i}}{\sum_{i=1}^{N} \frac{E_{total-demand}}{(1+r)^i}} \tag{4.12}$$

The different cost of constructing the buildings (SFH15, SFH45 and SFH100) or of retrofitting them to the corresponding thermal characteristics are not considered. For prosumers, we also use as indicators the self-consumption (SC), which is the share of on-site PV generation that is used to cover the local electricity demand (including the heat pump) and self-sufficiency (SS), which is the share of local demand

(including appliances, lighting, and heat pump) that is covered by the on-site PV generation as shown in Eqs. 4.13 and 4.14.

$$SC = \frac{\sum_{i=0}^{N} (E_{PV-total-demand} + E_{PV-batt})}{\sum_{i=0}^{N} E_{PV}} \tag{4.13}$$

$$SS = \frac{\sum_{i=0}^{N} (E_{PV-total-demand} + E_{batt-load})}{\sum_{i=0}^{N} E_{total-demand}} \tag{4.14}$$

Here N refers to the system lifetime (30 y); $E_{PV-total-demand}$ is the share of PV generation that directly meets local electricity demand; $E_{PV-batt}$ is the share of PV generation that is charged into the battery; E_{PV} is the total PV generation; and $E_{batt-load}$ is the amount of electricity discharged from the battery to cover local electricity demand. We graphically visualize these two indicators in an energy matching chart, which is a type of graph that shows the matching between PV generation and demand for different types of buildings (see Figure 4.5)(Luthander, A. M. Nilsson, et al. 2019). To analyze grid impacts, we finally consider the peak power flow which is defined as the maximum between imports from and exports to the grid (Pimm, Cockerill, and Taylor 2018).

4.3 Results

We present the results in three steps as a function of the thermal characteristics of the houses. Every building type (i.e., SFH15, SFH45 and SFH100), was matched with 549 electricity profiles (i.e., a total of 1647 profiles). Then, the optimization was run throughout a full-year and the results were scaled over a time period of 30 yr corresponding to the lifetime of the PV system. First, we display boxplots comparing LCOE and peak flows per building type for each configuration with and without demand peak-shaving (i.e., with and without the inclusion of a capacity-based tariff). Secondly, we display an energy matching chart to analyze self-consumption (SC) and self-sufficiency (SS) depending on the type of storage, namely batteries and hot water tanks (with and without DHW provision). Likewise, the LCOEs and peak flows are plotted in order to get an understanding of the trade-offs between prosumer benefits and grid impacts. To highlight statistically significant differences across the results, we perform a Shapiro-Wilk test to prove non-normality of the results (Royston 1982), followed by a paired Wilcoxon test with Holm procedure to control the family-wise error rate, to determine if two or more sets of pairs are different from one another in a statistically significant manner (Hollander, Wolfe, and Chicken 2013). All tests results are presented in Section B.8. The statistical analyses were performed in R (R Core Team) (Team R Core and others 2013). We use kW_{el} and kW_{th} to refer to electricity and heat respectively.

4.3.1 LCOE

Figure 4.3 displays the levelized cost of meeting the total electricity consumption for the three building types and eight configurations. Four major observations can be made. First, the LCOE of SFH15 (which corresponds to the Swiss Minergie-P or German Passivhaus) are significantly higher ($p - values \leq 0.001$) than for SFH45 (modern building from the years 2000-2010) or SFH100 (renovated building from before 1980 or a building from 1980-1990), in particular, when DHW provision is not

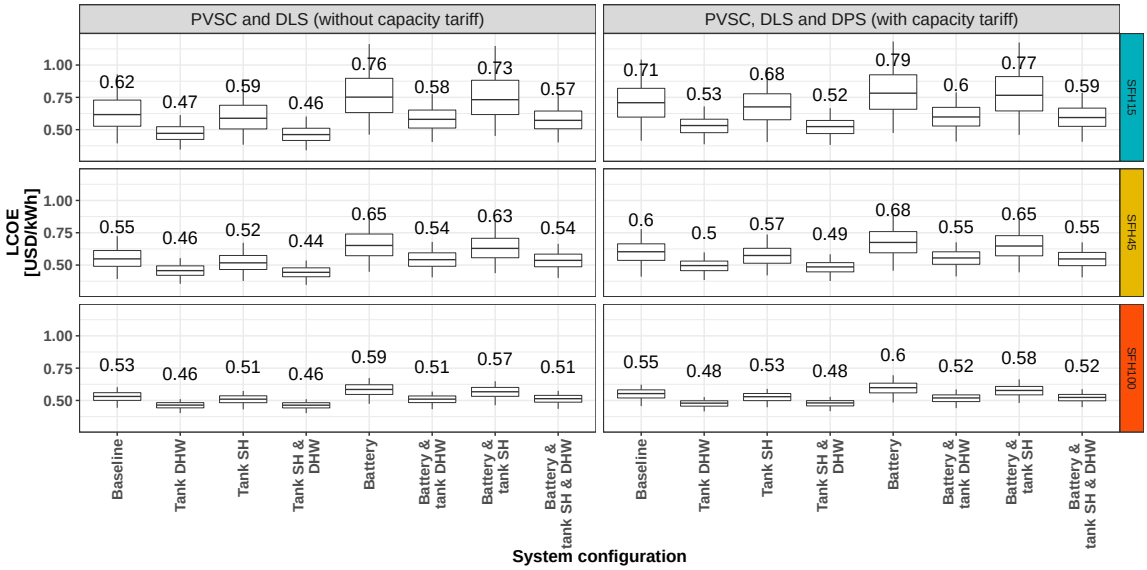

Figure 4.3: Boxplots (N=549) of the levelized cost of meeting the total electricity consumption, including space heating, hot water (if indicated) and all appliances, for all configurations depending on the combination of applications and the type of house. The line in the middle of the box and the number above the box represent the median LCOE. The box spans the first quartile to the third quartile, and the whiskers extend up to 1.5 times the interquartile range from the top or bottom of the box. PVSC stands for PV self-consumption, DLS for demand load shifting and DPS for demand peak-shaving. Note that low values of LCOE are beneficial for the consumer.

considered. For example, the difference between the median values of SFH15 and SFH100 reaches 0.17 USD/kWh_{el} for a PV-coupled heat pump connected to a battery and in the presence of a capacity-based tariff. The reason for these differences is twofold, on one hand the specific CAPEX and on the other hand, the electricity consumption of the heat pumps leads to very different electricity demand depending on the thermal envelope of the building, with medians of 8120 kWh_{el}, 3420 kWh_{el} and 2260 kWh_{el} p.a. for the SFH100, SFH45 and SFH15, respectively (see Section B.7). Secondly, DHW provision, which accounts for around 1300 kWh_{el} p.a. of heat pump electricity consumption, reduces significantly the LCOE ($p - values \leq 0.001$) regardless of the type of house. Furthermore, the better the thermal insulation of the house, the higher the impact of DHW on the LCOE. For instance, the median LCOE value is reduced by 0.05 USD/kWh_{el}, 0.11 USD/kWh_{el} and 0.17 USD/kWh_{el} for a PV-coupled heat pump system assisted with thermal storage for space heating and DHW in SFH100, SFH45 and SFH15, respectively, compared to the baseline (without storage).

Thirdly, the use of batteries significantly increases the median LCOE values by up to 0.08 USD/kWh_{el} relative to the baseline ($p - values \leq 0.001$), mainly as a consequence of the CAPEX of the battery. Finally, the inclusion of a capacity component in the retail tariff (to enable demand peak-shaving) entails a significant increase of the LCOE ($p - values \leq 0.001$) for houses with high thermal standard due to the lower impact of the volumetric component of the electricity tariff on the costs. The median increases of LCOE values due capacity-based tariffs are 0.05 USD/kWh_{el}, 0.03 USD/kWh_{el} and 0.01 USD/kWh_{el} for SFH15, SFH45 and SFH100, respectively.

4.3.2 Peak flow

Figure 4.4 displays the peak flow depending on the system configuration and the type of house. Three major observations can be made. First, the peak flow is significantly higher ($p-values \leq 0.001$) in houses with poor thermal envelope (SFH100), compared to houses with high (SFH45) and very high thermal performance (SFH15), which is a direct result of the heat pump capacity. For instance, the median of the peak flows across all configurations for SFH100 with (without) the capacity-based tariff are 9.1 kW_{el} (12.1 kW_{el}), 5.3 kW_{el} (6.5 kW_{el}) more than for SFH15.

Secondly, heat pump operation has only a rather small impact on the peak flow of SFH15 and SFH45, thanks to their envelope quality. Heat pumps only have a peak power of 1.7 kW_{el} and 2 kW_{el} respectively, which is lower than the median peak of the original demand for appliances and lighting (4.8 kW_{el}, see the case "No HP & no PV" in Figure 4.4). Furthermore, the peaks of the original demand and the heat pump are not simultaneous. In contrast, for renovated old houses (SFH100), the heat pump peak power (6.6 kW_{el}) strongly impacts the peak flow, doubling the original demand for appliances and lighting.

Figure 4.4 also shows that the impact of the type of storage depends on the thermal characteristics of the house and the presence of a capacity-based tariff. Batteries slightly reduce (increase) the peak flow by 0.8 kW_{el} (1.3 kW_{el}), depending on whether a capacity-based tariff is in place or not (this result is statistically significant, with $p-values \leq 0.001$). In poorly insulated houses, heat storage slightly reduces (increases) the peak flow by 1.2 kW_{el} (0.7 kW_{el}) depending on the capacity-based tariff. With batteries as energy storage, the peak flow of PV-coupled heat pumps varies very strongly depending on whether the electricity tariff includes or not a capacity-based tariff, decreasing by 1.2 kW_{el} and increasing by 2.6 kW_{el} respectively, regarding the base case (no storage), with differences being statistically significant, with $p-values \leq 0.001$ in both cases.

4.3.3 Graphical comparison electricity and heat storage

We compare electricity and heat storage, first in terms of self-consumption and self-sufficiency (Figure 4.5), and secondly in terms of LCOE and peak flow (Figure 4.6), assuming that a capacity-based tariff is included in the electricity tariff.

Figure 4.5 shows a limited increase in the median values of self-consumption (2-6%) and self-sufficiency (3-4%) for the inclusion of a hot water tank for space heating only (represented with a black circle, square and diamond according to the type of house) for the three types of house (despite being statistically significant, with $p-values \leq 0.001$). When a heat pump is used to provide both space heating and DHW, the increase in self-consumption is high (13-16%) and moderate for self-sufficiency 6-9%) (values are statistically significant, with $p-values \leq 0.001$). On the other hand, adding a battery to the PV-coupled heat pump system leads to important increases in self-consumption (15-16%) and self-sufficiency (11-29%), for the three types of house (statistically significant, with $p-values \leq 0.001$). Values for other configurations are shown in Section B.8, and similar patterns can be observed.

Figure 4.6 shows a graphical comparison of the LCOE and the peak flow by type of house for the different types of storage added to the PV-coupled heat pump system. The inclusion of heat storage for space heating marginally reduces the LCOE for SHF15, SFH45 and SFH100 by 0.03 USD/kWh_{el}, 0.03 USD/kWh_{el} and 0.02 USD/kWh_{el}, respectively ($p-values \leq 0.001$). More importantly, heat storage allows to maintain the peak flow at the same levels as the baseline case and even

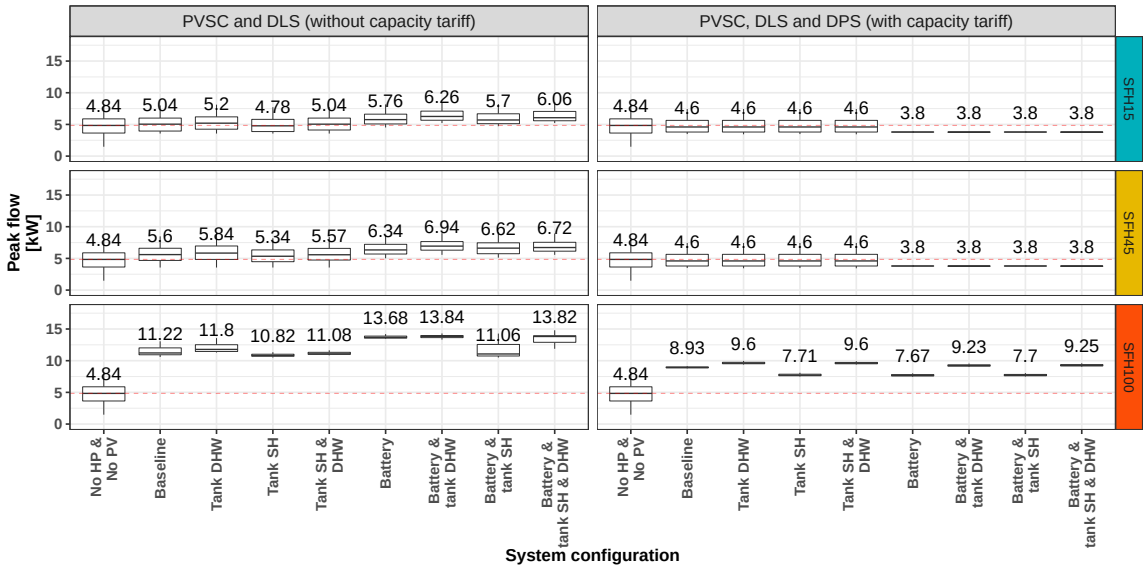

Figure 4.4: Boxplots (N=549) of the peak flow defined as the maximum peak power, considering import from and export to the grid, for all configurations depending number of storage applications (PVSC is PV self-consumption, DLS is demand load-shifting and DPS is demand peak-shaving with a capacity-based tariff) and the type of house (SFH15, SFH45 and SFH100). For comparison, the original electricity load, without PV generation or heat pump is also displayed (No HP & No PV). The line in the middle of the box and the number above the box represent the median peak flow. The box spans the first quartile to the third quartile, and the whiskers extend up to 1.5 times the interquartile range from the top or bottom of the box. The dashed red line represent the median of the classic electricity load distribution.

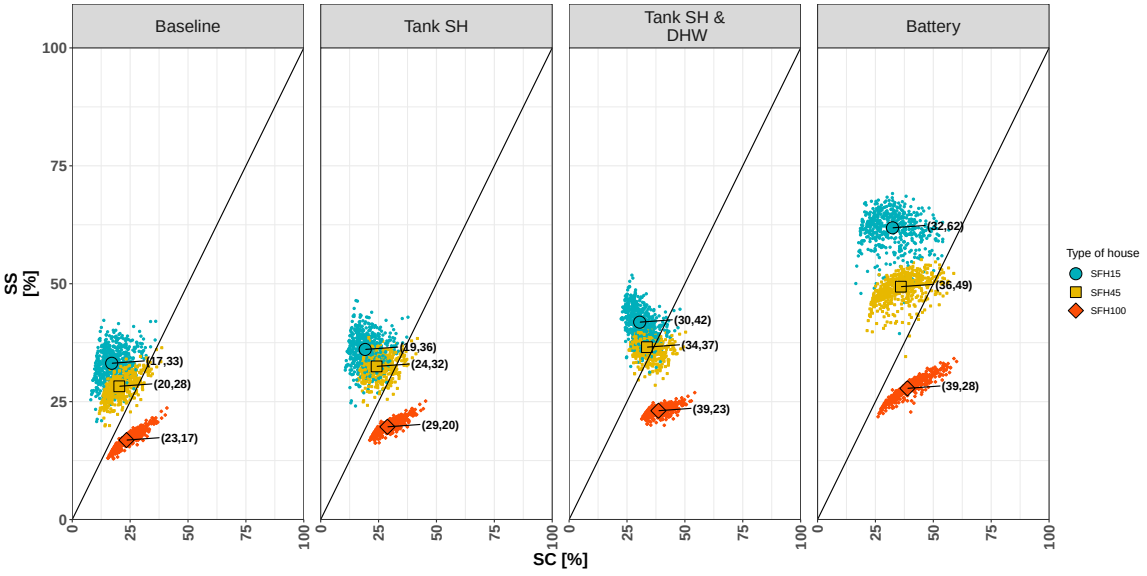

Figure 4.5: Energy matching chart to analyze self-consumption (SC) and self-sufficiency (SS) for a PV-coupled heat pump system as a function of the type of storage, namely, none (baseline case), heat storage for space heating alone, heat storage for space heating and with DHW and finally, with only a battery. The configurations presented here include a capacity-based tariff in the electricity tariff. The big black circle, square and diamond represent the median by type of house.

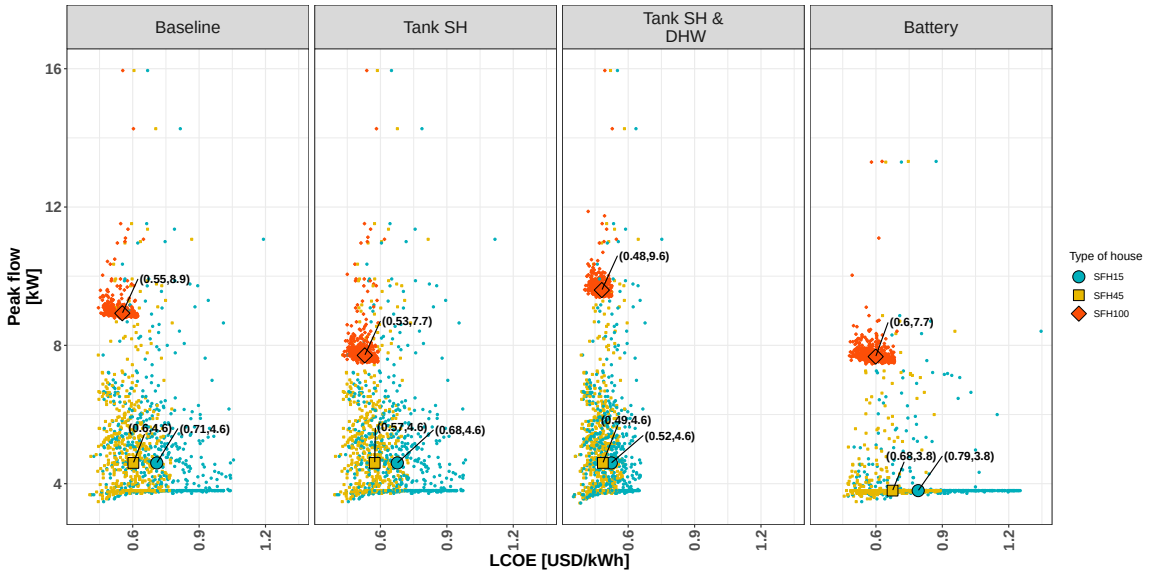

Figure 4.6: LCOE vs peak flow for a PV-coupled heat pump system as a function of the type of storage, namely, none (the baseline case), heat storage for space heating alone, heat storage for space heating and with DHW and finally, with only a battery. The configurations presented here include a capacity-based tariff in the electricity tariff. The big black circle, square and diamond represent the median by type of house.

helps to reduce it by 1.2 kW_{el} in inefficient houses (SFH100). When DHW is added as demand load, the LCOE decreases further by 0.16 USD/kWh_{el}, 0.08 USD/kWh_{el} and 0.07 USD/kWh_{el} for SHF15, SFH45 and SFH100, respectively. However, the median peak flow in the older house is pushed to 9.6 kW_{el} above the baseline median value (which excludes DHW, see Table 4.3), while in the more efficient houses the median peak flow remains at the same level.

On the other hand, the addition of a battery leads to an increase of the median LCOE between 0.04-0.08 USD/kWh_{el} depending on the type of house (statistically significant, $p - values \leq 0.001$). However, a battery decreases the peak flow if a capacity-based tariff is present, with a median peak reduction between 0.8-1.2 kW_{el} depending on the type of house ($p - values \leq 0.001$).

4.4 Discussion

Our results highlight some of the challenges, and opportunities associated with the electrification of heat demand in the context of decarbonization. First, installing heat pumps without retrofitting the thermal envelope, markedly increases (up to twice) the peak flow in poorly insulated houses (i.e., SFH100). This increase is a direct consequence of the size of the heat pump required to supply the heat demand. Secondly, the provision of DHW using heat pumps and electric backup heaters entails even a higher peak flow in poorly insulated houses. Consequently, thermal retrofitting does not only help to reduce carbon dioxide emissions and to increase comfort levels (Streicher, Padey, Parra, Bürer, S. Schneider, et al. 2019; Narula et al. 2019), but also to reduce grid stress.

Thermal retrofitting allows to defer investments on distribution grid upgrading, due to PV and heat pump penetration. In Switzerland, indicative costs of grid upgrading under a conservative scenario of PV penetration (4.2 GW_p) reach up to 0.49 billion USD, while they amount to 0.78 billion USD for 6.4 GW_{el} of installed

heat pump capacity (Gupta, Pena-Bello, et al. 2021). However, two main obstacles have to be overcome. First, the low retrofitting rate of 1% p.a., has to be increased. Secondly, the large investment for energy retrofitting, poses a second obstacle to reduce grid stress. For instance, retrofitting houses which are originally not well insulated (i.e., SFH100) to very high insulation standards (SFH15) costs around 730 USD/m^2 (Streicher, Padey, Parra, Bürer, and Patel 2018; Streicher, Padey, Parra, Bürer, S. Schneider, et al. 2019), i.e., 100.000 USD for a standard single-family houses of 140 m^2 as considered in this study. Additionally, the cost to improve the thermal performance of all the SFH in Switzerland is of 35 billion USD (Streicher, Mennel, et al. 2020). While these are very high prices for the tenants and may be subject of subsidies from the government, the economic saving potential of more than 50% for the Swiss residential building stock has been proved (Streicher, Padey, Parra, Bürer, and Patel 2018). Nevertheless, the extent of the economic saving potential for the distribution grid (avoidance of grid upgrade) remains an open question.

We find that the implementation and design of capacity-based tariffs are fundamental to limit the grid impacts associated with the performance of PV and heat pump technologies, as well as batteries charging from the grid (i.e., performing demand load shifting). Capacity-based tariffs provide price signals for prosumers to reduce their peak flow, which can help to defer distribution grid upgrades and to recover a portion of network costs (Azarova et al. 2018). On the other hand, policy makers and regulators need to carefully design such capacity-based tariffs in order to avoid costly household bill expenditures (Azarova et al. 2018). We acknowledge that although capacity-based tariffs have been widely applied for large consumers, their application has so far been more limited for residential customers. However, there are some first pilot projects and demonstrations, e.g., in the Netherlands, France, Italy, Finland, and Spain (Hennig et al. 2020; EMI 2015; Prettico et al. 2019). Their implementation for residential consumers is now being suggested following the penetration of PV, air conditioning, heat pumps and electric vehicles. As shown in this study, the performance of these various technologies modify the electricity demand profile and in particular, they increases the peak demand, leading to voltage issues, and overloading of lines and transformers (Perez-Arriaga, J. D. Jenkins, and Batlle 2017; Savelli and Morstyn 2021b; Fridgen et al. 2018).

It is important to highlight that energy storage can be a two-edged sword, reducing or increasing the peak flow depending whether a capacity-based tariff is present or not. When capacity-based tariffs are included, batteries allow to reduce the peak flow, even below the baseline case (which corresponds to houses with neither PV nor heat pump) in houses that are well and very well insulated. In houses which are poorly insulated, batteries also reduce the peak flow below the baseline as long as DHW is not met using electricity (i.e., an additional heat generator is used to meet DHW). Our results show a similar pattern for heat storage for space heating, however, heat storage reduces less the peak flow, even with high capacity-based tariffs (see Section B.10). The beneficial effect of heat storage could be increased by increasing the offset temperature and/or by allowing further flexibility, beyond the two hours-blocks assumed in this study. However, the use of larger tanks, under the same conditions (PV size of 4.8 kW_p, two hours-blocks and 10 K of temperature difference) only increase self-consumption and self-sufficiency by 1 percentage point, while the peak flow remains steady and the LCOE increases by 0.01 USD/kWh_{el} (see Section B.8). The peak flow is mainly determined by the PV export in well insulated houses, whereas the peak demand is predominant in poorly insulated houses.

This explains why the peak flow in well insulated houses is not reduced below the threshold determined by the PV nominal capacity unless PV curtailment is implemented.

The supply of DHW by heat pumps (around 1300 kWh_{el} p.a.) is highly beneficial for an investment of a PV-coupled heat pump system since it considerably reduces the LCOE (up to 0.17 USD/kWh_{el}) and increases the self-consumption rate by more than 10%, while incurring in a relatively small extra capital investment (960 USD). Conversely, DHW supply implies an increased peak flow in poorly insulated houses (SFH100). As an important finding, the use of batteries enables a significant increase in self-sufficiency and self-consumption, by up to 16% and 29%, respectively. However, the still high cost of batteries increases the LCOE markedly (up by 0.08 USD/kWh_{el}). Thus, battery cost reduction is urgently needed to pave the way towards win-win situations for prosumers and the grid, in particular for well insulated houses. Finally, access to low financing costs (i.e., reflected by the discount factor) is key to reduce the burden on prosumers who invest on low carbon technologies to decarbonize the heating sector, followed by subsidies to reduce the upfront cost of carbon-free technologies.

Our study proposes a robust framework to quantify the impacts of storage technologies on PV-coupled heat pump systems and the proposed model is rich in technology details. However, it is not without limitations, which in turn call for future research. Our methodological approach includes some simplifications such as the assumption of a steady state of the buildings' thermal performance and of perfectly-mixed water tanks. More detailed thermal modeling of both buildings and hot water tanks would have increased the computation time markedly. Daily schedule optimization could restrict heat storage flexibility and its economic case, but on the other hand, a longer optimization windows increases the forecast uncertainty, in particular of demand peaks. Forecast strategies (perfect forecast is assumed in this study), together with alternative optimization windows (midnight to midnight is assumed in this study) may cut down the peak flow reductions and increase LCOE values. We assume a rather limited thermal inertia of buildings implying that the heat supply must match the heat demand for each 2 hr time interval. In contrast, more flexible hot water tanks (larger size, higher temperature levels and stratification) and houses could boost the role of heat storage. However, we argue that extra thermal inertia and its associated flexibility (e.g., 24 hr) may not be representative for the entire building stock, in particular for houses with poor envelope quality, calling for further empirical evidence. In addition, we use a representative size of energy storage (both electricity and heat) for comparability reasons, whereas alternative sizes may modify the trade-offs between prosumer benefits and grid impacts (inclusion of sizing in the optimization could hence lead to different findings). Importantly, the design of future electricity tariffs including ToU and capacity-based components calls for further interdisciplinary research (Azarova et al. 2018). Future research can also include electric vehicles and use our open-source optimization model with different locations with temperate climate and fast diffusion of PV and heat pumps.

4.5 Conclusions and policy implications

This study analyzes the trade-offs between prosumer benefits and grid impacts for PV-coupled heat pumps, providing space heating and domestic hot water for residential buildings characterized by different thermal performance. We also compare

electricity and heat storage based on existing ToU tariffs and capacity-based tariffs.

Importantly, we find that energy retrofitting is effective (up to 50% smaller peak flow in well insulated buildings) for decreasing the grid impacts of heating electrification. Consequently, policy measures incentivizing building retrofitting are beneficial not only for the owners and tenants, in terms of improved thermal comfort and lower heating bills, but also for distribution grid operators that may defer (or completely avoid) upgrades. Secondly, we recommend the following steps to increase the share of PV self-consumption and self-sufficiency, based on our economic results, in houses with a PV-coupled heat pump system: first, to supply domestic hot water; secondly to install heat storage; and lastly, to use a battery.

Thirdly, the implementation and design of capacity-based tariffs are fundamental to relieve grid impacts from PV, batteries and electric heating with heat pumps. Based on our results, we conclude that heat storage reduces the levelized cost of meeting the electricity consumption, in particular when heat pumps are used for space heating and DHW, while it allows high self-consumption (30-39% comparable with batteries). On the other hand, both heat storage and batteries are found to be a two-edge sword, since they can either increase or decrease the peak demand depending on the presence of capacity-based tariffs. Based on representative sizes (i.e., 7 kWh_{el} battery and 1500 l hot water tank), we conclude that batteries are more effective than heat storage in increasing the self-sufficiency of houses with PV-coupled heat pumps.

However, decarbonizing heating demand using local PV supply enabled by storage is still costly (i.e., the cost of meeting the electricity related to the various energy services of the house, including space heating, hot water and all appliances is in the range of 0.55-0.71 USD/kWh_{el}) and therefore, appropriate policy incentives are needed. In order to be economically efficient, research and innovation policy should be designed in a way that reduces societal cost. Based on our analysis, we recommend that policy should support research and incentives on levers which simultaneously maximize prosumer benefits and minimize their grid impacts, such as building energy retrofitting, energy storage and capacity-based tariffs.

Chapter 5

Local level

Peer-to-peer (P2P) exchange of renewable energy is an attractive option to empower citizens to actively participate in the energy transition. Whereas previous research has assessed P2P communities primarily from a techno-economic perspective, little is yet known about prosumer preferences for solar power trading. Importantly, impacts of community members' trading decisions on key performance indicators such as individual electricity bills, community autarky, and grid stress remain unknown. Here, we assess P2P trading decisions of German homeowners based on an online experimental study and simulate how various decision-making strategies impact the performance of P2P communities. The findings suggest that community autarky is slightly higher when prosumers are enabled to trade energy compared to when they merely aim to maximize their self-consumption. Our analysis moreover shows that P2P energy trading based on human decision-making may lead to financial benefits for prosumers and traditional consumers, and reduced stress for the grid.

5.1 Introduction

Renewable energy communities (RECs) are expected to play a key role in the transition towards clean and affordable energy. The European Union, for instance, has put RECs in the spotlight of its energy strategy, the Clean Energy for all Europeans Package (European Union 2018). It enacted the right of citizens to consume, store, and sell self-generated renewable energy, either individually or in communities. RECs can be defined as renewable-based and distributed energy systems which are embedded within or close to consumption centers (Carlisle, Elling, and Penney 2008). Members of RECs share several attributes including space and networks and/or several interests, such as renewable electricity supplies and decarbonization, and actively participate in the project across one or more phases (Council of European Energy Regulators 2019). RECs may enable citizens to actively engage in the energy transition; for instance by participating in the collective investment in technology, the provision of self-generated electricity, and community decision-making processes (Savelli and Morstyn 2021a; Council of European Energy Regulators 2019).

Several types of RECs have been discussed in previous literature, such as cooperatives, self-consumption communities, virtual power plants, energy hubs, and peer-to-peer (P2P) electricity trading communities (Devine-Wright 2019; Koirala et al. 2016; Parra, Swierczynski, et al. 2017). Among them, P2P communities offer citizens real-time market participation (Ableitner et al. 2020). Specifically, P2P community members can buy and sell self-generated electricity on a local market;

a characteristic that differentiates P2P communities from other forms of RECs. In organic P2P electricity markets, which refer to fully distributed structures that rely on grassroots initiatives from citizens (Parag and Sovacool 2016; Hahnel, Herberz, et al. 2020), community members become an integral part of the community decision-making process, determining how much and when renewable energy is shared within the community (Lüth et al. 2018; Parag and Sovacool 2016; Wilkinson et al. 2020; Dudjak et al. 2021). In such P2P markets, community members with photovoltaic-coupled (PV-coupled) batteries have the highest degree of flexibility as they can decide whether they want to sell electricity to other community members, or increase their individual autarky.

It is indicated that a significant part of citizens from industrialized countries have a positive attitude towards P2P energy communities, and would generally be willing to participate in related projects. Previous studies involving citizens interested in renewable energy indicate willingness-to-participate rates ranging between 74.5-79.0% (Hahnel, Herberz, et al. 2020; Hackbarth and Löbbe 2020; Reuter and Loock 2017). In a representative UK survey, willingness-to-participate ranged from 54-67% depending on characteristics of the P2P community such as its geographical range (Fell, Schneiders, and Shipworth 2019). Moreover, 89.5% of a representative sample of 998 Swiss citizens reported that they would prefer P2P electricity trading to be based on their individual preferences over an entirely automatic decision-making process (see Section C.1). However, trading decisions in the context of P2P communities are complex, as multiple factors such as dynamic electricity prices, state of charge (SOC) of batteries, and PV generation forecasts need to be considered. Agents that both consume and produce energy (i.e., prosumers) further have to make trade-offs, since selling self-generated electricity at high market prices can be financially attractive, contribute to increased renewable energy consumption at the community level and lower grid stress, but can also reduce individual autarky. In contrast, prioritizing autarky at the individual level may forego financial benefits from trading, as well as potentially intensify grid stress. In light of these trade-offs, it is intriguing to ask under which conditions prosumers would be willing to provide electricity to a P2P community, and whether their trading decisions would lead to benefits at the individual, collective, and grid levels.

Recent research revealed factors that influence homeowners' P2P trading decisions (Hahnel, Herberz, et al. 2020; Ecker, Spada, and Hahnel 2018), but the impact of such decisions on key performance indicators has not yet been sufficiently examined. Past research on P2P energy communities has primarily addressed techno-economic aspects; for instance, underlying technologies (Andoni et al. 2019; Wörner et al. 2019), and pricing mechanisms (N. Liu et al. 2017; Zhou, J. Wu, and Long 2018; Hutty et al. 2021). User behavior has been reported for small P2P pilot trials, but has not been taken into account for the design and modeling of P2P communities yet (Ableitner et al. 2020). Instead, community members have been modeled as rational agents with exclusively economic interests (Andoni et al. 2019; Wörner et al. 2019; N. Liu et al. 2017; Zhou, J. Wu, and Long 2018; Hutty et al. 2021). This reductive view on human preferences and decision strategies is at odds with theories and empirical findings from psychology, which has illustrated that human preferences and decisions notably tend to deviate from assumptions made by standard economic theory (Gigerenzer and Gaissmaier 2011; Simon 1955; Hahnel, Chatelain, et al. 2020). Moreover, recent research on P2P energy trading has illustrated that individuals vary in their trading preferences, and apply different decision-making strategies in P2P scenarios rather than responding in a uniform fashion (Hahnel,

Herberz, et al. 2020). Thus, integrating actual human preferences and P2P decision strategies in energy modeling can result in more realistic projections of the potential of P2P communities at various levels. Finally, human-centered modeling more adequately responds to the principal idea that P2P communities foster social empowerment and participation in the energy transition (Ahl et al. 2019).

In this paper, we report an interdisciplinary approach, bridging psychology with the engineering sciences in order to address the need for integrating human decision preferences into the analysis of P2P energy communities. We first assessed homeowners' P2P trading preferences by means of an online experimental study and then integrated the decision data into an energy simulation. Our findings show that homeowners' trading decisions can result in benefits at the individual, collective and grid level. The benefits, however, vary across community members and depend on the applied P2P trading strategy of prosumers. The findings inform the design of P2P communities and provide new pathways towards human-centered REC design.

5.2 Material and methods

5.2.1 Experimental online study

Sample

The study was approved by the ethics committee of the Faculty of Psychology and Educational Sciences of the University of Geneva, Switzerland and was conducted in accordance with the ethical regulations of the university. All participants gave their consent to take part in the study and received financial compensation for participation. In total, 251 homeowners completed the study (of a total of 299 who began the study; i.e., 48 participants decided not to finish the study). Data collection was assigned to a market research institute (Consumerfieldwork; experimental study date: March 2020), which contacted panel members who owned a house and were older than 18 years old. Demographic characteristics, as well as information on PV and storage ownership and psychological variables of the full sample are depicted in Section C.2. The distribution of sex, age, educational level, and occupation largely corresponded to the general population of German citizens (but see subsection *Generalizability* for deviations). Participants completed the study online. The study was closed after the pre-defined number of 250 completions were attained.

Generalizability

The following aspects should be considered regarding the generalizability of our results. We specifically assessed decisions of German homeowners based on the rationale that homeowners should most likely be able to self-generate and trade electricity. This resulted in a higher median age in our sample than that of the German population, reflecting the circumstance that homeowners are on average older than the overall population. Additionally, the amount of women in our sample was slightly higher than in the German population. Moreover, trading decisions were only based on participants that reported to be willing to take part in a P2P community after a detailed information provision (70% of our sample, see subsection *Pre-assessment and P2P decision task*). Our rationale was to examine trading decisions of individuals that are likely to be members of future P2P communities. Table C.1 shows detailed demographic information on the total sample, the trading

sample, and the non-trading sample. Furthermore, our analyses of trading decisions were based on an experimental task using a predefined set of variables, and thus decisions might deviate from those made in real life (see main text, section *Limitations and future pathways* for a discussion). Finally, in order to test whether the results of the simulated P2P community can also be transferred to communities with different sizes and shares of PV and battery penetrations, we conducted sensitivity analyses with various community configurations and sizes. This sensitivity analysis can be found in Section C.4.

Pre-assessment and P2P decision task

Participants first answered a series of demographic questions including sex, age, civil status, employment status, highest achieved educational degree, and household size as well as their political ideology, general risk taking preferences, environmental values, and renewable energy technology purchase intentions (see Table C.1). Participants were then introduced to the P2P energy trading scenario which we designed to reflect future conditions in a realistic and vivid manner. The decision scenario was adapted from a recently published study by Hahnel et al. (Hahnel, Herberz, et al. 2020). In the scenarios, participants were asked to imagine that they installed PV modules on their roof to generate electricity as well as a 10 kWh battery in their basement to store the generated electricity. The PV system generated electricity with a levelized cost of €11 p/kWh, which was included as reference information for comparison with the P2P market price. Inside the P2P community, participants were able to trade electricity from their batteries.

Subsequently, the P2P choice task was introduced (see Figure C.1 for a visualization of the task). Participants were instructed that they would face several independent situations in the described scenario, and had to repeatedly decide whether or not they wanted to sell 1 kWh electricity from their battery to the community. In each situation, they were informed about the projected next PV surplus, the SOC of their battery, and the P2P market price. Prior to the task, participants were informed that when their battery was empty, they would have to buy their energy at the current community market price. Similarly, when their battery was fully charged they would have to sell their energy at the current market price. Afterward, participants reported their willingness to participate in the described P2P community. The specific question was: 'In general, could you imagine being part of an electricity community as described earlier, where electricity is traded among members?'; Response options: (1) 'Yes, I can imagine that in principle'; (2) 'No, I can't imagine that in any case.' When the answer was negative (i.e., 75 out of 251 participants, equivalent to 30% of the sample), participants were asked for the reason, and then the study was closed for those individuals (see Section C.2 and Figure C.2 for the reasons of respondents who did not want to participate in the proposed P2P community). Only in case of a positive answer, participants were forwarded to the energy trading section.

P2P experimental design

The P2P choice task was based on a 4 x 3 x 2 within-subjects design, with different electricity prices being offered in the community (€4 p/kWh to €28 p/kWh in steps of €8 p/kWh), SOC of the battery (30%–90% in steps of 30%), and time until the next surplus (more than or less than 12 hours). All possible combinations of prices and charging states were presented in a random order, resulting in a total of 24

decisions. The dependent variable was participants' choices to either sell electricity from the battery to the P2P community or not.

During the task, a reminder box was displayed informing participants that the levelized cost of PV was €11 p/kWh, that selling electricity would decrease the SOC of their battery by 10% (corresponding to 1 kWh), that a full battery is sufficient to cover the electricity demand for one day, approximately, and that their decisions would be valid for a one hour interval and could be revised afterwards.

5.2.2 Simulation

Modeling

We developed an open-source model, schematically represented in Figure 5.1, to analyze P2P communities including prosumers with and without batteries and traditional consumers. To understand the impacts and trade-offs of human decision-making preferences and strategies towards P2P trading, we used a baseline case with the same number of prosumers and consumers, as well as the same technology capacities. In this baseline case, prosumers maximized their self-consumption, which represented the status quo in Germany and many other countries after the decline of FiT (Ruf 2018). Our open-source model is based on prosumpy, a toolkit for the simulation and economic evaluation of self-consumption with solar home battery systems (Quoilin et al. 2016), which takes as inputs the community size, PV and battery penetration, and the demand and generation datasets. The model and data on which this article is based are available at `https://github.com/alpebexo/solar_communities`.

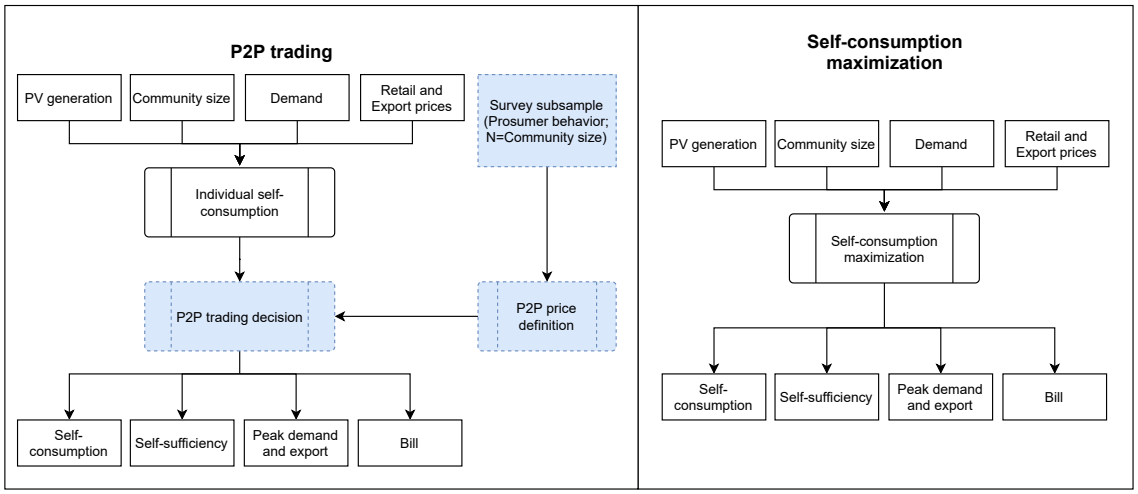

Figure 5.1: **Schematic representation of the proposed modeling of prosumers with PV and batteries depending on the strategy.** Households with a P2P trading strategy opt to self-consume their PV generated electricity before choosing to trade electricity from their batteries within the P2P community depending on the market price, the SOC and the time until the next surplus (more than or less than 12 hours). Prosumers with a self-consumption strategy opt to maximize their own self-consumption. They only inject surplus PV electricity into the main grid.

Community conformation

For both cases, P2P communities and self-consumption maximization, we considered 100 households in the same area behind a single PCC, which were fed by a single Low-Voltage/Medium-Voltage transformer. The two strategies were compared at the individual and at the aggregated levels (i.e., at the PCC). Table 5.1 shows the

main assumptions and technology characteristics for both P2P community trading and self-consumption maximization. We assumed 50% PV penetration (i.e., 50 households with PV) and 25% battery penetration (i.e., out of the 50 households with PV, 25 have access to a battery) for the main analysis. Analysis of other PV and battery penetration (25 and 75% for each device) scenarios and community sizes (20, 40, 60, and 80 households) are shown in Section C.4.

Table 5.1: Main assumptions and characteristics of the technologies for the P2P trading and self-consumption maximization strategies analyzed in this study. The mean values presented are for 1000 simulations.

Strategy	**Self-consumption maximization**	**P2P trading**
Number of simulations	1000	1000
Community size	100	100
Amount of households without PV nor battery	50	50
Amount of households with PV	50	50
Amount of households with PV and battery	25	25
Storage sitting	Distributed	Distributed
Retail price [EUR per kWh]	0,28	[0,04-0,28]
FiT [EUR per kWh]	0,04	[0,04-0,28]
Battery size [kWh per household]	10	10
Mean aggregated PV size [kW]	295	295
Mean aggregated demand [MWh per annum]	468.8	468.8
Simulation of trading preferences	No	Yes

Monte Carlo simulations

To increase the robustness of our results, we ran 1000 simulations for every community, randomly assigning to every household a demand profile and a PV system's size (prosumers only), as well as a set of decisions of one participant from the experimental study (prosumers with PV and battery only). We then referred to the mean values of the 1000 simulations across the figures in this paper.

Self-consumption maximization

Here, every prosumer, with and without batteries, maximized their own self-consumption to avoid expensive electricity imports from the main grid at the retail tariff. When the battery was full and PV generation was higher than demand, surplus PV electricity was sold to the grid at the FiT (see Section C.6 for more information). We used a flat tariff of €28 p/kWh as the retail price, which is close to the reported average retail price for households in Germany for the second half of 2019 (€28.7 p/kWh) (Eurostat 2020). The FiT was assumed to be constant at €4 p/kWh, which is close to the average German wholesale electricity price (€3.8 p/kWh) for the years 2017-2019. Under this strategy, there was no electricity trading. However, other households in the area can make use of the PV surplus electricity, contributing to aggregated self-consumption and autarky (measured at the PCC). Battery grid

charging and battery electricity injection into the main grid from the batteries were not allowed under this strategy.

P2P community

First proposed in 2007 (Beitollahi and Deconinck 2007), P2P trading is based on an interconnected platform that serves as an online marketplace where consumers and producers 'meet' to trade electricity directly, without the need for an intermediary (IRENA 2020). In particular, we modeled an organic market (behind the PCC) with a dynamic price structure (see subsection *Pricing mechanism in P2P community*) involving prosumers with and without batteries and traditional consumers (Hahnel, Herberz, et al. 2020; IRENA 2020). Therefore, electricity can be sold to the P2P community from both PV and battery systems. For the latter, we used homeowners' trading preferences derived from the experimental study, depending on the market price, battery SOC, and time until the next PV surplus (see Sections C.2 and C.6). Trading preferences were integrated into the simulation by randomly allocating each household with PV and batteries a decision profile of one participant from the experimental study.

Pricing mechanism in P2P community

Three assumptions were considered for the proposed P2P market: i) there is a competitive equilibrium; ii) electricity demand is inelastic; and iii) the market operator ensures that the platform is secured and trusted, and follows a balanced budget – i.e., all payments effectively flow between households and the utility grid, or among various households, without receiving any dedicated profit. There is a single market price at any time.

The price of a good is inversely related to the quantity offered, according to the law of supply and demand (N. Liu et al. 2017). Thus, the market price increases alongside limited PV surplus available to be sold relative to the amount of electricity demand, and vice versa. When PV surplus (including both PV and batteries) is higher than the community electricity demand, and therefore surplus PV electricity must be exported to the main grid at €4 p/kWh. Likewise, if the community electricity demand is higher than surplus PV electricity, electricity must be purchased from the main grid at the retail price (€28 p/kWh). To the extent that demand and supply match and to the extent that prosumers are willing to sell, electricity is available for trading inside the community, depending on prosumers preferences. We used Eq. 5.1 to calculate the amount of electricity that could be traded at every timeslot using the probabilities of selling electricity collected through the experimental study. To determine the market price, we used a two-step method, based on probabilities to sell (i.e., *ex-ante*, as opposed to actual sells): First, we calculated the probabilities of selling electricity from the batteries when the SOC was 60%, accounting for the time until the next PV surplus, using the data from the experimental study. Second, for the amount of traded electricity (calculated *ex-ante*, based on probabilities), we determined an equilibrium price for the P2P market, i.e., supply is equal to demand, and approximated the equilibrium price to those used for the experimental study (€4, €12, €20 and €28 p/kWh). Therefore, the market price was constrained to be a step function, with the FiT as the lower bound, and the retail price as the highest one (N. Liu et al. 2017). This dynamic price structure resulted in a uniform price for all community members. See Section C.6 for an example of two representative spring days.

$$E_{P-traded,t} = N \cdot \sum_{h=1}^{H} P((1KWh)_{h,t}|(SOC_{60\%}, t)) \tag{5.1}$$

Where N is the number of batteries in the community, and $P((1KWh)_{h,t}|(SOC_{60\%}, t))$ is the probability of trading 1 kWh from a prosumer with a battery when the SOC is 60% depending on the time until the next PV surplus based on the weather forecast.

Input data and assumptions

We used the distribution of PV sizes from the EEG register data and funding rates (which can be found here `https://bit.ly/37d0Q6L`) with 841,783 registers of small PV plants ($\leq$ 10 kW_p), from which we randomly generated for each Monte Carlo simulation the PV size attached to each one of the considered households. The PV generation was modeled using a single diode equivalent circuit model using outdoor temperature and clear sky global irradiation on a horizontal plane at ground level in Munich, Germany, taken from Soda-Pro (`http://www.soda-pro.com/`), from the year 2015. We generated one year of data with a 15-minute resolution, of a 1 kW_p PV system that was afterwards scaled up to the PV size assigned to a given household. In accordance with the experimental decision task, we used a 10 kWh battery system with 100% depth-of-discharge. It is worth noting that battery degradation is an important parameter to be considered by prosumers. Although we did not consider it in this study, in order to avoid trading electricity without a proper economic incentive, the battery degradation cost must be lower than the revenue created by the P2P trading (for a detailed discussion see Section C.7). In terms of electricity demand, we used electricity consumption data with a 15-minute temporal resolution of residential load profiles from a published German dataset (Tjaden, Bergner, et al. 2015).

Key performance indicators definition

To evaluate the performance of the two considered strategies, we used two economic indicators as well as three technical indexes. Firstly, we used the individual bill (Eq. 5.2) and the aggregated bill (Eq. 5.3). Additionally, we utilized the Benefit Index (BI, originally called participation willingness index (Zhou, J. Wu, and Long 2018)), which measures the percentage of prosumers who obtained more benefits by participating in P2P communities than those using a self-consumption maximization strategy, reflecting the overall financial benefit of the whole population (Eq. 5.4).

$$Bill_j = \sum_{i=0}^{t} (E_{grid-to-house_i} \cdot \pi_{retail_i} - E_{house-to-grid_i} \cdot \pi_{FiT_i}) \tag{5.2}$$

$$Bill_{agg} = \sum_{j=0}^{H} (Bill_j) \tag{5.3}$$

$$BI = N_{LowerCost}/N \tag{5.4}$$

Where, for the household j at time i, $E_{grid-to-house_i}$ is the amount of energy consumed and $E_{house-to-grid_i}$ is the amount of energy injected into the grid, π_{retail_i} and π_{FiT_i} are the retail prices and FiT respectively. In the case of the P2P community there is one price for electricity import and export within the community: the P2P

market price. The aggregated bill is the sum of the individual bills across the members of the P2P community, with the same households considered to calculate the aggregated bill for the self-consumption maximization strategy . In both strategies, we did not consider any cost associated with the community membership. In Eq. 5.4, $N_{LowerCost}$ represents the number of prosumers with a lower energy cost when they participate in the P2P community compared to the cost in the self-consumption maximization strategy.

In terms of technical performance, we used the indicators: PV self-consumption, which is the share of on-site PV generation (E_{PV}) that is used to cover one's own electricity demand (E_{demand}), and autarky, which is the share of one's own total demand that is covered by the on-site PV generation, at the individual and at the aggregated levels, as defined in Eqs. 5.5 and 5.6. We graphically show these two indicators in an energy matching chart (see Figure 5.2).

$$Self - consumption = \sum_{i=0}^{t} \frac{E_{PV-demand_i} + E_{PV-batt_i}}{E_{PV_i}} \tag{5.5}$$

$$Autarky = \sum_{i=0}^{t} \frac{E_{PV-demand_i} + E_{PV-batt_i}}{E_{demand_i}} \tag{5.6}$$

Where, $E_{PV-demand}$ is the PV electricity directly consumed, $E_{PV-batt}$ is the amount of PV electricity used to charge the battery, and E_{PV} is the annual PV generation. At the aggregated level, and to account for the interaction with the grid, we used the peak-to-peak amplitude difference in order to measure the daily variance of the interaction with the grid: in particular, the so-called duck-curve. The peak-to-peak amplitude difference measures the distance between the lower peak (maximum export of the day) and the higher peak (maximum import of the day), which in graphical terms, is the distance from the bottom to the top of the duck head (in kW, see Figure 5.3A). This indicator allowed us to highlight the differences between the two strategies beyond the year maxima.

Grid modeling

We included a complementary model of the distribution grid based on Hartvigsson et al. (2021a) and Hartvigsson et al. (2021b), using the average 15-minute profile of 100 households, and the PV profile with the same temporal resolution. We assumed that the households are embedded into an area of 0.01 km^2 in Germany. The proposed distribution grid model takes a simplified approach of a radial distribution grid with a uniform distribution of consumers in the area supplied by each transformer, involving horizontal and vertical connection lines (see Section C.5 for more information). The model considers the cost of installation for the distribution grid, taking into account the transformer cost, and the cost per km of the line, and takes into account losses and voltage constraints to calculate the transformer hosting capacity.

Statistical tests. To test for statistical differences across prosumer strategies, we performed a Shapiro-Wilk test to inspect the non-normality of the data, followed by a paired two-side Wilcoxon test with the Holm procedure to control the family-wise error rate. When more than two samples were compared (analysis of P2P trading groups), we used a Kruskal-Wallis test to test for differences. All statistical test results are presented in Section C.10.

5.3 Assessment and integration of prosumer decision- making.

We first conducted an online experimental study with 251 German homeowners willing to participate in a P2P community (see Methods for detailed sample information). We assessed decisions to trade self-generated PV electricity within a P2P community as a function of P2P market prices (€4 p/kWh to €28 p/kWh in steps of €8 p/kWh), SOC of privately owned 10 kWh batteries (30%–90% in steps of 30%), and time until the next solar generation surplus (more than or less than 12 hours). Figure C.16 depicts trading decisions of the sample as a function of the three above-mentioned factors.

We then integrated the data derived from the experimental study into an open-source model of P2P communities. Specifically, we simulated an organic P2P community (Parag and Sovacool 2016; Hahnel, Herberz, et al. 2020), where members buy and sell electricity directly among themselves, over a period of one year. Charging the battery from the grid was not considered. The community was located behind a single point of common coupling (PCC), a common interconnection point for different consumers connected to the same utility power supply (Sivaraman and Sharmeela 2021). The community encompassed 100 households in Germany, including both prosumers (with PV or with PV and battery) and consumers. Considering the future-oriented nature of P2P communities, we assumed a scenario with 50% PV penetration, and 25% battery penetration (see Section C.4 for a sensitivity analysis covering a broad range of community sizes, PV penetration, and battery penetration). In order to match demand and PV supply in the P2P community, we created a dynamic price structure with a uniform price for all community members at a given point in time. Furthermore, to increase the robustness of the results, we used the Monte Carlo method to sample 1000 P2P communities, in which all households were randomly assigned to an electricity demand profile (Tjaden, Bergner, et al. 2015), and prosumer households to a PV capacity, considering a representative distribution of PV plant sizes. Demand profiles and PV sizes were based on German data. Additionally, for every simulation, each prosumer with a battery was randomly assigned to a decision profile of one participant from the experimental study, reflecting their individual trading decisions. The link between the experimental psychological data and the simulation allowed us to determine for each point of time in the simulation whether or not a respective prosumer household would be willing to provide electricity to the community given the market price, battery SOC, and surplus forecast.

To assess the impact of homeowners' trading decisions at the individual, collective, and grid levels, we compared P2P communities with a baseline scenario with the same installed technologies and capacities but a different strategy (see Table 5.1). We refer to this baseline strategy as self-consumption maximization. In this baseline case, prosumers with PV-coupled batteries did not trade electricity from their batteries, in contrast to P2P communities. Thus, only surplus PV electricity was injected into the main grid, which is consumed locally if there is demand from other neighboring households located behind the same PCC. These conditions reflect the status quo in Germany at the time of data collection, in which a utility serves as an intermediary among households. Accordingly, consumed electricity was bought at the retail price (€28 p/kWh) and sold at the Feed-in Tariff (FiT, €4 p/kWh). We compared both prosumer models (P2P and self-consumption maximization) us-

ing various performance indicators, including the bill for prosumers and traditional consumers as well as self-consumption and autarky at the individual and aggregated level, measured at the PCC. Moreover, we accounted for grid exchanges in terms of maximum power imported from and exported to the main grid, and for the so-called 'duck-curve', which can be observed in areas with large PV generation (Kosowatz 2018). It reflects a need for fast-ramping up capacity after the sunset and represents a major challenge for grid stability (Kosowatz 2018).

5.4 Impact of prosumer decision-making at the individual level.

We find that P2P energy trading based on homeowners' trading strategies may lead to economic benefits for prosumers with and without batteries, as well as for traditional consumers compared to the baseline case where households maximize self-consumption (see Section C.3 for results considering a similar price structure for both models). Figure 5.2A illustrates that annual electricity bills were lower for all household types in P2P communities, compared to self-consumption maximization. The largest reduction, corresponding to a median value of €262.2 per annum (confidence interval based on 1000 simulations - CI 95% [€261.9; €262.6] per annum) was observed for traditional consumers. Prosumers with only PV showed the lowest annual bill reduction, with a median difference of €98.1 per annum (CI 95% [€97.9; €98.2] per annum). This amount slightly increased to €115.3 per annum (CI 95% [€114.7; €115.8] per annum) for prosumers with batteries. For consumers and prosumers, the differences between a P2P community and the use of self-consumption maximization strategy were statistically significant ($p - values \leq 0.001$).

Figure 5.2B presents the distribution of the average self-consumption and autarky for prosumers with PV-coupled batteries in P2P communities and the self-consumption baseline. In P2P communities, in contrast to self-consumption maximization, individual self-consumption was on average reduced by 6.6 percentage points (CI 95% [6.59; 6.61] percentage points) and autarky was reduced by 12.19 percentage points (CI 95% [12.17; 12.22] percentage points). For households with only PV, the indicators remained unchanged. Furthermore, prosumers with PV-coupled batteries were net producers of electricity regardless of the strategy, as indicated by their position above the diagonal in Figure 5.2B. This means that their aggregated annual PV generation was higher than their aggregated annual electricity consumption.

5.5 Impact of prosumer decision-making at the aggregated level.

Findings moreover show that P2P trading brings higher financial benefits for the community members at the collective level. In the P2P community, the annual aggregated bill was 22.8% lower (equivalent to €18479 per annum CI 95% [€18475; €18484] per annum), compared to self-consumption maximization ($p - values \leq 0.001$; see Figure 5.2C). The economic benefits of P2P communities can be further quantified through the benefit index (Zhou, J. Wu, and Long 2018), which measures the percentage of households who obtain more financial benefits when taking part in a P2P community (see Methods). We find that the benefit index ranges between

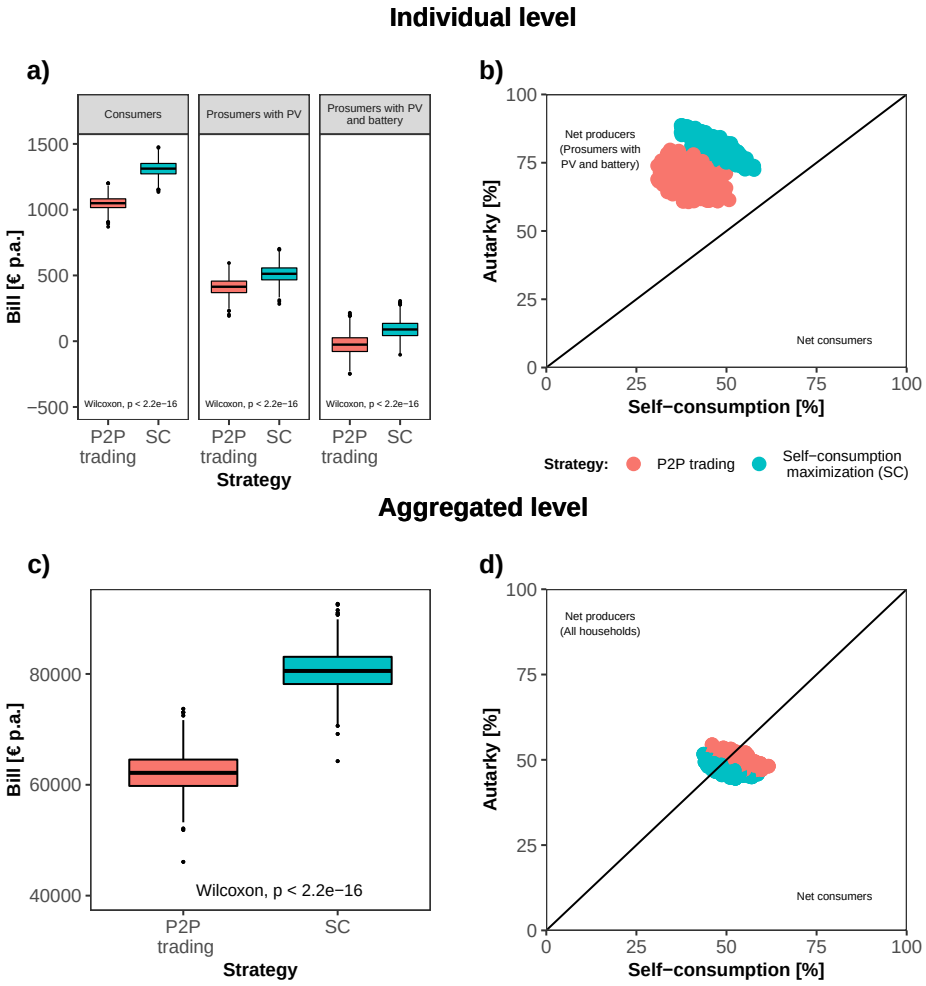

Figure 5.2: Impact of P2P trading and self-consumption maximization (SC) strategies at the individual and aggregated level (at the point of common coupling, PCC). **a)** Boxplot of the mean values of the individual annual bill depending on the type of household; namely traditional consumer, prosumer with PV, and prosumer with PV and battery for P2P trading and self-consumption maximization. Boxplots show the median (horizontal line) and the interquartile range (IQR; box outline). The whiskers extend from the hinge to the highest and lowest value that are within 1.5*IQR of the hinge, and the points represent the outliers. **b)** Energy matching chart at the individual level, for prosumers with PV and batteries. This graphical approach assesses matching between PV electricity generation and electricity demand, using self-consumption and autarky to visualize improved matching with energy storage and demand load shifting. Note that for prosumers with PV and without batteries, self-consumption and autarky are identical for P2P trading and self-consumption maximization, and therefore are not presented in the figure. **c)** Boxplot of the mean values of the aggregated bills at the PCC for P2P trading and self-consumption maximization. **d)** Energy matching chart at the aggregated level (PCC), thereby including all three types of households. The diagonal line represents the net zero energy households on an annual basis. Net producers of electricity are above the line and net consumers are below. The individual p-values of the two-sided Wilcoxon test with the Holm procedure to control the family-wise error rate are reported in the figure for panels b) and c), where N=1000 independent simulations.

95-100% (median of 100%, CI 95% [99%; 100%]), indicating that the majority of households benefited from P2P trading and dynamic prices.

Furthermore, trading within P2P communities led to a small but consistent increase of both, self-consumption and autarky at the aggregated level relative to prosumers maximizing self-consumption (see Figure 5.2D). Aggregated self-consumption increased from 49.6% (CI 95% [49.5%; 49.7%]) to 51.9% (CI 95% [51.8%; 52.0%]) while aggregated autarky increased from 48% to 50% on average. This finding can be explained by a more flexible distribution of locally produced PV electricity at the aggregated level, due to prosumers providing extra electricity from their batteries in P2P communities.

5.6 Impact of prosumer decision-making at the grid level.

In addition to the impact of P2P energy trading on households and communities, we analyzed power exchanges with the distribution grid. We further analyzed distribution grid reinforcement, taking into account the distribution grid constraints, which are vital factors for understanding future investments in electricity infrastructure (Gupta, Pena-Bello, et al. 2021; Heptonstall and Gross 2020; Hartvigsson et al. 2021a; Hartvigsson et al. 2021b). In order to visualize the duck-curve, we analyzed the average weekly grid exchanges across one year for one randomly selected simulation. As illustrated in Figure 5.3A, the data reflects a duck-curve pattern at the PCC: PV electricity exported to the grid shows a maximum around midday when solar generation is the highest. This grid injection is followed by a sharp ramp-up of net electricity demand of 22 kW per hour in the early evening when prosumers maximize self-consumption, due to both the solar sunset and electricity peak demand. Importantly, we notice that P2P trading can help to reduce the magnitude of the duck-curve by 10% when compared to self-consumption maximization (i.e., the ramp-up is 20 kW per hour for P2P). On average the import power peak in the P2P community is reduced by 19% around 8 p.m. (i.e., a reduction from 58 to 48 kW). Furthermore, the peak in exported PV power is reduced by 5% (i.e., reduction from 101 to 96 kW).

To compare the yearly differences in power exchanges with the grid, we used peak-to-peak amplitude differences per season for 1000 simulations. Figure 5.3B shows that the peak-to-peak reduction for P2P trading is maintained across all seasons, with the largest reductions occurring in spring (10.88 kW - CI 95% [10.85 kW; 10.90 kW], i.e., 4.49% - CI 95% [4.48%; 4.50%]), and the smallest reductions occurring in winter (4.96 kW - CI 95% [4.95 kW; 4.97 kW], i.e., 2.62% - CI 95% [2.61%; 2.62%], $p - values \leq 0.001$). Additionally, we modeled a synthetic distribution grid and transformer, including network constraints such as voltage violation, and cable and transformer overloading (see Methods and Section C.5). Based on our analysis, the main limiting factor to PV hosting capacity is transformer overloading, which can be addressed if maximum grid import and export peaks are reduced. Therefore, we analyzed the maximum grid import and export peaks across an entire year to understand whether P2P trading can alleviate them (see Figure 5.3C). We found that, relative to self-consumption maximization, the maximum export peak is marginally higher in a P2P community with a median difference of 1.69 kW ($p-values \leq 0.001$, CI 95% [1.67 kW; 1.71 kW]), while the maximum import peak is slightly lower with a median difference of -3.54 kW across the year (CI 95% [-3.57 kW; -3.5 kW]).

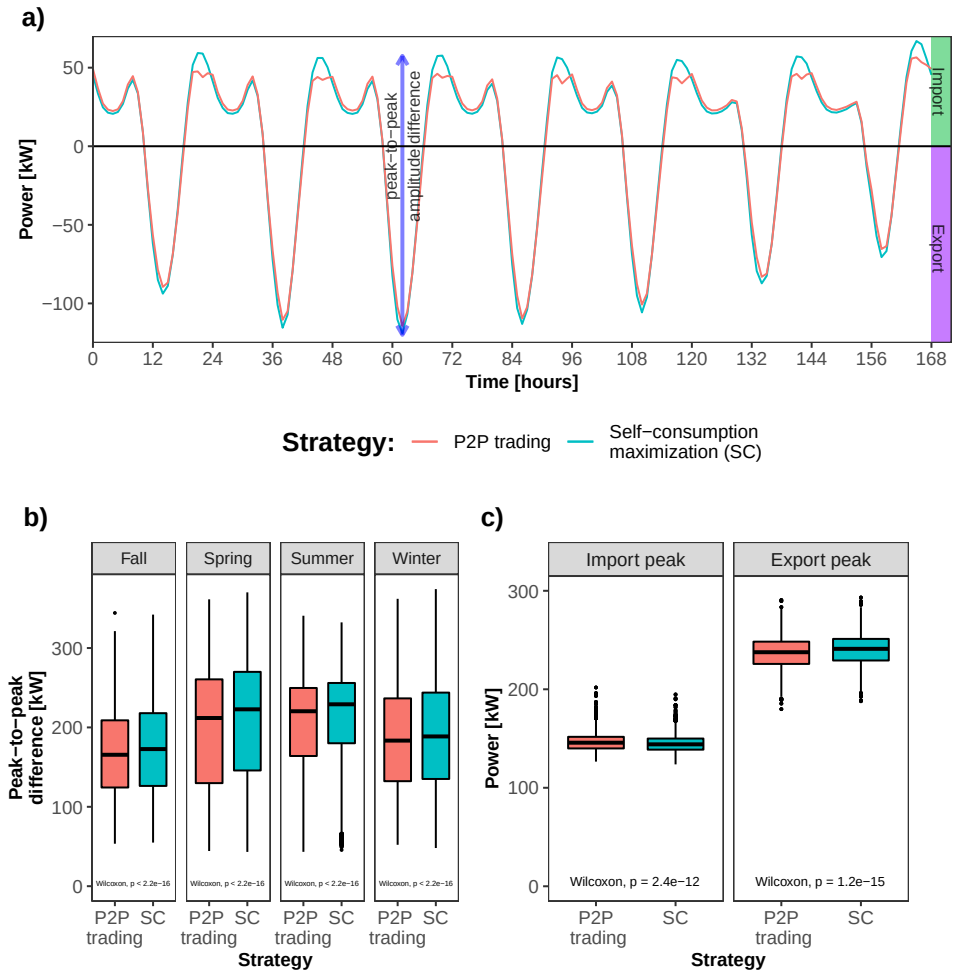

Figure 5.3: Impact of P2P community trading and self-consumption maximization strategies at the grid level. **a)** Average imports and exports for one randomly selected simulation to illustrate the duck-curve and peak-to-peak amplitude differences. Note that electricity exports are represented by negative values, and electricity imports by positive values on the y-axis; **b)** Boxplots of seasonal effect in grid exchange, based on the daily peak-to-peak amplitude difference. Boxplots show the median (horizontal line) and the interquartile range (IQR; box outline). The whiskers extend from the hinge to the highest and lowest value that are within 1.5*IQR of the hinge, and the points represent the outliers. **c)** Boxplots of the maximum import and export peak throughout the year across all simulations. The individual p-values of the two-sided Wilcoxon test with the Holm procedure to control the family-wise error rate are reported in the figure for panels b) and c), where N=1000 independent simulations.

5.7 Impact of different prosumer P2P decision-making strategies.

Finally, we examined the extent to which differences in P2P trading strategies impact autarky and electricity costs at the individual and community levels, as well as their impacts on the grid. To this end, we divided the sample into three groups based on the distribution of participants' trading decisions in the experimental task. Specifically, we composed three subgroups that either traded electricity in a restrained (those that are below μ-σ), moderate (those between μ-σ and μ+σ), or intensive way (those that are above μ+σ); represented by the red, green, and blue area in Figure 5.4A, respectively. We then created three P2P communities that were composed by the same share of traditional consumers (50%) and prosumers (25% with PV only, 25% with PV-coupled batteries), as in the previous analyses. The P2P communities differed with respect to whether their prosumers with PV-coupled batteries traded electricity in a restrained, moderate, or intensive way, using the three created trading subgroups. This approach allowed us to examine how different trading patterns impact the performance of P2P communities (see Figure 5.4B and C; see Figure C.17 for results on self-consumption).

The analysis points to an optimal trading window associated with a moderate trading pattern, which led to relatively high autarky at both the individual (70.13%, CI 95% [69.40%; 70.85%]) and community levels (49.71%, CI 95% [49.68%; 49.73%]). This decision pattern also resulted in the highest economic benefits at the individual level, with bill reductions for households with PV-coupled batteries of €46 and €43 per annum (CI 95% [€45; €47] and [€41; €45] per annum), compared to restrained and intensive trading patterns ($p - values \leq 0.001$). Similarly, it also resulted in significant bill reductions of €1226 and €918 per annum at the community level, compared to restrained and intensive trading respectively (CI 95% [€1224; €1254] and [€911; €920] per annum, $p - values \leq 0.001$). Moreover, the maximum weekly peak-to-peak magnitude of the duck-curve was on average 4.8 percentage points lower for moderate compared to restrained traders. In contrast, restrained traders achieved higher autarky at the individual level (77.57%, [76.93%; 78.20%]), but lower autarky at the community level compared to the moderate trading group (decrease by 1.3 percentage points - CI 95% [1.2; 1.4], $p - value \leq 0.001$). In contrast, intensive trading resulted in the highest community autarky, leading to an increase of 1 percentage points compared to moderate traders (CI 95% [0.9; 1.1], $p - value \leq 0.001$). Intensive trading has also the highest potential to reduce the duck-curve magnitude as it was, on average, reduced by 2.5 percentage points compared to moderate trading. However, this trading pattern reduced autarky at the individual level by 14 percentage points compared to moderate traders ($p - values \leq 0.001$). Lower individual autarky resulted in higher bills for intensive traders, with a bill increase of €44 per annum compared to moderate traders (CI 95% [€42; €46] per annum, $p - values \leq 0.001$), and statistically similar bills than restrained traders.

5.8 Discussion

Our study, bridging experimental psychological research with robust energy modeling, indicates that social empowerment in P2P communities may lead to multiple benefits for community members, including prosumers as well as traditional consumers. Our findings have four key implications for industry, policymakers, and

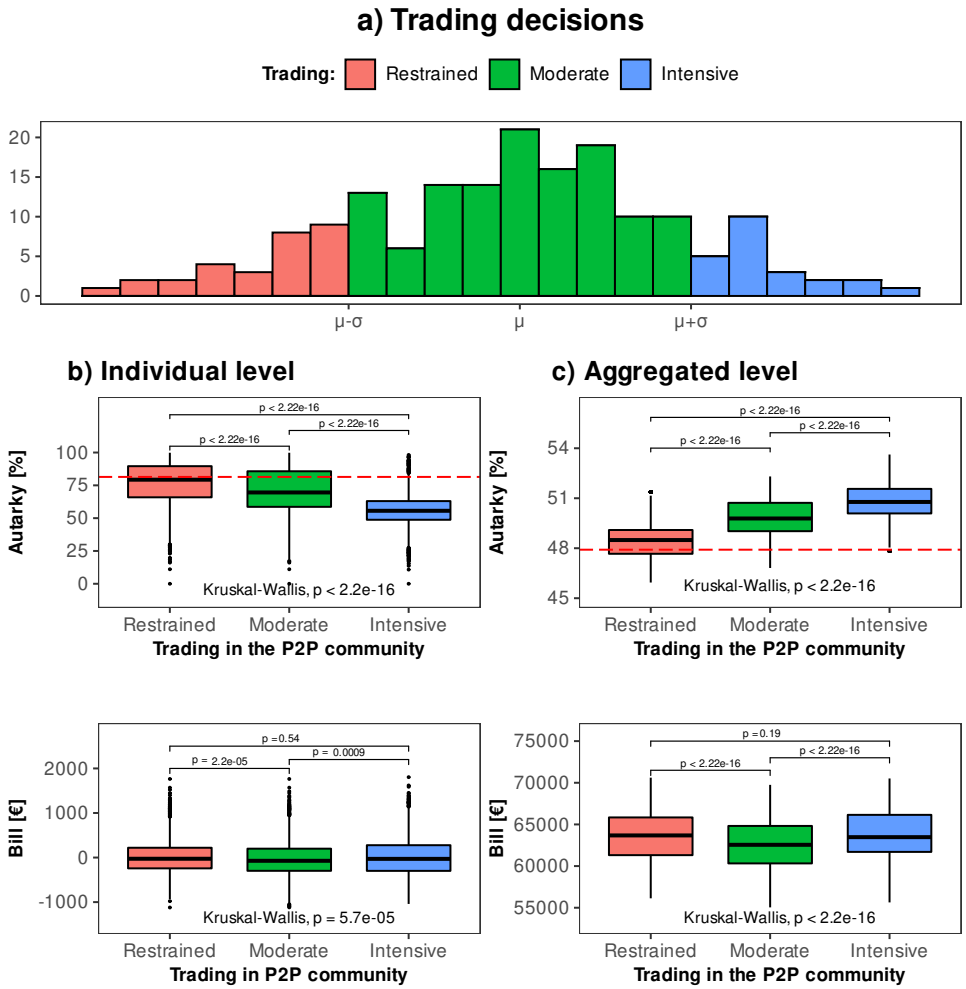

Figure 5.4: Impact of different P2P trading strategies on the individual and aggregated level (at the point of common coupling, PCC). **a)** Distribution of trading decisions assessed in the experimental study (a two-sided Shapiro-wilk test showed that the data is not significantly different from the normal distribution; W=0.98957, p-value=0.2276). The x-axis represents the amount of decisions to sell electricity to the community, covering the range from no trading at all (0 occurrences of trading), to always trading (24 occurrences of trading). The distribution was divided into three categories: restrained traders (red area: below μ-σ), moderate traders (green area: between μ-σ and μ+σ), and intensive traders (blue area: above μ+σ). The y-axis represents the number of participants for each trading value. **b)** Boxplots for autarky and annual bill for households with PV-coupled batteries depending on trading group; note that for prosumers with PV and without batteries, these performance indicators are identical across simulated P2P communities, and therefore are not presented in the figure. Boxplots show the median (horizontal line) and the interquartile range (IQR; box outline). The whiskers extend from the hinge to the highest and lowest value that are within 1.5*IQR of the hinge, and the points represent the outliers. **c)** Boxplots for autarky and annual bill at the aggregated level (PCC) depending on the trading group. The individual p-values of the two-sided Wilcoxon test with the Holm procedure to control the family-wise error rate and of the Kruskal-wallis test are reported in the figure for panels b) and c), where N=1000 independent simulations.

academics.

First, we find that traditional consumers obtain the highest financial benefits in P2P communities. As consumers do not generate their own electricity, they generally have higher electricity bills than prosumers, and thus have the largest reduction potential (Figure 5.2). This finding has implications for distributional energy justice; referring to the allocation of benefits and costs within a community (K. Jenkins et al. 2016; Morstyn, Savelli, and Hepburn 2021; Carley and Konisky 2020). On the one hand, P2P communities can foster energy justice as they increase access to renewable electricity at a low price, including households that do not have the financial resources to invest in renewable energy technology. On the other hand, investments in renewable energy technology need to pay off for community members to ensure availability of locally generated electricity. A fair distribution of the costs inherent to P2P communities, including investments in PV and storage systems, may be achieved by differentiated membership fees in the function of a member being a traditional consumer, prosumer with PV, or prosumer with both PV and battery.

Second, we find that aggregated autarky was overall slightly lower when prosumers maximized their self-consumption than when they shared energy within P2P communities. Prosumers who aim to maximize their individual autarky paradoxically reduce autarky at the aggregated level. In P2P communities, electricity trading liberates battery capacity, enabling recharging with more self-generated PV electricity when the next surplus occurs. In contrast, when prosumers aim to maximize self-consumption, their batteries remain idle for longer periods as no energy is shared from their batteries. Therefore, P2P communities reduce yearly PV electricity exports to and imports from the grid, increasing autarky at the collective level.

Third, our analysis of grid impacts shows that the duck-curve is flattened in P2P communities compared to a strategy where prosumers maximize self-consumption, *ceteris paribus*. P2P communities enable the supply of more PV electricity on-demand reducing the duck-curve and thereby decreasing the need for cost-intensive non-renewable energy supply, power balancing, and other ancillary services. However, extreme import peaks remain at similar levels for both types of prosumer strategies. Thus, while P2P communities may help to flatten the duck-curve, they can neither increase the hosting capacity of the distribution grids, nor defer their final upgrade. In order to further reduce the impact of high PV penetration on the grid (e.g., more than 75% of households with PV in the community, see Section C.5), the implementation of flexibility strategies such as demand side management can be considered. Implementing additional flexibility strategies would require close cooperation between P2P communities and network operators. Policy-makers should therefore promote such cooperation, and provide new regulation of data access, privacy, and cybersecurity to ensure that rights of P2P members are fully respected when enabling network operators to procure flexibility using P2P resources.

Fourth, our interdisciplinary analyses show that homeowners apply different P2P trading strategies (Hahnel, Herberz, et al. 2020) that may lead to more or less beneficial outcomes for themselves and the community. Specifically, either overly restrained or overly intensive trading strategies resulted in financial and autarky-related disadvantages at the individual and community levels. Our results pinpoint a moderate trading strategy to maximize benefits, reflecting decisions of the majority of participants in our sample (see Figure 5.4). For the design of a P2P community, this means that responsible stakeholders should dare to involve community members

in the operation of P2P communities, since their decisions seem well-calibrated to produce individual and collective benefits. As an additional effect, involvement in P2P operations may increase social empowerment, which eventually may lead to co-benefits, such as increased satisfaction, participation rates, and technology investments.

5.9 Limitations and future pathways

Our interdisciplinary approach is novel, but not without limitations. Although our methodology is based on the assessment of actual decisions of homeowners, it is important to note that these decisions were made in a controlled experimental setting. In our experimental design, homeowners received a pre-defined set of information, including energy prices, the SOC of their battery, and PV surplus forecasts. Our rationale was based on literature illustrating that laypersons have limited knowledge about energy-related variables and the energy system (Attari 2021; Marghetis, Attari, and Landy 2019). We, therefore, limited our focus to the factors that were previously identified as having a significant impact on homeowners' trading decisions (Hahnel, Herberz, et al. 2020; Wilkinson et al. 2020; Plewnia and Guenther 2020). Our research can thus be a starting point for future research considering additional factors in P2P trading including further technical information such as battery aging, either provided to prosumers or integrated into energy simulations and algorithms. For applications where batteries perform more cycles, such as batteries charging from both a PV system and the grid, or for batteries performing benefit stacking, aging may become relevant. Another limitation of our experimental approach is that real life prosumer decisions might be influenced by situational factors such as time constraints, which we did not consider in our experimental study. Large-scale field trials including an in-depth analysis of user decision-making would thus be a natural extension of our research, to increase external validity. Our findings can inform the design of future field trials that should aim to include broad samples of prosumers and consumers, and thereby go beyond existing pilot trials with restricted samples (Ableitner et al. 2020).

A discussion of external validity is closely linked to the question of how individual decisions could be implemented in future P2P communities. While it would be very demanding for prosumers to make each individual trading decision manually, their decision preferences could be integrated into trading algorithms that would administer trading in everyday life. To this end, prosumers would configure trading algorithms by means of prototypical decision situations similar to those applied in the present study, and the resulting decision profiles would then be used to calibrate decision algorithms. As illustrated in the Section C.1, 68.1% of citizens would prefer this option in which a trading algorithm administers trading in everyday life based on pre-assessed individual preferences, compared to 21.3% preferring manual scheduling, and 10.5% preferring entirely automatic decisions. Taken together, our research corroborates recent research on the need for responsible, human-centered, algorithm design and demonstrated methodological pathways to achieve such design objectives (Ransan-Cooper et al. 2021).

Future research can build upon our methodology to develop alternative pricing mechanisms or auction systems that account for user preferences. It would be of importance for such studies to exploit various means to integrate network charges in P2P market prices in order to ensure a fair distribution of costs for citizens within

and outside the community. Considering that P2P communities reduce the use of the main grid, reduced network charges for energy traded within the P2P community compared to existing charges are conceivable. Additionally, network charges may be distributed among community members according to their final peak flow (i.e., their peak export and import), to avoid free-riding and to increase distributional fairness within the community.

The grid-friendly operation of P2P communities should be further investigated by applying more detailed distribution grid models, which take into account the characteristics of local grids and trading decisions. Finally, the spectrum of considered technologies within P2P communities could be extended to other low-carbon technologies, such as heat pumps and electric vehicles. Given the high storage potential of electric vehicles, it is an intriguing question how prosumers would be willing to trade electricity when using electric vehicle batteries. We consider that future research with user-centered modelling approaches coupled with field trials can provide a more complete understanding of citizens' interactions in RECs, and thus may inform the design of future RECs that achieve both citizen empowerment and renewable flexibility procurement for the energy transition.

Chapter 6

National level

The Swiss Energy Strategy 2050 foresees, among other measures, a widespread adoption and integration of renewable energy technologies, in particular, distributed solar photovoltaics (PV). However, the massive increase of intermittent renewable generation capacity poses challenges for the control of the stability of the power grid. Battery energy storage can enable the penetration of distributed PV in two different ways. First, it increases the amount of PV self-consumption which makes PV more attractive for final consumers. Second, batteries can provide grid and market services to help keeping the grid stable. In this study, we aim to analyze the techno-economic benefits for the consumer and the grid associated with a pool of distributed storage, managed by an aggregator participating in the Swiss frequency market, as well as potential trade-offs. To this end, we apply a residential battery dispatching model to quantify the added value of frequency control for the prosumer. We use imbalance prices to quantify the total cost for the TSO that is equivalent to the payments to the frequency control service providers. Moreover, we look at future scenarios calculating the required regulating power quantities for 2030 and 2050, however, the future economic potential of the frequency control service was not calculated due to difficulties to model the manual frequency restoration reserve prices.

6.1 Introduction

Distributed solar PV is expected to reach 530 GW globally by 2024 and it has the highest growth potential across all the market segments mainly due to rapid consumer adoption (IEA 2020). In the residential sector, financial considerations speak for increased interest in PV, however, further motives have been found to influence investing on PV (Korcaj, Hahnel, and Spada 2015). For example, self-sufficiency, as the individual possibility to secure and control part of the energy provision and to reduce dependence on energy providers (Korcaj, Hahnel, and Spada 2015), was found to partially influence the intention to adopt PV systems (Korcaj, Hahnel, and Spada 2015; Ecker, Hahnel, and Spada 2017). Environmental motives are also often reported as key reasons for investing in PV (Stern et al. 2017). Finally, social influence plays an important role in the early take-off stage of the diffusion curve (Korcaj, Hahnel, and Spada 2015; Rai and Robinson 2015; Curtius et al. 2018; Alipour et al. 2020).

Massive residential PV integration poses several challenges to the distribution network. Local PV feed-in affects the voltage of the distribution grid, as well as

the operation of critical devices such as transformers and lines (Gupta, Pena-Bello, et al. 2021; Holweger et al. 2020). Unlike centralized generation, PV output cannot be easily controlled and would require large capacities of energy storage to enable on-demand supply (Gupta, Soini, et al. 2020). Additionally, with residential PV reaching grid-parity, defined as the cost level at which PV becomes competitive with retail electricity prices, policy schemes such as Feed-in tariffs (FiT) have declined and are now being phased out in different countries. This phase-out together with high electricity retail prices, the need to control PV power generation to avoid excessive PV power injection into the grid, are key drivers for PV self-consumption.

PV-coupled batteries can increase PV self-consumption while helping to mitigate the grid impact of distributed PV through the simultaneous provision of multiple applications (Stephan et al. 2016; Nousdilis, Christoforidis, and Papagiannis 2018; Gardiner et al. 2020). Despite having a steep learning curve with a learning rate of 20% for all types of cells (Ziegler and Trancik 2021), batteries are not yet profitable for the residential sector (do Nascimento and Rüther 2020; Litjens, Worrell, and van Sark 2018a). Nevertheless, expected battery cost reductions together with the simultaneous provision of multiple applications can help residential batteries to reach profitability before the end of the decade (Stephan et al. 2016; Gardiner et al. 2020; Pena-Bello, Barbour, Gonzalez, Yilmaz, et al. 2020; Englberger, Jossen, and Hesse 2020). Among several applications, batteries can provide frequency control to continuously match supply and demand, thereby replacing fossil-fuel based generation units, that are the conventional providers of frequency control.

Due to its great potential, diverse key factors impacting PV-coupled battery systems' profitability have been investigated. Self-consumption maximization, which is the principal residential application, has been the focus of various studies (Mohamed et al. 2021; Mulleriyawage and Shen 2020; Nousdilis, Kryonidis, et al. 2020). Authors have further studied other applications applications, either by comparing or stacking them, including demand peak-shaving, load-shifting and avoidance of PV curtailment (Mishra et al. 2020; Parra and Patel 2016; Pena-Bello, Barbour, Gonzalez, Patel, et al. 2019; Pena-Bello, Barbour, Gonzalez, Yilmaz, et al. 2020).

Frequency regulation has been addressed mostly for commercial consumers. Englberger, Jossen, and Hesse (2020) considered the role of power electronics in the combination of applications, taking into account not only energy but also power applications. They found commercial batteries to be highly profitable under the conditions of dynamic combination of applications (including self-consumption, demand peak-shaving, energy arbitrage, and frequency regulation). Standalone batteries combining the provision of frequency containment reserve (i.e., FCR, also known as primary control) together with load-shifting were analyzed for commercial consumers using approximate dynamic programming (Wen et al. 2021). Perez et al. (2016) included the effect of battery degradation in the provision of energy arbitrage and peak-shaving at the distributed level (to alleviate network congestion) as well as frequency regulation, divided into reserve (for available power) and response (for delivered energy). However, it is not clear from the study which types of frequency restoration reserves were analyzed (e.g., FCR, automatic Frequency Restoration Reserve - aFRR, or manual Frequency Restoration Reserve - mFRR). The authors found battery degradation to mainly affect services related to the energy market (e.g., energy price arbitrage). Additionally, the effect of restraining the battery state of charge (SOC) led to a revenue loss in the short-term that was compensated by long-term revenues due to a longer battery lifespan.

For residential consumers, Engels, Claessens, and Deconinck (2017) presented a

stochastic optimization of a residential battery providing FCR and self-consumption, and showed that there is a clear complementarity in combining these two services. Their combined provision added 25% of value compared to the use for frequency control alone, and increased the value threefold when compared to self-consumption alone. Hollinger et al. (2016) discussed the simultaneous provision of FCR and PV self-consumption for a single house under current regulatory conditions and market prices in Germany. Schopfer et al. (2017) modeled a virtual power plant able to pool distributed residential batteries to participate in the provision of FCR. They found the battery size to be a determining factor for the additional revenues that an individual household can generate within a virtual power plant. A hierarchical control with a double decision layer, one for the aggregator and one for the battery itself, was found to be effective to reduce frequency violations in a simulated real disturbance sequence, however, without the consideration of residential PV (Obaid et al. 2020). The only study focused on the provision of aFRR (also known as secondary control reserve) was prepared by Litjens, Worrell, and van Sark (2018a). They found the combination of aFRR and self-consumption to be profitable for residential and commercial consumers. Additionally, they found that the prioritized provision of aFRR over self-consumption enhancement resulted in higher revenues, but significantly reduced self-consumption.

Finally, Sossan et al. (2016) introduced the dispatched-by-design distribution systems paradigm, where batteries are deployed in the distribution grid to compensate traditionally stochastic prosumption peak flows. Along the same lines, Bozorg et al. (2018) investigated the effect varying penetration levels of dispatched-by-design distribution systems in the Danish bulk grid on the amount aFRR and mFRR required to ensure a predefined level of grid reliability.

To conclude, the available literature shows a high potential for the combination of self-consumption and frequency regulation (either FCR, aFRR or mFRR). However, only a few studies have investigated aFRR which is a more flexible market than FCR, compensating not only power availability, but also instantaneous energy balance, with only a few residential profiles with PV-coupled systems having been studied (Litjens, Worrell, and van Sark 2018a; Schelly 2014). Furthermore, mFRR has received only marginal attention.

In this study, we aim to analyze the added techno-economic benefits for the prosumer and the grid, associated with the pool of distributed storage under the management of an aggregator participating in the frequency market, taking Switzerland as case study. We evaluate the trade-offs between prosumer and market applications, namely PV self-consumption and frequency control, which are linked to different prosumer motivations such as keeping its own electricity for itself (self-sufficiency) or providing flexibility to the energy system, potentially with a higher economic benefit. We use techno-economic indicators such as self-consumption, self-sufficiency, net present value (NPV) of the battery as well as the levelized cost of energy storage, for different shares of battery capacity dedicated to frequency control. We then quantify the amount of reserve required to operate the Swiss electrical grid with a level of reliability considering different Swiss scenarios for 2030 and 2050.

6.2 Material and Methods

To analyze the added techno-economic benefits for prosumers maximizing their PV self-consumption that could be reaped via the aggregation of distributed storage

participating in the Swiss frequency market, as well as potential trade-offs, we use a residential battery dispatching model. In order to assess the impacts of renewable energy penetration on frequency control, we consider different scenarios for 2030 and 2050, modeling the future Swiss electrical grid mix with a dispatch sector coupling energy system model (referred to as GRIMSEL model - GeneRal Integrated Modeling environment for the Supply of Electricity and Low-temperature Heat) which minimizes the energy system costs. The optimal configuration of the Swiss energy system, considering the energy system of various neighbouring countries, allows us to determine the future spot electricity prices (or shadow prices). Then, to determine the energy capacity of battery storage required to operate the power systems with the desired reliability level, a Monte Carlo simulation is used. Finally, we use a linear model to estimate the price of regulating power (i.e., the energy that is produced (absorbed) by a generator (consumer) by deploying the booked reserve capacity, following a request from the TSO) and the imbalance costs. Note that residential PV is not used for frequency control, only batteries.

6.2.1 The Swiss frequency control market

The Swiss energy balancing and imbalancing markets follow the European directives (see below for further explanations). Switzerland counts with three balancing market products, FCR (provided together with the other members of continental Europe), aFRR and mFRR.

In Switzerland, FCR enters 0.5 minutes after a frequency deviation, then aFRR is called up by the TSO (i.e., Swissgrid) after 30 seconds of outage, and it is provided by online power stations working below the nominal capacity within the country, and is typically completed after 15 minutes (Swissgrid 2020). If the cause of the control deviation is not eliminated, aFRR gives way to mFRR, which is used for adjusting major, longer-lasting control deviations. TSOs send electronically transmitted messages to the providers, who within 15 minutes intervene to ensure the supply of power. In Switzerland, mFRR and restoration reserves (i.e., RR or slow tertiary control) are comparable products and integrated under a single product (called tertiary control) (Swissgrid 2020).

FCR is a daily product procured two days before real-time operation, and positive and negative power are jointly tendered (i.e., it is a symmetric product). Since 2018, aFRR has been separated into positive and negative power (asymmetric product), and it is procured on a weekly basis, and remunerated based on the Swiss market price (SwissIX) $\pm 20\%$ (Swissgrid 2019). Finally, mFRR corresponds to present-day fast and slow tertiary control reserves, it is an asymmetric product that is provided during one week or four hours, with the weekly product being tendered on Tuesdays and the four-hourly one day before real-time operation (Swissgrid 2020). The remuneration of mFRR is based on the energy price specified by the bidder. The power plants receive additional compensation for aFRR and mFRR energy, on top of power availability.

Finally, the imbalance settlement, i.e., the process of allocating costs to market actors that caused the imbalances, aims to charge (or pay) balance responsible parties (BRPs) for their imbalances during an imbalance settlement period (15-minutes in Switzerland). It includes incentives for the market to reduce imbalances while transferring the financial risk of imbalances to the BRPs. In Switzerland, it is done using the imbalance prices P_{Short} and P_{Long}, that are calculated using equations 6.1 to 6.4.

$$P_{Short} = (A + P_1) \cdot \alpha_1 \tag{6.1}$$

$$A = max(P_{spot}, P_{aFRR_+}, P_{mFRR_+}) \tag{6.2}$$

$$P_{Long} = (B - P_2) \cdot \alpha_2 \tag{6.3}$$

$$B = min(P_{spot}, P_{aFRR_-}, P_{mFRR_-}) \tag{6.4}$$

where α_1 is 1.1, α_2 is 0.9, P_1 is 1 Rp/kWh, and P_2 is 0.5 Rp/kWh. P_{spot} is the Swiss day-ahead spot price, P_{aFRR} is the price of secondary control energy, and P_{mFRR} is the price of tertiary control energy. In the case equation 6.1 results in a negative price, the factor α_1 is replaced by α_2. Similarly, in the case equation 6.3 results in a negative price, the factor α_2 is replaced by α_1 (Swissgrid 2018). Upward regulating power prices (i.e., positive control) are then addressed by the short imbalance prices (i.e., they are used when there is a deficit of energy and positive control is activated) and downward regulating power prices (i.e., negative control) are addressed by the long imbalance prices.

6.2.2 Modeling overview

We use an open-source 24-h optimization framework for battery dispatching (i.e., Battery Schedule OPtimizer for Residential Applications, BASOPRA) to analyze PV-coupled battery systems combining applications and to assess their added value (Pena-Bello, Barbour, Gonzalez, Patel, et al. 2019; Pena-Bello, Barbour, Gonzalez, Yilmaz, et al. 2020; Pena-Bello, Schuetz, et al. 2021). The model has been modified to allow the battery to perform frequency control (e.g., to provide upward regulation by battery discharge), as a response to the input prices (i.e., the difference between the spot price and the imbalance price). Thus, there is no obligation from the prosumer perspective to participate in the frequency market if the proposed prices are not economically attractive. Please note that it is the battery that provides frequency control, not the PV system.

Eq. 6.5 presents the objective function of the model, which is publicly available in `https://github.com/alefunxo/Basopra_FC`.

$$C = Min(\overbrace{\sum_{i=0}^{t}(E_{grid_i} * P_{import_i} - E_{PV-grid_i} * P_{export_i})}^{\text{Energy-based tariff}} - \underbrace{(E_{grid-batt} * P_{downwards} + E_{dis-FC} * \eta_{inv} * P_{upwards})}_{\text{Frequency Control}}) \tag{6.5}$$

$$P_{upwards} = P_{Short} - P_{spot} \tag{6.6}$$

$$P_{downwards} = P_{spot} - P_{Long} \tag{6.7}$$

where the energy-based tariff is given by E_{grid_i} which is the electricity drawn from the grid, P_{import_i} is the import price (i.e., retail price), $E_{PV-grid_i}$ is the PV-electricity exported to the grid, P_{export_i} is the export price (i.e., the spot price in this study), with the sub-index i representing every time step from 0 to t (i.e., 15-minutes step

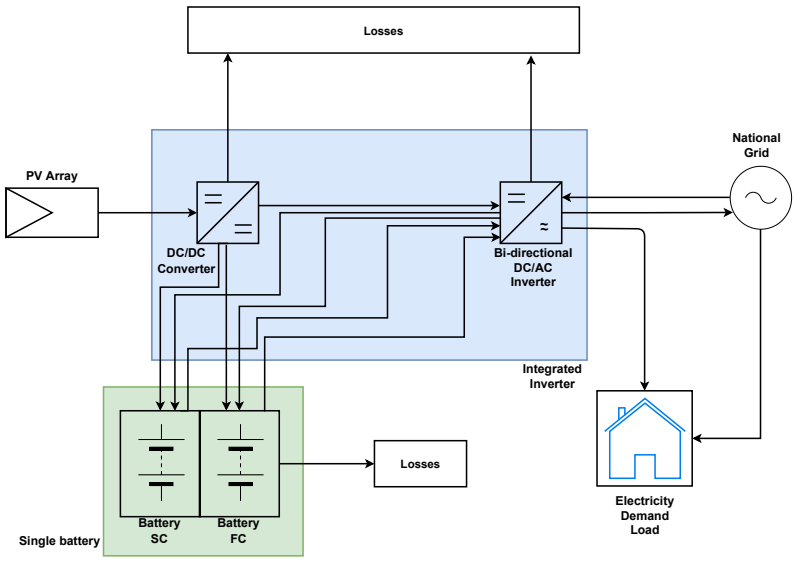

Figure 6.1: Simplified schematics of the DC-coupled PV-battery system with integrated inverter used in this study. Arrows indicate the direction of possible energy flows between the individual components. A single battery is used to provide self-consumption maximization and frequency control with dedicated capacity for each application.

for this study). As for the frequency control application, it is considered that prosumers could provide upward regulating power by increasing their production (represented by the injection of electricity from the battery to the grid E_{dis-FC}) or provide downward regulating power by increasing their consumption (i.e., represented by the battery charging $E_{grid-batt}$). $P_{upwards}$ and $P_{downwards}$ are the differences between the balance energy prices and the spot prices, in each direction.

Using the BASOPRA model we analyze the extra value for the prosumer provided by PV-coupled battery systems, assuming that a fraction of the battery capacity is used for PV self-consumption, which is the main application for prosumers, while the other fraction of the battery capacity is used for frequency control, which is the key application for an aggregator. We then investigate the trade-offs between PV self-consumption and frequency regulation (see Figure 6.1).

Moreover, we consider two future years of the Swiss energy transition, 2030 and 2050. Based on the future scenarios from Rinaldi et al. (2020), we consider two cases, business as usual (BAU), with a heat pump deployment similar to the rather moderate current market diffusion rate, and a more ambitious "fossil phase-out" case where all the residential sector fossil heating is progressively replaced by heat pumps. In all the future scenarios, we consider a building stock retrofitting rate of 1%. Therefore, we explore four future scenarios, namely "2030 BAU", "2030 fossil phase-out", "2050 BAU", and "2050 fossil phase-out".

With the scenarios defined, GRIMSEL, a quadratic dispatch and capacity retirement model of the electricity supply in five countries (Switzerland, Austria, Germany, France and Italy) (Soini, Parra, and Patel 2019) is used to identify optimal power investments as a function of building retrofitting as well as distribution capacity upgrade (Rinaldi et al. 2020). GRIMSEL approximates perfect electricity market conditions by minimizing variable and fixed costs, while satisfying predefined hourly demand under perfect foresight. GRIMSEL considers significant changes for the Swiss residential sector, while for the other Swiss sectors, e.g., industry, only the demand is modified. The model also takes into account changes in Germany, France, Italy, and Austria, such as nuclear or coal phase-out, however, the model

assumptions for these large countries are kept constant across the scenarios modeled for Switzerland. Finally, GRIMSEL determines the resulting power assets required to drive the decarbonization of the heating sector, as well as the resulting spot prices for each scenario.

Using the power capacity per technology from GRIMSEL, we subsequently apply a Monte Carlo simulation to investigate the effect of varying the penetration level of dispatched-by-design distribution systems in the bulk grid on the amount of reserve required to operate the global electrical grid with a predefined level of reliability. The main hypothesis made in this model include: absence of significant changes on the transmission system in the future, thus continuing to use the actual transmission system of 163 internal buses and 18 international interconnections, according to the Strategic Grid 2025 from Swissgrid (Swissgrid 2015); PV capacity distribution is proportional to the hosting capacity of the nodes (Gupta, Sossan, and Paolone 2021); no use of imported and exported automatic or manual frequency regulation services; compensation of only 25% of the imbalances regarding day-ahead forecasts using Swissgrid resources, while the remaining 75% are either compensated through the intraday market or internally by the BRPs (according to authors' analysis of Swissgrid imbalance data and ENTSO-E data); unavailability rate of generators as reported by Guerrero-Mestre et al. (2020); mean time to repair assumed to be 1 hr (instead of the average 8-24 hr), since following an unplanned outage, in less than an hour the generation company could purchase energy from intraday markets or make use of bilateral agreements in order to avoid mismatches and imbalances which would be penalized by Swissgrid; finally, it is assumed that there is a comparable amount of available automatic and manual reserve (i.e., aFRR and mFRR, respectively; 50-50% distribution with respect to the total required reserves in each direction). This model was run ten times per hour per scenario, due to its long computational time (3 to 4 hours per run). The outputs of the simulations are the probability distribution of transmission system responses such as deployed regulating power (both automatic and manual, as well as upwards and downwards).

A linear model is then used to determine the regulating power price, and thereby the extra costs of using the regulating power market instead of the spot market to fulfil a commitment made on the day-ahead market (Skytte 1999). For this purpose, we use the spot price (from GRIMSEL) and the activated amount of regulating power quantities in both directions (from the Monte Carlo simulation). Using linear models and real data from 2019 to mid-2021, we calculate the aFRR prices using the spot price (by definition the aFRR prices are the tied to spot price ±20%), and mFRR prices using the spot price and the activated volume using Eq. 6.8 (see also Table 6.1).

$$P_X = a_3 * P_{Spot} * Q_X + a_2 * Q_X + a_1 * P_{Spot} + b \tag{6.8}$$

where X represents the type and direction of regulating power (i.e., aFRR or mFRR, upwards or downwards), P refers to prices (spot or regulating power price) and Q refers to the quantities of regulating power. Finally, a_1, a_2, a_3 and b are the linear model coefficients, that are displayed in Table 6.1. Supplementary Table D.4 displays the differences between the reported (real) and the modeled regulating power prices for the year 2020. Outliers (i.e., observations that lie at an abnormal distance from other values) are difficult to predict, in particular for mFRR. Moreover, it is noteworthy to mention that the amount of outliers also reduces the proportion of the regulating power price variance that is explained by the independent variables in the linear model (R^2 in Table 6.1). Note that we opt to model the

Table 6.1: Linear model coefficients of the regulating power price as a function of the spot price and the regulating power quantities, based on real data from 2020.*,** and *** indicate 0.05, 0.01 and 0.001 significance levels, respectively.

	a_3	a_2	a_1	b	R^2
P_{aFRR_+}	0	0	1.040559^{***}	8.529436^{***}	87.47
P_{aFRR_-}	0	0	0.76195^{***}	1.20292^{***}	92.10
P_{mFRR_+}	$8.46e-06^{***}$	$4.75e-05^{***}$	$-8.31e-03^{*}$	1.659	60.00
P_{mFRR_-}	$-4.90e-06^{***}$	$1.65e-04^{***}$	0.1854^{***}	-3.667^{***}	31.00

regulating power prices instead of the imbalance prices due to the low variance of the imbalance prices that can be explained based on a linear model using the spot price and the regulating power quantities as independent variables (R^2 is equal to 30% for long and 7% for short imbalance prices).

Using the spot price and automatic and manual frequency reserves prices, the imbalance prices are calculated based on Eqs. 6.1 to 6.4. The imbalance prices are the prices seen from the TSO point of view (i.e., Swissgrid). Since the TSO has to pay reserve and flexibility providers, the approach just explained allows us to determine the cost of the transaction and in that way to transfer the cost to the BRP, establishing the total cost of dispatched-by-design distribution systems.

6.2.3 Input data

A Swiss dataset comprising 636 households in Geneva (Pena-Bello, Barbour, Gonzalez, Yilmaz, et al. 2020) with a temporal resolution of 15-minute is used for the BASOPRA model. This temporal resolution provides a reasonable compromise between modeling technology performance and computational speed (Beck et al. 2016). Households included in the dataset have a median electricity consumption of 2.5 MWh per annum, within a range of 0.2-7.4 MWh per annum

We simulate PV generation using a standard one-diode model (Parra, Walker, and Gillott 2014) and PV technology with a nominal efficiency of 18.6% (*HIT photovoltaic module HIT-N2XXSE10 datasheet* n.d.), representative of the current state taking into account outdoor temperature and horizontal solar irradiance monitored for the year 2017. The model also includes a maximum power point tracker system, as is the case of most PV systems in order to maximize the output regardless of the environmental conditions (temperature and solar irradiance). For this model, the residential PV system sizes were established using a ratio of 1 kWp of PV for each 1 MWh of annual energy consumption (Litjens, Worrell, and van Sark 2018a; Hoppmann et al. 2014; Pena-Bello, Barbour, Gonzalez, Yilmaz, et al. 2020). Similarly, the battery sizes installed are of 1 kWh for each MWh of electricity demand, for instance, an annual electricity consumption of 5 MWh leads to a nominal PV capacity of 5 kWp and a battery capacity of 5 kWh (see Supplementary Information D.2.1 for further details on the model).

For the GRIMSEL model, the same input data that is presented by Rinaldi et al. (2020) is considered, with a building stock retrofitting rate of 1% per annum, and the use of air-source and ground-source heat pumps progressively replacing fossil heating in future scenarios (BAU and Fossil phase-out, in 2030 and 2050), with

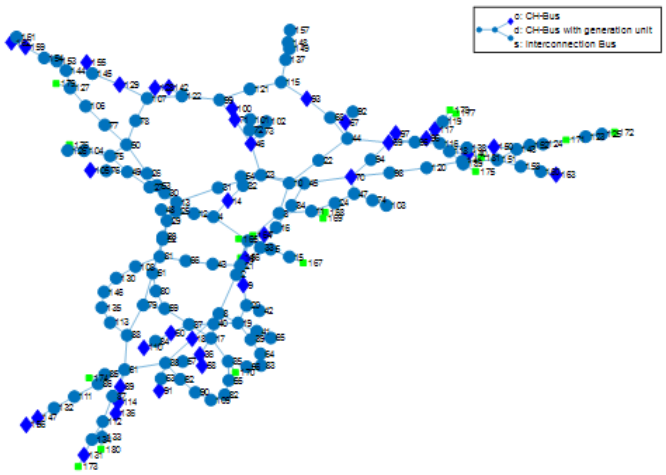

Figure 6.2: Swiss grid topology

COP values as a function of the outlet temperature.

For the Monte Carlo simulation, the extended high voltage grid topology for Switzerland including the interconnections with the neighboring countries is considered. The grid composed of 181 buses at either 380 kV or 220 kV connected through 209 transmission lines and transformers is depicted in Figure 6.2, with a total of 163 buses located in Switzerland and 18 in the neighboring countries. The unavailability and failure rates of the main components like transmission lines and transformers are obtained from the statistical data provided by European Network of Transmission System Operators for Electricity (ENTSO-E). Overall, 36 power generation units are connected to the grid representing medium and large power plants with total capacity of 17.2 GW. The unavailability and the failure rates of the generation units are determined as a function of the type of each unit according to the statistical data available in Guerrero-Mestre et al. (2020). For the base case, the total power demand is 8.1 GW which is distributed among the buses. Future scenarios for the capacity of generation units and distributed generations are generated with GRIMSEL. Moreover, for each scenario GRIMSEL provides the power generation per generation type, total demand, and interconnection power exchanges with one-hour resolution for one year. In the power system reliability simulator, the hourly generation, demand, and interconnection power are distributed among the buses and additional scenarios for unavailability of units and components as well as real-time uncertainties related to both demand and distributed renewable sources are considered in order to find the amount of flexibility required for a secure operation of the system. These uncertainties represent the difference between real-time power generation/demand and the outcomes of the markets (modeled in GRIMSEL) based on normal distributions. For the outage and unavailability, the value of Mean Time To Repair (in average between 8 to 24 hours) was assumed to be equal to 1 hour (Mousavi, Cherkaoui, and Bozorg 2012).

6.2.4 Electricity tariff design and battery applications

In this study, we consider the maximization of PV self-consumption in the residential sector and frequency control through an aggregator. The procurement of frequency regulation by means of an aggregator should be enabled by proper policy, whereas the maximization of self-consumption does not depend on the electricity tariff. A flat tariff of 0.22 USD/kWh throughout the year is assumed for all households. Based

on the sharp decline of FiT across many countries, the PV export price is assumed to correspond to the spot electricity price, as is the case for traditional electricity generators. Spot electricity prices from the day-ahead market in Switzerland (from EPEXSPOT, average price of 0.05 USD/kWh) are assumed. We use the difference between the balance energy price and the spot price for the year 2020 (see Eqs. 6.6 and 6.7), to calculate the revenue from frequency control, with an average price of 0.28 USD/kWh for upward control and 0.17 USD/kWh for downward control.

6.2.5 Techno-economic indicators

We use several indicators to analyze the evolution of the frequency market and the trade-offs between prosumer benefits and grid impacts when combining frequency control and self-consumption. To quantify the trade-offs for the prosumer and the grid, we study total self-consumption (TSC), which is the share of on-site PV generation that is used to cover the local electricity demand, and self-sufficiency (SS), which is the share of local demand that is covered by the on-site PV generation as shown in Eqs. 6.9 and 6.10. Additionally, we use the peak flow, i.e., the maximum between export and import power, and the equivalent full cycles (EFC, see Eq. 6.11).

$$TSC = \frac{\sum_{i=0}^{N} \left(E_{PV-total-demand} + E_{PV-batt}\right)}{\sum_{i=0}^{N} E_{PV}} \tag{6.9}$$

$$SS = \frac{\sum_{i=0}^{N} \left(E_{PV-total-demand} + E_{batt-load}\right)}{\sum_{i=0}^{N} E_{total-demand}} \tag{6.10}$$

$$EFC = \frac{\eta \cdot E_{PV-bat}}{C} \tag{6.11}$$

where $E_{PV-total-demand}$ is the share of PV generation that directly meets local electricity demand; $E_{PV-batt}$ is the share of PV generation that is charged into the battery; E_{PV} is the total PV generation; $E_{batt-load}$ is the amount of electricity discharged from the battery to cover local electricity demand; and C is the battery capacity.

In addition, we use the Net Present Value (NPV) to quantify the economic viability of installing a battery in an otherwise stand-alone PV system, which is relevant for prosumers from a financial point of view (see Eqs. 6.12 and 6.13). The NPV is calculated using annual project cash flows (CF) taking into account the difference between the cash flows from a PV-coupled battery system and a system with only PV. We also use the levelized cost of energy storage, LCOES (USD/kWh), that quantifies the cost associated with the total electricity supplied by the battery throughout the life of the system (see Eq. 6.14).

$$CF_{Batt_i} = CF_{PV-Batt_i} - CF_{PV_i} \tag{6.12}$$

$$NPV = \sum_{i=1}^{N} \frac{CF_{Batt_i}}{(1+r)^i} - \sum_{i=0}^{N} \frac{CAPEX}{(1+r)^i} \tag{6.13}$$

$$LCOES = \frac{\sum_{i=0}^{N} \frac{CAPEX}{(1+r)^i} + \sum_{i=1}^{N} \frac{OPEX}{(1+r)^i}}{\sum_{i=1}^{N} \frac{E_{dis-D}+E_{dis-FC}}{(1+r)^i}} \tag{6.14}$$

where $CF_{PV-Batt_i}$ is the cash flow of the PV-coupled battery system, CF_{PV_i} is the cash flow of the PV system alone and CF_{Batt_i} is the cash flow due to the installation of the battery system in Eq. 6.12. The $CAPEX$ represents the total capital expenditures (excluding the PV system), the OPEX are the operational expenditures (in USD), r is the discount factor (a weighting term that multiplies value to discount it back to the present value), i is the year and N is the lifetime of the project (30 years) in Eq. 6.13. Finally, E_{dis-D} and E_{dis-FC} are the energy discharged to cover the local demand and the energy discharged used for frequency control, respectively.

To quantify the total regulating power cost per year, the price of regulating power is multiplied by the average regulating power quantity obtained form the ten Monte Carlo simulations. To calculate the final cost of the imbalances that the TSO should cover (and charge to the BRPs), the total regulating power per direction and year is multiplied by the difference between the imbalance price and the spot price (see Eqs. 6.15 and 6.16).

$$Cost_{upwards} = (P_{upwards}) * (aFRR_{+} + mFRR_{+}) \tag{6.15}$$

$$Cost_{downwards} = (P_{downwards}) * (aFRR_{-} + mFRR_{-}) \tag{6.16}$$

6.3 Results

6.3.1 BASOPRA

The size of PV systems was established using a ratio of 1 kWp of PV for each 1 MWh of annual electricity consumption (Litjens, Worrell, and van Sark 2018a; Hoppmann et al. 2014; Pena-Bello, Barbour, Gonzalez, Yilmaz, et al. 2020). Similarly, the capacity of the batteries was sized to match 1 kWh for each MWh of electricity consumption. We set a reference case in which the batteries exclusively perform PV self-consumption as an application. Then, we compare various scenarios where the capacity of the batteries is shared to perform both PV self-consumption and frequency control (including both aFRR and mFRR), increasing the ratio dedicated to frequency control in steps of 25% up to 75%.

Self-consumption, self-sufficiency and equivalent full cycles

The median values of TSC and SS of residential PV-coupled batteries exclusively used for PV self-consumption are 39.7% and 56.7%, respectively, as shown in Figure 6.3a. However, the amount of TSC and SS is moderately reduced when a share of the battery capacity is further used for frequency control. With each increase of 25% of the battery capacity share dedicated to frequency control, there is a reduction of 4-5 percentage points on TSC and 6-7 percentage points on SS (p-values$<$0.05), reaching 25.7% and 36.9%, respectively when 75% of the battery is used for frequency control. Interestingly, the use of the battery for frequency regulation is significantly more cycle intensive than the use of the battery for PV self-consumption. For example, the median EFC values for a battery capacity share of 25%, 50% and 75% dedicated to frequency regulation are 456, 673 and 830 EFC per annum (p-values$<$0.05), compared to 231 EFC per annum in the case for PV self-consumption only. With such increase of EFC, the residential battery needs to be replaced up to

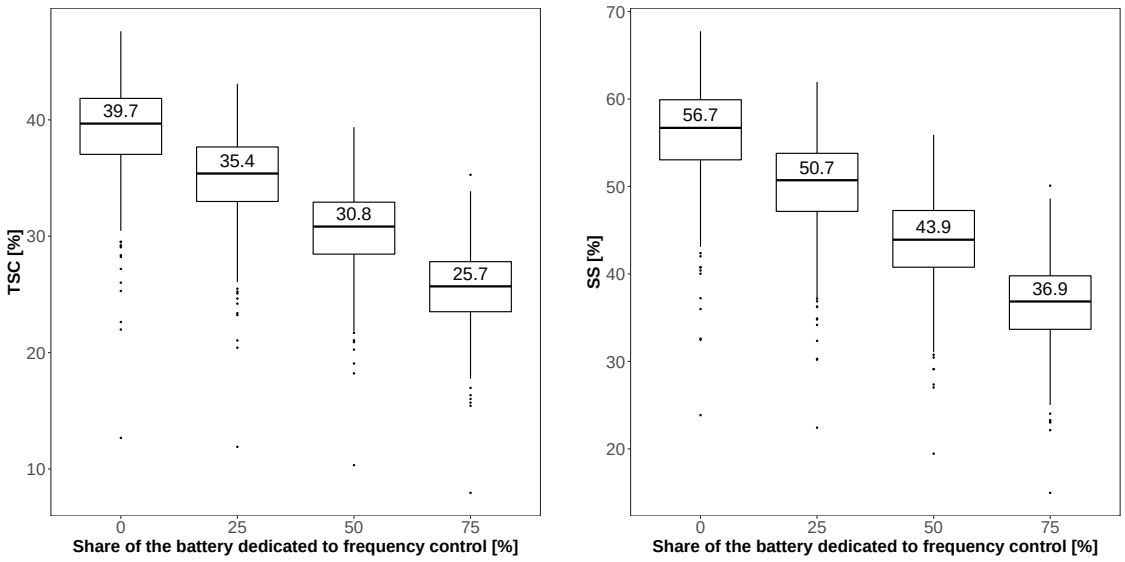

(a) Total self-consumption. (b) Self-sufficiency

Figure 6.3: Boxplots (N=636) of total self-consumption and self-sufficiency achieved by PV-coupled batteries depending on the share of the battery dedicated to frequency control. The median value for each boxplot is indicated in the figure

Table 6.2: Descriptive statistics of the peak flow (i.e., maximum between export and import power) of households with PV-coupled batteries depending on the share of the battery dedicated to frequency control.

FC Battery share	Min	Q1	Median	Mean	Q3	Max
0%	0.67	3.09	4.32	4.51	5.36	16.78
25%	0.64	3.34	4.72	4.87	5.82	18.81
50%	0.63	3.54	5.00	5.14	6.20	19.53
75%	0.67	3.63	5.16	5.31	6.51	20.27

five times throughout the PV lifetime, instead of one when it is used exclusively for PV self-consumption.

Peak flow

Table 6.2 shows the peak flow (i.e., maximum between export and import power) for the whole dataset of households, as a function of the share of the battery dedicated to frequency control. As there is more capacity dedicated to frequency control, the peak flow slightly increases from the reference case median peak flow of 4.3, to 4.7, 5 and 5.2 for a battery share of 25%, 50% and 75%, respectively, dedicated to perform frequency control (p-values$<$0.05, except for the difference between 50% and 75%, p-value=0.15).

Net present value and levelized cost

Figures 6.4a and 6.4b show the boxplots of the NPV and LCOES for all the households depending on the share of the battery dedicated to frequency control. The use

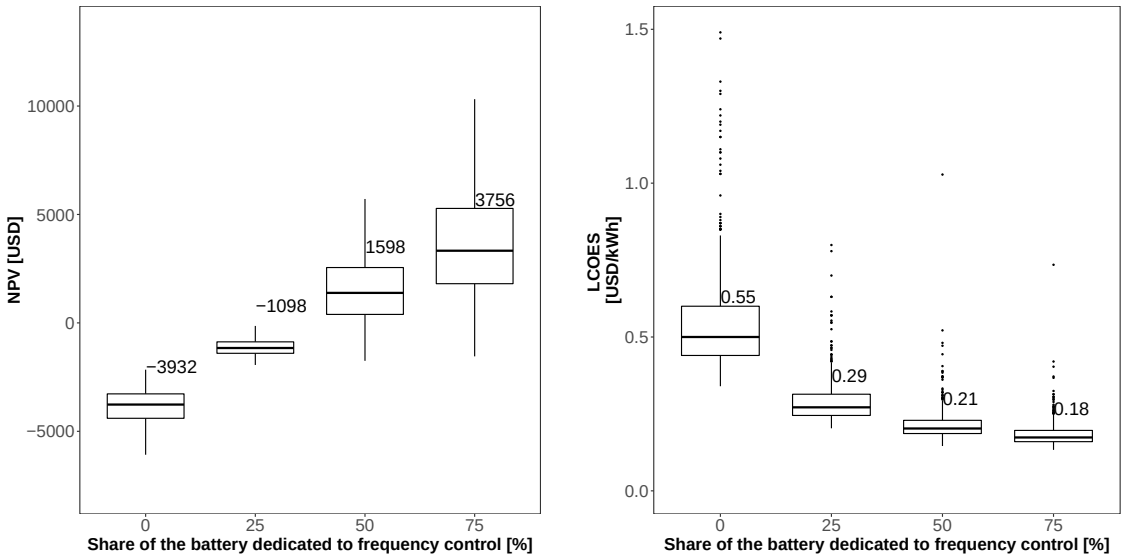

(a) Net present value (NPV)

(b) LCOES

Figure 6.4: Boxplots (N=636) NPV and LCOES achieved by PV-coupled batteries depending on the share of the battery dedicated to frequency control. The median value for each boxplot is indicated in the figure

of the battery exclusively for PV self-consumption yields negative NPV values with a median of -3932 USD, and LCOES values of 0.55 USD/kWh. With the addition of frequency control, the NPV increases considerably, reaching median values of -1098, 1598 and 3756 USD, for shares of battery capacity dedicated to frequency control of 25%, 50% and 75%, respectively. It should be noted that the NPV is positive even taking into account the more frequent battery replacement related to the performance of frequency control. As for LCOES, the median values decrease from 0.55 to 0.29, 0.21 and 0.18 USD/kWh. Especially the first step of increasing the frequency control from zero to 25% allows to significantly decrease by 47% the LCOES, while reducing TSC and SS levels by around 11%. All values are statistically significant (p-values$<$0.05). Finally, the median revenue from upwards regulating power is twice the revenue of downwards regulating power (346.3 USD per annum vs. 178 USD per annum), see Supplementary Table D.2, for descriptive statistics.

6.3.2 GRIMSEL results

For the four proposed future scenarios (i.e., 2030 BAU, 2030 fossil phase-out, 2050 BAU, and 2050 fossil phase-out), GRIMSEL models the Swiss energy system including various types of consumers and urban settings. Table 6.3 presents the capacity per technology for each scenario, showing that the output for PV capacity is close to the Swiss 2050 target (i.e., 36 TWh of PV energy), equivalent to a PV capacity of 31.5 GW, under the assumption of a capacity factor of 13% (Gupta, Sossan, and Paolone 2021). Figure 6.5 displays the spot price distribution per scenario using boxplots. The spot prices reflect the marginal costs of the most expensive power plant used at a given moment. The spot prices are similar across the scenarios for the same years but with respect to 2020 values, 2030 and 2050 median spot prices are 3.5 and 4.7 times higher, respectively. This high difference in the spot price reflects the use of the most expensive power plant, probably gas, and the future increase in fuel prices (Rinaldi et al. 2020).

Table 6.3: Installed capacity (in MW) and total demand (in TWh per annum) per technology per scenario

	Biomass	Geothermal	Li Batteries	Mineral oil	Natural gas	Nuclear	PV	Pumped hydro	Reservoirs	Run of river	VRFB	Waste	Wind onshore	Demand
2020	191.3	13.0	0.0	64.5	675.6	2874.5	1666.0	2435.5	9698.3	5334.4	0.0	470.2	240.6	60.7
2030 BAU	585.7	88.3	2392.9	17.2	1751.8	1194.0	11520.7	2469.4	9833.4	5408.6	0.0	532.1	705.8	64.1
2030 Fossil phase-out	585.7	88.3	2393.1	17.2	1751.8	1194.0	11520.9	2469.4	9833.4	5408.6	0.0	532.1	705.8	64.9
2050 BAU	674.8	556.8	16948.6	0.0	3449.1	0.0	27767.9	2580.4	10275.3	5651.7	1885.4	535.0	2334.2	71.5
2050 Fossil phase-out	674.8	556.8	18233.7	0.0	3449.1	0.0	28171.4	2580.4	10275.3	5651.7	2272.7	535.0	2334.2	73.3

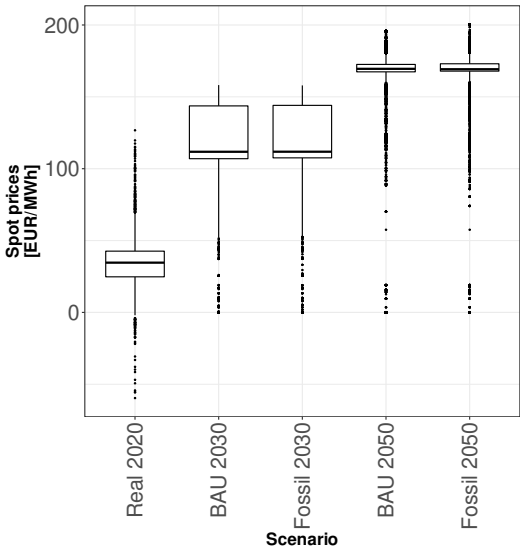

Figure 6.5: spot price boxplot (N=8760) per scenario

6.3.3 Monte Carlo simulation results

Figure 6.6 shows the statistical distribution of regulating power for a single simulation. Each simulation represents the occurrence of the uncertain parameters of the system including generation and load forecast error at each bus, availability of the transmission lines and transformers, and availability of generation units. Regarding the scenarios, the inter-quartile range (IQR) of the regulating power per total load distribution increases with the years, and remains similar within the same year. For example, the mean IQR for the ten simulations is 0.0135 for 2020, and for 2030 BAU and fossil phase-out scenarios, the mean IQR is 0.0152 and 0.0153, respectively. A higher IQR indicates a greater chance of extreme positive or negative events, in this case more regulated power per total load. A comparison of the activated reserves can be found in the Supplementary Table D.3. Table 6.4 presents the results of the Monte Carlo simulation per scenario.

Table 6.4: Average of the Monte Carlo simulation outputs per scenario per annum

	2020 Real	2020 Modeled	2030 BAU	2030 Fossil phase-out	2050 BAU	2050 Fossil phase-out
Positive regulating power [GWh]	311.15	307.45	360.18	355.1	478.85	502.49
Negative regulating power [GWh]	-340.88	-356.88	-428.68	-405.19	-501.36	-528.75
Positive regulating power per total demand	44.32	44.76	50.27	48.86	59.86	61.24
Negative regulating power per total demand	-48.89	-52.03	-59.15	-55.16	-62.4	-64.71

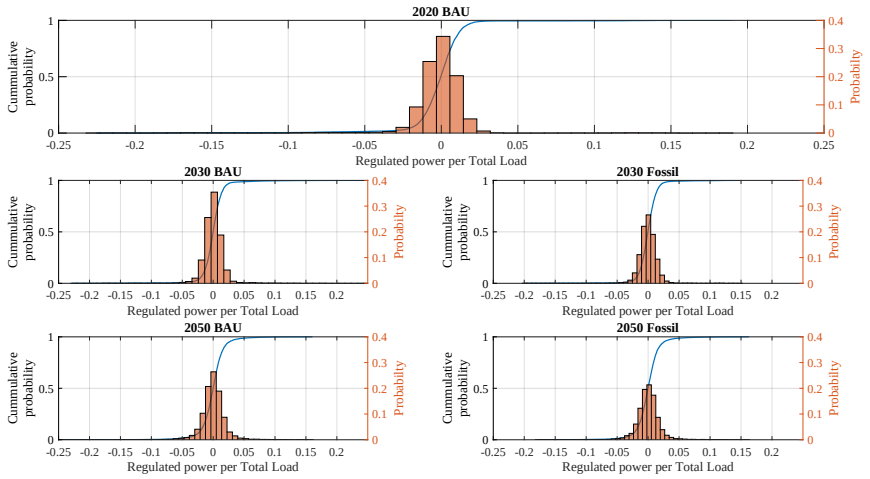

Figure 6.6: Regulating power per total load per scenario for one simulation

6.3.4 Linear model results

Making use of the spot electricity prices calculated with the GRIMSEL model and the total regulating power from the Monte Carlo simulation, we calculate the total annual cost per type of restoration reserve and per year, as indicated in Table 6.5.

For aFRR, the modeled values for the year 2020 are relatively close to the real values, with percentage errors of 2.2% and 18.5%, for positive and negative control, respectively. However, the errors for mFRR are important despite several efforts to reduce them (including consideration of transmission congestion, peak and non-peak, weekday and weekend, and seasonality). For more information about these errors, refer to Table 6.1, which shows the linear model coefficients of the regulating power price and the coefficient of determination, that is, the proportion of the variance for the regulating power prices that is explained by the spot electricity price and the regulating power. The coefficient of determination is very high for aFRR in both directions (87% and 92%), but for mFRR it is much lower (60% and 31%). These values for mFRR suggest that even if the predictors (the spot price and the regulating power quantities) are able to explain a non-negligeable part of the regulating power prices, the standard deviation of the errors is only 37% of the standard deviation of the real $mFRR_+$ price, and only 17% of the real $mFRR_-$ price (differences in descriptive statistics are shown in Supplementary Table D.4). This results in a underestimation of the total annual cost according to Table 6.5. Positive mFRR, however, has been the more costly service in 2019 and 2020 (18.6 and 21.7 millions of Euros, respectively), accounting for 82 and 94% of the total activation cost of the regulating power. Therefore, it is impossible for us to draw conclusions on the total projected cost of frequency control.

Figure 6.7 shows the imbalance prices for each scenario, however, these depend on the prices of the spot, aFRR and mFRR (see Eqs. 6.1-6.4), which make the modeled imbalance prices highly uncertain and rather unreliable (see also Supplementary Table D.4, for differences on descriptive statistics).

Table 6.5: Total cost of regulating power in Millions of Euros per annum per scenario.

	2020 real	2020 Modeled	2030 BAU	2030 fossil phase-out	2050 BAU	2050 fossil phase-out
$Cost_{aFRR_+}$	6,85	7.00	11,87	11,8	19,27	20,7
$Cost_{aFRR_-}$	-4,22	-5.00	-9,97	-9,51	-14,32	-15,37
$Cost_{mFRR_+}$	21,71	0,21	0,06	0,06	0,06	0,06
$Cost_{mFRR_-}$	-1,37	-0,51	-2	-1,91	-2,99	-3,22

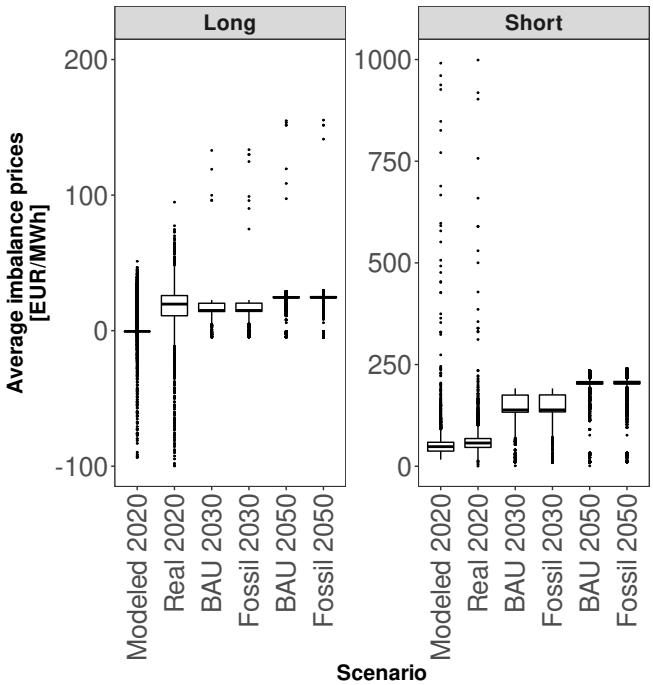

Figure 6.7: Boxplot (N=8760) of imbalance prices per scenario (based on the average regulating power of ten Monte Carlo simulations)

6.4 Discussion

Our results highlight that, to maximise the profitability of battery investments, prosumers should also provide flexibility to the energy system with frequency control. In this study, we consider that prosumers can directly participate in the frequency control market, by providing upwards and downwards regulating power (i.e., without considering the aggregator perspective in first instance). Without taking into account the compensation for power availability (i.e., remuneration for availability, in USD/kW), this approach allows us to consider the maximum revenues that prosumers can draw from regulating power (i.e., energy service only).

From the prosumer perspective, in line with the results from previous research (Schelly 2014; Engels, Claessens, and Deconinck 2017; Litjens, Worrell, and van Sark 2018b), it is clear that the provision of frequency control adds significant value, and it makes economic sense to increase the share of the battery that is used for frequency control. The combination of such application together with PV self-consumption reduces the levelized cost of battery storage, while also increasing the NPV, despite increasing ageing and related battery replacements. Importantly, the break even point is reached for cases where at least 50% of the battery is used for frequency control.

The use of the battery for frequency control also brings important trade-offs for prosumers, since self-sufficiency is moderately reduced by 6-7 percentage points with each increase of 25% of the battery capacity share dedicated to frequency control. Considering that motivations for investing on PV-coupled battery systems are diverse, e.g., self-sufficiency versus financial results (Korcaj, Hahnel, and Spada 2015), we argue that combining PV self-consumption and frequency control may not appeal all prosumers despite the economic advantage. It is worth mentioning that we did not find any indication of meaningful increase on the peak flow due to the participation of distributed batteries in frequency control services, which suggests that it is a grid-friendly strategy.

From our analysis of future scenarios for the Swiss energy system, we see that the amount of regulating power (i.e., the sum of aFRR and mFRR in each direction) is expected to increase by up to 60% throughout the energy transition, mainly due to the projected massive increase in PV capacity (see Table 6.4). This expansion of PV capacity will require further reserve capacities to be contracted by the TSO, to preserve the frequency in the required region. The TSO, however, will not bear with the cost of such reserve capacity and regulating power. This cost will be transferred (as it is now) to the Balancing Responsible Parties that cause the imbalances in the system, and this cost will probably be reflected in the bill of the final consumers of electricity.

With an increase in future reserve capacities, the figure of an aggregator in a future energy system is conceivable. However, in order to enable the emergence of aggregators, TSO requirements to provide aFRR and mFRR should evolve to allow the pool of such distributed energy resources. The relaxation of some of the requirements for prequalification, for instance on the verification of each individual asset that participates in the frequency regulation provision, would facilitate a business model for aggregators (Leisen, Steffen, and C. Weber 2019).

This paper also highlights the challenges associated with modeling prices of frequency control, and in particular those of manual frequency restoration reserves (mFRR). The mFRR prices proved to be hard to model, most probably due to their definition through auctions using pay-as-bid strategies. Moreover, it is difficult to

predict the future prices of mFRR, and therefore, there is an inherent uncertainty linked to this service. Accordingly, aggregators should be careful when designing the contract of mFRR services from distributed batteries to avoid economic losses. Deeper insight could be obtained by analysing the real probabilities of winning bids on the procurement of aFRR and/or mFRR in each direction. From the aggregator perspective, the provision of aFRR in Switzerland is more straightforward, since the prices are tied to the spot price, and therefore more easily forecasted for short time periods (e.g., intraday). Moreover, the upward regulating power (i.e., the increase of generation using both aFRR and mFRR) proved to offer more economic appeal for prosumers, since the median of the value associated to upwards frequency control was twice of the median value associated to downwards frequency control (i.e., median annual values of 346 USD and 178 USD per annum, respectively), across all the cases.

The limitations of this study lie mainly on the fact that we consider the maximum revenues that can be drawn from frequency control provision, for which we consider both aFRR and mFRR products, that are weekly or four-hourly products, and therefore the provision of both products may not be guaranteed throughout the whole year. Additionally, our analyses are based on the maximum economic potential since we assume that residential batteries can deliver the four frequency control services (namely $aFRR_+$, $aFRR_-$, $mFRR_+$, and $mFRR_-$) all year round, which may not be plausible in reality (see for instance the work of Biggins et al. (2022) on probabilities to get auction bids accepted in the UK frequency market). Another caveat to be considered, is the accumulation of the model-specific uncertainties about parameter values, input data or model structure, which leads to a cascade of uncertainty. Moreover, while the future diffusion of heat pumps has been accounted for in our model, their use for frequency control has not been considered. Similarly, we have not considered the electricity demand increase due to the grow of the electric vehicle market, which could become important in the coming years, also for aggregators providing frequency services. From the regulatory point of view, Switzerland is expected to join the European integration of frequency control services, MARI, PICASSO and TERRE. This European integration would change the requirements to participate and potentially reduce the amount of regulating power required in the future, since it would be an integrated European service, however, at the moment it is still unclear whether Switzerland will be part of such integration as a third-country or not due to the lack of an electricity agreement with the European Union. Finally, further uncertainty is linked to Swissgrid's plan to carry out a reform of the pricing mechanism to improve market liquidity and price signals, by harmonising prices and creating incentives for an efficient balancing (Swissgrid 2020).

6.5 Conclusions

This paper quantifies the various impacts for prosumers related to the use of PV-coupled batteries for increasing their self-sufficiency and providing flexibility to the whole energy system with frequency control, under the management of an aggregator. We present an open-source PV-coupled battery model which use input data of historical market prices data for 2020 and monitored smart meter electricity consumption from 636 Swiss households. We quantify the Swiss capacity requirements of dispatched-by-design distribution systems, where batteries are deployed in the

distribution grid to dispatch the operation of traditionally stochastic prosumption peak flows. Finally, we attempt to model future frequency control prices with limited data (spot prices and regulating power quantities), which proved to be complex, in particular for mFRR.

According to our results, the participation of prosumers in the frequency control market through an aggregator makes economic sense, since performing both frequency control and PV self-consumption significantly reduces the levelized cost and increases the net present value, in spite of the considerably reduced battery lifetime as a consequence of frequency control. However, the self-consumption and self-sufficiency rates of prosumers are reduced by 6 and 4 percentage points, as the share of the battery dedicated to frequency control increases by 25%. This limitation may prevent some prosumers who prioritize self-sufficiency from joining an aggregator. Based on our results, we also recommmend that prosumers interested in providing frequency control consider a 25% share of the batteries dedicated to frequency control, for which an attractive trade-off between LCOES on the one hand and total PV self-consumption and self-sufficiency levels on the other is found. A 25% may also be accepted by a large share of prosumers, since most of the battery capacity is still used to run their own houses.

Chapter 7

Conclusions

7.1 Summary

This thesis aims to contribute to the literature by analyzing trade-offs between prosumers benefits, in particular in the residential sector, and grid impacts for various PV-coupled battery configurations. As distributed PV is expected to continue to massively grow in the context of the energy transition across the globe, increased stress on the distribution grid is expected mainly due to PV feed-in, but also to the increase of peak power demand through the decarbonization of the transport and heating sectors. To mitigate these impacts in a decarbonized energy system, synergies among low-carbon technologies are required. Increased levels of flexibility facilitate the integration of high amounts of PV, since they optimize grid asset use to maintain the balance between demand and supply, can manage network congestion, and defer network reinforcement. However, this flexibility needs to be enabled through incentives and managed by technology and algorithms that allow the users to respond in real-time to such incentives.

Through this study, we seek to shed light on different technologies and strategies to jointly increase prosumers benefits and to reduce the stress on the distribution grid. The use of PV-coupled batteries, heat pumps, and thermal storage is studied and compared when promoting self-consumption, flexibility, and services to the grid such as peak reduction and frequency control while quantifying the benefits for the prosumers. We further explore the unexploited economic benefit that can be reaped by adding different applications performed by the storage system, along with the increase of self-consumption, referred to as the combination of application or benefit stacking. In a first instance, we analyze avoidance of PV curtailment, demand load shifting, demand peak-shaving, peer-to-peer trading and frequency control, on top of PV self-consumption. These applications respond to different policy mechanisms, incentives and tariff structures. In this regard, we address the following two research questions:

Research question A

To which extent can the combination of applications help to increase the financial revenue of energy storage in the residential sector?

Research question B

What are the trade-offs between prosumer benefits and grid impacts in single-family houses with PV and energy storage with access to multiple revenue streams?

To answer these questions, we develop an open-source 24-h optimization framework for battery dispatching (i.e., Battery Schedule OPtimizer for Residential Applications, BASOPRA), subsequently expanded to optimize heat pumps and thermal storage operation, for space heating and domestic hot water (DHW). This optimization framework allows us to explore the performance of the storage systems when combining applications such as self-consumption, avoidance of PV curtailment, demand shifting, demand peak-shaving, and frequency control.

The operation of smart residential storage systems and heat pumps, and the applications that can be considered, mainly depend on the energy tariff structure (e.g., capacity-based tariffs) and on energy policy and regulation (e.g., PV curtailment). In the context of this thesis, we consider the deployment of capacity-based tariffs to reduce the grid impacts of PV, heat pumps, and EVs in the near future. Additionally, we consider the possibility of a physical feed-in limit of 50% of the nameplate PV-system capacity as a preventive measure to keep the power system stable during periods of high PV production, and the reduction of the feed-in tariffs, which is assumed to match the wholesale electricity price as is the case for traditional electricity generators.

Furthermore, we look into two emerging electricity market participants, namely aggregators and P2P communities. The former are considered in the case of residential batteries providing frequency control, to pool together enough storage capacity to participate in the Swiss frequency market, whereas the latter are considered to explore the influence of trading preferences, translating the findings from the psychological research to the engineering field, and expanding the development of human-centered energy systems, which leads to the last research question of this thesis:

Research question C

How does a P2P community based on actual trading preferences performs at the individual, collective and grid level?

We address this question through an interdisciplinary study that assesses P2P trading decisions of German homeowners on the basis of an online experimental study, and simulates how various decision-making strategies could impact the performance of P2P communities.

7.2 Key findings in the context of the energy transition

The studies in this thesis build upon the importance of decentralized energy storage, and in particular, of lithium-ion batteries, for the energy transition as means to increase PV adoption while reducing PV impacts on the distribution grid. However, batteries are not yet cost-effective. Economies of scale, innovation, and competition between different types of lithium-ion batteries have enabled average lithium-ion

battery cell cost to drop by 82% since 2012, but further cost reductions are still required, in particular, for residential storage to become cost-effective.

In order to make residential storage cost-effective, we study how the combination of applications can contribute to earlier break-even points for residential batteries than when batteries are used only for PV self-consumption, in two different geographies, Geneva (Switzerland) and Austin (U.S.). In order to reach economic profitability, batteries require further cost reductions regardless of battery technology. When all applications are combined, NCA-based batteries are closest to profitability. They require only 35% reduction in total costs to be profitable in Switzerland and 40% in the U.S. NMC-based batteries in Switzerland require a 30% reduction in total costs, however, in the U.S. this increases up to 55% (see Figure 2.7). Analogously, from the prosumer point of view, it represents an increase of the battery Net Present Value (NPV) of the battery system by 66%. The combination of applications hence allows to reach cost-effectiveness of residential storage more quickly under the condition of adequate incentives, while incentivizing the prosumers to optimize the use of their batteries. Importantly, the combination of applications for residential batteries significantly increases their value without substantially reducing the battery life nor prosumer's PV self-consumption (see Subsection 3.3.2).

In addition, we have highlighted the importance of energy policy and electricity tariff design to alleviate grid stress, modify prosumer interactions with the grid and mitigate the impact of PV penetration. We analyzed the impact of regulation-based PV curtailment and found it to be more interesting from the grid perspective than from the prosumer perspective, offering indirect benefits for grid operation and grid stability that cannot be neglected. On the other hand, PV curtailment can potentially discourage prosumers to install large PV systems, depending on how PV curtailment is enforced from the regulatory side. Moreover, we evaluated the use of TOU tariffs to reduce the consumption of grid electricity during peak time, which in general increases the number of cycles of the battery due to grid charging at off-peak time, reducing the levelized cost of the battery, and provides synergies with demand peak-shaving. However, it barely increases the NPV of batteries.

Throughout this thesis, we explore the combination of volumetric tariffs and capacity-based tariffs. The main reason for the promotion of capacity-based tariffs is the reduction of electricity consumption due to PV penetration and therefore the decrease of the prosumers' contribution to cover the grid costs, resulting in losses for the DSOs. Capacity-based tariffs may hence allow DSOs to recover their investment while ensuring the supply of energy and the safety of the grid.

Capacity-based tariffs can additionally be seen as a mechanism to reduce the impact of PV feed-in on the distribution grid, incentivizing batteries to perform demand peak-shaving while increasing self-consumption. Capacity-based tariffs can also provide benefits for the wider energy system, since electricity peaks are typically met by more costly and carbon-intense generators, and therefore the reduction of such peaks may lead to a reduction of energy costs and carbon dioxide emissions at the aggregated level. Moreover, at the residential level, batteries performing demand peak-shaving, which is enabled by capacity-based tariffs, were found to have on average a 15% higher NPV than other combination of applications. Therefore, through the implementation of capacity-based tariffs, prosumers with smart systems and residential storage can help to reduce the stress on the grid while improving battery profitability for all household types, regardless of the consumption bracket or the load profile. Regarding the impact of capacity-based tariffs on residential heating decarbonization (see Chapter 4), we found that depending on their presence

or absence, energy storage can be a two-edged sword by either reducing or increasing the household's peak flow compared to a base case without energy storage. Without capacity-based tariffs an increase in peak demand is, therefore, to be expected as electrification of the heating sector advances, in particular in poorly insulated single-family houses.

However, capacity-based tariffs may incur significantly higher costs for some households and may consequently have a disruptive impact if implemented without accompanying measures (Azarova et al. 2018). In addition, for the Swiss case, under the presence of capacity-based tariffs, it was found that the power exported by prosumers determined the maximum peak flow in well-insulated houses (i.e., renovated and new single-family houses, see Chapter 4). Depending on the regulatory framework, charging prosumers for their power injections into the main grid may not be possible (as is the case in Switzerland today), to avoid charging the users two times for the same service (if prosumers have already been charged on the imported power). This opens a new regulatory debate as the countries pursue the energy transition, since policy-makers aim to rapidly increase PV penetration to decarbonize the energy system, and DSOs need to continue to ensure the security of the distribution grid (and their revenue), but they may not be in the position to address the main cause of future power peaks, i.e., PV installations. In the particular case of Switzerland, where most PV installations are expected to be roof-mounted, larger residential installations than those assumed in this thesis (based on the median residential size or on the total demand) are expected as PV cost declines and therefore higher peaks of injected power.

Concerning the decarbonization of the heating sector, the differences in building envelope quality were found to be crucial for the grid impact of single-family houses using heat pumps. In modern and renovated single-family houses, the peak flow after the installation of PV and heat pumps was found to remain around the same values as before the installation of both systems. However, in poorly insulated single-family houses, the need to install larger heat pumps to cover the heat demand induces an increase in the peak flow that can only be slightly reduced when capacity-based tariffs are used. Therefore, in addition to reduce carbon dioxide emissions and increasing comfort levels (Streicher, Padey, Parra, Bürer, S. Schneider, et al. 2019; Narula et al. 2019), thermal retrofitting has an important role to play in the reduction of grid stress in the future decarbonized heating sector.

We found that prosumers with PV-coupled heat pumps systems aiming to increase their share of PV self-consumption and self-sufficiency in an economically viable way should use their heat pump to also supply domestic hot water next to space heat. This reduces the levelized cost of electricity consumption and it increases the self-consumption by 10%, while representing only a small extra capital investment for the DHW storage (around 1000 CHF, in Switzerland). As a second step, the installation of a heat storage system allows to increase self-consumption and self-sufficiency by another 2 to 6 percentage points at relatively low cost. Batteries are the last option, mainly due to their high cost, despite their capacity to increase self-consumption and self-sufficiency by 2-20% beyond the levels of the previously mentioned systems.

For P2P communities, we found evidence that social empowerment may lead to benefits for the community members, independently whether they are prosumers or traditional consumers. The latter were found to reap the highest financial benefits under the proposed market mechanism, which may lead to distributional energy justice problems, since the actors that invest less enjoy higher benefits. Therefore, fairer

distribution of P2P community costs should be explored, for instance, through differentiated membership costs. In terms of power exchanges with the grid, despite the reduction of average power peaks due to higher self-consumption at the aggregated level in P2P communities, compared to a traditional self-consumption maximization strategy, the extreme events (i.e., maximum power drained and injected) remained unchanged. This result implies the need to introduce other strategies to reduce grid stress at the community level, as the ones previously discussed here (e.g., PV curtailment or capacity-based tariffs), or to further use of flexibility through demand-side management or changed prosumer behavior through incentives, before tapping into more costly solutions at the distributed level such as the installation of voltage regulated distribution transformers or even grid reinforcement.

Finally, we considered the procurement of frequency regulation by means of an aggregator. According to our results, the provision of such a service can be a profitable service for the prosumer, but it is linked to a high degree of uncertainties that should be mainly bore by the aggregator at the moment of bidding and committing assets to provide frequency control services. In line with previous research, frequency control was found to bring high value to the battery, considerably reducing the median levelized cost from 0.55 to 0.29 USD/kWh when only 25% of the PV-coupled battery capacity is dedicated to frequency control. In this same case, the median net present value increases by USD 2830, however, the battery lifetime is considerably reduced from 13 to 9 years due to additional cycling for frequency control. As expected, there is a trade-off, which implies a reduction in self-consumption and self-sufficiency, however, it is moderated up to 6 and 4 percentage points, respectively, as the share of the battery dedicated to frequency control increases by 25%. This limitation may prevent some prosumers who prioritize self-sufficiency from joining an aggregator. Prosumers and aggregators interested in entering the frequency market may consider testing the economic viability with a 25% share of the batteries dedicated to frequency control, for which an attractive trade-off between LCOES on the one hand and total self-consumption and self-sufficiency levels on the other is found.

The amount of regulating power was found to increase by up to 60% across the energy transition, mainly as a result of the PV capacity increase. This increment in regulating power opens the door to new business models, like aggregators, in particular, because distributed energy resources, such as PV, batteries, electric vehicles, and heat pumps, continue to grow. However, the future revenues from frequency regulation services were found to be difficult to model, reflecting a high degree of uncertainty for the aggregator's business model.

7.3 Summary for policy and decision-makers

Figure 7.1 displays a summary of the trade-offs that are found across this thesis, in the form of a schematic. Please note that the comparisons are done inside every chapter and not across chapters since some hypothesis, applications and indicators change from chapter to chapter. Moreover, in Chapter 4 for the three analyzed devices (battery, DHW storage and space heating storage), two options appear depending on the presence or absence of a capacity-based tariff, and therefore of demand peak shaving.

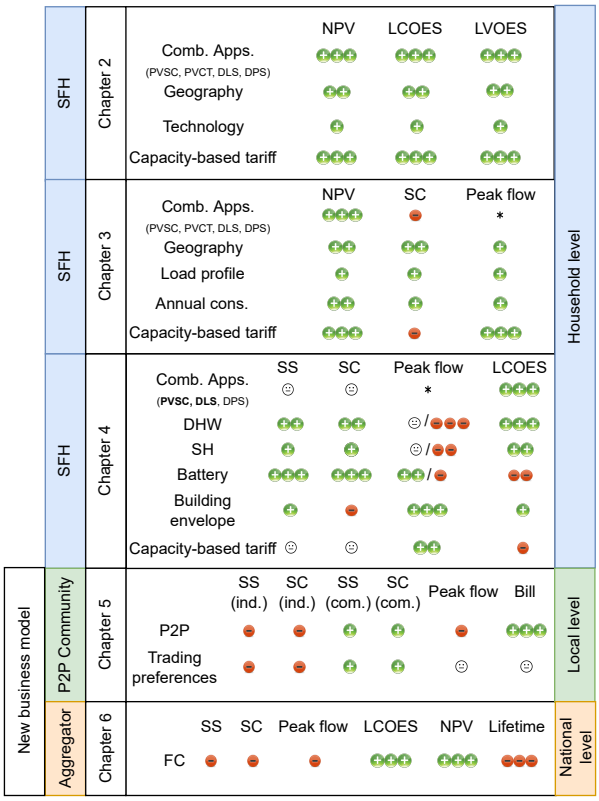

Figure 7.1: Schematic representation of the trade-offs per chapter. The comparisons are made within chapters and not across chapters. The asterisk (*) indicates a dependency on the presence of a capacity-based tariff. The neutral emoji indicates indifference. Note that in Chapter 4 we compare PV self-consumption and demand load shifting with PV self-consumption, demand load shifting and demand peak shaving. In Chapter 5, *ind.* stands the for individual level and *com.* stands for the community level, and the comparison of P2P is made with prosumers following a self-consumption strategy. In Chapter 6 the comparison is between PV self-consumption and frequency control (FC).

Recommendation I:

Electricity tariffs which fit for the purpose can effectively increase residential PV system flexibility, e.g., by enabling energy storage to perform different applications that can help to reduce the grid stress and increase the financial benefits for the prosumers.

Recommendation II:

Capacity-based tariffs can effectively mitigate distribution grid impacts by promoting a reasonable exchange with the grid, but should be carefully designed to avoid disruptive impacts on households' budgets while ensuring DSO revenue.

Recommendation III:

Under current technology costs, the following steps are recommended to increase the share of PV self-consumption and self-sufficiency in single-family houses with PV-coupled heat pump systems: first, to supply also domestic hot water in addition to space heating; secondly to install heat storage; and lastly, to use a battery.

Recommendation IV:

Systematic building energy retrofitting holds the key to substantial energy savings, carbon dioxide emissions reduction, and to help alleviate the impact of electrification of the heating sector on the grid.

Recommendation V:

In P2P communities, a fairer distribution of community costs is needed to avoid distributional energy justice problems, since pure consumers reap the highest financial benefits under the proposed market mechanism.

Recommendation VI:

P2P communities are useful to reduce the so-called duck-curve (based on average power exchanges with the grid), but not to mitigate the maximum power exchanges with the grid. Therefore, other mechanisms to reduce the impact on the grid should be explored.

Recommendation VII:

The provision of frequency control by means of an aggregator can be a profitable service for the prosumer reaching positive NPV (with a median value of USD 3756) and lower levelized cost of storage (up to 67% reduction with respect to a battery providing PV self-consumption only), but it is linked to a high degree of uncertainties that should be mainly bore by the aggregator.

Recommendation VIII:

Frequency control provision by residential batteries was found to reduce self-consumption and self-sufficiency by 6 and 4 percentage points as the share of the battery dedicated to frequency control increases by 25%. Furthermore, the battery lifetime decreases to five years (with 75% of the battery used for frequency control) instead of 13 years, when the battery is used for PV self-consumption only (median values), due to the increase in the number of cycles.

Recommendation IX:

The amount of regulating power was found to increase by up to 60% across the energy transition, mainly as a result of the PV capacity increase.

7.4 Future work

The presented work could be advanced in several different directions to further increase and accelerate PV penetration, supporting the energy transition, and reducing the distribution grid stress. In particular, in a near future with a high penetration of EVs, it is important to assess the behavior of EVs under different tariff scenarios and policy incentives, as well as their synergies or trade-offs when compared to stationary storage providing grid services. Moreover, the role of EVs at the community scale, and the role of trading preferences with respect to the possibility to allow a

third actor to interact with their vehicle appear as the next steps to continue the research on human-centered energy systems.

The inclusion of power flow analysis and the analysis from the DSO point of view are as well two important next steps to better understand the impact of low-carbon technologies as enablers for PV. These analyses should be done together with local DSOs since the data is not publicly available and the results of such studies may be interesting for local actors, however, they may lose generalizability due to the significant differences among distribution grids across different areas and countries, therefore calling for a sufficiently large number of distribution grids to be assessed. Different forecast strategies and their accuracy may lead to different results. Having assumed perfect foresight, forecast strategies were not within the scope of this thesis. However, their financial implications for the prosumers may be significant, in particular when monthly capacity-based tariffs are involved. Capacity-based tariffs with lower resolution (e.g., weekly or daily) can result in better results for the prosumers and the grid, due to lower errors of forecasting and higher capability of adaptation from the prosumers.

The analysis of buildings' thermal inertia and its simplified representation in the model (average inertia) could lead to more accurate results, in particular for buildings with poor envelope quality. However, this needs further empirical analysis and dedicated modeling.

Alternative pricing mechanisms or auction systems that account for user preferences in P2P communities should be explored. Finally, in order to ensure the validity of the results presented, large-scale field trials, including an in-depth analysis of user decision-making, would be a logical extension of this work.

Appendices

Appendix A

Supplementary Information - Electrochemical storage Part A

A.1 Material and method

Fig. A.1 is a schematic representation of our method. In first place, we specify the input data for electricity demand and PV generation (Section A.1.1). The applications and their combinations are subsequently defined along with the respective electricity tariff structure (Section A.1.1). Then, the battery technologies, system topology and components are presented (Sections A.1.2 and A.1.3). Thirdly, our schedule optimization is described (Section A.1.4). Finally, we present the techno-economic performance indicators (Section A.1.5). Across the study we use USD as common currency for both locations[a].

A.1.1 Input data

Demand and PV generation

We use electricity consumption data with 15-minute temporal resolution monitored in single dwellings in Western Switzerland (636 dwellings) and Austin, Texas (308 dwellings) during the year 2015. Considering this amount of data, we opt to form representative consumer groups in order to reduce the computational time required. To generate these representative consumer groups, we employ clustering to produce groups of consumers with similar behaviors. We split the consumers according to their annual consumption into 3 separate groups, i.e., a low, medium and high consumption group in both locations. Finally, within these 3 groups we cluster based on the average daily load profile. We opt to produce 4 clusters in each consumption bracket, noting that the selecting the number of clusters in highly dimensional data is a difficult task. From each cluster we select the household that is closer to the centroid which is subsequently optimized. The results presented in this study are the average of the four representative households of each cluster per consumption bracket.

Environmental variables including outdoor temperature and horizontal solar irradiance monitored across both locations are used to model PV generation. We simulate PV generation using a standard one-diode model and PV panel input data with a nominal efficiency of 18.6%, representative of the current state of the art

[a]Exchange rate used: 1 USD/CHF.

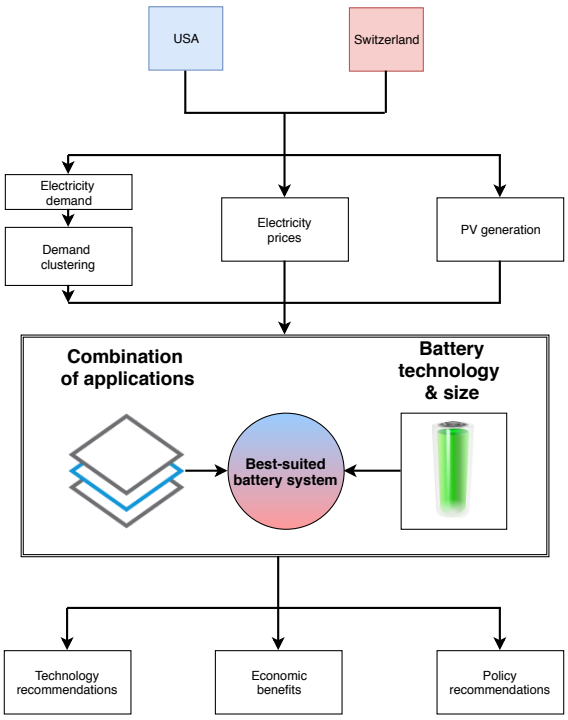

Figure A.1: Schematic representation of the modeling approach proposed.

(*HIT photovoltaic module HIT-N2XXSE10 datasheet* n.d.). The model also includes a maximum power point tracker system, as is the case of most PV systems, to maximize the output regardless of the environmental conditions. The PV system's installed capacity is modeled based on the empirical distribution across Switzerland[b] and Texas[c] (see Section 1.3 of the supplementary information). We finally focus on the median PV size of the distributions for our baseline results (i.e., unchanged PV size), while alternative scenarios including the 25th and 75th percentile are shown in Section 5 of the supplementary information.

Electricity tariff and battery applications

The operation of a residential battery as well as the number of applications it can deliver depends on the tariff structure. In this study we include all existing consumer applications (see Fig. A.2), excluding back-up power since we focus on distribution areas with a high level of grid stability (for both utilities referred in this study, the number of minutes of power failure experienced by a typical customer in a year was below 100 minutes in 2016[d]). Since there is not a market mechanism incentivizing the export of electricity from residential batteries to the main grid, this case is not considered either.

Electricity prices used in this study are based on available tariffs which are offered by the local utility companies in the two locations. Both, single tariffs and double tariffs (with a peak and off-peak periods) are considered in the analysis. In Switzerland, double tariffs are applied all-year-round, while in the U.S. they are applied only in summertime. The export price is assumed to be the wholesale

[b]Swiss Federal Office of Energy

[c]https://openpv.nrel.gov

[d]For the utility in Texas, the number of minutes of power failure amounted to 95.6 minutes (which is 30% lower than the average in the U.S. (Lim and Yurukoglu 2018)) while it was only 7.8 minutes in the canton of Geneva.

Table A.1: Various electricity tariffs components depending on the bill structure and for the two locations used in this study to test various battery applications.

Name		Units	U.S.	Switzerland	Based on
Flat Tariff		USD/kWh	0.073	0.22	Energy
Double Tariff	On-peak[a]	USD/kWh	0.183	0.24	Energy
	Off-peak	USD/kWh	0.056	0.152	Energy
Export price		USD/kWh	0.027[b]	0.047[b]	Energy
Capacity tariff		USD/kW/month	10.14	9.39	Power
Feed-in limit		$\%kW_{p-PV}$	50%	50%	Regulation

[a] In the U.S. on-peak time is only from June to September from 1 p.m. to 7 p.m. on weekdays. In Switzerland, on-peak time is all year-round from 7 a.m. to 10 p.m. on weekdays and from 5 p.m. to 10 p.m. on weekends.
[b] We use real hourly wholesale price for ERCOT and EPEXSPOT markets. The price shown in the table is the average wholesale price.

electricity price as is the case for traditional electricity generators. This is already the case in Switzerland for installations which are on the waiting list to be granted a one-off subsidy for the capital investment in PV (Husser, Pius 2017) and this is expected to become a widespread policy as a consequence of falling cost of PV technology. We use 2015 wholesale electricity prices from the day-ahead market for Texas (ERCOT southern load zone) and Switzerland (EPEXSPOT). It is important to note that, apart from the electricity price, electricity bills include other fixed costs as well, such as taxes and grid usage.

Capacity tariffs, which bill the peak electricity demand (i.e., in USD/kW) during a billing period, have been widely applied for large consumers, typically belonging to the secondary and tertiary economic sectors. For residential customers capacity tariffs have only being marginally applied (e.g., by the Arizona Public Services in the U.S.), although their implementation is being suggested following the penetration of air conditioning, heat pumps and electric vehicles (AEMC 2014). As a first attempt to include them we assume capacity tariffs applied to large consumers by the local utilities in the two locations. Finally, following the example in Germany, a (physical) feed-in limit of 50% of the nameplate PV-system capacity for both countries is assumed as a preventive measure to keep the power system stable during periods of high PV production (Hesse, Martins, et al. 2017). Table 2.1 provides the input data for every battery application depending on the tariff structure.

For the baseline scenario, we assume a flat retail tariff and the exclusive usage of batteries for PV self-consumption in agreement with most residential grid-tied battery systems installed worldwide (Pena-Bello, Burer, et al. 2017). Then, the bill structure is modified by adding step by step the components shown in Table A.2 (Combination 2-5) and the various combinations of applications are therefore always tested including PV self-consumption. For instance, in combinations assuming a double tariff instead of a flat tariff, we assume inclusion of demand load-shifting as strategy. Finally, a case in which all applications are combined is also presented below while results for other combinations including three applications are shown in Section 5 of the Supplementary Information.

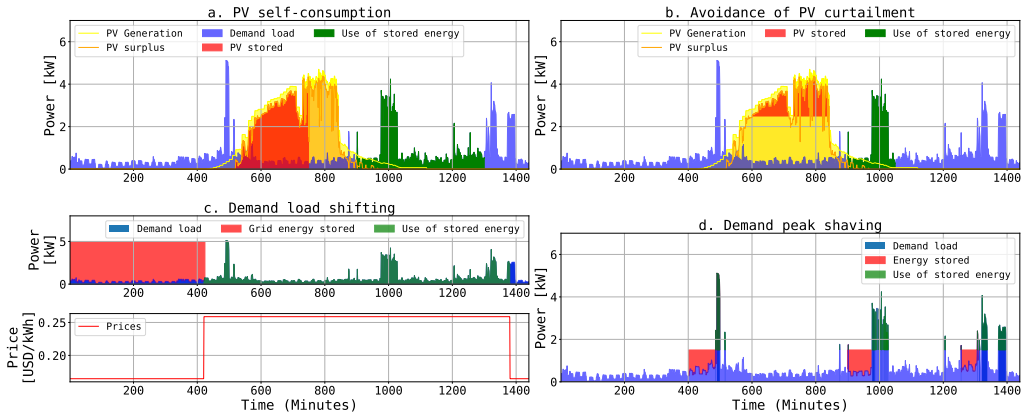

Figure A.2: Schematic representation of the four applications analyzed in this study. a. PV self-consumption, b. Avoidance of PV curtailment, c. Demand load shifting and d. Demand peak shaving.

Table A.2: Various combination of applications and the respective electricity tariff structure compared in this study. If the application indicator is ON, it means that the referred application is included in the combination, same is valid for the electricity tariff structure indicators.

Combination name	Applications				Electricity tariff structure			
	PV Self-consumption (PVSC)	Avoidance of PV curtailment (PVCT)	demand-load shifting (DLS)	Demand peak shaving (DPS)	Flat tariff (FT)	Double tariff (DT)	Capacity tariff	Feed-in limit
Combination 1 (Baseline scenario)	ON	OFF	OFF	OFF	ON	OFF	OFF	OFF
Combination 2	ON	OFF	OFF	ON	ON	OFF	ON	OFF
Combination 3	ON	OFF	ON	OFF	OFF	ON	OFF	OFF
Combination 4	ON	ON	OFF	OFF	ON	OFF	OFF	ON
Combination 5	ON	ON	ON	ON	OFF	ON	ON	ON

Table A.3: Battery specifications for the six technologies compared in this study. SOC denotes the state of charge.

Technology	Cathode Material	Cycles @ DoD	Maximum lifetime [years]	Roundtrip Efficiency	Energy Costs [USD/nominal kWh]	Maximum charge/ discharge rate [kW]	ΔSOC	Maximum SOC	Minimum SOC	Cycle & calendar aging factor per year[a]	Reference
Li-ion	NMC	5000 @ 100%	15	91.8%	410	0.4*C	1	1	0	0.059 & 0.07	(ITP Renewables 2016; ITP Renewables 2017; Tesla 2015)
	NCA	8000 @ 100%	20	92.5%	650	1*C	1	1	0	0.047 & 0.05	(Trina BESS 2017)
	LFP	6000 @ 100%	20	94%	980	2*C	1	1	0	0.024 & 0.05	(ITP Renewables 2016; ITP Renewables 2017; Sony 2017)
	LTO	15000 @ 100%	25	96.7%	1630	4*C	1	1	0	0.003 & 0.04	(Leclanche 2015), personal communication
Lead-acid	VRLA	1500 @ 50%	10	85%	330	0.1*C	0.5	1	0.5	0.236 & 0.1	(Hesse, Martins, et al. 2017; Sonnenschein 2013)
	ALA	4500 @ 70%	15	91%	750	1*C	0.7	0.9	0.2	0.06 & 0.07	(ITP Renewables 2016; ITP Renewables 2017; Ecoult 2017)

[a] The cycle aging factor is given for a 50% depth-of-discharge. For further information please refer to the section 2 of the supplementary information.

A.1.2 Battery technologies

We compare and optimize the operation of the most deployed battery technologies for residential applications, including the two main families, lithium-ion and lead-acid. A total of six different technologies are analyzed: for the lithium family, these include lithium nickel manganese cobalt oxide (NMC), lithium nickel cobalt aluminum oxide (NCA), lithium iron phosphate (LFP), and lithium titanium oxide (LTO) batteries; and for the lead-acid family, we consider traditional valve regulated lead-acid (VRLA) and advanced lead-acid (ALA) batteries. The technical and economic battery input data required by the model were collected from publicly available data-sheets and personal communication with representative manufacturers. Table A.3 presents the key specifications for the six battery technologies defined by the type of cathode material. Three currently available battery sizes were assessed, small (3 kWh), medium (7 kWh) and large (14 kWh). Moreover, aging is modeled on a daily basis for the first year using the maximum among the daily calendar factor and the daily cyclic factor. The former is calculated as the multiplicative inverse of the calendar lifetime, whereas the cyclic aging factors are based on Woehler curves[e] for every technology. The cyclic aging is then given by the number of cycles per day at the given depth of discharge (depth-of-discharge), divided by the maximum number of cycles at a given depth-of-discharge (Sauer et al. 2009). Further details are presented in Section 2 of the Supplementary Information.

A.1.3 PV-coupled battery system

This study focuses on the combined investment in a PV-coupled battery system; more specifically, we analyze the techno-economic implications of adding a battery system when purchasing a new PV system that would otherwise be installed on its own. We consider a DC-coupled topology since a lower investment is required and the overall efficiency of stored PV electricity is higher than in AC-coupled topologies (Ardani et al. 2017). Moreover, the prevention of PV curtailment is possible (for further information see section 3 of supplementary information). The DC-coupled system used in this study is illustrated in Fig. A.3 and it includes an integrated inverter with a buck-boost charge controller with a maximum power point tracking system and a bi-directional inverter (required to charge from the grid). An inverter loading ratio (i.e., the ratio between the inverter rating and the PV rating, referred to as ILR) of 1.2 is considered for this study (Burger and Rüther 2006). Since manufacturers claim no operational costs required for residential PV and battery technologies, we set them to zero (Tesla 2015; Sonnenschein 2013). Installation

[e] The Woehler curves show the number of remaining cycles of a battery as a function of depth of discharge until the end of lifetime. This curve is given by some battery manufacturers in data sheets.

Table A.4: Values selected for the technical and economic assessment of PV-coupled battery systems.

Component	Units	Value	Reference
Charge controller efficiency	%	98	Energy 2017
Inverter efficiency	%	94	Energy 2017
Bi-directional inverter cost	[USD/kW]	600	Ardani et al. 2017
Bi-directional inverter lifetime	years	15	Fu et al. 2017
Balance of plant cost	[USD/kW]	100	Pena-Bello, Burer, et al. 2017
Installation costs	[USD]	2000	Baumann and Baumgartner 2017
O&M	[USD/kW]	0	Tesla 2015; Sonnenschein 2013
Discount rate	%/a	4	Stephan et al. 2016
End of life (EoL)	%	70	Käbitz et al. 2013
ILR	p.u.	1.2	Burger and Rüther 2006

costs are considered for the inverter and battery and are assumed to be high for both countries (i.e., $ 2000). Other technical and economic characteristics of the PV-coupled battery system considered in this study are shown in Table A.4.

A.1.4 Optimization of the battery schedule

The management problem of a PV-coupled battery system is solved by Linear Programming, using Pyomo, an open-source tool for modeling optimization applications in Python (Hart et al. 2012) and solved with CPLEX. The model parameters and variables are presented in Table A.5. The battery schedule is optimized for every day (i.e., 24 h optimization framework) and we assume perfect day-ahead forecast of the electricity demand load, solar PV generation and wholesale prices in order to determine the maximum economic potential regardless of the forecast strategy used. Aging was treated as an exogenous parameter, calculated on daily basis and was not subject to optimization (for further information see section 2 of the supplementary information). The temporal resolution of the input data and simulation is 15 minutes , with this value providing a reasonable compromise between the modeling real performance and computational speed (Beck et al. 2016). The model objective function have two components, namely the energy and power components of the electricity bill. As the tariff structure depends on the applications considered, a boolean parameter activates the power-based factor of the bill when is necessary.

Every optimization was run for one year and then the results are linearly-extrapolated to reach the battery end of life. We assume 30% of capacity depletion as the end of life (Käbitz et al. 2013) and when the battery lifetime exceeds the inverter lifetime, the residual value of the battery is considered using straight-line depreciation (Moore et al. 2015). Replacement is considered when the battery cannot match the inverter lifetime which is taken as the project lifetime, we take a conservative approach maintaining the same price in the future discounted to the

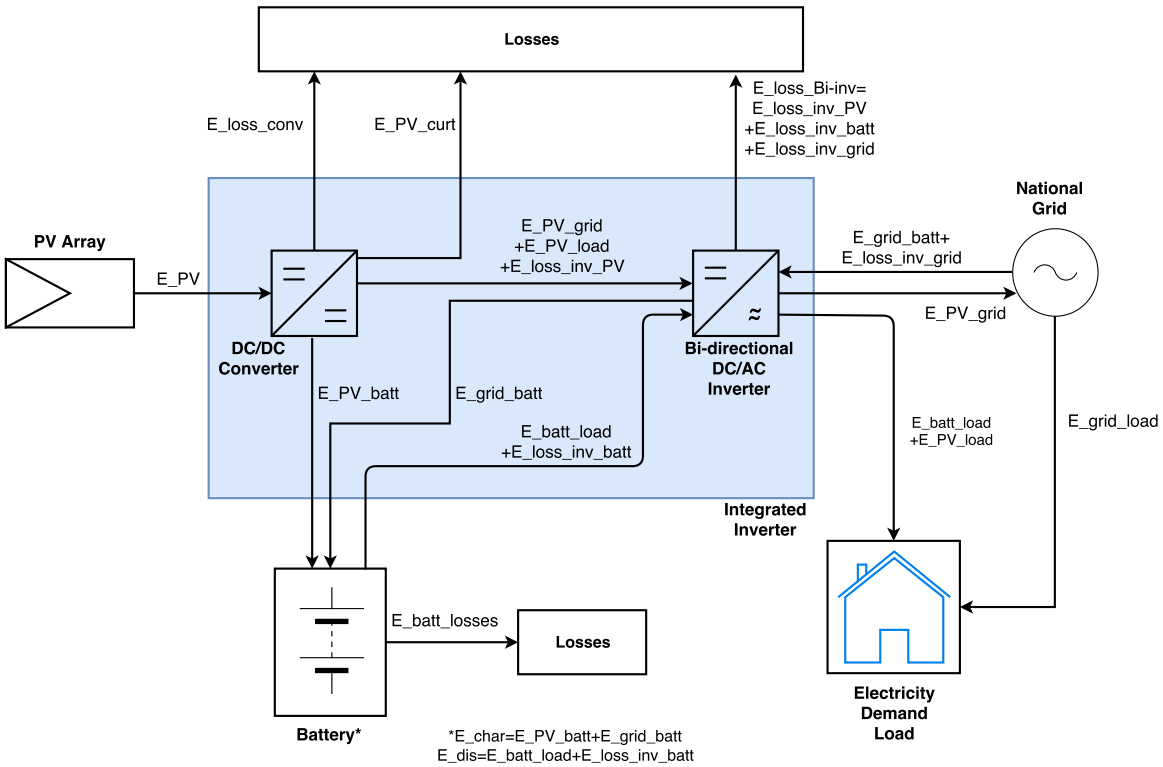

Figure A.3: DC-coupled PV-battery system with integrated inverter used in this study. Arrows indicate the direction of possible energy flows between the individual components.

present[f]. The analysis is done with same prices for all years across battery lifetime. The validation of the model can be found in Section 4 of the supplementary information. The objective function and constraints are presented below.

$$Min(\overbrace{\sum_{i=0}^{t}(E_{grid_i} * \pi_{import_i} - E_{PV-grid_i} * \pi_{export_i})}^{\text{Energy-based tariff}} + \underbrace{(P_{max-day} * \pi_{capacity} * PS)}_{\text{Power-based tariff}}) \tag{A.1}$$

Subject to:
Battery constraints:

$$SOC_{min} \leq SOC_i \leq SOC_{max} \tag{A.2}$$

$$E_{char_i} = E_{PV-batt_i} + E_{grid-batt_i} \tag{A.3}$$

$$E_{dis_i} \leq (SOC_{i-1} - SOC_{min}) * C_{batt}^{nom} \tag{A.4}$$

Energy balance constraints:

$$E_{grid_i} = E_{grid-load_i} + E_{grid-batt_i} + E_{loss-inv-grid_i} \tag{A.5}$$

$$E_{PV_i} = E_{PV-load_i} + E_{PV-batt_i} + E_{PV-grid_i} + E_{PV-curt_i} + E_{loss-conv_i} + E_{loss-inv-PV_i} \tag{A.6}$$

$$E_{load_i} = E_{PV-load_i} + E_{grid-load_i} + E_{dis_i} * \eta_{inv} \tag{A.7}$$

$$SOC_i = \frac{(SOC_{i-1} * C_{batt}^{nom} + E_{char_i} - E_{dis_i} - E_{loss-batt_i})}{C_{batt}^{nom}} \tag{A.8}$$

[f]This due to the high uncertainty linked to future battery prices for different battery technologies.

$$E_{dis_i} = E_{batt-load_i} + E_{loss-battinv_i} \tag{A.9}$$

Efficiency losses constraints:

$$E_{loss-conv_i} = (1 - \eta_{conv}) * (E_{PV-load_i} + E_{PV-batt_i} + E_{PV-grid_i}) \tag{A.10}$$

$$E_{loss-biinv_i} = E_{loss-inv-PV_i} + E_{loss-inv-grid_i} + E_{loss-inv-batt_i} \tag{A.11}$$

$$E_{loss-inv-PV_i} = (E_{PV-load_i} + E_{PV-grid_i}) * (1 - \eta_{inv}) \tag{A.12}$$

$$E_{loss-inv-grid_i} = E_{grid-batt_i} * (1 - \eta_{inv}) \tag{A.13}$$

$$E_{loss-inv-batt_i} = E_{dis_i} * (1 - \eta_{inv}) \tag{A.14}$$

$$E_{loss-batt_i} = E_{char_i} * (1 - \eta_{batt}) \tag{A.15}$$

Power constraints:

$$P_{char_i} \leq P_{max-char} \tag{A.16}$$

$$P_{dis_i} \leq P_{max-dis} \tag{A.17}$$

$$P_{PV-grid_i} + P_{PV-load_i} + P_{dis_i} + P_{loss-biinv_i} \leq P_{inv} \tag{A.18}$$

$$P_{PV-grid_i} + P_{PV-batt_i} + P_{PV-load_i} + P_{loss-conv_i} \leq P_{inv} \tag{A.19}$$

$$P_{grid-batt_i} + P_{loss-inv-grid_i} \leq P_{inv} \tag{A.20}$$

Application selection:

$$P_{PV-curt_i} \leq P_{limit} \quad \forall \quad i \quad if \quad PVCT = 1 \tag{A.21}$$

$$E_{grid-batt_i} = 0 \quad \forall \quad i \quad if \quad DLS = 0 \tag{A.22}$$

$$P_{grid_i} \leq P_{max-day} \quad \forall \quad i \quad if \quad DPS = 1 \tag{A.23}$$

A.1.5 Techno-economic indicators

Three complimentary indicators are used to analyze the techno-economic performance of batteries coupled with PV systems, i.e., the PV system is excluded in the analysis since we are interested in the decision of adding a battery. The levelized cost of energy storage, LCOES (USD/kWh) quantifies the cost associated with the total electricity supplied by the battery throughout the life of the system (see Eq. A.24). The second indicator is the levelized value of energy storage, LVOES (USD/kWh). It quantifies the revenue associated with the battery discharge throughout the life of the system (see Eqs. A.25 and A.26). Finally, the net present value (NPV) calculated as the sum of the discounted cash flows over the lifetime of the battery system (Eq. A.27) is used to appraise the overall impact of the system configuration and operation for each combination (geography, technology, consumer type and combination of applications) on the economic profitability of residential batteries.

$$LCOES = \frac{\sum_{i=0}^{N} \frac{CAPEX}{(1+r)^i} + \sum_{i=1}^{N} \frac{OPEX}{(1+r)^i}}{\sum_{i=1}^{N} \frac{E_{dis}}{(1+r)^i}} \tag{A.24}$$

$$LVOES = \frac{\sum_{i=1}^{N} \frac{CF_{Batt_i}}{(1+r)^i}}{\sum_{i=1}^{N} \frac{E_{dis}}{(1+r)^i}} \tag{A.25}$$

$$CF_{Batt_i} = CF_{PV-Batt_i} - CF_{PV_i} \tag{A.26}$$

$$NPV = \sum_{i=1}^{N} \frac{CF_{Batt_i}}{(1+r)^i} - \sum_{i=0}^{N} \frac{CAPEX}{(1+r)^i} \tag{A.27}$$

Table A.5: List of model parameters and variables.

Modeling parameters	Name	Units	Modeling variables	Name	Units
Converter efficiency	η_{conv}	%	PV generation fed to the load	$E_{PV-load}$	kWh
Inverter efficiency	η_{inv}	%	PV generation exported to the grid	$E_{PV-grid}$	kWh
Inverter rating	P_{inv}	kW	PV generation injected to the battery	$E_{PV-batt}$	kWh
Battery Efficiency	η_{batt}	%	PV generation curtailed	$E_{PV-curt}$	kWh
Maximum discharge power	$P_{max-dis}$	kW	Energy lost due to converter efficiency	$E_{loss-conv}$	kWh
Maximum charge power	$P_{max-char}$	kW	Total energy lost due to bi-directional inverter efficiency	$E_{loss-binv}$	kWh
Battery nominal capacity	C_{batt}^{nom}	kWh	PV energy lost due to bi-directional inverter efficiency	$E_{loss-PVinv}$	kWh
Battery lifetime	N	years	Grid energy lost due to bi-directional inverter efficiency	$E_{loss-gridinv}$	kWh
Battery maximum state of charge	SOC_{max}	%	Battery energy lost due to bi-directional inverter efficiency	$E_{loss-battinv}$	kWh
Battery minimum state of charge	SOC_{min}	%	Energy lost due to battery efficiency	$E_{loss-batt}$	kWh
Retail prices	π_{import}	USD/kWh	Energy drained from the battery	E_{dis}	kWh
Export prices	π_{export}	USD/kWh	Energy injected to the battery	E_{char}	kWh
Capacity tariff	$\pi_{capacity}$	USD/kW	Energy delivered from the battery to the load	$E_{batt-load}$	kWh
Feed-in limit	P_{limit}	%	Energy imported from the grid to the battery	$E_{grid-batt}$	kWh
Combination of applications	[PVCT, PVSC, DLS, DPS]	Boolean array	Energy imported from the grid to the load	$E_{grid-load}$	kWh
Load demand	E_{load}	kWh	Energy drained from the grid	E_{grid}	kWh
PV generation	E_{PV}	kWh	Maximum power drained from the grid	$P_{max-day}$	kW
Optimization time framework	t	minutes	Power related to any energy parameter	$P_x = E_x/\Delta t$	kW
Temporal resolution	Δt	fraction of hour	State of charge	SOC_i	%

A.2 Demand, PV generation and tariffs data

A.2.1 Demand datasets

Two demand datasets covering Austin, Texas in USA and a western Swiss city with 15-minute smart meter data covering the whole year 2015 were used in this study. For Austin the data were obtained from the Pecan Street project, for 322 households, as for the 667 Swiss dwellings data confidentiality agreements apply, however we treated the data as if it was from Geneva. In terms of average yearly electricity consumption the American household use 3.7 times more electricity than Swiss households from the datasets. The two cities present a completely different consumption behavior, while in Austin there is a clear seasonality with a summer peak that is the double of winter or fall consumption, in Geneva summer is the less electricity-demanding season and winter and fall present comparatively only 16% more electricity demand. In terms of monthly average consumption, in Austin, excluding summer months, the average consumption is 837 kWh/month and almost two times greater during summer months. On the other hand, in Geneva a clear mean of 274 kWh/month is maintained all year-round with a slightly lower consumption in spring and fall (see Fig. A.4).

A.2.2 Demand clustering

Rather than run individual simulations for all the household consumers (322 US households and 667 Swiss households), which would lead to very long simulation times, we instead aim to find representative consumers which exemplify typical consumption patterns within the datasets for both countries. Therefore, for both the US and CH we create groups of consumers with similar behaviour in terms of the

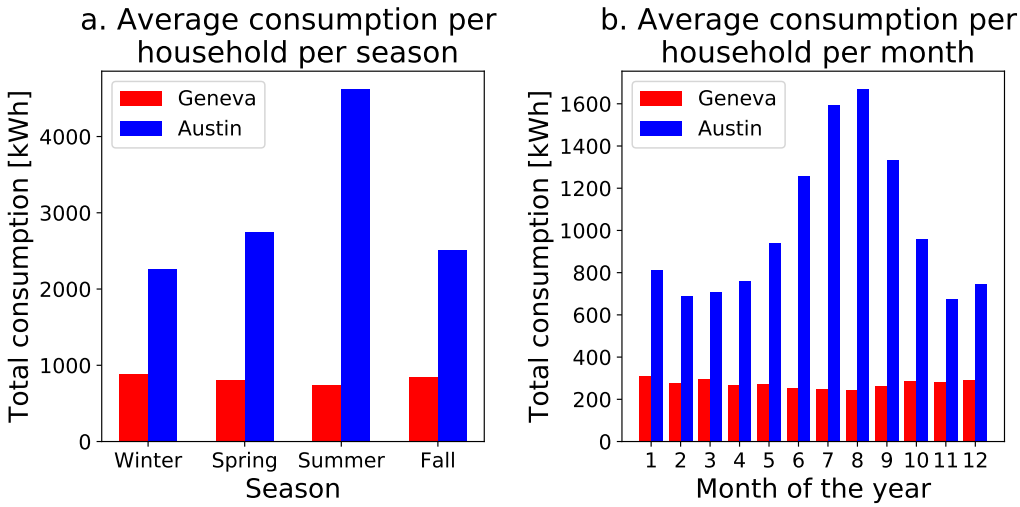

Figure A.4: Average consumption per household in both locations, Geneva, Switzerland is shown in red while Austin, Texas is presented in blue. a. Per season and b. Per month.

shape and overall magnitude of their average daily load profiles. From each group, we then select the consumer whose load is closest to the centroid of the group, designating that consumer as the representative from that group. Simulations are run for each representative consumer for all scenarios.

To generate the representative consumer groups, we employ a clustering method. In the literature, a range of clustering methods have been employed to form consumer segments (for a review of the clustering techniques applied to electricity load data see (Chicco 2012)), however k-means is the most commonly used clustering framework and has been used in a range of studies regarding household load profiles *i.e.* (Kwac, Flora, and Rajagopal 2014; Xu, Barbour, and González 2017; Benıétez et al. 2014; Al-Wakeel, J. Wu, and N. Jenkins 2017). Therefore, we form our consumer groups using k-means clustering.

When clustering daily load profiles, it is a normal step to normalise the load profiles, bringing the daily shapes to a similar scale for pattern recognition (Kwac, Flora, and Rajagopal 2014; Xu, Barbour, and González 2017). This is described by Equation A.28:

$$e_c(t) = \frac{l_c(t)}{\sum_{t=1}^{t=24} l_c(t)} \tag{A.28}$$

$e_c(t)$ is the normalised load at time t and $l_c(t)$ is consumer c's load at time t before normalisation.

While directly clustering normalised load profiles is effective for forming groups of load profiles with similar shapes independent of consumption magnitudes, in this work we also want to study the effect of differing levels of overall consumption. Therefore, first we look at the distributions of total yearly consumption in both locations and form groups with similar consumption levels. As shown in Figure A.5, there are several consumers with abnormally high consumption in both locations (above 7500 kWh in Switzerland is considered an outlier and above 25000 kWh in Pecan Street is considered an outlier) and we do not consider these consumers, since our ultimate aim is to find representative consumer groups. We then split the remaining consumers whose consumption is within our defined normal range into 3 separate groups - a low consumption group, a medium consumption group and a high consumption group in both locations. The low consumption group is defined by

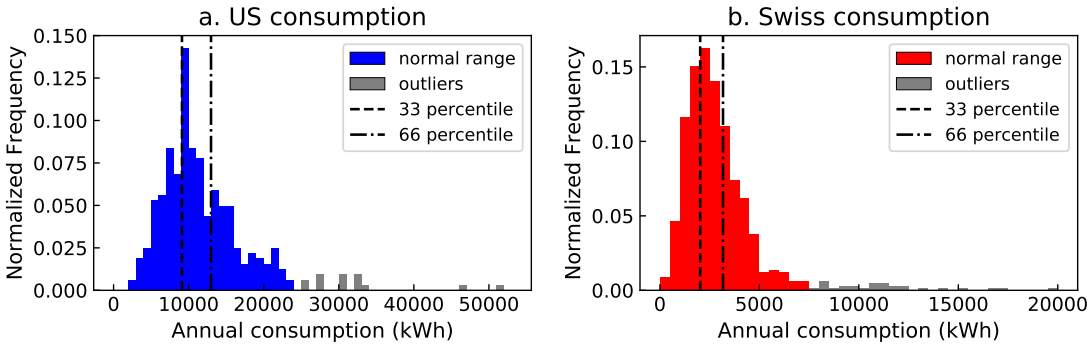

Figure A.5: Distributions of annual household electricity consumption for our data from a. Austin, USA and b. Geneva, Switzerland.

consumers in the 0^{th}—33^{rd} percentiles, the medium consumption group is defined by consumers in the 34^{th}—66^{th} percentiles, and the high consumption group contains consumers with yearly consumption greater than the 67^{th} percentile.

After forming the consumption brackets based on overall consumption, we further subdivide these by clustering according to the load shape. We use the k-means clustering method, which randomly assigns an initial set of centroids, and then iteratively moves these to minimize the objective function shown in Equation A.29.

$$J = \sum_{j=1}^{K} \sum_{i=1}^{n_j} \sqrt{\sum_{t=1}^{t=24} (e_{i,j}(t) - \zeta_j(t))^2} \tag{A.29}$$

Here, j indexes the clusters from 1 to K and i indexes the load shapes assigned to cluster j, where n_j is the total number of shapes in cluster j. $e_{i,j}$ is the i^{th} load shape assigned to cluster j and ζ_j is the centroid of cluster j. As can be seen, we minimise the Euclidean distance between centroids and the normalised load profiles.

Since we cluster average daily load profiles, we ultimately produce groups with similar average behaviours, recognising that there may be significant deviation away from the average daily load shape for an individual on any given days (Kwac, Flora, and Rajagopal 2014; Xu, Barbour, and González 2017). We opt to produce 4 clusters in each consumption bracket, noting that the selecting the number of clusters in highly dimensional data where it is not known is a difficult task. However, to provide some justification we look at the variance explained by the cluster centroids compared to the total variance in the data. Figure A.6 shows the elbow plots for both locations, and illustrates that in general the additional variance accounted for by an extra cluster diminishes below 5—7% after adding more than 4 clusters.

The clusters in each consumption bracket for both locations are shown in Figure A.7.

A.2.3 PV generation

In this section we refer to a generation profile generated for each location using a PV installation of 1 kW_p of nominal power. In terms of yearly generation, a PV system in Austin generates 15% more electricity than the same PV system in Geneva. The capacity factor in Austin is 18.8% while in Geneva is 16.3%, being these values congruent with related literature (Pfenninger and Staffell 2016). We assume the same generation for every PV system for every household in this study being then adjusted according to the PV size distribution in each location. Fig. A.8

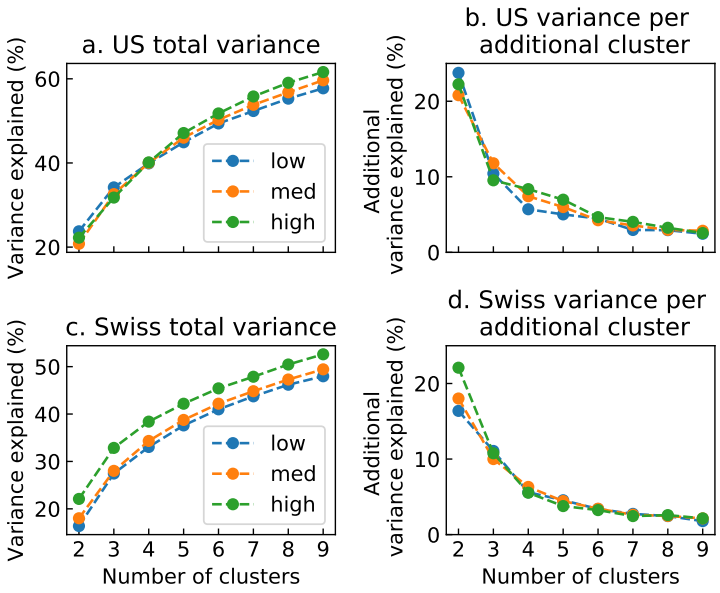

Figure A.6: The percentage variance explained against the number of clusters. a. The total percentage variance explained as a function of the number of clusters for Austin and b. the increase in variance explained between the cluster centroids by adding an additional cluster. c. and d. show the respective plots for Switzerland

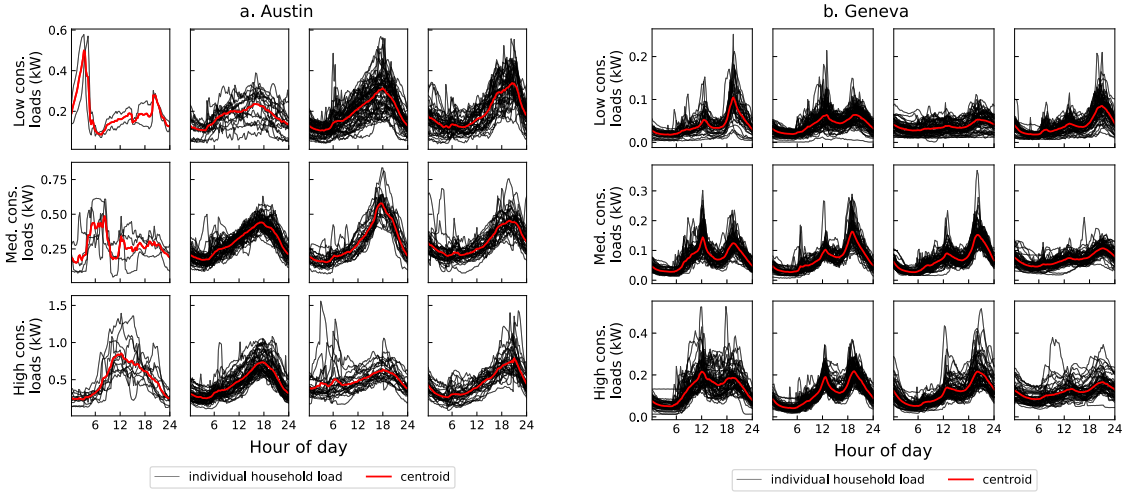

Figure A.7: The clusters formed for a. Austin and b. Geneva.

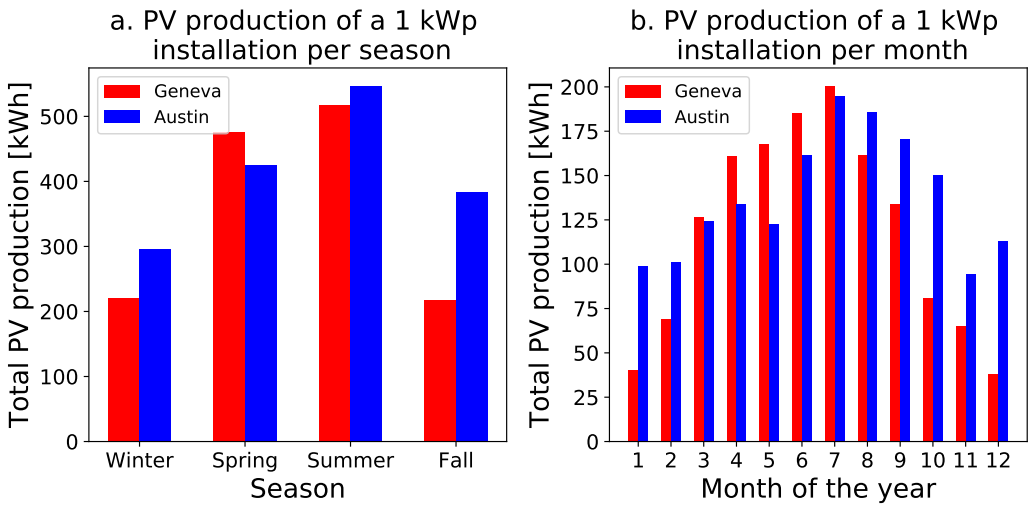

Figure A.8: Electricity generation of a 1 kW_p PV installation in both locations, Geneva, Switzerland is shown in red while Austin, Texas is presented in blue. a. Per season and b. Per month.

presents the differences per season and per month between the two locations, as can be observed throughout the year Austin have more generation than Geneva, except during spring when the PV system in Geneva produces 11% more electricity than in Austin. As for fall and winter, a PV system in Austin produces 75% and 34% more electricity than the same PV system in Geneva, respectively. In summer the difference is less than 6%.

The distribution of PV sizes for both locations and the first, second and third quartiles are presented in Fig. A.9. Since A limit of 10 kW_p of nominal power for residential systems is usually used by national reports (Fu et al. 2017; Husser, Pius 2017), we selected the same limit for this study. We take into account all the country installations under the mentioned threshold, as for USA we take only Austin installations under the same threshold. For both datasets the three quartiles are very close, the first quartile is 3.15 kW_p and 3.2 kW_p for Austin and Geneva, respectively, as for the third quartile Austin presents a smaller system size (6.4 kW_p) than Geneva (6.9 kW_p). The medians are again very close, being only 0.2 kW greater in Austin (5 kW_p) than in Geneva.

A.2.4 Tariffs

Energy tariffs are based on "Electricité vitale Bleu" for households in Geneva and on TOU for residential customers in Austin. Both, single tariffs and double tariffs are considered in the analysis.

A.2.5 Export prices

In general, Swiss export prices are larger than prices in Texas with average daily prices of 0.04 USD/kWh and 0.027 USD/kWh respectively. However, the differences among average electricity prices per season indicate a general trend in Geneva where spring and summer months are usually low (around 0.033 USD/kWh) while fall and winter prices are around 0.047 USD/kWh (see figure A.10). As for Austin, prices are similar among winter, spring and fall (around 0.024 USD/kWh), however in summer prices are larger (0.035 USD/kWh in average) but can be as high as 2.25 USD/kWh.

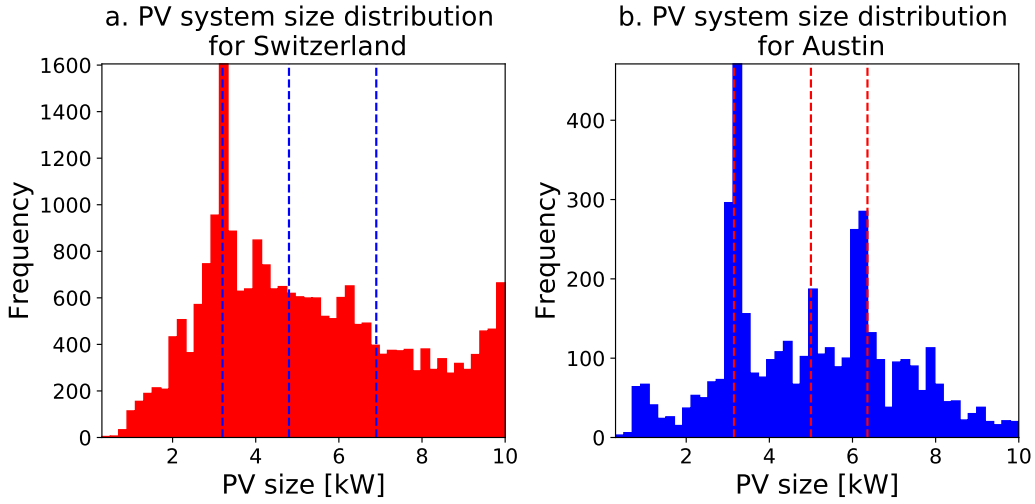

Figure A.9: PV system size distribution smaller than 10 kW_p for a. Switzerland (22807 data points) and b. Texas (4295 data points). The dashed lines represent the dataset first, second (median) and third quartiles.

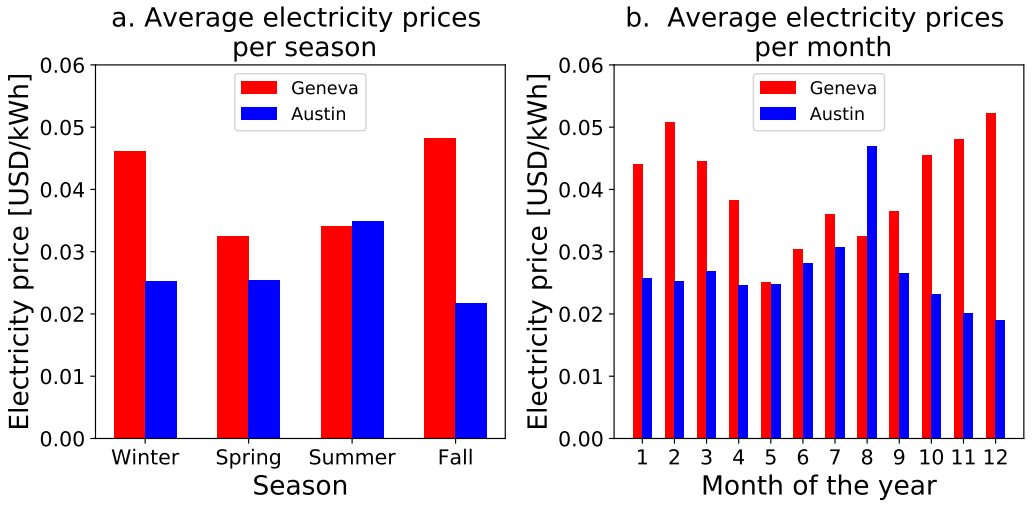

Figure A.10: Electricity prices in both locations, Geneva, Switzerland is shown in red while Austin, Texas is presented in blue. a. Per season and b. Per month.

A.3 Aging

Battery aging and durability are parameters with a great uncertainty for battery energy storage technologies (Hesse, Schimpe, et al. 2017). In this paper, we model battery aging process through the battery capacity depletion since it limits the battery lifetime. The aging behavior is typically divided in two, calendar aging (when the battery is standby) and cycle aging (when the battery is used) (Sauer et al. 2009). We acknowledge the battery aging process is non-linear, particularly in the first hundreds of cycles, but as pointed out in earlier papers, capacity losses can be assumed to be linear without compromising lifetime predictions markedly (Hesse, Martins, et al. 2017; Sauer et al. 2009) and this approach is followed in this study. Furthermore, previous studies have reported that one of the two aging factors dominates (typically cycle aging for small batteries) in typical operation conditions (Sauer et al. 2009), thus the model can be simplified across the different technologies through the use of the maximum of both, see Eq. A.30. The aging factor is calculated in daily basis.

Typically a 20% reduction of the initial capacity is applied to define the end of life (EoL) of a battery (Sauer et al. 2009), especially for industrial application since under this value the manufacturers do not guarantee the battery performance. However, lower values are often stated for residential applications which are less demanding (Hesse, Martins, et al. 2017; Käbitz et al. 2013), in this study we use a 30% capacity depletion as EoL.

Calendar losses have been previously modeled using the Arrhenius formula since they are mainly dependent on the battery temperature (Käbitz et al. 2013). However, the temperature is controlled by the battery management system in new models available in the market. Therefore, the proposed model neglects its effect on the battery aging. Eq. A.31 defines daily calendar aging as the multiplicative inverse of the battery calendar lifetime.

As for the cyclic aging, we use a similar approach as the presented by Magnor et al. (Sauer et al. 2009) which is based on Woehler curves[g] for different battery technologies. We extend this method to other technologies adapting the maximum number of cycles performed by the battery. The cyclic aging is then given by the number of cycles per day at the given DoD, divided by the maximum number of cycles at a given DoD, as indicated by Eqs.

A.32 and A.33.

$$aging_d = max(cyc_d, cal_d) \tag{A.30}$$

$$cal_d = \frac{1}{Batt_{cal-life}} \tag{A.31}$$

$$DoD^\star = \frac{\sum_{i=1}^{t} E_{dis_i}}{E_{batt}^{nom}} \tag{A.32}$$

$$cyc_d = \frac{N_{cycles_d}^{DoD^\star}}{N_{max}^{DoD^\star}} \tag{A.33}$$

The Woehler curves used in this study are displayed in Fig. A.11 and the equation that mathematically describes every curve is presented in Table A.6. Each curve is based on manufacturers' datasheets.

[g]The Woehler curves show the number of cycles of a battery as a function of depth of discharge until the end of lifetime. This curve is given by most battery manufacturers in data sheets.

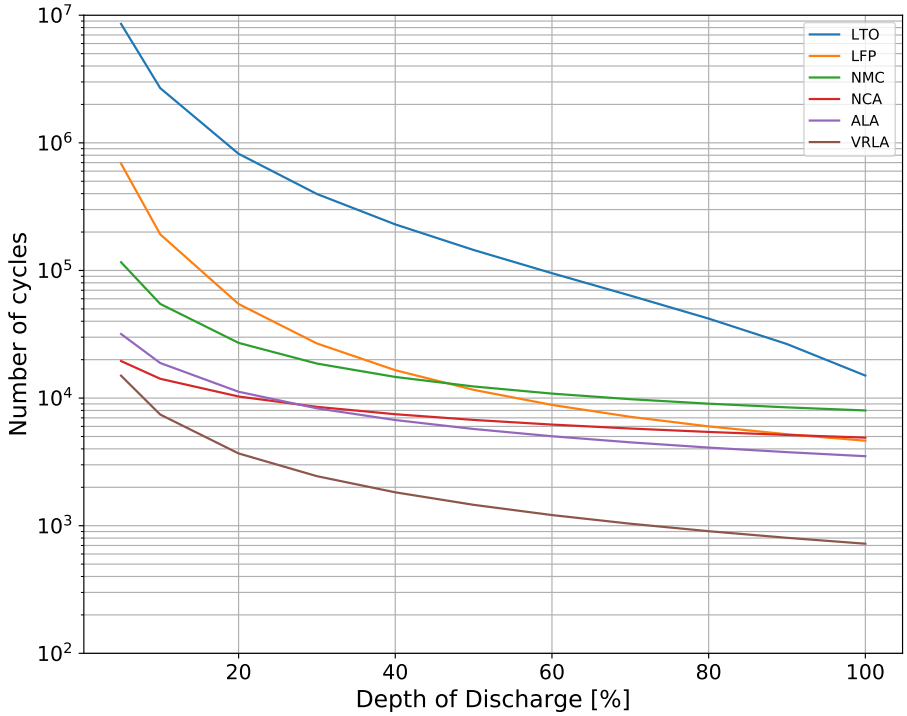

Figure A.11: Woehler curves for every technology used in this study.

Table A.6: Number of cycles for every technology used in this study.

Technology	Number of cycles as a function of DoD	Reference
LTO	$\exp\left(\frac{\log(DoD)-\log(771.51)}{-0.604}\right) - 45300$	*XALT 60Ah High Power Lithium-Ion LTO Cell* 2018
LFP	$\exp\left(\frac{\log(DoD)-\log(70.869)}{-0.54}\right) + 1961.37135$	Omar et al. 2014
NCA	$\exp\left(\frac{\log(DoD)-\log(1216.7)}{-0.869}\right) + 4449.67011$	Trina BESS 2017
NMC	$\exp\left(\frac{\log(DoD)-\log(1E8)}{-2.168}\right)$	Truong et al. 2016
ALA	$\exp\left(\frac{\log(DoD)-\log(37403)}{-1.306}\right) + 330.656417$	*FCP-1000 Lead Carbon Battery* 2018
VRLA	$\exp\left(\frac{\log(DoD)-\log(667.61)}{-0.988}\right)$	Sonnenschein 2013

A.4 PV-coupled battery system

This topology allows to select a smaller inverter (i.e., increase the ratio between the inverter rating and the PV rating beyond 1) and store otherwise clipped energy (Denholm, Margolis, and Eichman 2017). Likewise, this topology prevents from curtailing PV export exceeding a regulatory threshold as in Germany where PV generators with a installed capacity of maximum 30 kW must be able to reduce the feed-in power in case of network overload or limit the power supply of the PV-system to the grid to 70% of installed capacity which can be enforced to 50% if a storage installation is funded by the government subsidy program (Bundestag Deutscher 2017; KfW Bank 2016)[hi].

DC -coupled systems require a single power conversion to store energy (through the charge controller), whereas AC-coupled systems require two power conversions (from the PV array through the PV inverter and then through a bi-directional inverter to the battery). Therefore, in applications where PV output storage is frequent, DC-coupled systems are generally more efficient than AC-coupled systems. In the DC-coupled system, the efficiency of the charge controller is set at 98% while that from the bi-directional DC/AC inverter is set at 95% (Energy 2017). Thus, the DC/AC efficiency from the PV system to the grid or to the demand load is 93%. On the other hand, when PV electricity is stored, one must consider battery roundtrip efficiency, therefore lowering efficiency depending on battery technology, for instance, it goes down to 79% for the VRLA. As for grid charging, the AC-AC efficiency (i.e., grid-to-battery-to-load efficiency) is within a range of 76% (for VRLA) to 87% (for LTO).

[h] §9 subsection 2

[i] In the literature curtailed and clipped energy are often interchangeable, however in this work we use the term "clipped energy" to refer to wasted energy due to technical restrictions (e.g., inverter rating) while "curtailed energy" is used when we refer to wasted energy due to legal restrictions.

A.5 Model validation

In order to validate the model, some test scenarios with intuitive solutions for the optimum schedule of operation of the battery are considered. The three scenarios are run with a LFP battery with a large capacity (100 MWh) and efficiency of 100%. The demand is considered to be constant at 100 kW.

In the first case, presented in figure A.12, the time-series test price presents a single time slot with a low price of 10 USD/kWh and a peak price of 100 USD/kWh. The battery charging and discharging limits are set at 2*C. The output is as expected a schedule where the battery is charged in the low-price time slot and discharged afterwards.

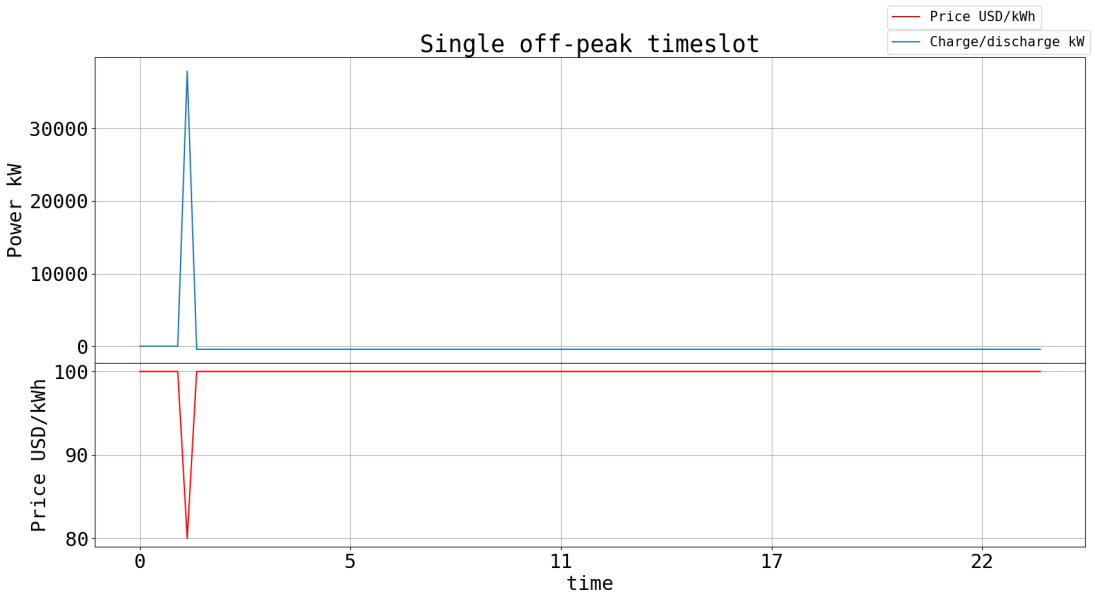

Figure A.12: Result for optimization of the single off-peak time slot test case. The output schedule for charge (positive y-axis) and discharge of the battery with the given price input.

In the second test, shown in figure A.13 the time-series test price is a square wave varying between 100 USD/kWh and 10 USD/kWh. The battery charging and discharging limits are set at 100 kW. Therefore, we would expect the optimized result to output a schedule that charged when the prices are low, then discharged to cover the demand when the prices are high. The figure of the model results is an excellent fit with the expected schedule. A positive power flow means the battery is charging.

In the last test, shown in figure A.14 the time-series test price is a sinus wave varying between 50 USD/kWh and -50 USD/kWh. The battery charging and discharging limits are set at 100 kW. Therefore, we would expect the optimized result to output a schedule that charged when the prices are lower than 0 USD/kWh, then discharged to cover the demand when the prices are high. We can see how at the end of the day, the battery charges only when prices are strictly below 0 USD/kWh, since the battery does not charge if it does not need the energy before the end of the day.

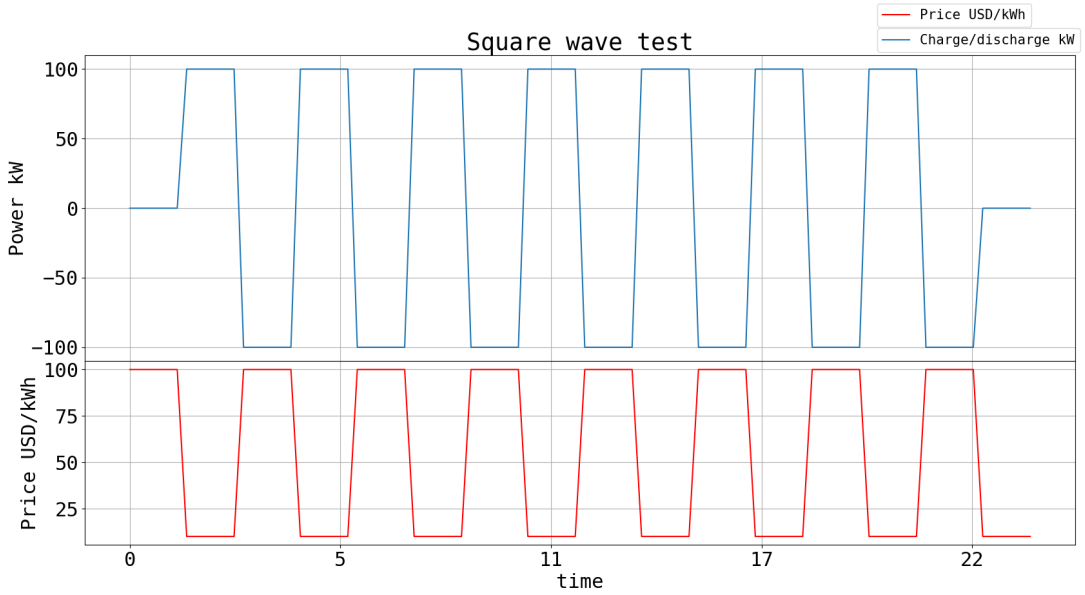

Figure A.13: Result for optimization of the square wave price test case. The output schedule for charge (positive y-axis) and discharge of the battery with the given price input.

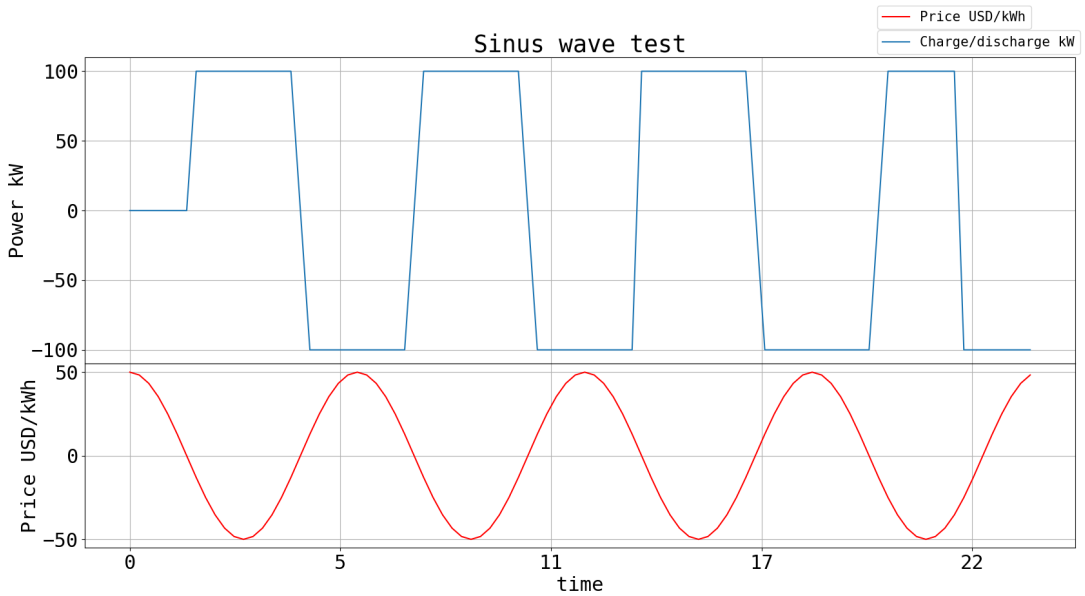

Figure A.14: Result for optimization of the sinus wave price test case. The output schedule for charge (positive y-axis) and discharge of the battery with the given price input.

A.6 Other combinations of applications

Results are presented here for a typical size of 7 kWh depending on the battery technology and for both locations. Since we aim to analyze the impact of geography, battery technology and size on the attractiveness of the combination of applications, our baseline results are based on a representative (median) fixed PV size in each geographical region. Three additional combinations of applications are analyzed besides the five presented in the main paper. In order to give the reader a point of comparison, PV self-consumption only and the full combination of applications are as well deployed.

The main result drawn from Figs. A.15,A.16 and A.17 is the influence of demand load shifting when combined with PV self-consumption and demand peak shaving, which helps to reduce the levelized cost and slightly enhance the added value. At the end it results in an improved NPV which is significantly higher than the scenario where avoidance of PV curtailment is combined with the same two applications.

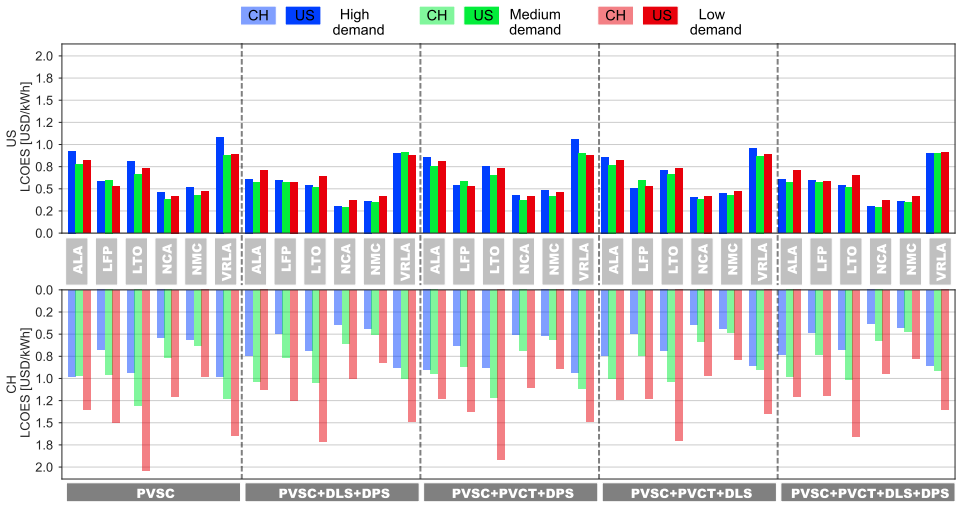

Figure A.15: Levelized cost of energy storage of a 7 kWh battery for all battery technologies depending on the type of combination of applications for the U.S. (top) and Switzerland (bottom). The size the PV system correspond to the medium installed capacity across both locations.

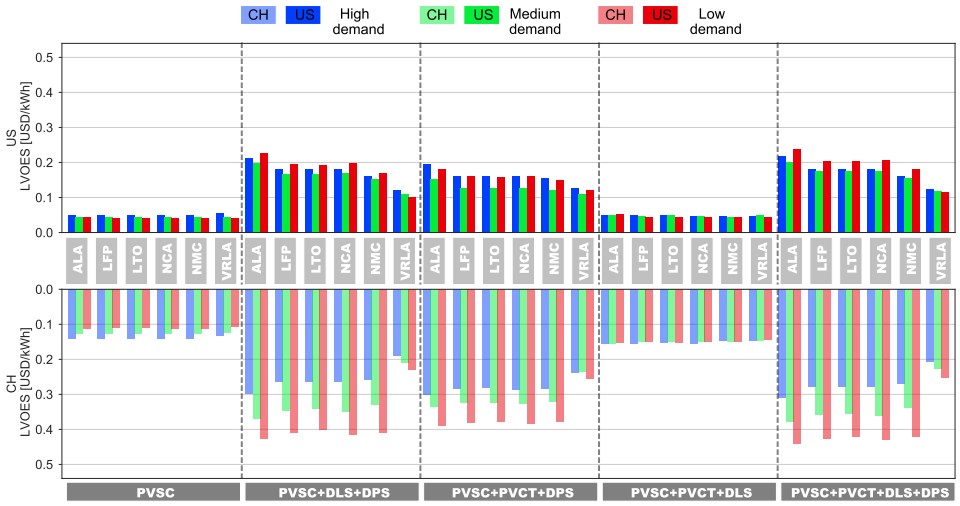

Figure A.16: Levelized value of energy storage of a 7 kWh battery for all battery technologies depending on the type of combination of applications for the U.S. (top) and Switzerland (bottom). The size the PV system correspond to the medium installed capacity across both locations.

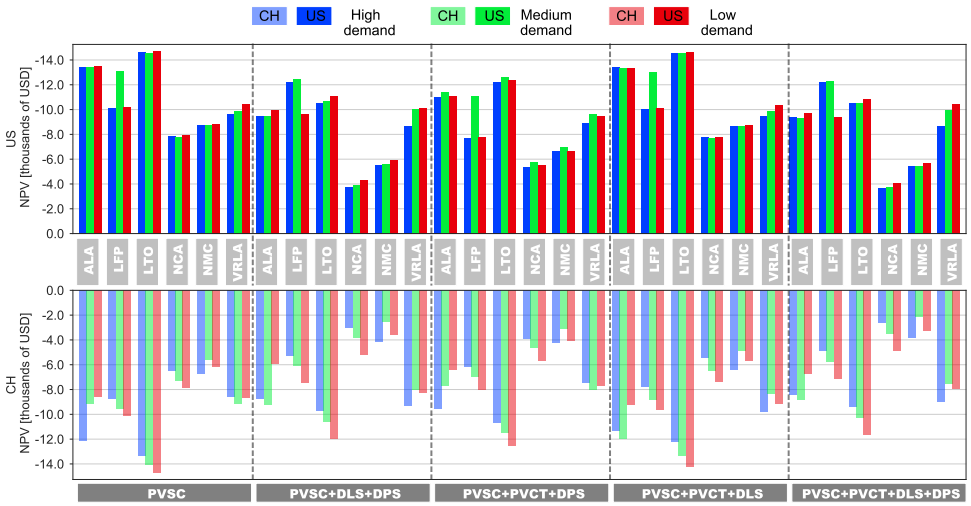

Figure A.17: Net present value of energy storage of a 7 kWh battery for all battery technologies depending on the type of combination of applications for the U.S. (top) and Switzerland (bottom). The size the PV system correspond to the medium installed capacity across both locations.

A.7 PV size impact

Fig. A.18 displays the average LCOES, LVOES and NPV across the three groups of consumers, for the 25th, median and 75th quartiles of the PV size distribution for Switzerland and Fig A.19 for the U.S., for a 7 kWh battery performing simultaneously all consumer applications depending on the battery technology.

In general, the combination of applications reaches smaller levelized cost, higher levelized value and higher NPV for all batteries, with the exception of LFP-based batteries in the U.S. when median PV size is assessed (due to replacement near the end of life). Moreover, the difference between a battery performing PV self-consumption only and one performing all the applications simultaneously is higher as the PV size raises for the levelized value and the NPV, as for the levelized cost the difference diminishes with PV size.

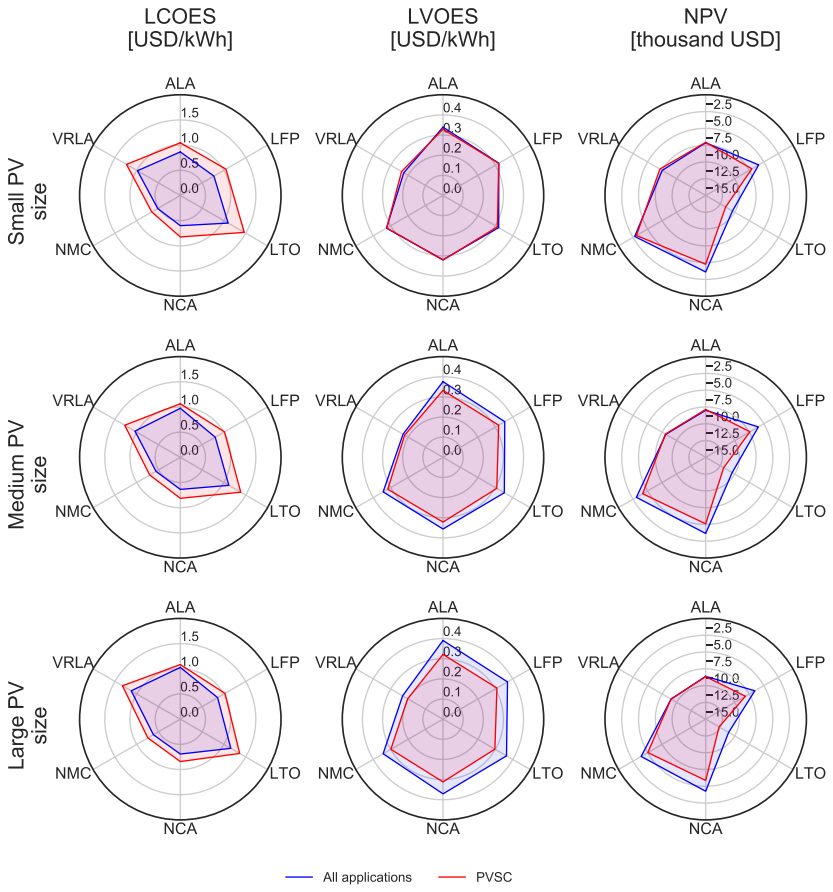

Figure A.18: Comparison of the average LCOES (left), LVOES (middle) and NPV (right) for various battery technologies and a 7 kWh battery performing only PV self-consumption (red) and all consumer applications simultaneously (blue) in Switzerland, depending on the size of PV, namely small (top), medium (middle) and large (bottom).

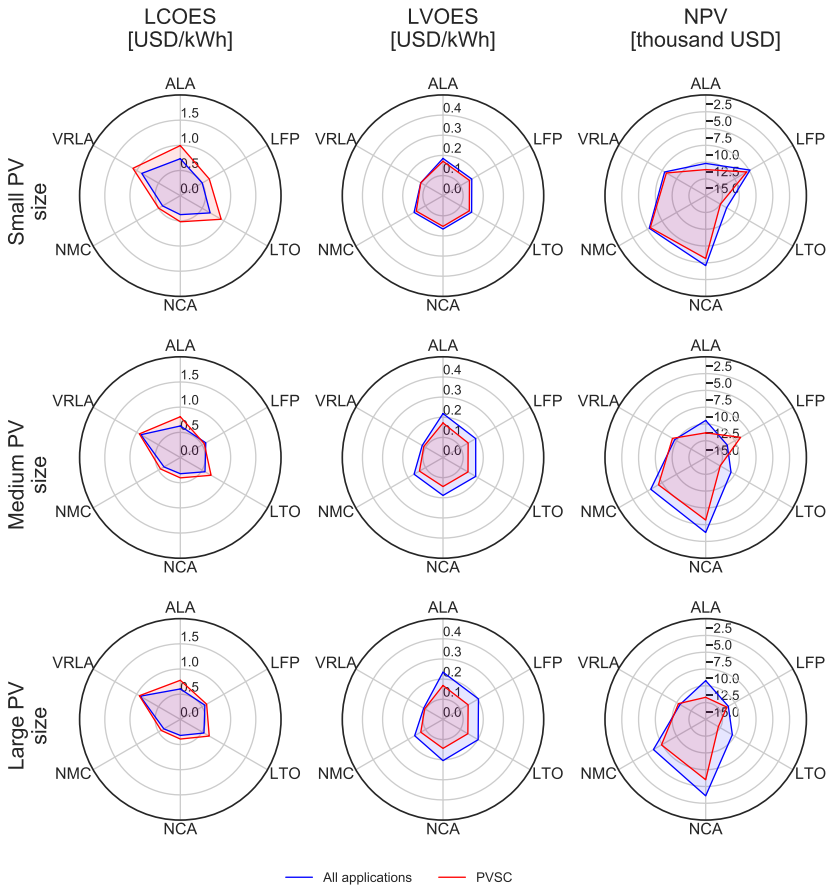

Figure A.19: Comparison of the average LCOES (left), LVOES (middle) and NPV (right) for various battery technologies and a 7 kWh battery performing only PV self-consumption (red) and all consumer applications simultaneously (blue) in the U.S., depending on the size of PV, namely small (top), medium (middle) and large (bottom).

Appendix B

Supplementary Information - Thermal and Electrochemical storage

B.1 Heat demand

The space heating and DHW demands for the three types of houses are calculated using a calibrated dynamic simulation tool (Schuetz, Scoccia, et al. 2018), and are presented in Fig. B.1. The simulation tool calculates the dynamics of the building and energy system by solving the coupled differential equations of the individual components using a Runge-Kutta integrator (see the end of this section for implementation details). The coarse model layout is shown in Fig. B.2.

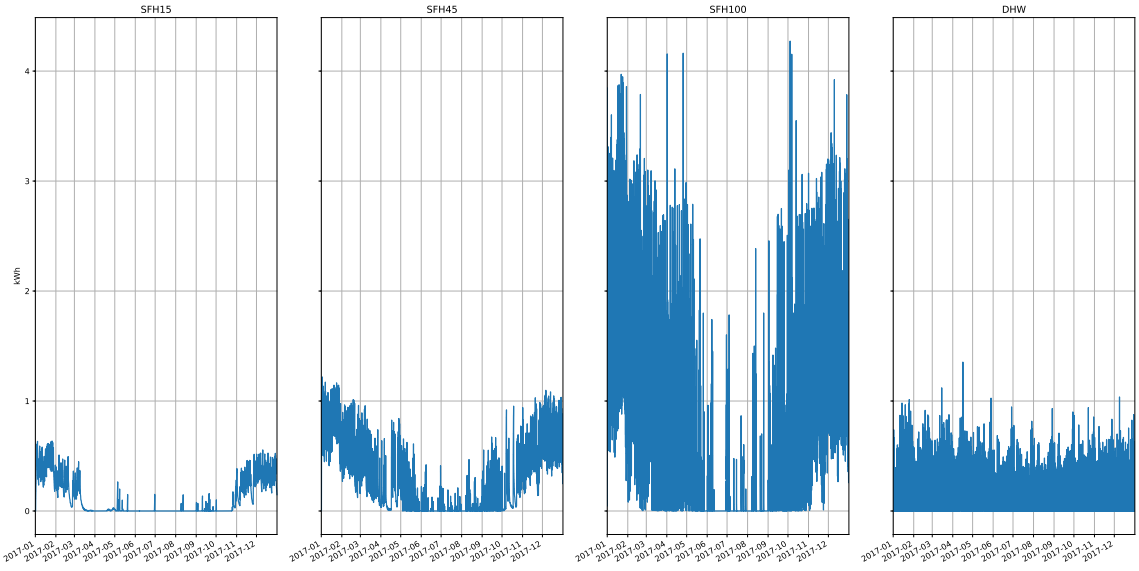

Figure B.1: Space heat demand for the three types of houses and domestic hot water demand for the year 2017.

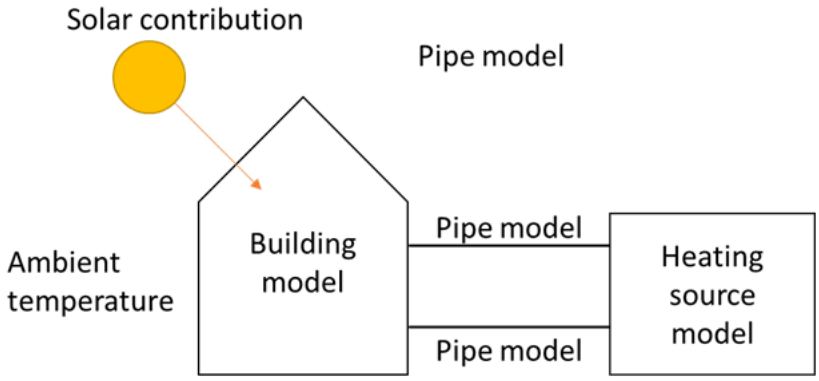

Figure B.2: Dynamic building and energy system model configuration. The system is simulated by solving the coupled differential equation model describing the individual components.

The dynamics of the building are described by the model presented in Eq. B.1

$$\frac{\partial T_{room}}{\partial t} = -H \cdot (T_{room} - T_{amb}) + g \cdot I + \dot{Q}_{emitter-system} + \dot{Q}_{internal} \tag{B.1}$$

adapted from Burmeister et al. (Burmeister and Keller 1998). This model describes the change of the room temperature T_{room} and considers the current ambient temperature T_{amb}, the solar radiation I, the heat flux generated by the emitter system $\dot{Q}_{emitter-system}$ $[kWh_{th}]$ and the internal heat loads $\dot{Q}_{internal}$. The building is characterized by three coefficients: C for the lumped heat storage capacity; g the solar factor; and H the lumped losses. These values are calculated based on the specifications of the three reference simulation buildings SFH15, SFH45 and SFH100 with an annual heating energy demand of 15, 45 and 100 kWh_{th}/m^2 as defined in the Reference framework for system simulation (Dott, Haller, et al. 2013). The internal heat loads $\dot{Q}_{internal}$ are taken from the Reference framework for system simulation (Dott, Haller, et al. 2013) according to SIA2024 (Swiss Society of Engineers and Architects 2015).

The heat flux of the emitter system to the building is described by the radiator equation (Eq. B.2).

$$\dot{Q}_{emitter-system} = \dot{Q}_{design} \cdot \left(\frac{\frac{T_{in}+T_{emitter-system}}{2} - T_{room}}{\Delta T_{design}} \right)^{n_r} \tag{B.2}$$

Here, $\dot{Q}_{emitter-system}$ is the heat flux to the room; $\dot{Q}_{design}$ is the design capacity of the emitter system at the design temperature split ΔT_{design}; T_{in} describes the inlet temperature of the emitter system (given by the pipe temperature); $T_{emitter-system}$ is the temperature of the emitter system; and n_r is the radiator exponent. The dynamics of the emitter system is modeled as a one-node storage model with $\dot{Q}_{emitter-system}$ as a loss term and the heat contribution of inlet and outlet pipe (see Fig. B.2). For SFH15 and SFH45, a floor heating system is modelled (radiator exponent 1.1), for SFH100, a radiator-based system is modelled (radiator exponent 1.3). The radiator exponent describes the relation between the mean temperature difference and the heat output of the radiator. This exponent is important since the relationship between the two is non-linear (Østergaard and Svendsen 2016a). The radiator exponents of 1.1 and 1.3 correspond to the values describing heat emissions from typical underfloor heating systems and radiators, respectively (Østergaard and Svendsen

2016b; Dott, Haller, et al. 2013). The design powers of the emitter systems are chosen to match the heat demand at -10°C ambient temperature. In the energy system model the heating source is connected to the emitter systems via two pipes modelled as a one-node storage model. The heating source is modelled as a resistance heater with an efficiency of 100%, i.e., the consumed energy is the energy inserted into the pipes or the energy system, which allows us to model the heat demand independently from the energy system (a heat pump in this paper, that is modeled afterwards). The heating system is controlled such that a target room temperature of $20°C$ is maintained within a dead band of $1°C$. The climatic data are taken for Geneva. The energy demand for the DHW preparation is integrated in the energy demand of the heating source. The energy demand for DHW is calculated based on a DHW profile assuming that the water is heated from an inlet temperature of 15°C to target temperature of 60°C. The DHW profile are calculated using the DHWcalc tool (Jordan and Vajen 2001) simulating the DHW profile of a family with two adults and two children. The coupled differential equations model are solved in a program implemented in C++ using Visual Studio 2017 community edition and the boost library version 1.64.0.). The heat load is determined based on hourly integrals of the energy demand of the houses simulated in the dynamic model and it is resampled to 15-min to match the electricity demand resolution(Schuetz, Scoccia, et al. 2018).

B.2 Heat pump sizing and modelling

To size the air-source heat pump, both the design point and the heat emission system' supply temperature have to be calculated. Following the reference framework for system simulations of the IEA (Dott, Haller, et al. 2013, Appendix A), the distribution of the outdoor temperature (see Fig. B.3) is used and the design temperature is defined as the lowest temperature to lie in the confidence interval of 0.99 (*i.e.*, where $z = 2.57 * \sigma$). For the case of Geneva, the design temperature is -11°C (see Fig. B.3). Then, as shown in Fig. B.4, the heat load at the design temperature is calculated as an extrapolation of a linear fit to the daily heating power consumption (Dott, Haller, et al. 2013, Appendix D).

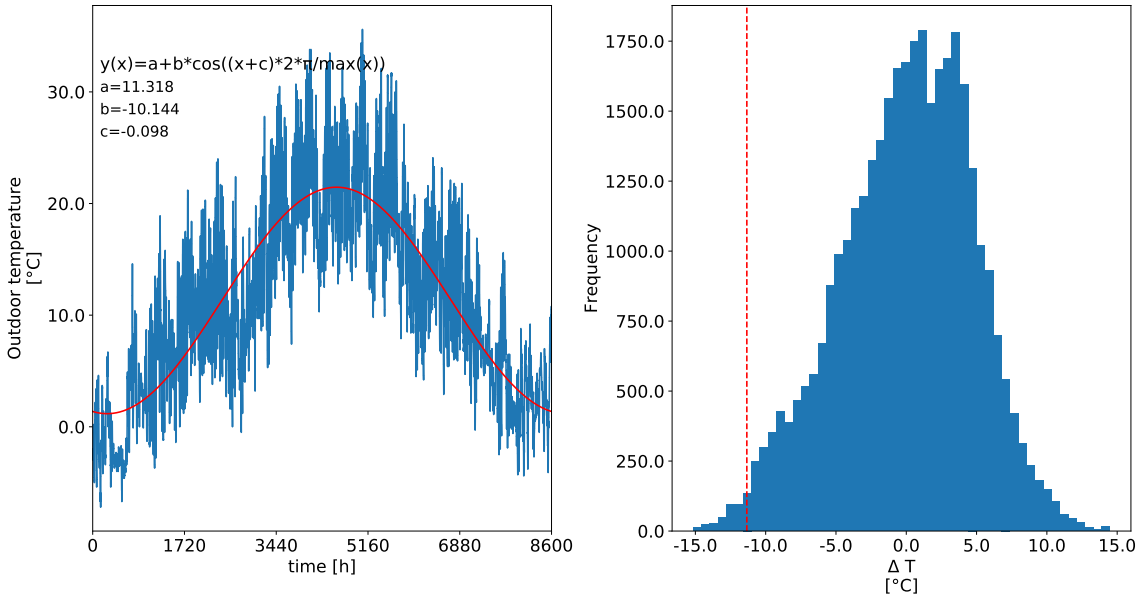

Figure B.3: Left: temperature distribution for Geneva, with sine fit (red curve); Right: Probability density distribution of temperature deviation from sine fit for Geneva.

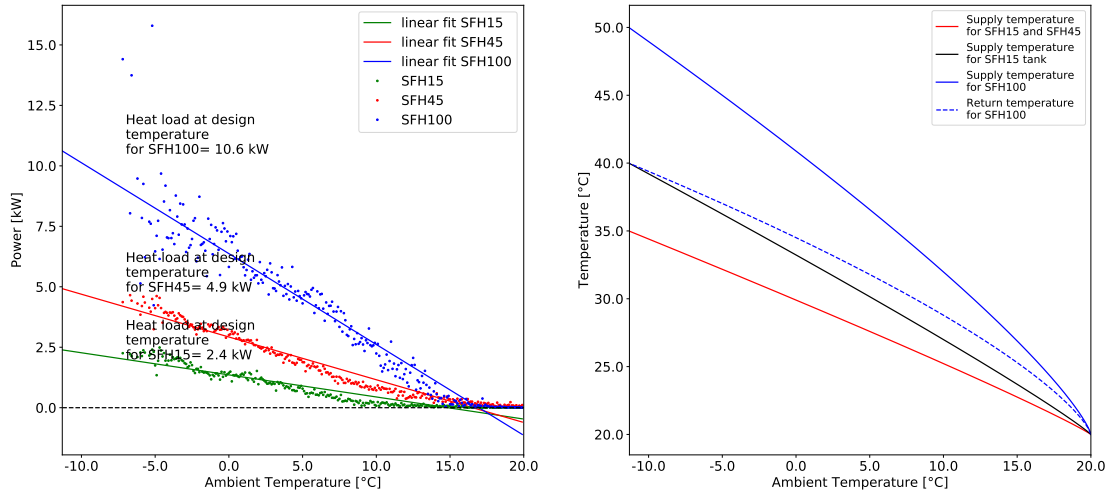

(a) (b)

Figure B.4: (a): Heat load at the design temperature and required heating power of the building in function of the outside temperature of the three building types SFH100, SFH45, SFH15; (b): Supply and return temperatures as a function of the ambient temperature of the building types SFH100, SFH45 and SFH15 with a heating limit at the ambient temperature of 15°C

To calculate the heating system' supply and return temperatures, represented in see Fig. B.4, we use the average daily outdoor temperature and the set-point temperature (20°C), following the IEA approach (Dott, Haller, et al. 2013, Section 5 and Appendix E).

The closest heat pump size in Fig. B.5 that meets the peak heat demand load at the design temperature is used, in case the closest heat pump size is not able to provide the required heat power at the design point, a backup heater is used to supply the missing power (its COP is assumed to be one, and is assumed to be connected to the thermal storage).

B.3 Heat pump lookup table

Belaria SRM (4-16) — Hoval

Leistungsdaten - Heizung

Hoval Belaria® SRM (4-16)
Angaben gemäss EN14511

Typ tVL °C	tQ °C	Qh kW	(4) P kW	COP	Qh kW	(6) P kW	COP	Qh kW	(8) P kW	COP	Qh kW	(11) P kW	COP	Qh kW	(14) P kW	COP	Qh kW	(16) P kW	COP
30	-20	2,3	1,5	1,48	3,2	1,9	1,67	3,8	2,4	1,57	7,3	3,7	1,98	9,0	4,9	1,82	9,6	5,6	1,71
	-15	3,3	1,5	2,16	4,1	1,9	2,22	5,0	2,4	2,08	8,8	3,9	2,25	10,3	5,0	2,08	10,6	5,8	1,84
	-10	4,2	1,5	2,73	5,0	1,8	2,72	6,0	2,3	2,55	9,0	3,4	2,63	11,3	4,7	2,44	11,8	5,3	2,25
	-7	4,7	1,5	3,07	5,5	1,8	3,03	6,6	2,3	2,84	9,1	3,1	2,91	11,9	4,5	2,68	12,6	5,0	2,53
	-2	4,8	1,4	3,56	6,2	1,8	3,44	7,4	2,3	3,24	9,6	2,9	3,29	11,4	3,7	3,06	12,1	4,2	2,86
	2	4,9	1,2	4,12	6,6	1,8	3,74	7,9	2,3	3,51	9,5	2,6	3,71	11,2	3,3	3,46	11,7	3,7	3,21
	7	5,3	1,0	5,30	8,5	1,8	4,61	10,2	2,4	4,33	11,9	2,3	5,21	15,1	3,1	4,92	16,6	3,5	4,81
	12	5,3	0,8	6,87	9,2	1,8	5,05	11,0	2,3	4,76	12,9	2,2	5,82	16,0	3,0	5,38	17,3	3,4	5,16
	15	5,5	0,8	7,20	10,0	1,8	5,60	12,0	2,3	5,28	14,0	2,2	6,36	17,3	3,0	5,85	18,8	3,4	5,60
	20	6,0	0,7	8,14	11,5	1,8	6,54	13,8	2,3	6,14	15,9	2,1	7,43	19,8	2,9	6,75	21,5	3,3	6,43
35	-20	2,2	1,7	1,29	3,1	2,1	1,47	3,7	2,7	1,38	7,3	4,1	1,80	8,9	5,3	1,70	9,7	5,9	1,64
	-15	3,1	1,7	1,80	4,0	2,1	1,94	4,8	2,6	1,82	8,7	4,3	2,03	10,2	5,3	1,91	10,6	6,2	1,71
	-10	4,0	1,7	2,36	4,8	2,0	2,37	5,8	2,6	2,23	8,8	3,8	2,34	11,1	5,0	2,20	11,7	5,7	2,04
	-7	4,6	1,7	2,81	5,3	2,0	2,64	6,4	2,6	2,48	8,8	3,4	2,57	11,7	4,9	2,40	12,3	5,4	2,28
	-2	4,8	1,5	3,13	6,1	2,0	3,10	7,3	2,5	2,92	9,2	3,2	2,88	11,1	4,1	2,72	11,8	4,6	2,55
	2	4,8	1,3	3,59	6,4	1,9	3,37	7,7	2,4	3,17	9,1	2,8	3,20	10,9	3,6	3,05	11,4	4,0	2,85
	7	5,1	1,1	4,57	8,4	2,0	4,20	10,0	2,5	3,94	11,4	2,6	4,46	14,6	3,3	4,36	16,1	3,7	4,30
	12	5,2	0,9	6,05	9,0	2,0	4,60	10,8	2,5	4,32	12,3	2,5	4,98	15,4	3,3	4,70	16,7	3,7	4,54
	15	5,3	0,8	6,53	9,8	1,9	5,12	11,7	2,4	4,80	13,3	2,5	5,44	16,7	3,3	5,11	18,2	3,7	4,92
	20	5,9	0,8	7,22	11,2	1,9	5,99	13,5	2,4	5,66	15,2	2,4	6,33	19,0	3,2	5,88	20,8	3,7	5,64
40	-20	2,2	1,9	1,15	2,9	2,4	1,24	3,5	3,0	1,16	7,3	4,5	1,63	8,8	5,6	1,57	9,6	6,3	1,52
	-15	3,2	1,9	1,67	3,8	2,3	1,64	4,5	2,9	1,54	8,5	4,7	1,82	9,7	5,6	1,75	9,9	6,2	1,59
	-10	4,0	1,9	2,12	4,7	2,3	2,10	5,7	2,9	1,98	8,5	4,1	2,07	10,8	5,4	1,99	11,2	6,0	1,87
	-7	4,5	1,9	2,40	5,3	2,2	2,38	6,4	2,8	2,24	8,5	3,8	2,26	11,4	5,3	2,14	12,0	5,9	2,05
	-2	4,6	1,7	2,71	6,0	2,1	2,82	7,3	2,7	2,66	8,8	3,5	2,51	10,8	4,5	2,41	11,5	5,1	2,27
	2	4,7	1,5	3,05	6,2	2,1	3,00	7,4	2,6	2,83	8,6	3,1	2,75	10,5	3,9	2,69	11,1	4,4	2,52
	7	5,0	1,3	3,82	8,2	2,2	3,80	9,8	2,7	3,58	11,2	2,8	3,95	13,9	3,7	3,74	15,5	4,2	3,71
	12	5,1	1,0	5,00	8,7	2,1	4,14	10,5	2,7	3,88	12,2	2,8	4,42	14,7	3,6	4,07	16,1	4,1	3,97
	15	5,2	1,0	5,27	9,5	2,1	4,55	11,4	2,7	4,27	13,2	2,7	4,83	16,0	3,6	4,43	17,5	4,1	4,30
	20	5,7	1,0	5,97	10,9	2,1	5,29	13,0	2,6	4,97	15,1	2,7	5,60	18,3	3,6	5,10	20,0	4,1	4,94
45	-20	2,2	2,1	1,01	2,8	2,5	1,10	3,3	3,2	1,03	6,8	4,7	1,44	7,2	5,6	1,28	7,7	6,3	1,22
	-15	2,9	2,2	1,36	3,6	2,5	1,47	4,3	3,1	1,39	7,8	4,7	1,67	8,9	5,6	1,60	9,6	6,3	1,53
	-10	3,8	2,1	1,81	4,6	2,4	1,91	5,5	3,1	1,80	8,0	4,3	1,87	10,2	5,6	1,83	10,7	6,3	1,71
	-7	4,3	2,1	2,10	5,2	2,4	2,19	6,3	3,0	2,06	8,2	4,1	2,01	11,0	5,6	1,97	11,4	6,3	1,82
	-2	4,5	1,9	2,41	5,7	2,3	2,50	6,8	2,9	2,34	8,6	3,8	2,25	10,5	4,8	2,17	11,4	5,5	2,06
	2	4,6	1,7	2,71	6,1	2,2	2,77	7,3	2,8	2,61	8,9	3,4	2,58	10,7	4,3	2,45	11,4	4,8	2,39
	7	4,9	1,4	3,40	8,0	2,3	3,43	9,5	3,0	3,22	11,0	3,2	3,48	13,6	4,1	3,29	15,2	4,6	3,29
	12	4,9	1,2	4,06	8,4	2,3	3,66	10,1	2,9	3,44	12,0	3,1	3,89	14,4	4,0	3,59	15,8	4,5	3,51
	15	5,1	1,2	4,22	9,1	2,3	4,03	10,9	2,9	3,78	13,1	3,1	4,24	15,6	4,0	3,90	17,1	4,5	3,81
	20	5,5	1,1	4,88	10,4	2,2	4,66	12,5	2,9	4,39	15,0	3,0	4,93	17,9	4,0	4,48	19,6	4,5	4,35
50	-20	2,1	2,3	0,89	2,7	2,6	1,05	3,3	3,2	1,02	-	-	-	-	-	-	-	-	-
	-15	2,9	2,3	1,22	3,5	2,5	1,40	4,2	3,2	1,32	6,9	4,7	1,47	8,2	5,6	1,47	8,8	6,3	1,40
	-10	3,6	2,3	1,57	4,5	2,5	1,80	5,3	3,2	1,69	7,6	4,6	1,64	9,2	5,6	1,65	9,7	6,3	1,55
	-7	4,1	2,3	1,78	5,0	2,5	2,04	6,0	3,1	1,91	8,0	4,6	1,74	9,8	5,6	1,75	10,3	6,3	1,63
	-2	4,3	2,1	2,03	5,6	2,4	2,35	6,7	3,0	2,22	8,6	4,3	2,00	10,2	5,2	1,95	10,4	5,8	1,81
	2	4,4	1,9	2,29	6,0	2,3	2,61	7,2	2,9	2,45	8,4	3,8	2,21	10,3	4,7	2,19	11,0	5,4	2,04
	7	4,7	1,7	2,83	7,5	2,4	3,14	9,0	3,1	2,94	10,7	3,5	3,03	13,4	4,6	2,93	14,5	5,1	2,86
	12	4,7	1,5	3,22	8,0	2,4	3,35	9,6	3,1	3,15	11,7	3,5	3,38	14,2	4,4	3,19	15,1	5,0	3,05
	15	4,8	1,4	3,47	8,7	2,4	3,65	10,4	3,0	3,43	12,7	3,5	3,69	15,4	4,5	3,46	16,4	5,0	3,31
	20	5,2	1,3	3,92	9,9	2,4	4,19	11,9	3,0	3,94	14,2	3,4	4,16	17,2	4,4	3,87	18,8	5,0	3,78
55	-15	2,6	2,4	1,08	3,3	2,6	1,28	3,9	3,3	1,20	4,5	4,8	0,94	6,6	6,2	1,06	7,0	7,1	0,98
	-10	3,4	2,4	1,39	4,1	2,5	1,61	4,9	3,2	1,52	6,3	4,7	1,34	8,2	5,8	1,41	8,6	6,6	1,31
	-7	3,8	2,4	1,58	4,6	2,5	1,82	5,5	3,2	1,71	7,1	4,7	1,52	8,7	5,6	1,56	9,2	6,3	1,46
	-2	4,1	2,2	1,85	5,1	2,5	2,09	6,2	3,1	1,96	7,8	4,6	1,70	8,9	5,2	1,70	9,3	5,8	1,62
	2	4,3	2,0	2,11	5,5	2,4	2,29	6,6	3,1	2,15	7,6	4,2	1,81	9,8	5,2	1,90	10,3	5,8	1,78
	7	4,5	1,8	2,58	7,1	2,5	2,85	8,5	3,2	2,69	10,0	3,9	2,54	12,7	5,1	2,52	13,9	5,6	2,48
	12	4,6	1,5	3,01	7,5	2,5	3,04	9,0	3,2	2,87	11,0	3,9	2,84	13,5	4,9	2,75	14,5	5,5	2,64
	15	4,6	1,5	3,13	8,1	2,5	3,30	9,8	3,2	3,10	12,0	3,9	3,11	14,7	4,9	2,99	15,8	5,5	2,86
	20	4,9	1,5	3,37	9,3	2,5	3,77	11,2	3,2	3,55	13,5	3,8	3,51	16,4	4,9	3,33	18,1	5,5	3,27

tVL = Heizungsvorlauftemperatur (°C)
tQ = Quellentemperatur (°C)
Qh = Heizleistung bei Volllast (kW), gemessen nach Standard EN 14511
P = Aufnahmeleistung Gesamtgerät (kW) inkl. Hocheffizienzpumpe, gemessen nach EN 14511
COP = Leistungszahl Gesamtgerät nach Standard EN 14511

Figure B.5: Lookup table for heat pump size, COP and power calculations used in this study

B.4 Electric storage modelling

$$SOC_{min} \leq SOC_i \leq SOC_{max} \tag{B.3}$$

$$E_{char_i} = E_{PV-batt_i} + E_{grid-batt_i} \tag{B.4}$$

$$E_{dis_i} \leq (SOC_{i-1} - SOC_{min}) * C_{batt}^{nom} \tag{B.5}$$

$$SOC_i = \frac{(SOC_{i-1} * C_{batt}^{nom} + E_{char_i} - E_{dis_i} - E_{loss-batt_i})}{C_{batt}^{nom}} \tag{B.6}$$

$$E_{dis_i} = E_{batt-load_i} + E_{batt-hp_i} + E_{batt-hpw_i} + E_{loss-battinv_i} \tag{B.7}$$

B.5 System lifetime

Every optimization was run for one year and then the results are scaled over a time period of 30 years, corresponding to the PV lifetime (Bauer et al. 2017). The battery is assumed to reach its end of life once the capacity has decreased by 30% (Pena-Bello, Barbour, Gonzalez, Yilmaz, et al. 2020). We consider replacements for all the components of the system and take a conservative approach by keeping the same capital cost for future components, which are discounted to the present considering the time value of money. If the lifetime of a replaced component exceeds 30 years, the residual value of the component is deduced from the capital expenditures (CAPEX) using straight-line depreciation and a discount factor of 4% (Moore et al. 2015). Table B.1 shows the present value of the CAPEX per device for each type of house considered in this study, including replacements. The specific technology costs for PV, battery, heat pumps and hot water tanks are given in Table B.2.

Table B.1: CAPEX (USD) including replacements for the various technologies included in this study depending on the type of house. Detailed values are presented in Table B.2

Device	Size	SFH15	SFH45	SFH100	Reference
PV	4.8 [kW_p]	10360	10360	10360	Bauer et al. 2017
Heat pump	4/6/16 [kW_{th}]	10300	15500	41200	Fischer et al. 2016
Battery[a]	7 [kWh_{el}]	12120	13180	13280	Schmidt et al. 2019
Tank SH	17.4 [kWh_{el}]	0[b]	0[b]	1790	Fischer et al. 2016
Tank DHW	4.7 [kWh_{el}]	960	960	960	Fischer et al. 2016

a Average values to account aging.
b The concrete of the floors and the heating water content are used as existing heat storage and thus no additional costs are considered.

Table B.2: Values selected for the technical and economic assessment of PV-coupled heat pump systems supported by electricity and heat storage.

Component	Units	Value	Reference
PV size	[kW]	4.8	
PV lifetime	[years]	30	Bauer et al. 2017
PV module cost	[USD/kW]	1032	Bauer et al. 2017
PV Balance of plant cost	[USD/kW]	240	Bauer et al. 2017
PV Installation costs (labour costs)	[USD/kW]	514	Bauer et al. 2017
PV Installation costs (other costs)	[USD/kW]	163.5	Bauer et al. 2017
PV O&M	[USD/kW]	103	Bauer et al. 2017
PV inverter cost	[USD/kW]	190	Fu et al. 2017
PV inverter lifetime	years	15	Fu et al. 2017
Inverter efficiency	%	94	Pena-Bello, Barbour, Gonzalez, Yilmaz, et al. 2020
ILR	p.u.	1.2	Burger and Rüther 2006
Charge controller efficiency	%	98	Pena-Bello, Barbour, Gonzalez, Yilmaz, et al. 2020
Bi-directional inverter cost	[USD/kW]	600	Ardani et al. 2017
Bi-directional inverter lifetime	years	15	Fu et al. 2017
Battery pack cost	[USD/kWh_{el}]	335	Schmidt et al. 2019
Battery balance of plant cost	[USD]	2000	Baumann and Baumgartner 2017
Battery O&M	[USD/kW]	0	Schmidt et al. 2019
Battery round-trip efficiency	%	89	Schmidt et al. 2019
End of life (EoL)	%	70	Pena-Bello, Barbour, Gonzalez, Yilmaz, et al. 2020
HP lifetime	[years]	20	Fischer et al. 2016
HP module cost	[USD/kW]	1650	Fischer et al. 2016
HP Installation costs	[USD/kW]	2200	Fischer et al. 2016
HP O&M	% of CAPEX p.a.	1.1	Fischer et al. 2016
Hot water tank lifetime	[years]	20	Fischer et al. 2016
Hot water tank cost @ 10 K ΔT	[USD/kWh_{th}]	66	Fischer et al. 2016
Hot water tank cost @ 20 K ΔT	[USD/kWh_{th}]	132	Fischer et al. 2016
Hot water tank Installation costs	[USD/kWh_{th}]	0	Fischer et al. 2016
Hot water tank O&M	[USD/kWh_{th}]	0	Fischer et al. 2016
Discount factor	%/a	4	Pena-Bello, Barbour, Gonzalez, Yilmaz, et al. 2020
EUR to USD rate	p.u.	1.1	

B.6 Optimization model validation

In order to validate the model, some test scenarios with intuitive solutions for the optimum schedule of operation of the battery and the heat pump, separately, are considered. For the battery, we use a scenario using a battery with a capacity of 20 kWh_el and efficiency of 100%. We use the demand of one day for a randomly selected house from the dataset. Figure B.6, presents the time-series test price with a time slot with a low price of 20 USD/kWh_{el} and a peak price of 100 USD/kWh_{el}. The battery charging and discharging limits are set at 2*C. The output is as expected a schedule where the battery is charged in the low-price time slot and discharged afterwards.

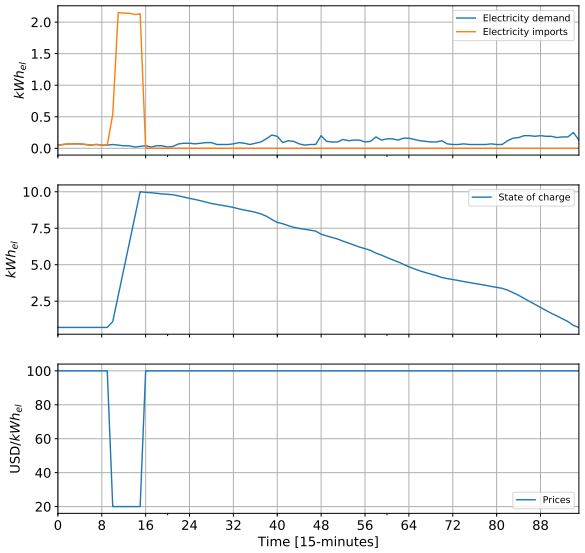

Figure B.6: Result for battery scheduling optimization of the off-peak time slot test case. On top the electricity demand and imports are shown. In the middle the state of charge of the battery is displayed. At the bottom the price is displayed.

As for the heat pump, we use three test scenarios. The first one, as in the case of the battery presents the time-series test price with a time slot with a low price of 20 USD/kWh_{el} and a peak price of 100 USD/kWh_{el}. The thermal storage is charged at when prices are low and discharged at once when there is heat demand, as displayed in B.7. It is worth to recall that we assume an intrinsic thermal flexibility of the houses of 2 hours.

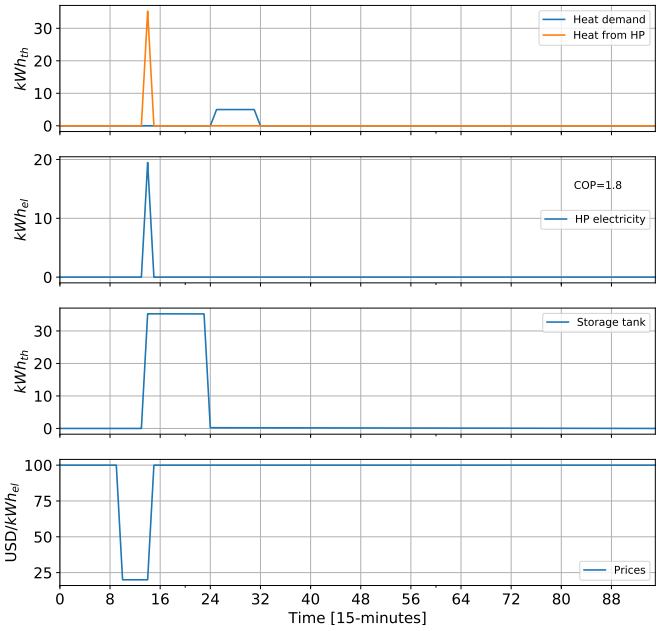

Figure B.7: Result for heat pump and thermal storage scheduling optimization of the off-peak time slot test case. On top the heat demand and heat provided by the HP are shown. The second panel shows the HP electricity demand (note the COP of 1.8, at that time of the day, which is a function of the outdoor temperature). The third panel displays the amount of energy stored in the storage tank. Finally, at the bottom the price is displayed.

The second test scenario consists of a heat pump without storage of any kind. As in the previous case, there is a time slot with low price. Moreover, the heat demand is extended across two 2-hour-blocks to show the behavior of the heat supply. As shown in Figure B.8, when the prices are low, the heat pump provides the heat to cover the demand of the first 2-hours block, later on a second peak represents the delivery of heat to cover the demand of the second block. Finally, Figure B.9 displays a situation where the low price does not match the heat demand and therefore, the heat pump cannot profit from the price difference and is forced to cover the heat demand at the same time as it appears.

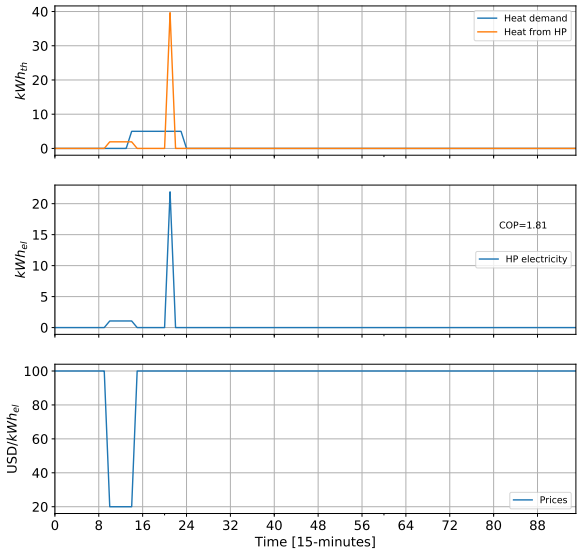

Figure B.8: Result for heat pump scheduling optimization of the off-peak time slot test case. On top the heat demand and heat provided by the HP are shown. The middle panel shows the HP electricity demand (note the COP of 1.8, at that time of the day, which is a function of the outdoor temperature). Finally, at the bottom the price is displayed.

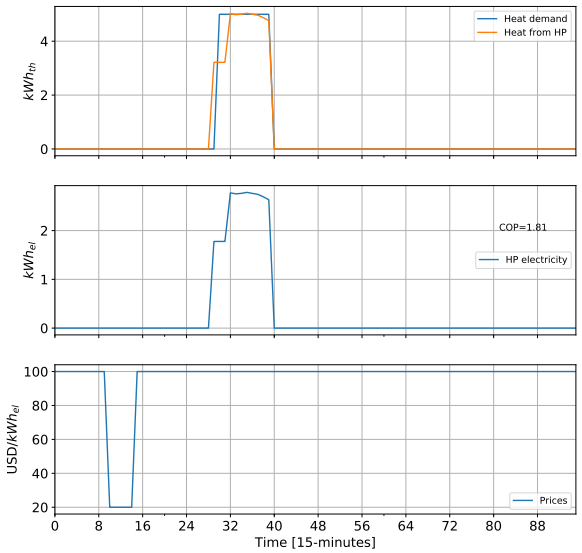

Figure B.9: Result for heat pump scheduling optimization of the off-peak time slot test case. On top the heat demand and heat provided by the HP are shown. The middle panel shows the HP electricity demand (note the COP of 1.8, at that time of the day, which is a function of the outdoor temperature). Finally, at the bottom the price is displayed.

Table B.3: List of model parameters and variables.

Modeling parameters	Name	Units	Modeling variables	Name	Units
Converter efficiency	η_{conv}	%	PV generation fed to the load	$E_{PV-load}$	kWh_{el}
Inverter efficiency	η_{inv}	%	PV generation exported to the grid	$E_{PV-grid}$	kWh_{el}
Inverter rating	P_{inv}	kW	PV generation injected to the battery	$E_{PV-batt}$	kWh_{el}
Battery Efficiency	η_{batt}	%	PV generation curtailed	$E_{PV-curt}$	kWh_{el}
Maximum discharge power	$P_{max-dis}$	kW	Energy lost due to converter efficiency	$E_{loss-conv}$	kWh_{el}
Maximum charge power	$P_{max-char}$	kW	Total energy lost due to bi-directional inverter efficiency	$E_{loss-binv}$	kWh_{el}
Battery nominal capacity	C_{batt}^{nom}	kWh_{el}	PV energy lost due to bi-directional inverter efficiency	$E_{loss-PVinv}$	kWh_{el}
Battery lifetime	N	years	Grid energy lost due to bi-directional inverter efficiency	$E_{loss-gridinv}$	kWh_{el}
Battery maximum state of charge	SOC_{max}	%	Battery energy lost due to bi-directional inverter efficiency	$E_{loss-battinv}$	kWh_{el}
Battery minimum state of charge	SOC_{min}	%	Energy lost due to battery efficiency	$E_{loss-batt}$	kWh_{el}
Retail prices	π_{import}	USD/kWh_{el}	Energy drained from the battery	E_{dis}	kWh_{el}
Export prices	π_{export}	USD/kWh_{el}	Energy injected to the battery	E_{char}	kWh_{el}
Capacity tariff	$\pi_{capacity}$	USD/kW	Energy delivered from the battery to the load	$E_{batt-load}$	kWh_{el}
Feed-in limit	P_{limit}	%	Energy imported from the grid to the battery	$E_{grid-batt}$	kWh_{el}
Combination of applications	[PVCT, PVSC, DLS, DPS]	Boolean array	Energy imported from the grid to the load	$E_{grid-load}$	kWh_{el}
Load demand	E_{load}	kWh_{el}	Energy drained from the grid	E_{grid}	kWh_{el}
PV generation	E_{PV}	kWh_{el}	State of charge	SOC_i	%
Space heat demand (SH)	Q_{load}	kWh_{th}	PV generation fed to the HP for SH	E_{PV-hp}	kWh_{el}
Domestic heat water demand	Q_{dhw}	kWh_{th}	PV generation fed to the HP for DHW	E_{PV-hpw}	kWh_{el}
Nominal power of the HP	$P_{HP_{nom}}$	kW	Energy from the battery fed to the HP for SH	$E_{batt-hp}$	kWh_{el}
Coefficient of Performance	COP_i	-	Energy from the battery fed to the HP for DHW	$E_{batt-hpw}$	kWh_{el}
Temperature minimum of SH tank	$T_{ts_{min}}$	K	Energy from the grid fed to the HP for SH	$E_{grid-hp}$	kWh_{el}
Temperature maximum of SH tank	$T_{ts_{max}}$	K	Energy from the grid fed to the HP for DHW	$E_{grid-hpw}$	kWh_{el}
Temperature minimum of DHW tank	$T_{tsw_{min}}$	K	Thermal energy in the SH tank	Q_{ts}	kWh_{th}
Temperature maximum of DHW tank	$T_{tsw_{max}}$	K	Thermal energy in the DHW tank	Q_{tsw}	kWh_{th}
U-value SH tank	U_{ts}	$kW * m^{-2} * K^{-1}$	Thermal energy lost in the SH tank	$Q_{losses_{ts}}$	kWh_{th}
U-value DHW tank	U_{tsw}	$kW * m^{-2} * K^{-1}$	Thermal energy lost in the DHW tank	$Q_{losses_{tsw}}$	kWh_{th}
Surface SH tank	A_{ts}	m^2	Thermal energy flow from SH tank to SH	Q_{ts-sh}	kWh_{th}
Surface DHW tank	A_{tsw}	m^2	Thermal energy flow from DHW tank to DHW	$Q_{tsw-dhw}$	kWh_{th}
Specific heat SH tank fluid	$c_{p_{ts}}$	$kWh * kg^{-1} * K^{-1}$	Thermal energy supplied by the HP to the SH tank	Q_{hp-ts}	kWh_{th}
Specific heat DHW tank fluid	$c_{c_{tsw}}$	$kWh * kg^{-1} * K^{-1}$	Thermal energy supplied by the HP to the DHW tank	$Q_{hpw-tsw}$	kWh_{th}
Mass SH tank fluid	m_{ts}	kg	Thermal energy supplied by the HP SH demand	Q_{hp-sh}	kWh_{th}
Mass SH tank fluid	m_{tsw}	kg	Temperature of the SH tank	T_{ts}	K
Configuration	[Batt, heating, ts, DHW]	Boolean array	Temperature of the DHW tank	T_{ts}	K
Optimization time framework t	minutes	-	Maximum power drained from the grid	$P_{max-day}$	kW
Temporal resolution	Δt	fraction of hour	Power related to any energy parameter	$P_x = E_x/\Delta t$	kW

B.7 Total electricity demand

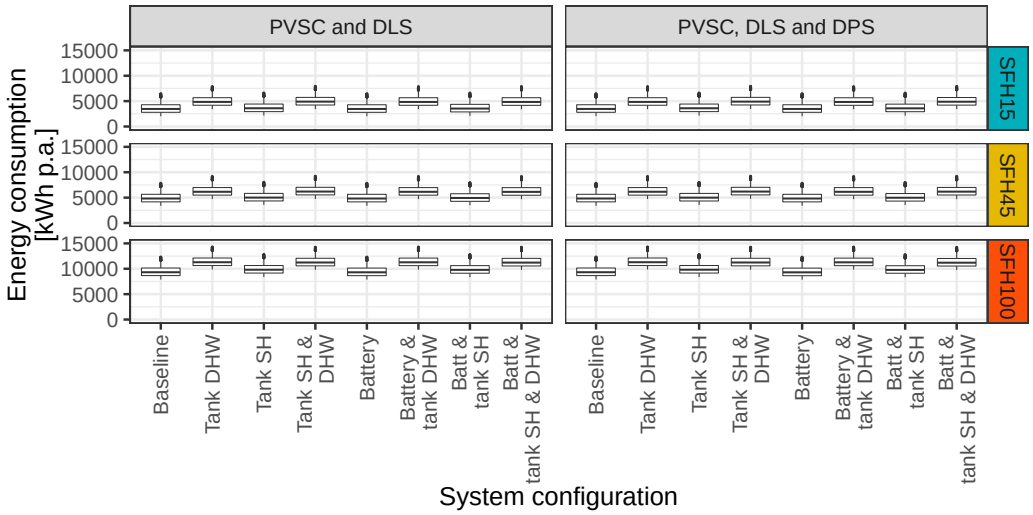

Figure B.10: Boxplots (N=549) of the total electricity demand including appliances, lighting and heat pump, for all configurations depending number of storage applications (PVSC is PV self-consumption, DLS is demand load-shifting and DPS is demand peak-shaving with a capacity-based tariff) and the type of house (SFH15, SFH45 and SFH100). The line in the middle of the box represents the median electricity use. The box spans the first quartile to the third quartile, and the whiskers extend up to 1.5 times the interquartile range from the top or bottom of the box.

B.8 Other results

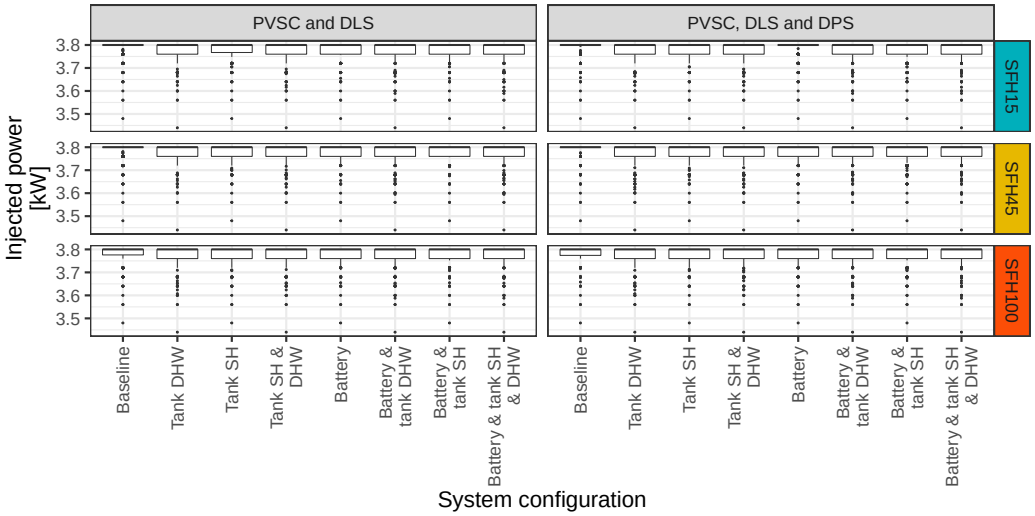

Figure B.11: Boxplots (N=549) of the injected power, for all configurations depending number of storage applications (PVSC is PV self-consumption, DLS is demand load-shifting and DPS is demand peak-shaving with a capacity-based tariff) and the type of house (SFH15, SFH45 and SFH100). The line in the middle of the box represents the median electricity use. The box spans the first quartile to the third quartile, and the whiskers extend up to 1.5 times the interquartile range from the top or bottom of the box.

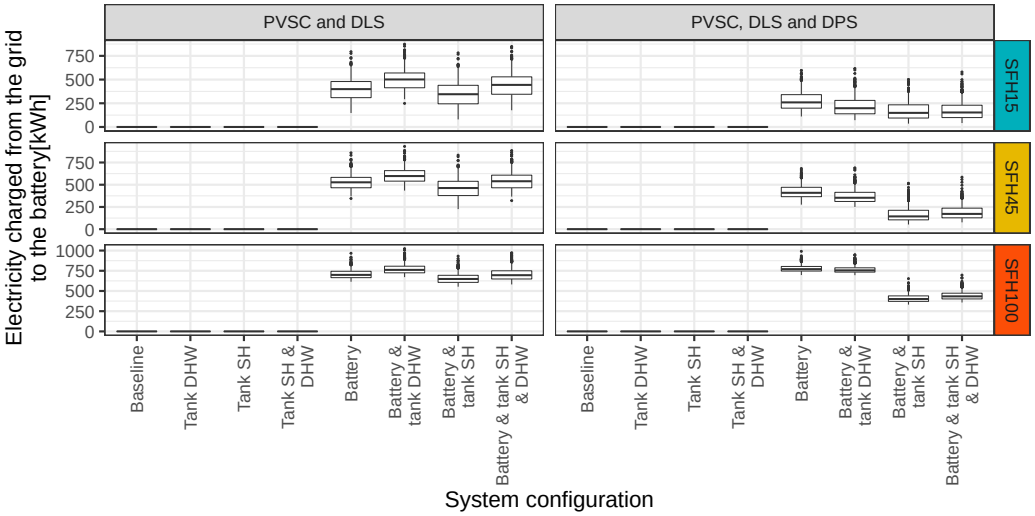

Figure B.12: Boxplots (N=549) of the total electricity charged from the grid to the battery, for all configurations depending number of storage applications (PVSC is PV self-consumption, DLS is demand load-shifting and DPS is demand peak-shaving with a capacity-based tariff) and the type of house (SFH15, SFH45 and SFH100). The line in the middle of the box represents the median electricity use. The box spans the first quartile to the third quartile, and the whiskers extend up to 1.5 times the interquartile range from the top or bottom of the box.

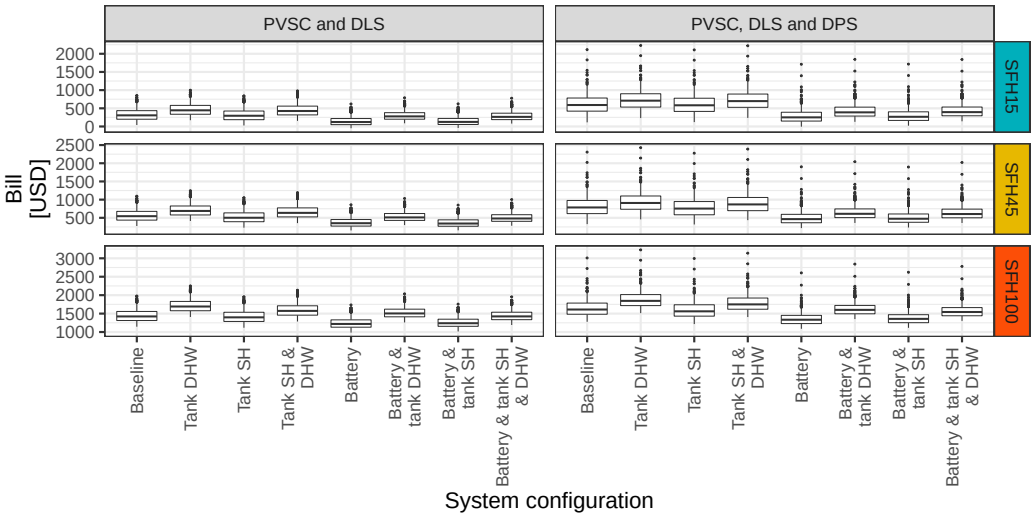

Figure B.13: Boxplots (N=549) of the total electricity bill accounting for appliances, lighting and heat pump, for all configurations depending number of storage applications (PVSC is PV self-consumption, DLS is demand load-shifting and DPS is demand peak-shaving with a capacity-based tariff) and the type of house (SFH15, SFH45 and SFH100). The line in the middle of the box represents the median electricity use. The box spans the first quartile to the third quartile, and the whiskers extend up to 1.5 times the interquartile range from the top or bottom of the box.

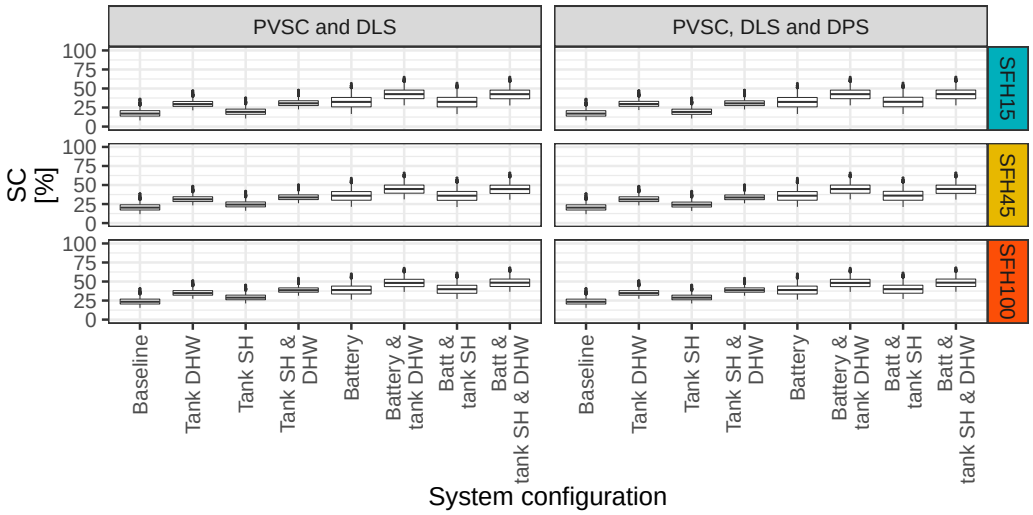

Figure B.14: Boxplots (N=549) of the self-consumption, for all configurations depending number of storage applications (PVSC is PV self-consumption, DLS is demand load-shifting and DPS is demand peak-shaving with a capacity-based tariff) and the type of house (SFH15, SFH45 and SFH100). The line in the middle of the box represents the median electricity use. The box spans the first quartile to the third quartile, and the whiskers extend up to 1.5 times the interquartile range from the top or bottom of the box.

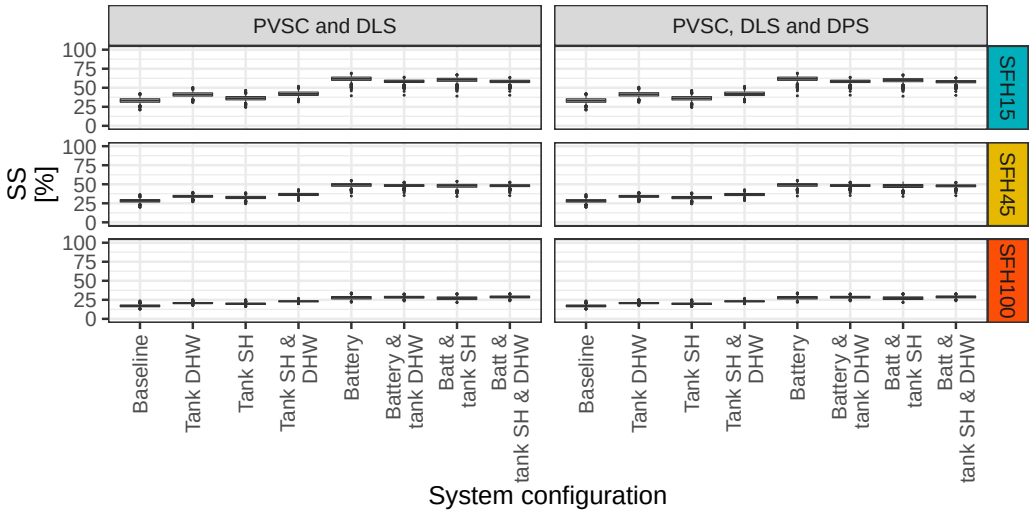

Figure B.15: Boxplots (N=549) of the self-sufficiency, for all configurations depending number of storage applications (PVSC is PV self-consumption, DLS is demand load-shifting and DPS is demand peak-shaving with a capacity-based tariff) and the type of house (SFH15, SFH45 and SFH100). The line in the middle of the box represents the median electricity use. The box spans the first quartile to the third quartile, and the whiskers extend up to 1.5 times the interquartile range from the top or bottom of the box.

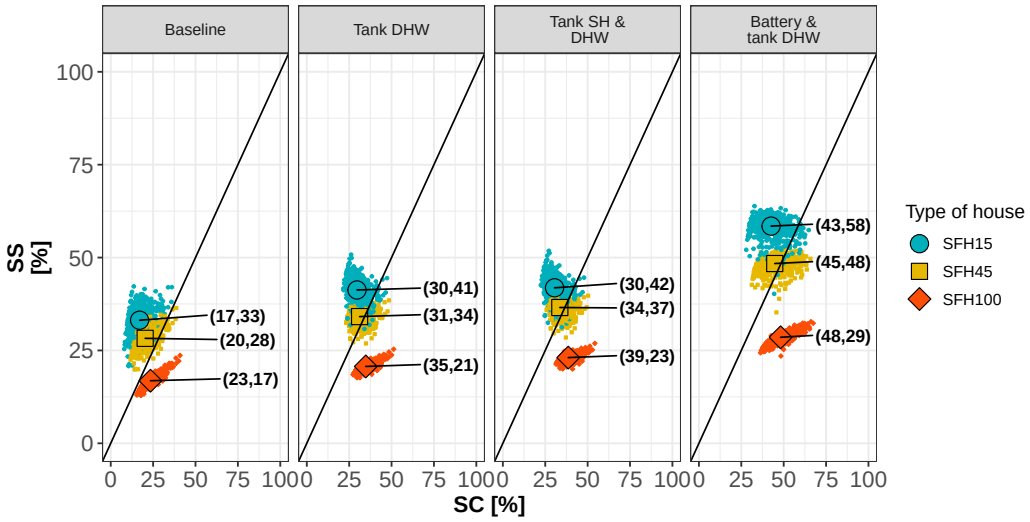

Figure B.16: Energy matching chart to analyze self-consumption (SC) and self-sufficiency (SS) for a PV-coupled heat pump system as a function of the type of storage, namely, none (baseline case), heat storage for DHW, heat storage for space heating and with DHW and finally, with DHW storage and a battery. The configurations presented here include a capacity-based tariff in the electricity tariff. The big black circle, square and diamond represent the median by type of house.

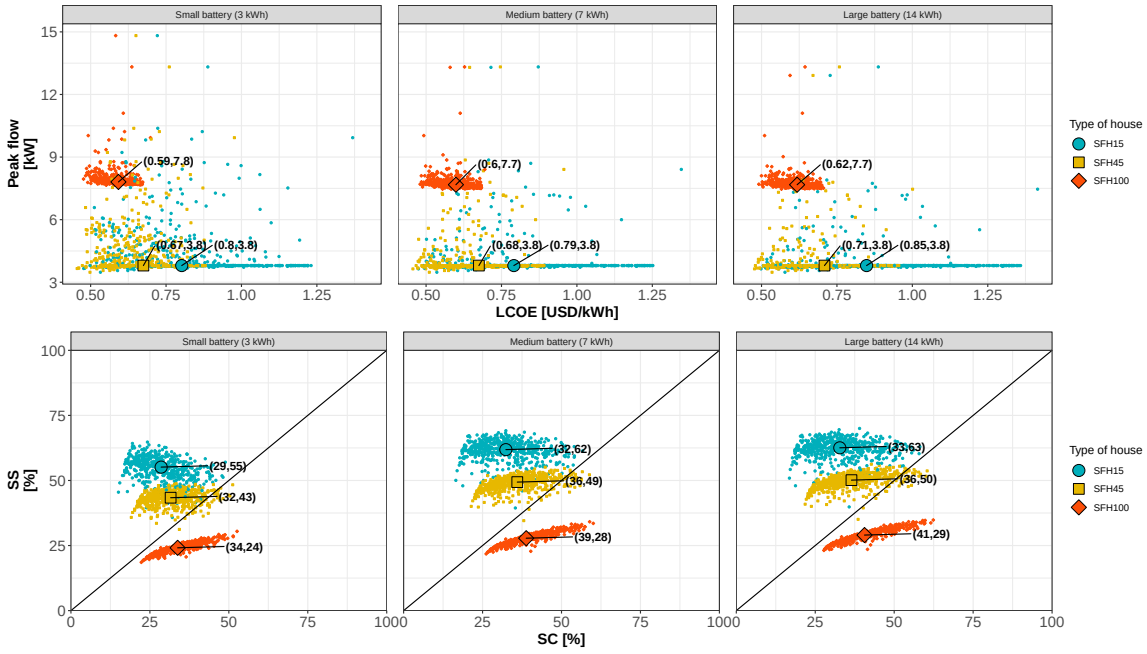

Figure B.17: LCOE vs peak flow (top) for a PV-coupled heat pump system as a function of the electricity storage size, namely, small (3 kWh), medium (7 kWh), and large (14 kWh); Energy matching chart (bottom) to analyze self-consumption (SC) and self-sufficiency (SS) for a PV-coupled heat pump system as a function of the electricity storage size, namely, small (3 kWh), medium (7 kWh), and large (14 kWh). The configurations presented here include a capacity-based tariff in the electricity tariff. The big black circle, square and diamond represent the median by type of house.

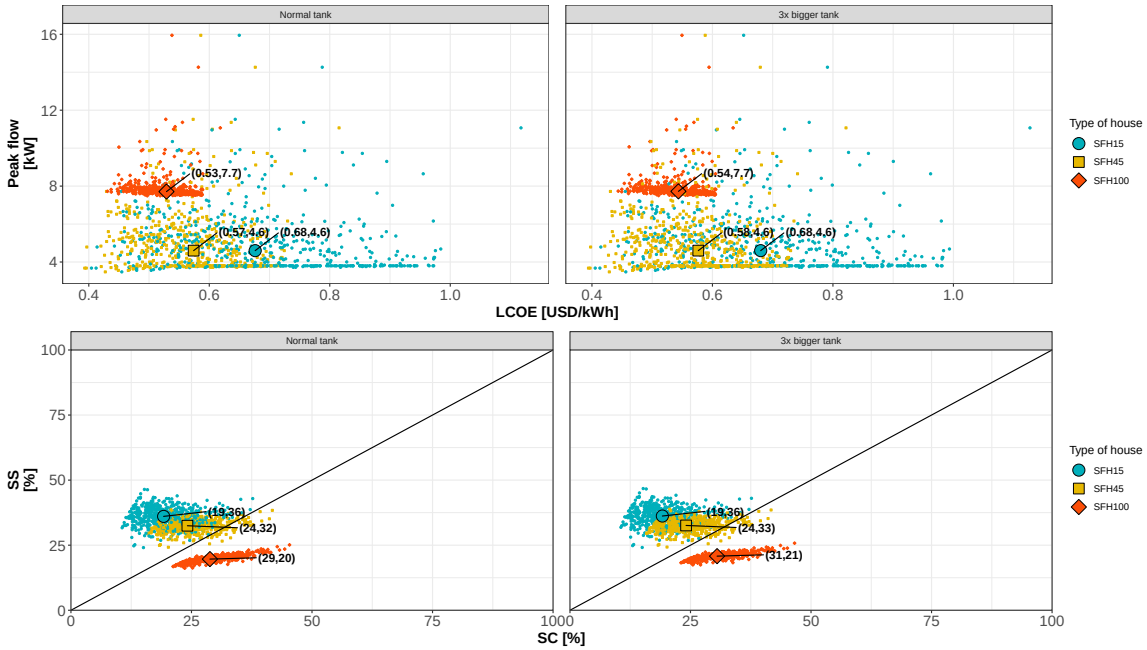

Figure B.18: LCOE vs peak flow (top) for a PV-coupled heat pump system as a function of the electricity thermal size, namely, normal (17.5 kWh), and large (52.5 kWh); Energy matching chart (bottom) to analyze self-consumption (SC) and self-sufficiency (SS) for a PV-coupled heat pump system as a function of the thermal storage size, namely, normal (17.5 kWh), and large (52.5 kWh). The configurations presented here include a capacity-based tariff in the electricity tariff. The big black circle, square and diamond represent the median by type of house

B.9 Statistical tests

Table B.4: Results of Shapiro test performed on different subsets for Figures 4.3 and 4.4 of the main paper.

				PVSC and DLS		PVSC, DLS AND DPS						PVSC and DLS		PVSC, DLS AND DPS	
		Figure	subset	W	p-value	W	p-value			Fig. 4.4	subset	W	p-value	W	p-value
LCOE	SFH15	Fig. 4.3	No HP No PV					Peak flow	SFH15	Fig. 4.4	No HP No PV				
		Fig. 4.3	Baseline	0,9657	7,95E-10	0,97999	1,09E-06			Fig. 4.4	Baseline	0,81892	<2.2e-16	0,77253	<2.2e-16
		Fig. 4.3	Tank DHW	0,97951	8,22E-07	0,99134	0,0033			Fig. 4.4	Tank DHW	0,84277	<2.2e-16	0,7744	<2.2e-16
		Fig. 4.3	Tank SH	0,96814	2,36E-09	0,98217	4,15E-06			Fig. 4.4	Tank SH	0,7994	<2.2e-16	0,77285	<2.2e-16
		Fig. 4.3	Tank SH and DHW	0,97971	9,28E-07	0,99135	0,003338			Fig. 4.4	Tank SH and DHW	0,82455	<2.2e-16	0,77442	<2.2e-16
		Fig. 4.3	Battery	0,96461	4,98E-10	0,96904	3,56E-09			Fig. 4.4	Battery	0,78572	<2.2e-16	0,35877	<2.2e-16
		Fig. 4.3	Battery and tank DHW	0,97994	1,06E-06	0,98327	8,40E-06			Fig. 4.4	Battery and tank DHW	0,77419	<2.2e-16	0,36624	<2.2e-16
		Fig. 4.3	Battery and tank SH	0,96279	2,31E-10	0,96983	5,16E-09			Fig. 4.4	Battery and tank SH	0,78133	<2.2e-16	0,36075	<2.2e-16
		Fig. 4.3	Battery and tank SH and DHW	0,97818	3,82E-07	0,98277	6,07E-06			Fig. 4.4	Battery and tank SH and DHW	0,7778	<2.2e-16	0,36873	<2.2e-16
	SFH45	Fig. 4.3	No HP No PV						SFH45	Fig. 4.4	No HP No PV				
		Fig. 4.3	Baseline	0,9791	6,48E-07	0,98892	4,64E-04			Fig. 4.4	Baseline	0,87929	<2.2e-16	0,77306	<2.2e-16
		Fig. 4.3	Tank DHW	0,98192	3,54E-06	0,99169	4,45E-03			Fig. 4.4	Tank DHW	0,89746	<2.2e-16	0,77496	<2.2e-16
		Fig. 4.3	Tank SH	0,9798	9,73E-07	0,98937	6,60E-04			Fig. 4.4	Tank SH	0,85769	<2.2e-16	0,77316	<2.2e-16
		Fig. 4.3	Tank SH and DHW	0,98211	4,00E-06	0,99188	5,21E-03			Fig. 4.4	Tank SH and DHW	0,87473	<2.2e-16	0,77512	<2.2e-16
		Fig. 4.3	Battery	0,97674	1,71E-07	0,98401	1,36E-05			Fig. 4.4	Battery	0,81298	<2.2e-16	0,3609	<2.2e-16
		Fig. 4.3	Battery and tank DHW	0,98013	1,19E-06	0,98656	7,97E-05			Fig. 4.4	Battery and tank DHW	0,77557	<2.2e-16	0,36888	<2.2e-16
		Fig. 4.3	Battery and tank SH	0,9793	7,26E-07	0,98215	4,10E-06			Fig. 4.4	Battery and tank SH	0,83445	<2.2e-16	0,36522	<2.2e-16
		Fig. 4.3	Battery and tank SH and DHW	0,98275	6,00E-06	0,9849	2,48E-05			Fig. 4.4	Battery and tank SH and DHW	0,75742	<2.2e-16	0,3742	<2.2e-16
	SFH100	Fig. 4.3	No HP No PV						SFH100	Fig. 4.4	No HP No PV				
		Fig. 4.3	Baseline	0,98031	1,32E-06	0,98205	3,84E-06			Fig. 4.4	Baseline	0,73406	<2.2e-16	0,32685	<2.2e-16
		Fig. 4.3	Tank DHW	0,97881	5,48E-07	0,98074	1,72E-06			Fig. 4.4	Tank DHW	0,68744	<2.2e-16	0,4223	<2.2e-16
		Fig. 4.3	Tank SH	0,97993	1,06E-06	0,98182	3,32E-06			Fig. 4.4	Tank SH	0,48729	<2.2e-16	0,41031	<2.2e-16
		Fig. 4.3	Tank SH and DHW	0,97885	5,61E-07	0,98074	1,72E-06			Fig. 4.4	Tank SH and DHW	0,51377	<2.2e-16	0,38675	<2.2e-16
		Fig. 4.3	Battery	0,98059	1,57E-06	0,98164	2,97E-06			Fig. 4.4	Battery	0,60603	<2.2e-16	0,37434	<2.2e-16
		Fig. 4.3	Battery and tank DHW	0,97965	8,95E-07	0,9801	1,16E-06			Fig. 4.4	Battery and tank DHW	0,47703	<2.2e-16	0,4475	<2.2e-16
		Fig. 4.3	Battery and tank SH	0,9805	1,49E-06	0,98195	3,61E-06			Fig. 4.4	Battery and tank SH	0,76735	<2.2e-16	0,37721	<2.2e-16
		Fig. 4.3	Battery and tank SH and DHW	0,97994	1,06E-06	0,97964	8,89E-07			Fig. 4.4	Battery and tank SH and DHW	0,81946	<2.2e-16	0,46405	<2.2e-16

Table B.5: Results of Wilcoxon pairwise tests performed on different subsets for Figures 4.3 and 4.4 of the main paper.

					PVSC and DLS	PVSC, DLS and DPS						PVSC and DLS	PVSC, DLS and DPS
		Figure	subset A	subset B	p-value	p-value			Figure	subset A	subset B	p-value	p-value
LCOE	SFH15	Fig. 4.3	Baseline	Tank DHW	<2.2e-16	<2.2e-16	Power	SFH15	Fig. 4.4	Baseline	Tank DHW	0,1663	1
		Fig. 4.3	Baseline	Tank SH	1,30E-09	<2.2e-16			Fig. 4.4	Baseline	Tank SH	0,3811	1
		Fig. 4.3	Baseline	Tank SH and DHW	<2.2e-16	<2.2e-16			Fig. 4.4	Baseline	Tank SH and DHW	1	1
		Fig. 4.3	Baseline	Battery	<2.2e-16	<2.2e-16			Fig. 4.4	Baseline	Battery	7,60E-16	<2.2e-16
		Fig. 4.3	Baseline	Battery and tank DHW	<2.2e-16	<2.2e-16			Fig. 4.4	Baseline	Battery and tank DHW	<2.2e-16	<2.2e-16
		Fig. 4.3	Baseline	Battery and tank SH	<2.2e-16	<2.2e-16			Fig. 4.4	Baseline	Battery and tank SH	<2.2e-16	<2.2e-16
		Fig. 4.3	Baseline	Battery and tank SH and DHW	<2.2e-16	<2.2e-16			Fig. 4.4	Baseline	Battery and tank SH and DHW	<2.2e-16	<2.2e-16
		Fig. 4.3	Tank DHW	Tank SH	<2.2e-16	<2.2e-16			Fig. 4.4	Tank DHW	Tank SH	0,0015	1
		Fig. 4.3	Tank DHW	Tank SH and DHW	0,0055	0,00071			Fig. 4.4	Tank DHW	Tank SH and DHW	0,3811	1
		Fig. 4.3	Tank DHW	Battery	1,40E-06	<2.2e-16			Fig. 4.4	Tank DHW	Battery	6,70E-11	<2.2e-16
		Fig. 4.3	Tank DHW	Battery and tank DHW	<2.2e-16	<2.2e-16			Fig. 4.4	Tank DHW	Battery and tank DHW	<2.2e-16	<2.2e-16
		Fig. 4.3	Tank DHW	Battery and tank SH	2,50E-07	<2.2e-16			Fig. 4.4	Tank DHW	Battery and tank SH	5,70E-13	<2.2e-16
		Fig. 4.3	Tank DHW	Battery and tank SH and DHW	<2.2e-16	<2.2e-16			Fig. 4.4	Tank DHW	Battery and tank SH and DHW	<2.2e-16	<2.2e-16
		Fig. 4.3	Tank SH	Tank SH and DHW	<2.2e-16	<2.2e-16			Fig. 4.4	Tank SH	Tank SH and DHW	1,66E-01	1
		Fig. 4.3	Tank SH	Battery	<2.2e-16	<2.2e-16			Fig. 4.4	Tank SH	Battery	<2.2e-16	<2.2e-16
		Fig. 4.3	Tank SH	Battery and tank DHW	<2.2e-16	<2.2e-16			Fig. 4.4	Tank SH	Battery and tank DHW	<2.2e-16	<2.2e-16
		Fig. 4.3	Tank SH	Battery and tank SH	<2.2e-16	<2.2e-16			Fig. 4.4	Tank SH	Battery and tank SH	<2.2e-16	<2.2e-16
		Fig. 4.3	Tank SH	Battery and tank SH and DHW	<2.2e-16	<2.2e-16			Fig. 4.4	Tank SH	Battery and tank SH and DHW	<2.2e-16	<2.2e-16
		Fig. 4.3	Tank SH and DHW	Battery	4,60E-03	<2.2e-16			Fig. 4.4	Tank SH and DHW	Battery	2,40E-16	<2.2e-16
		Fig. 4.3	Tank SH and DHW	Battery and tank DHW	<2.2e-16	<2.2e-16			Fig. 4.4	Tank SH and DHW	Battery and tank DHW	<2.2e-16	<2.2e-16
		Fig. 4.3	Tank SH and DHW	Battery and tank SH	0,0043	<2.2e-16			Fig. 4.4	Tank SH and DHW	Battery and tank SH	<2.2e-16	<2.2e-16
		Fig. 4.3	Tank SH and DHW	Battery and tank SH and DHW	<2.2e-16	<2.2e-16			Fig. 4.4	Tank SH and DHW	Battery and tank SH and DHW	<2.2e-16	<2.2e-16
		Fig. 4.3	Battery	Battery and tank DHW	<2.2e-16	<2.2e-16			Fig. 4.4	Battery	Battery and tank DHW	2,10E-13	1
		Fig. 4.3	Battery	Battery and tank SH	1	<2.2e-16			Fig. 4.4	Battery	Battery and tank SH	1	1
		Fig. 4.3	Battery	Battery and tank SH and DHW	<2.2e-16	<2.2e-16			Fig. 4.4	Battery	Battery and tank SH and DHW	7,90E-11	1
		Fig. 4.3	Battery and tank DHW	Battery and tank SH	<2.2e-16	1,30E-15			Fig. 4.4	Battery and tank DHW	Battery and tank SH	5,30E-11	1
		Fig. 4.3	Battery and tank DHW	Battery and tank SH and DHW	1,00E+00	0,00724			Fig. 4.4	Battery and tank DHW	Battery and tank SH and DHW	3,59E-01	1
		Fig. 4.3	Battery and tank SH	Battery and tank SH and DHW	<2.2e-16	<2.2e-16			Fig. 4.4	Battery and tank SH	Battery and tank SH and DHW	7,00E-07	1
	SFH45	Fig. 4.3	Baseline	Tank DHW	<2.2e-16	<2.2e-16		SFH45	Fig. 4.4	Baseline	Tank DHW	0,18535	1
		Fig. 4.3	Baseline	Tank SH	<2.2e-16	<2.2e-16			Fig. 4.4	Baseline	Tank SH	0,09976	1
		Fig. 4.3	Baseline	Tank SH and DHW	<2.2e-16	<2.2e-16			Fig. 4.4	Baseline	Tank SH and DHW	0,997712	1
		Fig. 4.3	Baseline	Battery	<2.2e-16	<2.2e-16			Fig. 4.4	Baseline	Battery	<2.2e-16	<2.2e-16
		Fig. 4.3	Baseline	Battery and tank DHW	<2.2e-16	<2.2e-16			Fig. 4.4	Baseline	Battery and tank DHW	<2.2e-16	<2.2e-16
		Fig. 4.3	Baseline	Battery and tank SH	<2.2e-16	<2.2e-16			Fig. 4.4	Baseline	Battery and tank SH	<2.2e-16	<2.2e-16
		Fig. 4.3	Baseline	Battery and tank SH and DHW	<2.2e-16	<2.2e-16			Fig. 4.4	Baseline	Battery and tank SH and DHW	<2.2e-16	<2.2e-16
		Fig. 4.3	Tank DHW	Tank SH	<2.2e-16	<2.2e-16			Fig. 4.4	Tank DHW	Tank SH	0,00036	1
		Fig. 4.3	Tank DHW	Tank SH and DHW	1,00E-14	<2.2e-16			Fig. 4.4	Tank DHW	Tank SH and DHW	0,0992	1
		Fig. 4.3	Tank DHW	Battery	<2.2e-16	<2.2e-16			Fig. 4.4	Tank DHW	Battery	1,00E-10	<2.2e-16
		Fig. 4.3	Tank DHW	Battery and tank DHW	<2.2e-16	<2.2e-16			Fig. 4.4	Tank DHW	Battery and tank DHW	<2.2e-16	<2.2e-16
		Fig. 4.3	Tank DHW	Battery and tank SH	<2.2e-16	<2.2e-16			Fig. 4.4	Tank DHW	Battery and tank SH	4,60E-15	<2.2e-16
		Fig. 4.3	Tank DHW	Battery and tank SH and DHW	<2.2e-16	<2.2e-16			Fig. 4.4	Tank DHW	Battery and tank SH and DHW	<2.2e-16	<2.2e-16
		Fig. 4.3	Tank SH	Tank SH and DHW	<2.2e-16	<2.2e-16			Fig. 4.4	Tank SH	Tank SH and DHW	1,23E-01	1
		Fig. 4.3	Tank SH	Battery	<2.2e-16	<2.2e-16			Fig. 4.4	Tank SH	Battery	<2.2e-16	<2.2e-16
		Fig. 4.3	Tank SH	Battery and tank DHW	<2.2e-16	<2.2e-16			Fig. 4.4	Tank SH	Battery and tank DHW	<2.2e-16	<2.2e-16
		Fig. 4.3	Tank SH	Battery and tank SH	<2.2e-16	<2.2e-16			Fig. 4.4	Tank SH	Battery and tank SH	<2.2e-16	<2.2e-16
		Fig. 4.3	Tank SH	Battery and tank SH and DHW	<2.2e-16	<2.2e-16			Fig. 4.4	Tank SH	Battery and tank SH and DHW	<2.2e-16	<2.2e-16
		Fig. 4.3	Tank SH and DHW	Battery	5,60E-05	<2.2e-16			Fig. 4.4	Tank SH and DHW	Battery	<2.2e-16	<2.2e-16
		Fig. 4.3	Tank SH and DHW	Battery and tank DHW	<2.2e-16	<2.2e-16			Fig. 4.4	Tank SH and DHW	Battery and tank DHW	<2.2e-16	<2.2e-16
		Fig. 4.3	Tank SH and DHW	Battery and tank SH	4,80E-05	<2.2e-16			Fig. 4.4	Tank SH and DHW	Battery and tank SH	<2.2e-16	<2.2e-16
		Fig. 4.3	Tank SH and DHW	Battery and tank SH and DHW	<2.2e-16	<2.2e-16			Fig. 4.4	Tank SH and DHW	Battery and tank SH and DHW	<2.2e-16	<2.2e-16
		Fig. 4.3	Battery	Battery and tank DHW	<2.2e-16	7,80E-09			Fig. 4.4	Battery	Battery and tank DHW	7,70E-12	1
		Fig. 4.3	Battery	Battery and tank SH	1	1,20E-13			Fig. 4.4	Battery	Battery and tank SH	0,07577	1
		Fig. 4.3	Battery	Battery and tank SH and DHW	<2.2e-16	5,40E-15			Fig. 4.4	Battery	Battery and tank SH and DHW	4,20E-08	1
		Fig. 4.3	Battery and tank DHW	Battery and tank SH	<2.2e-16	0,0082			Fig. 4.4	Battery and tank DHW	Battery and tank SH	7,90E-04	1
		Fig. 4.3	Battery and tank DHW	Battery and tank SH and DHW	1	0,0202			Fig. 4.4	Battery and tank DHW	Battery and tank SH and DHW	3,13E-01	1
		Fig. 4.3	Battery and tank SH	Battery and tank SH and DHW	<2.2e-16	0,4597			Fig. 4.4	Battery and tank SH	Battery and tank SH and DHW	7,12E-02	1
	SFH100	Fig. 4.3	Baseline	Tank DHW	<2.2e-16	<2.2e-16		SFH100	Fig. 4.4	Baseline	Tank DHW	<2.2e-16	<2.2e-16
		Fig. 4.3	Baseline	Tank SH	<2.2e-16	<2.2e-16			Fig. 4.4	Baseline	Tank SH	<2.2e-16	<2.2e-16
		Fig. 4.3	Baseline	Tank SH and DHW	<2.2e-16	<2.2e-16			Fig. 4.4	Baseline	Tank SH and DHW	0,00019	<2.2e-16
		Fig. 4.3	Baseline	Battery	<2.2e-16	<2.2e-16			Fig. 4.4	Baseline	Battery	<2.2e-16	<2.2e-16
		Fig. 4.3	Baseline	Battery and tank DHW	<2.2e-16	<2.2e-16			Fig. 4.4	Baseline	Battery and tank DHW	<2.2e-16	<2.2e-16
		Fig. 4.3	Baseline	Battery and tank SH	<2.2e-16	<2.2e-16			Fig. 4.4	Baseline	Battery and tank SH	0,16499	<2.2e-16
		Fig. 4.3	Baseline	Battery and tank SH and DHW	<2.2e-16	<2.2e-16			Fig. 4.4	Baseline	Battery and tank SH and DHW	<2.2e-16	<2.2e-16
		Fig. 4.3	Tank DHW	Tank SH	<2.2e-16	<2.2e-16			Fig. 4.4	Tank DHW	Tank SH	<2.2e-16	<2.2e-16
		Fig. 4.3	Tank DHW	Tank SH and DHW	<2.2e-16	<2.2e-16			Fig. 4.4	Tank DHW	Tank SH and DHW	<2.2e-16	0,56271
		Fig. 4.3	Tank DHW	Battery	<2.2e-16	<2.2e-16			Fig. 4.4	Tank DHW	Battery	<2.2e-16	<2.2e-16
		Fig. 4.3	Tank DHW	Battery and tank DHW	<2.2e-16	<2.2e-16			Fig. 4.4	Tank DHW	Battery and tank DHW	<2.2e-16	<2.2e-16
		Fig. 4.3	Tank DHW	Battery and tank SH	<2.2e-16	<2.2e-16			Fig. 4.4	Tank DHW	Battery and tank SH	2,50E-08	<2.2e-16
		Fig. 4.3	Tank DHW	Battery and tank SH and DHW	<2.2e-16	<2.2e-16			Fig. 4.4	Tank DHW	Battery and tank SH and DHW	<2.2e-16	<2.2e-16
		Fig. 4.3	Tank SH	Tank SH and DHW	<2.2e-16	<2.2e-16			Fig. 4.4	Tank SH	Tank SH and DHW	<2.2e-16	1
		Fig. 4.3	Tank SH	Battery	<2.2e-16	<2.2e-16			Fig. 4.4	Tank SH	Battery	<2.2e-16	0,00034
		Fig. 4.3	Tank SH	Battery and tank DHW	<2.2e-16	<2.2e-16			Fig. 4.4	Tank SH	Battery and tank DHW	<2.2e-16	<2.2e-16
		Fig. 4.3	Tank SH	Battery and tank SH	<2.2e-16	<2.2e-16			Fig. 4.4	Tank SH	Battery and tank SH	<2.2e-16	0,04825
		Fig. 4.3	Tank SH	Battery and tank SH and DHW	<2.2e-16	<2.2e-16			Fig. 4.4	Tank SH	Battery and tank SH and DHW	<2.2e-16	<2.2e-16
		Fig. 4.3	Tank SH and DHW	Battery	1	<2.2e-16			Fig. 4.4	Tank SH and DHW	Battery	<2.2e-16	<2.2e-16
		Fig. 4.3	Tank SH and DHW	Battery and tank DHW	<2.2e-16	<2.2e-16			Fig. 4.4	Tank SH and DHW	Battery and tank DHW	<2.2e-16	<2.2e-16
		Fig. 4.3	Tank SH and DHW	Battery and tank SH	0,033	<2.2e-16			Fig. 4.4	Tank SH and DHW	Battery and tank SH	0,0023	<2.2e-16
		Fig. 4.3	Tank SH and DHW	Battery and tank SH and DHW	<2.2e-16	<2.2e-16			Fig. 4.4	Tank SH and DHW	Battery and tank SH and DHW	<2.2e-16	<2.2e-16
		Fig. 4.3	Battery	Battery and tank DHW	0,06	8,10E-08			Fig. 4.4	Battery	Battery and tank DHW	3,90E-09	<2.2e-16
		Fig. 4.3	Battery	Battery and tank SH	<2.2e-16	3,80E-05			Fig. 4.4	Battery	Battery and tank SH	<2.2e-16	0,01961
		Fig. 4.3	Battery	Battery and tank SH and DHW	<2.2e-16	4,40E-14			Fig. 4.4	Battery	Battery and tank SH and DHW	2,00E-06	<2.2e-16
		Fig. 4.3	Battery and tank DHW	Battery and tank SH	1	<2.2e-16			Fig. 4.4	Battery and tank DHW	Battery and tank SH	<2.2e-16	<2.2e-16
		Fig. 4.3	Battery and tank DHW	Battery and tank SH and DHW	<2.2e-16	0,0055			Fig. 4.4	Battery and tank DHW	Battery and tank SH and DHW	<2.2e-16	0,00876
		Fig. 4.3	Battery and tank SH	Battery and tank SH and DHW	<2.2e-16	<2.2e-16			Fig. 4.4	Battery and tank SH	Battery and tank SH and DHW	<2.2e-16	<2.2e-16

Table B.6: Median LCOE in USD/kWh_{el} for the three types of houses, depending on the CAPEX reduction per device and configuration for various configurations of PV-coupled heat pumps, thereby assuming that the retail tariff includes a capacity-based component. The median values for which the LCOE reduction is higher than for the baseline scenario (i.e., without CAPEX reduction) are printed bold .

CAPEX reduction		Baseline	Tank SH	Tank SH and DHW	Battery
No reduction	SFH15	0.71	0.68	0.52	0.79
	SFH45	0.6	0.57	0.49	0.68
	SFH100	0.55	0.53	0.48	0.60
Battery 50%	SFH15	0.71	0.68	0.52	**0.72**
	SFH45	0.60	0.57	0.49	**0.63**
	SFH100	0.55	0.53	0.48	0.57
HP 50%	SFH15	0.67	0.64	0.5	0.76
	SFH45	0.57	0.54	0.46	0.64
	SFH100	**0.5**	**0.48**	**0.44**	**0.55**
PV 50%	SFH15	0.67	0.64	0.49	0.75
	SFH45	0.57	0.55	0.46	0.65
	SFH100	0.54	0.53	0.47	0.58

B.10 Sensitivity analysis

In this section, we address the influence of three major input parameters, namely, i) the CAPEX of PV, heat pump, battery and space heating storage tank in Table B.6 (we exclude the DHW tank since the CAPEX is relatively low), ii) the discount factor in Table B.7 and iii) the impact of the capacity-based tariff on the power peak flow in Table B.8. This is done for the baseline PV-coupled heat pump system and configurations with electricity and heat storage for space heating.

According to Table B.6, a 50% reduction in the CAPEX of a heat pump has the greatest effect on the LCOE for the poorly insulated houses (SFH100), reducing the LCOE by 0.05 USD/kWh_{el} (9%). In well and very well insulated houses (SFH45 and SFH15), the CAPEX of the battery has the greatest effect on the LCOE, and for example a 50% reduction would improve the LCOE by 0.05 (7%) and 0.07 USD/kWh_{el} (9%), respectively.

The discount factor (i.e., 4%) has a marked impact on the LCOE, which is also statistically significant ($p - values \leq 0.001$). For example, the LCOE increases by 0.15 USD/kWh_{el} (21%) for the SFH15 if the discount factor increases from 4% to 8% in the baseline scenario (see Table B.7). A higher discount factor represents a higher time value of money and uncertainty and thus, reduces the economic viability.

Finally, Table B.8 firstly shows that, the peak flow is not very sensitive to the

Table B.7: Median LCOE in USD/kWh_{el} for the three types of house, depending on the discount factor and for various configurations of PV-coupled heat pumps considering that the retail tariff includes capacity-based component. In bold are presented the median LCOE values for the baseline scenario (discount factor equal to 4%) are presented in bold.

Configuration	Discount factor	SFH15	SFH45	SFH100
Baseline		0.63	0.54	0.49
Tank SH	2%	0.61	0.51	0.46
Battery		0.68	0.58	0.52
Baseline		**0.71**	**0.60**	**0.55**
Tank SH	**4%**	**0.68**	**0.57**	**0.53**
Battery		**0.79**	**0.68**	**0.6**
Baseline		0.78	0.67	0.62
Tank SH	6%	0.75	0.64	0.60
Battery		0.92	0.78	0.69
Baseline		0.86	0.75	0.70
Tank SH	8%	0.83	0.71	0.67
Battery		1.05	0.89	0.79

value of the capacity-based component of a retail tariff. Secondly, there is a threshold value of the capacity component below which energy storage cannot reduce the peak flow further, which is mainly given by the PV export peak (3.8 kW_{el} in this study). To reduce the peak flow under these circumstances, PV curtailment would be needed. PV-coupled heat pump systems increase the peak flow if retail tariffs do not include a capacity-based component, even when supported by electricity or heat storage.

Table B.8: Median peak flow in kW_{el} for the three types of house, depending on the capacity-based tariff for the configurations of PV-coupled heat pumps with heat storage and with battery. The peak import is shown in parentheses. In bold is presented the capacity-based tariff used across this study.

Capacity-based tariff	Space heating storage			Battery		
$(USD/kW_{el}/month)$	SFH15	SFH45	SFH100	SFH15	SFH45	SFH100
0	4.8 (4.8)	5.3 (5.3)	10.8 (10.8)	5.8 (5.8)	6.3 (6.3)	13.7 (13.7)
1.2	4.6 (4.6)	4.8 (4.8)	7.7 (7.7)	3.8 (2.6)	3.8 (3.2)	10.6 (10.6)
4.7	4.6 (4.6)	4.6 (4.6)	7.7 (7.7)	3.8 (2.5)	3.8 (2.9)	7.7 (7.7)
9.4	**4.6 (4.6)**	**4.6 (4.6)**	**7.7 (7.7)**	**3.8 (2.5)**	**3.8 (2.6)**	**7.7 (7.7)**
18.8	4.6 (4.6)	4.6 (4.6)	7.7 (7.7)	3.8 (2.5)	3.8 (2.5)	7.7 (7.7)

Appendix C

Supplementary Information - Local level

C.1 P2P electricity trading and individual preferences

Personal preferences concerning how P2P trading decisions should be administered in everyday life were assessed using the Swiss Household Energy Data Survey (S. Weber et al. 2017), a representative survey of energy behaviors conducted in April 2019. In order to achieve a representative sample of the Swiss population, quotas on age, gender, region, and living situation (i.e., tenants and owners) were applied. After conducting a P2P decision task similar to the one applied in the present study, 998 participants were asked to report their preference about how their decisions should be executed in a P2P community. Choice options: (1) "I decide manually each time to sell self-generated electricity or not" (response rate: 21.34%), (2) "A computer system executes the decisions to sell or not sell electricity based on my pre-set preferences" (response rate: 68.14%), and (3) "A computer system executes all decisions without my influence" (response rate: 10.52%).

C.2 Experimental study and survey

Overall, 299 German homeowners started the study. Out of these participants, 251 completed it, i.e., we got a response rate of 84%. This section provides an overview and summary of the two key analytical points of the study. See Supplementary Table C.1 for the characterization of the sample.

Table C.1: Characterization of the total sample as well as the sub-samples including both the respondents who took part in the P2P electricity trading experiment and the respondents who did not. The following terms apply: PV = photovoltaic system, EV = electric vehicle, ESS = energy storage system. To show statistically significant differences among the participants willing to take part in the P2P trading strategy and the participants that were not interested in taking part in the P2P community, we use the two-sided t test and a chi-square test for categorical data. Significant differences are marked as follows: ***p $<$ .001; **p $<$ .01; *p $<$ .05.

	Total sample (100%)	CI 95%	Taking part (70%)	CI 95%	Not interested (30%)	CI 95%	Significant difference
Sex							
Female	53,0%	n/a	50,6%	n/a	58,6%	n/a	No
Age (mean)	52,6	[50,8; 54,4]	51,6	[49,4; 53,8]	55	[52,0; 58,0]	No
Civil status							
Single	15,9%	n/a	18,3%	n/a	10,7%	n/a	***
In a relationship	15,9%	n/a	16,4%	n/a	14,7%	n/a	**
Married	58,2%	n/a	54,5%	n/a	66,9%	n/a	***
Divorced	5,2%	n/a	5,1%	n/a	5,4%	n/a	No
Widow	4,8%	n/a	5,7%	n/a	2,7%	n/a	*
Employment status							
Student	4,8%	n/a	6,3%	n/a	1,3%	n/a	**
Unemployed	6,0%	n/a	6,3%	n/a	5,4%	n/a	No
Full-time	42,2%	n/a	43,8%	n/a	38,5%	n/a	***
Part-time	22,3%	n/a	24,4%	n/a	17,4%	n/a	***
Retiree	24,7%	n/a	19,3%	n/a	37,5%	n/a	No
Education							
Secondary school	9,2%	n/a	7,4%	n/a	13,4%	n/a	No
High school	33,9%	n/a	31,8%	n/a	38,8%	n/a	**
Abitur	21,5%	n/a	23,2%	n/a	17,4%	n/a	***
Bachelor	8,8%	n/a	8,0%	n/a	10,7%	n/a	No
Master	24,7%	n/a	26,7%	n/a	20,1%	n/a	***
PhD	2,0%	n/a	2,9%	n/a	0,0%	n/a	*
Energy mix							
100% fossil	11,9%	n/a	9,1%	n/a	18,4%	n/a	No
100% renewable	27,9%	n/a	27,8%	n/a	28,1%	n/a	***
Fossil/renewable mix	32,3%	n/a	35,8%	n/a	24,1%	n/a	***
Do not know	27,9%	n/a	27,2%	n/a	29,5%	n/a	**
PV possession	13,5%	n/a	17,7%	n/a	3,7%	n/a	
ESS possession	0,05%	n/a	0,05%	n/a	0,04%	n/a	
Purchase intention[1]							
PV	2,4	[2,3; 2,6]	2,7	[2,5; 2,9]	1,7	[1,5; 1,9]	***
EV	2,1	[1,9; 2,3]	2,3	[2,1; 2,5]	1,6	[1,4; 1,9]	***
ESS	2,5	[2,4; 2,7]	2,8	[2,6; 3,0]	1,8	[1,5; 2,1]	***
Heat pump	2,3	[2,1; 2,4]	2,5	[2,3; 2,7]	1,8	[1,5; 2,1]	***
Others							
Household members (mean)	2,5	[2,4; 2,7]	2,57	[2,4; 2,7]	2,4	[2,2; 2,6]	No
Political ideology[2]	5,2	[5,0; 5,4]	5,1	[4,9; 5,3]	5,4	[5,1; 5,7]	No
Risk seeking[3]	5,4	[5,1; 5,7]	5,7	[5,4; 6,0]	4,8	[4,2; 5,4]	**
Respect of the earth[4]	6,2	[6,0; 6,4]	6,3	[6,1; 6,5]	5,9	[5,6; 6,3]	No
Unity with nature[4]	5,9	[5,7; 6,1]	6,1	[5,8; 6,3]	5,6	[5,1; 6,0]	*
Environmental protection[4]	6,4	[6,2; 6,5]	6,6	[6,4; 6,8]	5,8	[5,4; 6,2]	***
Pollution prevention[4]	6,3	[6,1; 6,5]	6,4	[6,2; 6,6]	6	[5,6; 6,3]	*

1 Technology purchase intention (within next 5 years) ranged from 1 – very small intention to 5 – very strong intention.
2 political ideology ranged from 1 – extremely left to 10 – extremely right.
3 risk seeking ranged from 0 – not willing to take risks at all to 10 – very willing to take risks.
4 altruistic and biospheric values ranged from 0 – opposite to my life principles to 8 – of supreme importance.

C.2.1 P2P Decision task

Supplementary Figure C.1 displays one example of the P2P choice task, based on a 4 x 3 x 2 within-subjects design with the different electricity prices being offered in the P2P community (€0.04 per kWh to €0.28 per kWh in steps of €0.08 per kWh), SOC of the battery (30–90% in steps of 30%), and time until the next surplus (more than or less than 12 hours). All possible combinations of price and SOC were presented in random order resulting in a total of 24 decisions. The dependent variable was participants' choices to either sell electricity from the battery to the community or not.

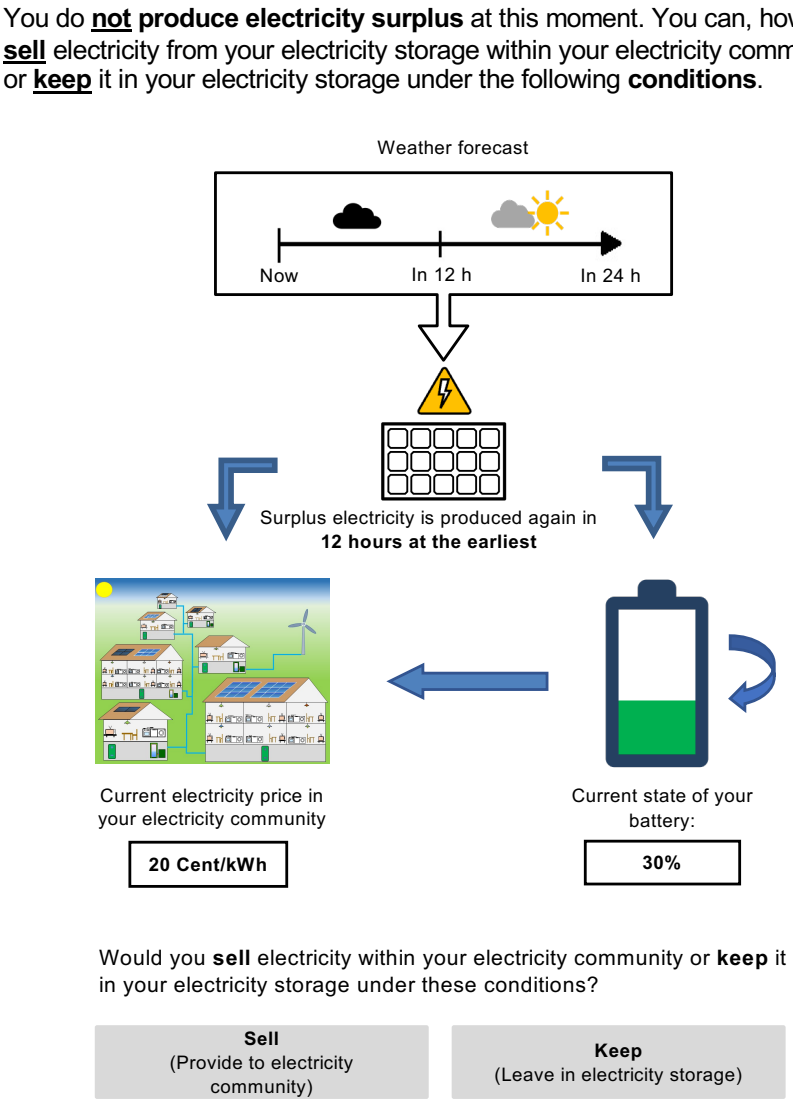

Figure C.1: **Example of the trading decision task.** Based on the experimental P2P decision task in the online study. Please note that this figure is slightly different to the task displayed to participants, since some icons were changed due to copyright reasons. The source of weather, electricity, and battery icons: Microsoft PowerPoint; source of solar module icon: Martin Markstein from thenounproject.com, licensed under CC BY 3.0.

C.2.2 Willingness to participate in P2P communities

The large majority of the sample (70%) admitted to be interested in becoming a member of a P2P community. On the other hand, those who declared their reluctance to be part of a P2P community claimed several reasons. Since a broad range

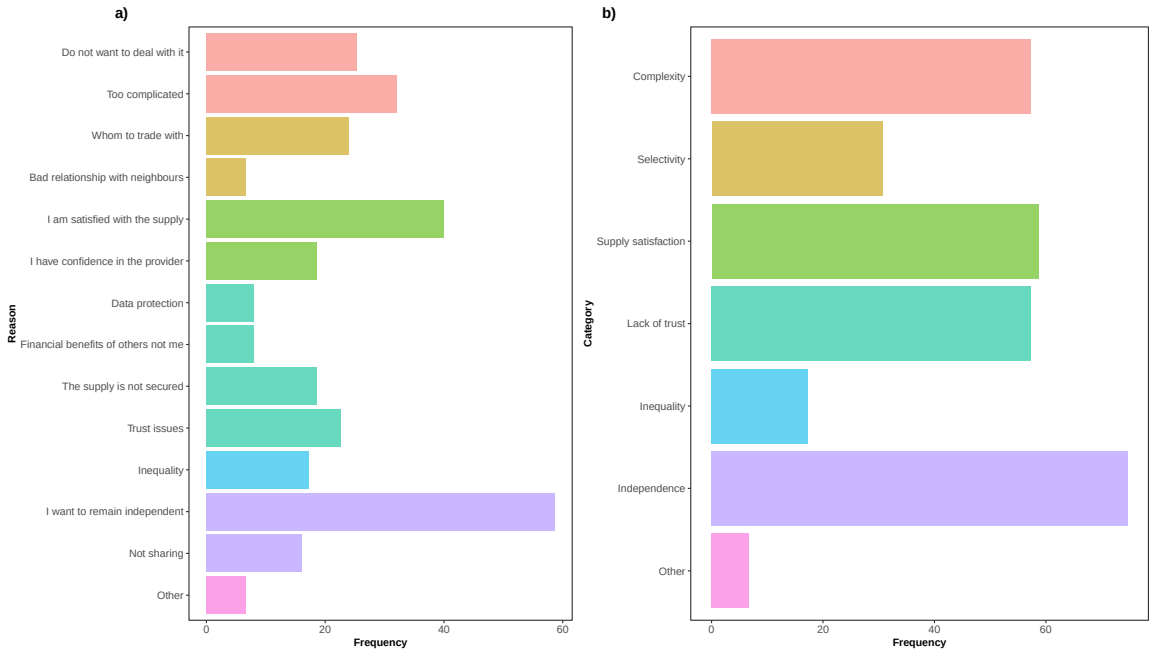

Figure C.2: **Reported reasons why participants are not interested in becoming a member of a P2P community. a)**: Detailed reasons to not be part of the P2P community. **b)**: Aggregated categories of reasons to not be part of the P2P community.

of reasons were given by the participants, we aggregate them in categories. Supplementary Figure C.2 shows the most stated reasons given and the corresponding categories. The most important categories of reasons to not be part of the P2P community were "Independence" (75%), "Supply satisfaction" (59%), "Complexity" (57%), "Lack of trust" (57%) and "Selectivity" (31%, i.e., refers to the choice with whom the members of P2P communities want to trade with). Almost two thirds of the sample declared to be familiar with trading (64%), but only 42% of the sample indicated to have a high tendency to trade. Beyond the factual answers of the participants reluctant to take part in P2P communities, we found statistically significant differences on risk aversion by willingness to participate in P2P communities, in that the group that expressed reluctance to participate in P2P trading was more risk averse than the group that expressed willingness to be part of a P2P community ($p - values \leq 0.005$).

C.3 Individual self-consumption with P2P price structure

In order to verify the validity of our results, here we implemented a self-consumption maximization strategy using the same pricing mechanism as in a P2P community; results are presented in Supplementary Figure C.3 and C.4. In this way, we confirmed that P2P communities performed better than the self-consumption maximization strategy, even under a similar price structure. At the individual level, self-consumption and autarky in the self-consumption maximization strategy remained unchanged while were reduced in P2P communities. The annual bill, however, was smaller under the self-consumption maximization strategy with P2P price structures than in the self-consumption maximization strategy evaluated in the main paper, and even lower in P2P communities, except for prosumers with PV only.

At the aggregated level, self-consumption and autarky under the self-consumption maximization strategy remained at equal levels while comparatively higher in P2P communities. As for the aggregated bill, P2P prices help to reduce it for the self-consumption maximization strategy, however, P2P communities remained, comparatively, the best option to reduce the electricity bill.

Since there were no supplementary exchanges of electricity when changing the price structure under the self-consumption maximization strategy, the power exchanges remain unchanged, thus we do not show them here. Finally, the Benefit Index that compares the share of households that are better-off being part of a P2P community compared with pursuing a self-consumption maximization strategy, even under a similar price structure, is 72.5%.

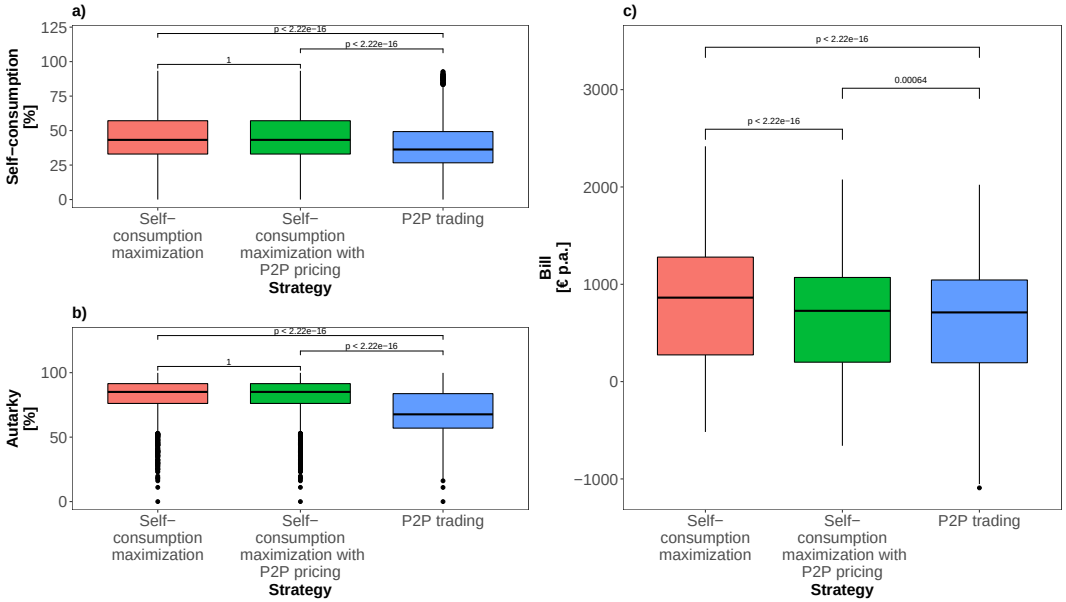

Figure C.3: **Comparison of self-consumption maximization strategy under traditional retail tariff and FiT, self-consumption maximization strategy with P2P price structure, and P2P communities at the individual level. a)**: Boxplots of annual self-consumption. Boxplots show the median (horizontal line) and the interquartile range (IQR; box outline). The whiskers extend from the hinge to the highest and lowest value that are within 1.5*IQR of the hinge, and the points represent the outliers. **b)**: Annual autarky. **c)**: Annual bill for all types of prosumers. Note that self-consumption and autarky are presented only for the prosumers with PV and battery, since for the other cases these indicators do not change. The individual p-values of the two-sided Wilcoxon test with the Holm procedure to control the family-wise error rate are reported in the figure for panels b) and c), where N=1000 independent simulations.

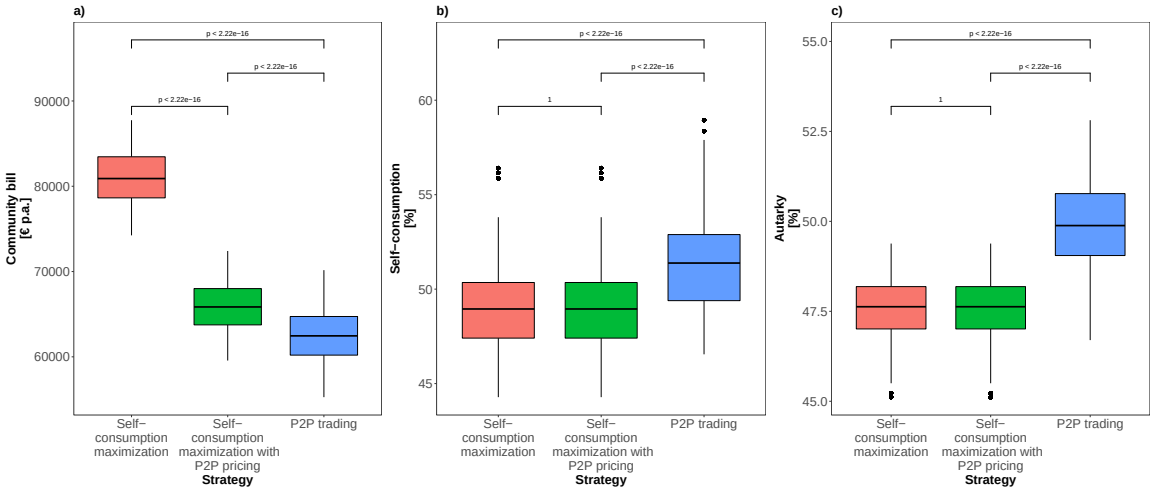

Figure C.4: **Comparison of self-consumption maximization strategy under traditional retail tariff and FiT, self-consumption maximization strategy with P2P price structure, and P2P communities at the aggregated level. a)**: Boxplot of the annual bill. Boxplots show the median (horizontal line) and the interquartile range (IQR; box outline). The whiskers extend from the hinge to the highest and lowest value that are within 1.5*IQR of the hinge, and the points represent the outliers. **b)**: Annual self-consumption. **c)**: Annual autarky. The individual p-values of the two-sided Wilcoxon test with the Holm procedure to control the family-wise error rate are reported in the figure for all panels, where N=1000 independent simulations.

C.4 Sensitivity analysis

In order to verify the validity of our results, we implemented a sensitivity analysis of self-consumption, autarky and the annual cost to PV penetration, battery penetration and community size at both the individual and community level. Supplementary Figure C.5 displays the results at the individual level. The increase of battery penetration reduced the annual bill of classical consumers, however, it increased the annual bill of prosumers with PV and battery. For prosumers with PV only there was an optimal level of battery penetration that remains to be studied. Self-consumption and autarky levels remained at similar levels at the individual level, independently of the PV and battery penetrations.

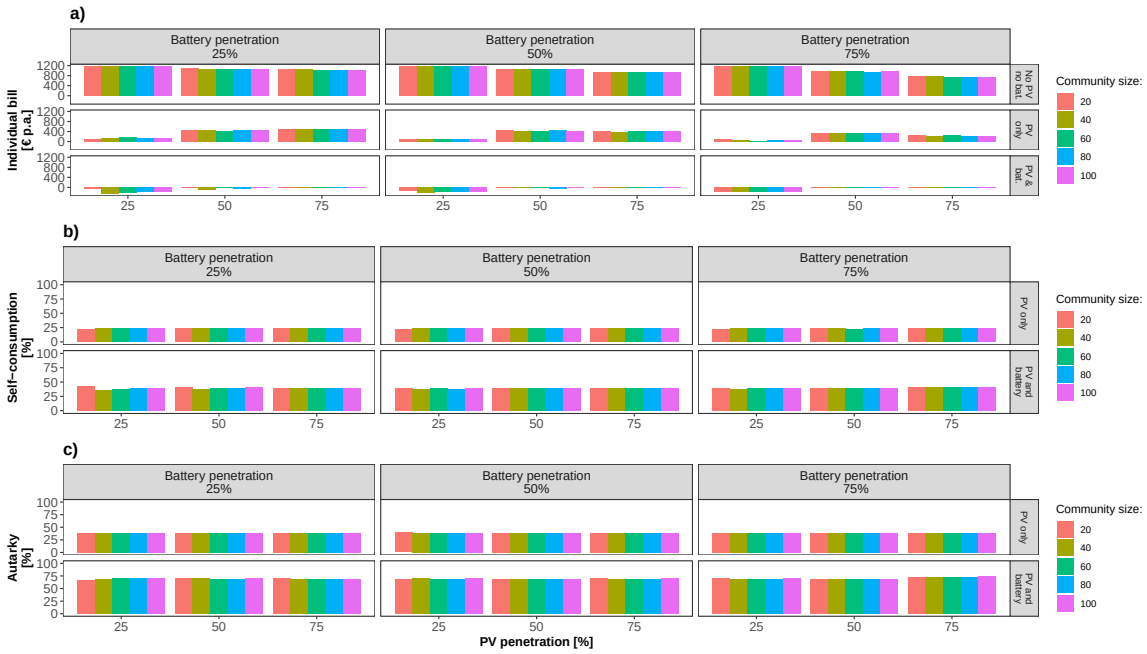

Figure C.5: **Sensitivity of the key performance indicators with respect to community size, PV and battery penetration at the individual level, depending on the type of prosumer. a)**: Annual bill. **b)**: Annual self-consumption. **c)**: Annual autarky. Note that self-consumption and autarky are not presented only for the classical consumers, since these indicators are zero.

Results of the community level are shown in Figure C.6. We found an important impact of PV and battery penetration in the community, whereas the community size impact was reduced at both levels. As PV and battery penetrations increased, the autarky at the community level increased, while the self-consumption and the annual bill reduced, which suggests a saturation beyond a given threshold of technology penetration, which remains to be studied.

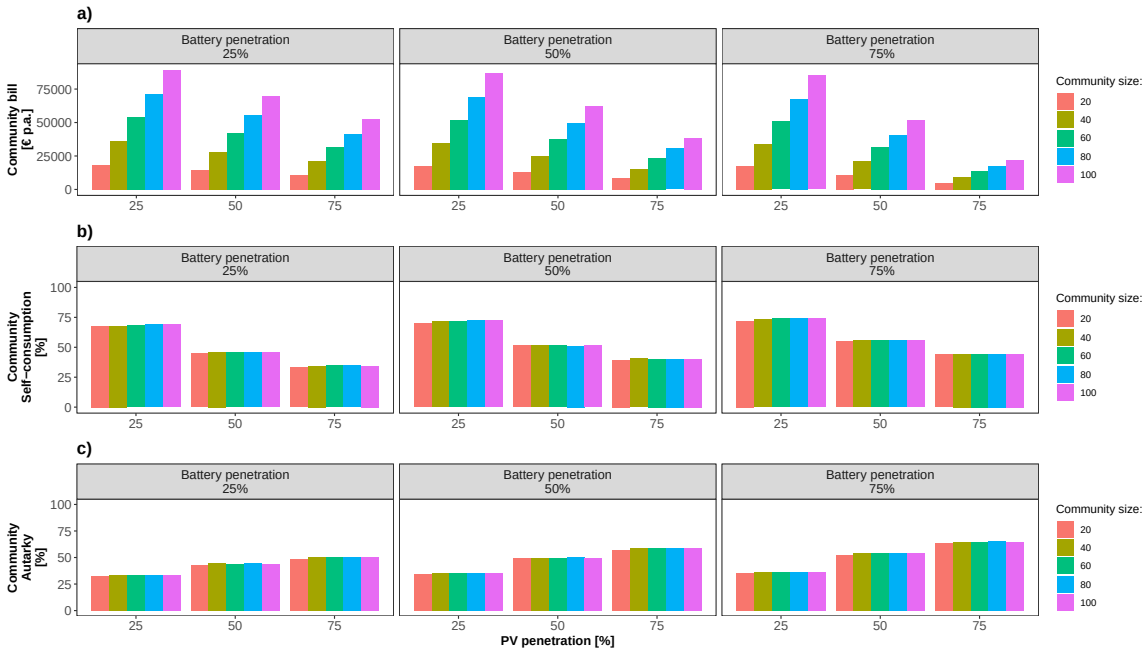

Figure C.6: **Sensitivity of the key performance indicators with respect to community size, PV and battery penetration at the aggregated level. a)**: Annual bill. **b)**: Annual self-consumption. **c)**: Annual autarky.

C.5 Distribution grid

C.5.1 Overview of the distribution grid design, problems and solutions

The approach of distribution system operators (DSOs) to design distribution grids mainly considered the demand of their consumers and centralized power supply provided by a public grid infrastructure (in a safe and efficient manner). To ensure reliable electricity supply under peak demand, DSOs estimate the peak power demand of an area and use this estimate to size the grid assets (Ruf 2018). Peak demand per household in Germany ranges from 2-6 kW for households with traditional appliances and from 7-13 kW for households with electric heating, e.g., electric boilers for domestic hot water (Heinhold 1965). Moreover, to estimate the peak demand of the area, DSOs consider the active power and a coincidence factor that varies depending on the number of customers (being 1 for one household and between 0.2-0.4 for a very large number of consumers Heinhold 1965; Hartvigsson et al. 2021a; Hartvigsson et al. 2021b). In Germany, a three-phase connection is commonly used to connect households (Ruf 2018), which improves the power factor, voltage stability and reduces losses.

Now, with the increase of distributed energy resources such as electric vehicles, and heat pumps as well as an increasing amount of electronic devices, the peak power per household is increasing. Moreover, PV systems pose a new challenge to the distribution grid infrastructure, which was designed to provide electricity and not to absorb it. Important challenges for DSOs in Germany have been caused by a high number of small PV systems, as well as some large PV systems which are installed far away from the load in rural areas (Ruf 2018). DSOs must guarantee grid stability and power quality, however, since PV injection was not considered in the planning of distribution grids, the local PV feed-in affects the voltage of the distribution grid, as well as the operation of critical devices such as transformers and lines (Gupta, Pena-Bello, et al. 2021). These effects have to be taken into account in both the planning as well as a safe and efficient operation of the electric grid.

The amount of distributed generation for which constraints are violated is denoted as hosting capacity (Bollen and Hassan 2011). The hosting capacity is highly dependant on local conditions, such as transformer size, amount of consumers covered by a transformer, lines length, local consumption and PV generation matching (based on irradiance and PV panels orientation). Three main problems arise from PV feed-in in the low voltage distribution grid area, namely, grid voltage alteration due to load profile modification, thermal loading of lines and transformers due to violations of the thermal limits of the devices, and reverse power flow, in the case that feed-in in the distribution grid exceeds local consumption (i.e., the low voltage distribution grid area then operates as a power plant instead of a demand hub).

The hosting capacity of an existing grid is determined by its topology, assets and local conditions. In Germany the main limiting factors of the hosting capacity are voltage increase and lack of transformer capacity(Ruf 2018; Bayer et al. 2018; Hartvigsson et al. 2021a; Hartvigsson et al. 2021b). Cable capacity is the least common problem. Usual techniques to increase hosting capacity without incurring in traditional grid reinforcement are voltage regulated distribution transformers (VRDT), PV curtailment, capacity-based tariffs, demand side management, reactive power compensation by PV inverters, and energy storage (Ruf 2018; Pena-Bello, Barbour, Gonzalez, Patel, et al. 2019).

Standard long-term solution grid reinforcement is slow to implement and costly (Varela et al. 2017), and therefore DSOs search to avoid it. VRDT are transformers with on-load tap changers at the low-voltage level. The tap changer varies the transformer ratio, controlling the value of the secondary voltage under load (Ruf 2018). This technique has been widely applied in high voltage to medium voltage transformers but only recently developed for medium voltage to low voltage commercial devices. With VRDT, a decoupling of the low voltage grid from the medium voltage grid is achieved and the voltage band is increased (even doubled) at the low voltage level (Hinz and Sojer 2012). In Germany, however, VRDTs are not widely available and its cost is 1.5 to 2 times higher compared with regular distribution transformers (van Amelsvoort 2014), which is still lower than grid reinforcement (Schwarz and Kollmann 2014). PV curtailment is a regulation measure that refers to the limitation (in power terms) of PV feed-in. In some regions with substantial PV penetration, a feed-in limit is set to keep the grid stability. Electricity dissipation is typically done using the PV inverter (Pena-Bello, Barbour, Gonzalez, Patel, et al. 2019). Reactive power compensation by PV inverters allows to reduce voltage deviations operating the PV inverters at power factors lower than 1, however, it increases the losses at the inverter (Vlahinić et al. 2019). This technique is particularly interesting in distribution grids with high shares of PV (Vlahinić et al. 2019). Demand side management consists of demand loads shifting in time to match renewable generation, and/or lower electricity prices (Fidalgo, Couto, and Fournie 2016). Eligible loads for demand side management include air conditioning, heating and refrigeration (displaceable load) and also a small percentage of other household devices, e.g., wet appliances, which when matched with PV surplus may alleviate grid stress. Capacity-based tariffs which are proportional to the maximum peak power (i.e., in €/kW) during a billing period, have been widely applied for large consumers. To reduce the grid impacts of PV, heat pumps and electric vehicles and enabled by the deployment of smart meters, capacity-based tariffs are already being tested in some countries, e.g., France, Belgium, Austria and Sweden (Pena-Bello, Schuetz, et al. 2021). Capacity-based tariffs provide price signals for prosumers to reduce their peak flow, which can help to defer distribution grid upgrades and to recover a portion of network costs. However, its implementation requires thoughtful roll-out to allow households to adapt to new price signals (Azarova et al. 2018). Finally, energy storage is able to increase self-consumption (and therefore reduce PV feed-in), and provide additional applications such as avoidance of PV curtailment (if PV curtailment is enforced), peak shaving (reduction of the peak flow, if capacity tariffs are implemented), as well as ancillary services (Pena-Bello, Barbour, Gonzalez, Patel, et al. 2019; Battke et al. 2013).

C.5.2 Distribution grid modeling

In this section, the results of a complementary model of a distribution network based on Hartvigsson et al. are presented (Hartvigsson et al. 2021a; Hartvigsson et al. 2021b). This model uses a top-down approach, from a DSO perspective, to design a distribution grid and the transformer capacity based on several parameters, e.g., nominal voltage, fuse rating, population density, load coincidence, etc. Using the average 15-min profile of 100 German houses used in this study, the model calculates the required capacity of the transformer to cover the demand in a given area. We assumed that the community is conformed entirely by single-family houses, in a rural area, and within a surface of 0.01 km^2. The model relies on the coincidence factor

to calculate the peak demand, and focuses on the longest feeder, e.g., a continuous stretch of cable or power line, from each transformer. The coincidence factor allows us to simplify comparisons and reduce the complexity of the problem and make it computational feasible, however, it may cause a bias towards voltage violations in the results. Moreover, it excludes the impact of harmonics and flicker, which is generally small(Hartvigsson et al. 2021a; Hartvigsson et al. 2021b). The distribution grid model includes costs for the transformers and cables (for both low voltage and medium voltage lines). It takes into account losses and voltage constraints to calculate the transformer hosting capacity. The distribution network model takes a simplified approach of a radial distribution network with a uniform distribution of customers in the area supplied by each transformer and with horizontal and vertical connection lines (see Supplementary Figure C.7) (Hartvigsson et al. 2021a; Hartvigsson et al. 2021b). For detailed information on the model, please refer to Hartvigsson et al. 2021a; Hartvigsson et al. 2021b.

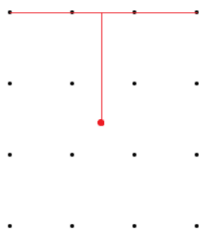

Figure C.7: **Schematic representation of the simplified approach of the distribution network with uniform distribution of customers.** The red dot represents the MV/LV transformer, while the black dots represent the customers.

Two options were modeled: first, the model used the least costly option to allocate the transformer capacity. Second, the model was modified to cover the demand of the 100 households using a single transformer, following the assumption in this study of a single point of common coupling (PCC) for the whole community. The results of the simulations are presented in Supplementary Table C.2. The difference of cost between the two options was in the range of €415-6570 (i.e., 0.5-9.3%). The hosting capacity ranged between 500-1250 kW, whereas the main limiting factor was always the transformer capacity (the other limiting factors being voltage increase and cable capacity), which is in line with the literature(Ruf 2018; Bayer et al. 2018; Hartvigsson et al. 2021a; Hartvigsson et al. 2021b).

Overall, our results indicate that for a PV size distribution between 1-10 kWp (with a median of 6 kWp) and the PV penetration scenarios of 25%, 50%, and 75%, the transformer can allocate the amount of PV in every scenario, with the maximum feed-in power being 160 kW, 303 kW. and 450 kW, respectively. However, in the cases where the hosting capacity is close to being reached (e.g., a PV penetration equal or higher to 75% and a single transformer of 1 kVA), P2P gently reduces the maximum feed-in (6%), but other flexibility solutions should be explored such as demand-side management and reactive power compensation by PV inverters (Fidalgo, Couto, and Fournie 2016; Vlahinić et al. 2019).

Table C.2: Results of transformer allocation and hosting capacity using the model presented by Hartvigsson et al. (Hartvigsson et al. 2021a; Hartvigsson et al. 2021b), and adapted for the present study. Two options are presented, least cost and a single transformer used to feed the whole community. The peak demand is directly related with a 20 A fuse installed at the household level.

Variable	Least cost (Option a)						One single transformer (Option b)					
Fuse rating [A]	20	20	20	20	20	20	20	20	20	20	20	20
Nominal voltage [V]	400	400	400	400	400	400	400	400	400	400	400	400
Margin	1	1,2	1,5	1,8	2,1	2,4	1	1,2	1,5	1,8	2,1	2,4
Hosting capacity	600	600	1000	1000	1000	1250	500	800	800	1000	1000	1250
Capacity per customer	6	6	10	10	10	12,5	5	8	8	10	10	12,5
Solar energy	921498,8	921498,8	1535831,4	1535831,4	1535831,4	1919789,2	767915,7	1228665,1	1228665,1	1535831,4	1535831,4	1919789,2
Feeder length	0,081	0,081	0,081	0,081	0,081	0,11	0,11	0,11	0,11	0,11	0,11	0,11
Transformer capacity	315	315	500	500	500	1250	500	800	800	1000	1000	1250
Number of transformers	2	2	2	2	2	1	1	1	1	1	1	1
Customers per feeder	13	13	13	13	13	25	25	25	25	25	25	25
Customers per transformer	50	50	50	50	50	100	100	100	100	100	100	100
Peak demand	446,4	446,4	446,4	446,4	446,4	446,4	446,4	446,4	446,4	446,4	446,4	446,4
Cost [SEK]	714066,5	714066,5	776194,5	776194,5	776194,5	840912,3	747205,3	780391,3	780391,3	805161,3	805161,3	840912,3
Cost [€]	70692,59	70692,59	76843,26	76843,26	76843,26	83250,32	73973,33	77258,74	77258,74	79710,97	79710,97	83250,32
Limiting factor	Tr. Cap.	Tr. Cap.	Tr. Cap.	Tr. Cap.	Tr. Cap.	Tr. Cap.	Tr. Cap.	Tr. Cap.	Tr. Cap.	Tr. Cap.	Tr. Cap.	Tr. Cap.
Overcost [€]	-	-	-	-	-	-	3280,7	6566,2	415,5	2867,7	2867,7	0,0
Overcost %	-	-	-	-	-	-	4,6%	9,3%	0,5%	3,7%	3,7%	0,0%

C.6 Modeling

In this paper, we analyzed P2P communities with a size of 100 households and compared them with a baseline strategy where prosumers aimed to maximize their self-consumption, i.e., the status quo in Germany (and many other countries), where 185,000 prosumers were maximizing their self-consumption with individual batteries in 2019 (Figgener, Stenzel, et al. 2021). We compared these two strategies at the individual, and at the aggregated level, using key performance indicators such as self-consumption, autarky, and peak demand. The aggregated level corresponds to a single point of Common Coupling (PCC), which matches the size of the community for P2P trading. For both strategies, we further considered a single low-voltage/medium-voltage transformer behind the single PCC, using 15-minute resolution demand and PV generation data (see Section C.5 for more details).

C.6.1 Self-consumption maximization

Supplementary Figure C.8 illustrates the self-consumption maximization strategy (baseline) for which prosumers aimed to minimize electricity imports from the main grid at the retail price by using their local PV generation on-site (instead of being exported to the main grid with the FiT). First, PV generation met the household demand if they matched, and any PV surplus was used to charge the battery until it was full. On the other hand, the battery discharged to meet the household electricity demand if demand was greater than PV generation until it was empty. Surplus PV electricity from prosumers was injected into the local grid and was considered to be consumed locally if there was demand from other neighboring houses located behind the same PCC. For this strategy, we also calculated the aggregated autarky and self-consumption at the PCC, which was then compared with the values obtained with

P2P communities. Moreover, Supplementary Figure C.9 is a flowchart that displays the schedule of a PV-coupled battery system maximizing self-consumption at every time step, as well as the amount of PV electricity that was directly self-consumed and exported to the grid. Supplementary Figure C.10 shows the aggregated flows for two representative spring days achieved with the self-consumption maximization strategy.

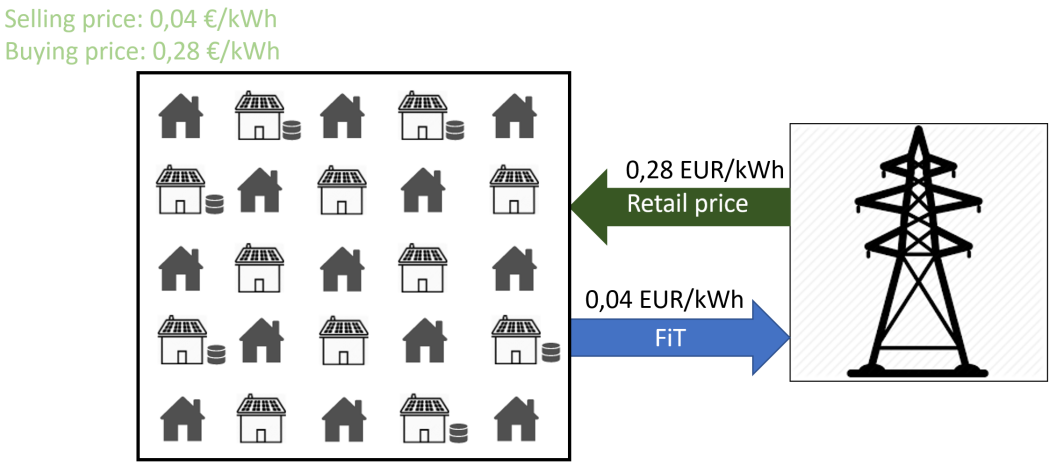

Figure C.8: **Schematic representation of the self-consumption maximization strategy.** Source: Own elaboration. Source of solar panel roof and electricity tower icons: Creative Mahira from thenounproject.com. Source of house icon: Larea from thenounproject.com. Icons licensed under CC BY 3.0.

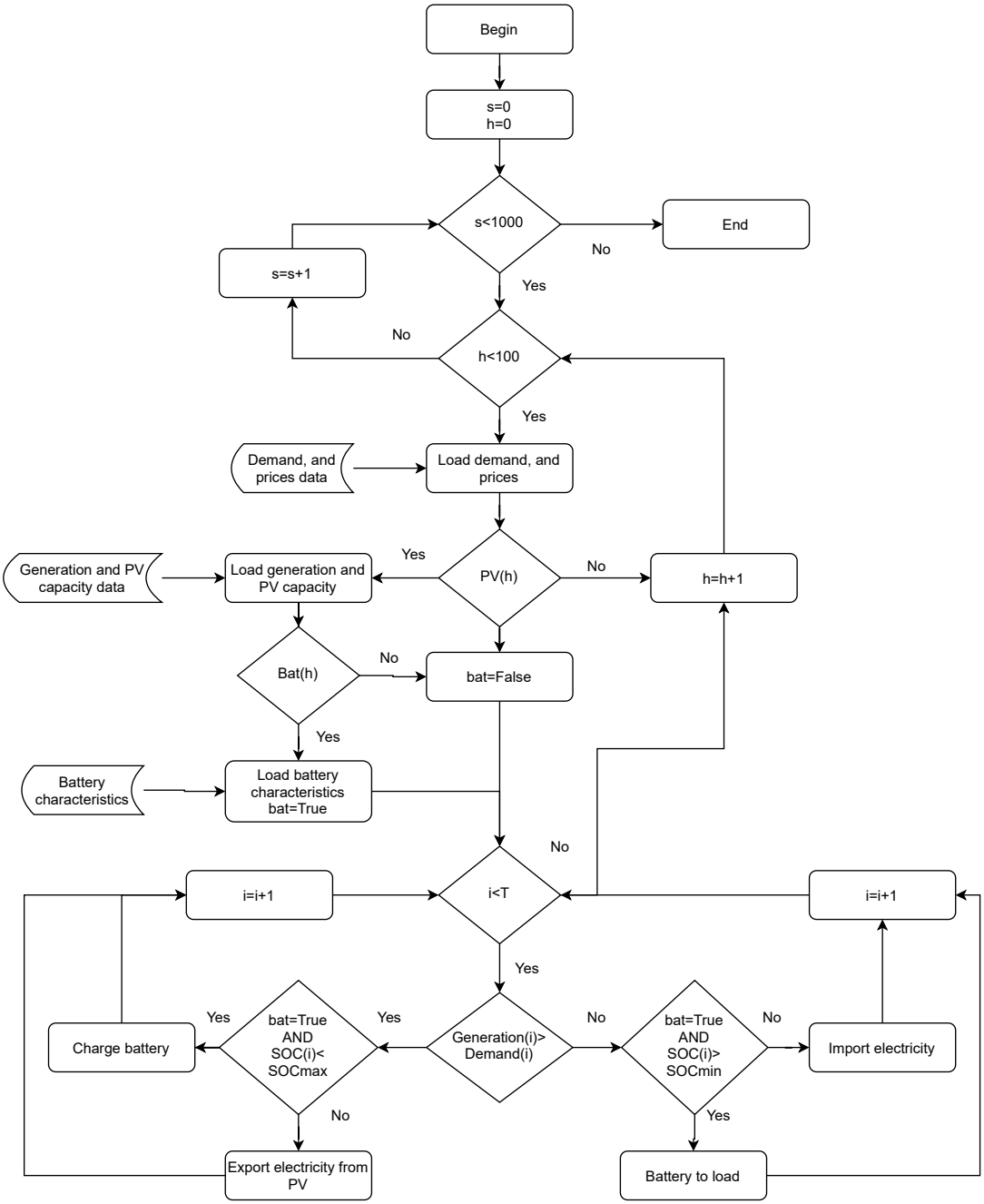

Figure C.9: **Flowchart of the energy management model for self-consumption maximization strategy.**

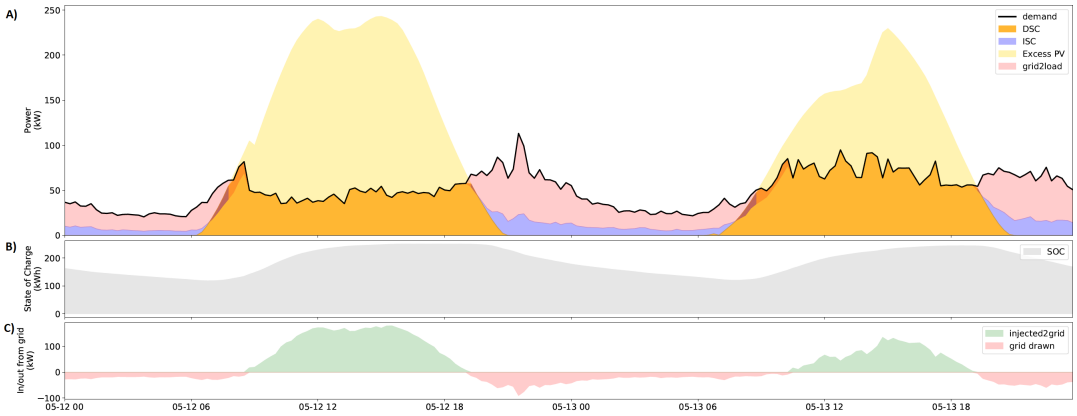

Figure C.10: **Energy flows of the self-consumption maximization strategy. a)**: Sample of two days with aggregated flows at the PCC. **b)**: Aggregated SOC. **c)**: Aggregated grid exchanges.

C.6.2 P2P communities

Supplementary Figure C.11 illustrates a P2P community where PV trading occurred among the same households considered for the baseline strategy assuming the same PCC. Households' surplus PV generation was traded within the P2P community, and only if there was not any community demand to be met locally, residual PV electricity was sold to the main grid at the FiT. Electricity from batteries was traded according to the prosumers' preferences given in Supplementary Figure C.1. Moreover, Supplementary Figure C.12 displays a flowchart of the schedule of a PV-coupled battery system trading electricity in a P2P community at every time step, as well as the amount of PV electricity that was directly self-consumed and exported to the grid. Likewise the self-consumption maximization strategy, PV generation met the household demand if they matched, and any PV surplus was used to charge the battery until it was full.

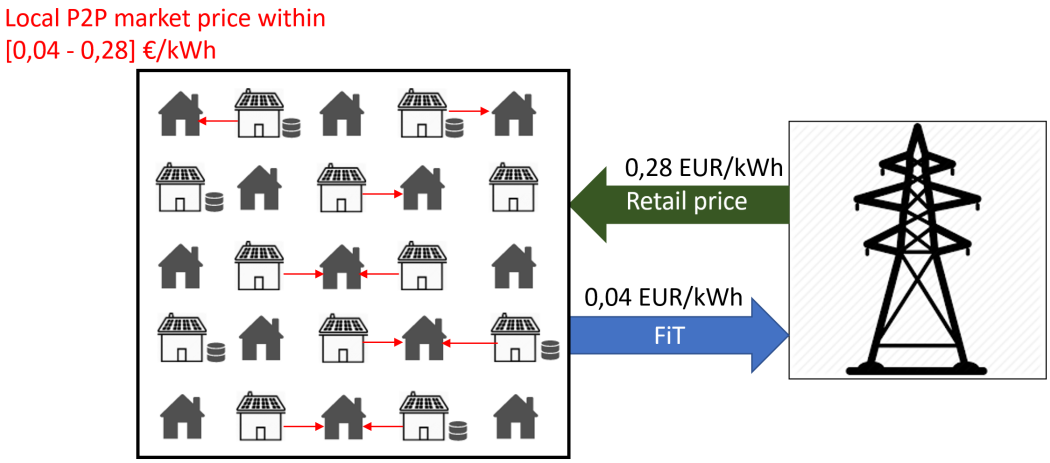

Figure C.11: **Schematic representation of the P2P community.** Source: Own elaboration. Source of solar panel roof and electricity tower icons: Creative Mahira from thenounproject.com. Source of house icon: Larea from thenounproject.com. Icons licensed under CC BY 3.0.

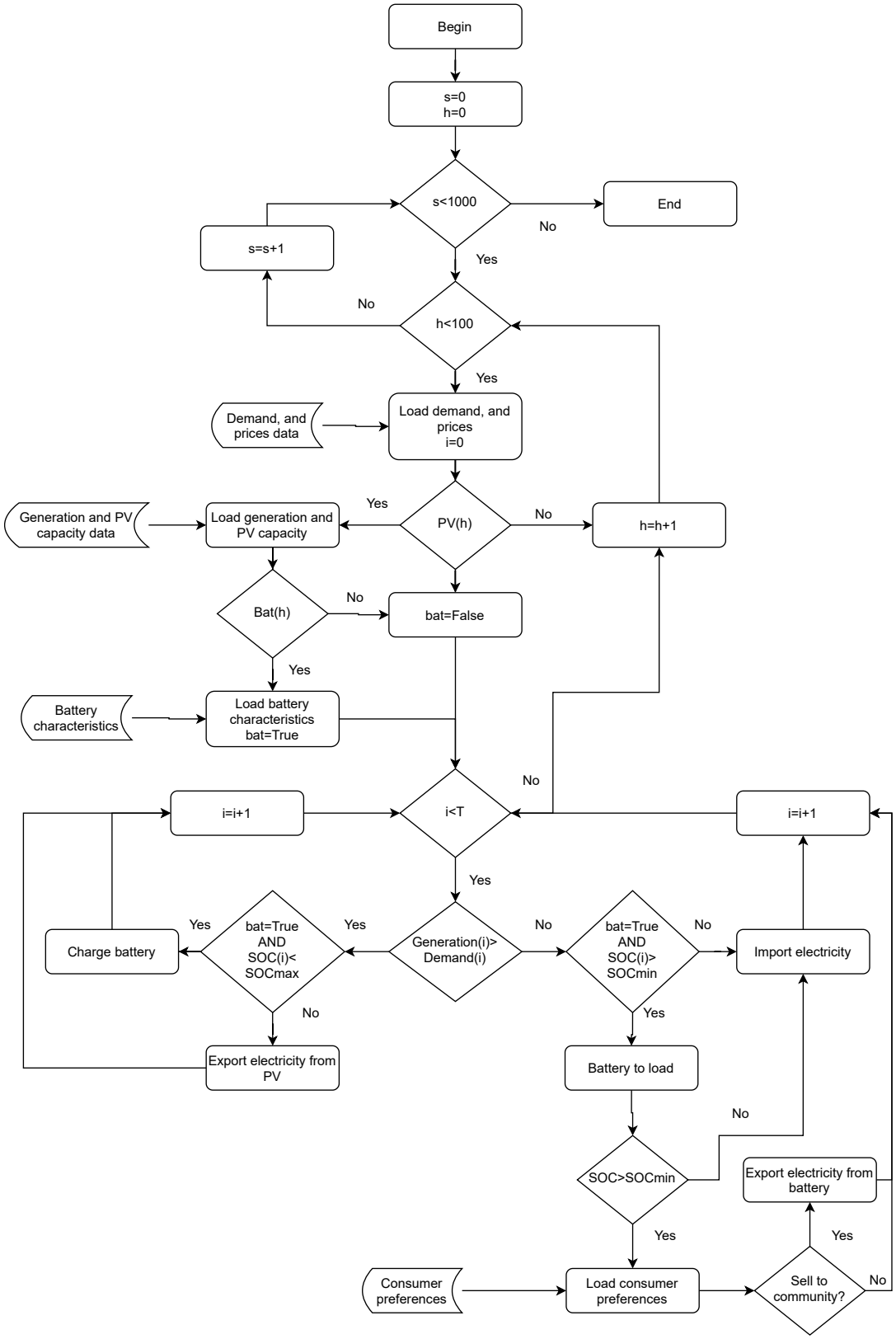

Figure C.12: **Flowchart of the energy management model for the P2P community.**

On the other hand, the battery discharged to meet the household electricity demand if demand was greater than PV generation until it was empty. Surplus PV electricity from prosumers was injected into the local grid and was considered to be consumed locally if there was demand from other neighboring houses located behind the same PCC. If the household demand was satisfied and the battery was full, the remaining PV electricity was traded into the P2P community. Furthermore,

the battery can then be discharged to cover the household demand or to trade into the P2P community taking into account the consumer preferences. Supplementary Figure C.13 shows the aggregated flows at the PCC for the same two representative spring days achieved by P2P community trading. Trading achieved with batteries within a P2P community (in blue in the Supplementary Figure C.13), as well as the P2P market price are shown in the bottom box.

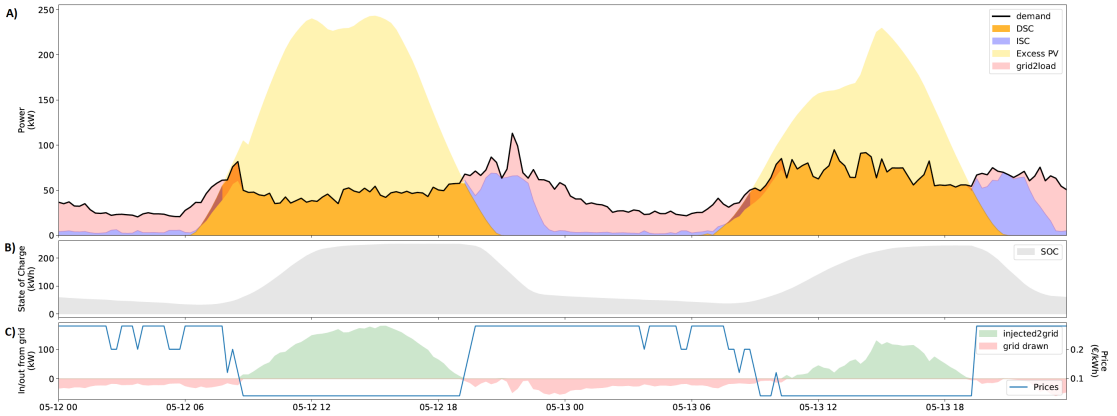

Figure C.13: **Energy flows of the P2P trading strategy. a)**: Sample of two days with aggregated flows at the PCC. **b)**: Aggregated SOC. **c)**: Aggregated grid exchanges and P2P prices.

C.6.3 Flowchart of the pricing mechanism in P2P community

Supplementary Figure C.14 displays a flowchart of the pricing mechanism in P2P communities. Supplementary Figure C.15 shows the energy flows at the aggregated level, with time slots when there is PV surplus at the aggregated level represented in green.

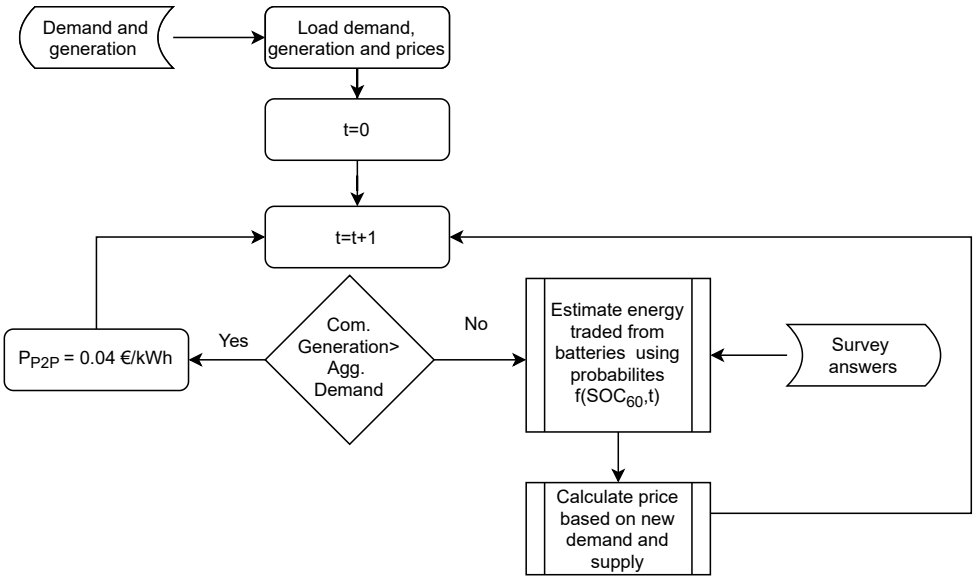

Figure C.14: **Flowchart of the pricing mechanism in P2P community.**

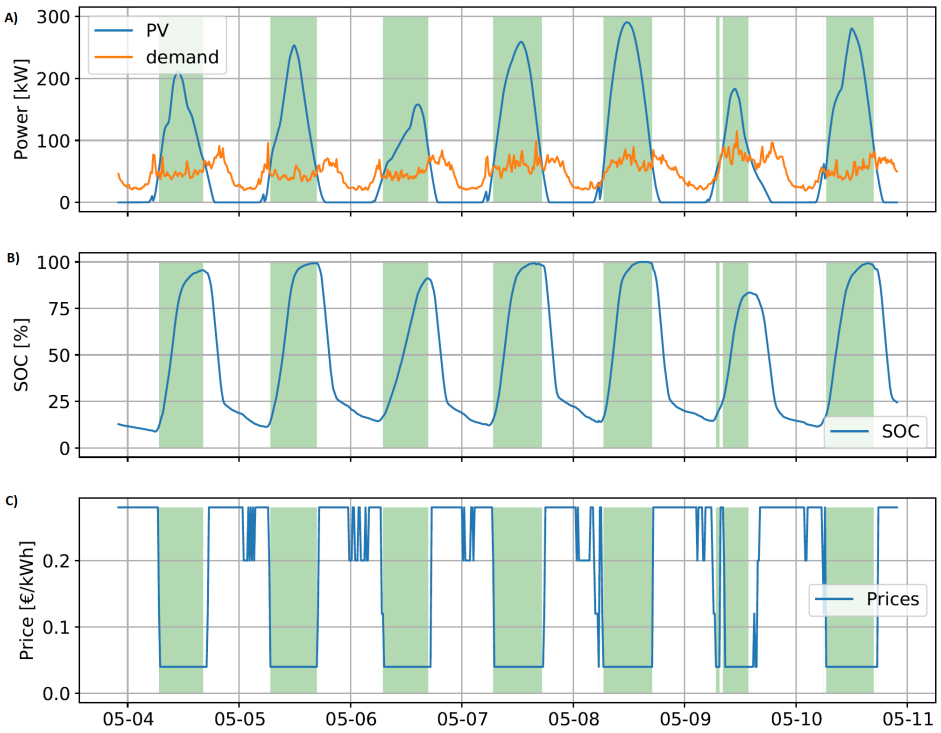

Figure C.15: **Energy flows at the aggregated level, showing the market price behavior in P2P communities in presence of surplus (green areas)**. **a)**: Aggregated PV generation and demand at the community level. **b)**: Aggregated State of Charge (SOC) of the 25 batteries across the P2P community. **c)**: Market price.

C.6.4 Comparison of the households' main motivations in both strategies.

Table C.3: Comparison of the role of each type of household for P2P communities and the baseline case in which prosumers maximize their self-consumption. In parentheses are presented the nature of the motivations.

Prosumer strategy \ Type of household	Prosumer with battery	Prosumer	Traditional consumer
P2P community	Self-determined trading of their PV electricity to other community members at higher value than the FiT (economic, social and environmental)	Weather-constrained trading of their PV electricity to other community members at a higher value than the FiT (economic, social, and environmental)	Purchasing of local PV electricity at a lower or equal price than the conventional grid electricity (economic, social, and environmental)
Self-consumption maximization	Avoiding conventional grid electricity imports at a high price by using their local PV generation directly and with storage (economic, and environmental)	Avoiding conventional grid electricity imports at a high price by using their local PV generation directly (economic, and environmental)	Purchasing main grid electricity at conventional price (retail tariff) with a high share of PV surplus electricity generated by neighbours (environmental)

C.7 Impact of battery degradation on P2P trading

In this study, battery degradation was not considered for neither of both battery strategies, namely, P2P trading and self-consumption. There are two main reasons for this. First, we do not model technology cost for PV nor battery systems that can be very heterogeneous within a P2P community (i.e., different technologies and costs). We assume the use of similar technologies and capacities in both strategies, namely, P2P trading and self-consumption maximization. In our paper, we focus on the extra value brought by P2P trading regarding individual self-consumption maximization, which is the main objective pursued by battery owners nowadays (Parra and Patel 2019; Dong et al. 2021). Second, degradation costs will be significantly lower than the value generated by batteries in the near future and, therefore, we do not consider them. This assumption is based on a comparison between cost and revenue of batteries which is explained below, assuming lithium-manganese-cobalt-oxide (NMC) batteries for our simulations with the following technical characteristics now: 5000 EFC, 15 years of lifetime, and 91% round trip efficiency.

The assumption that degradation costs will be significantly lower than the value generated by batteries can be derived as follows for the strategy of self-consumption maximization. The economic driver for a battery to increase PV self-consumption is given by Eqs. C.1 and C.2.

$$Rev_{PVSC} = E_{dbat} \cdot P_e - E_{PV-bat} \cdot P_{FiT} \tag{C.1}$$

$$Rev_{PVSC} = E_{PV-bat} \cdot P_e \cdot (\eta - \frac{P_{FiT}}{P_e}) \tag{C.2}$$

Whereas the revenue per kWh charged is given by Eq. C.3

$$Rev_{PVSC} = P_e \cdot (\eta - \frac{P_{FiT}}{P_e}) \tag{C.3}$$

Where P_e is the retail price, P_{FiT} is the Feed-in Tariff, η is the battery round-trip efficiency,E_{dbat} and E_{PV-bat} are the energy charged into and discharged from the battery, respectively. We modeled self-consumption maximization with the following electricity prices: P_{FiT}=€0.04 per kWh and P_e =€0.28 per kWh, which resulted in a battery revenue of €0.215 per kWh.

Battery aging/degradation results from both cycle and calendar losses which reduce the battery capacity throughout its lifetime, both in operation and stand-by, respectively. The state of health (SOH) of a battery has been used in the literature to measure the continuous loss of capacity of a battery (in parallelism with the state-of-charge, SOC). A percentage of the initial battery capacity is used for assessing the end of the lifetime, typically corresponding to 70% or 80% (Truong et al. 2016; Hesse, Martins, et al. 2017; He et al. 2018). For this study, we use a lithium-ion battery with 5000 EFC before the remaining capacity reaches 80%. The cost associated per kWh (Eq. C.7), taking a uniform degradation rate over the battery life cycle approach(Truong et al. 2016; Hesse, Martins, et al. 2017; He et al. 2018), can be derived using Eqs. C.4- C.7:

$$CAPEX = C \cdot Cost_{bat} \tag{C.4}$$

$$EFC = \frac{\eta \cdot E_{PV-bat}}{C} \tag{C.5}$$

$$Cost_{deg} = \frac{CAPEX}{E_{PV-bat}} \tag{C.6}$$

$$Cost_{deg} = \frac{\eta \cdot CAPEX}{EFC \cdot C} \tag{C.7}$$

Where $Cost_{bat}$ is the cost of the storage medium per kWh assumed to be €390 per kWh for this exercise, C is the nominal capacity of the battery, EFC are the equivalent full cycles and $CAPEX$ is the capital expenditure. Considering the above-mentioned battery characteristics, the degradation cost is equal to €0.072 per kWh. Therefore, in the case of self-consumption, the revenue stemming from the battery is markedly higher (threefold higher) than the cost of using the battery, and a profit can be easily made.

For batteries integrated in a P2P community, a similar approach can be used using the local market price P_{P2P}, instead of the retail price in Eq. C.2. With P_{FiT}=€0.04 per kWh, the minimum P_{P2P} that makes the revenue positive should be higher than the FiT to counterbalance the round trip efficiency penalty, and equal to €0.044 per kWh. But if we consider the same degradation cost, the local market price (P_{P2P}) should be higher than €0.123 per kWh

$$Rev_{P2P} = P_{P2P} \cdot (\eta - \frac{P_{FiT}}{P_{P2P}}) > Cost_{deg} \tag{C.8}$$

Based on these calculations, we conclude that either the battery CAPEX should be reduced by 55% or the EFC increased by the same amount (ceteris paribus) to achieve a revenue which is higher than degradation cost when the local market price is €0.04 per kWh (this is the lowest market price, which can be up to €0.28 per kWh). Given the projected development of battery technologies, this cost reduction seems to be feasible in the near future (in particular, some batteries available in the market already offer more than 8000 cycles - e.g., trinaBEss at similar prices, although it is a different chemistry Trina BESS 2017). Additionally, based on Eq. C.8, the minimum price at which trading electricity from batteries is profitable (which depends on the battery and the P2P market price specifications), should be properly indicated to the prosumers and incorporated into the battery scheduling management to avoid trading electricity without a proper economic incentive.

C.8 Willingness to sell

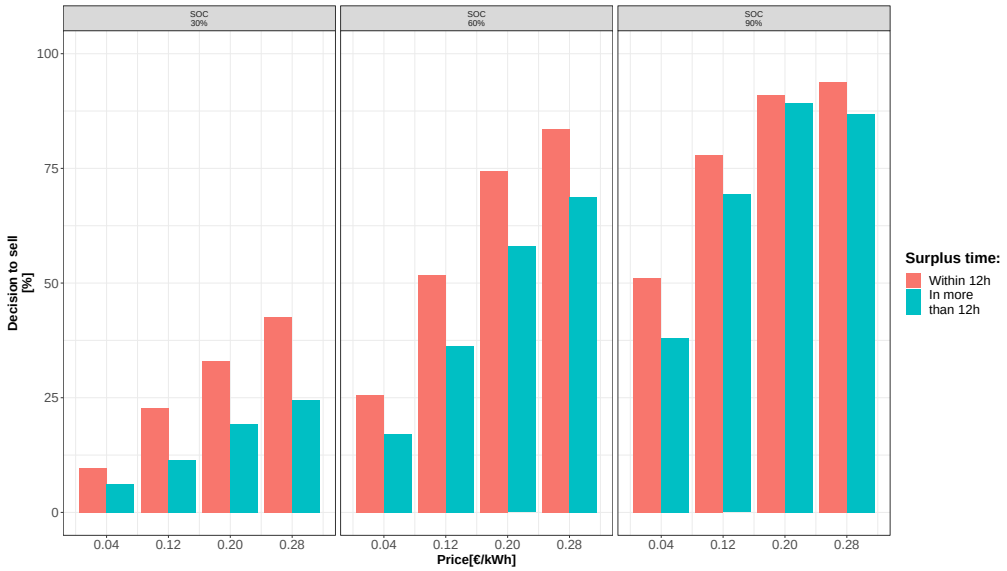

Figure C.16: **Willingness to sell electricity within the P2P community based on the experimental study.** Decisions to sell self-generated PV electricity to the P2P community as a function of P2P market prices (€0.04 per kWh to €0.28 per kWh in steps of €0.08 per kWh), SOC of privately owned 10 kWh batteries (30–90% in steps of 30%), and time until the next solar generation surplus (more than or less than 12 hours) as factors.

C.9 P2P community modeling for communities with different patterns of trading

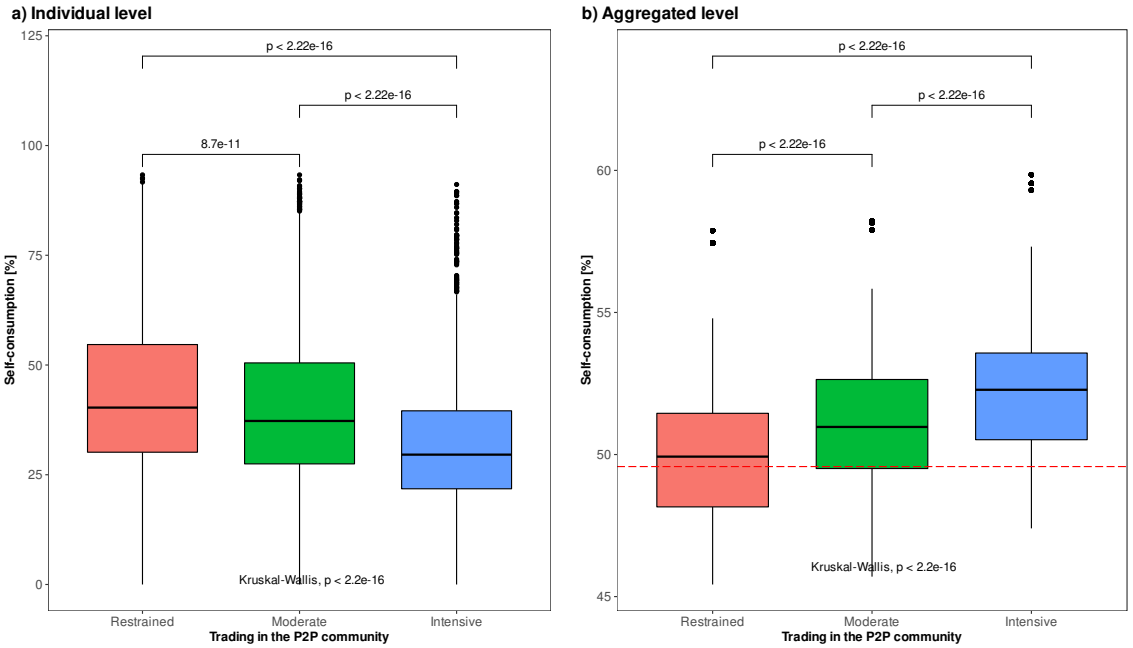

Figure C.17: **Results of the P2P community modeling for communities with different patterns of trading. a)** Boxplots for self-consumption for households with PV-coupled batteries; **b)** Boxplots for self-consumption at the aggregated level (PCC). Boxplots show the median (horizontal line) and the interquartile range (IQR; box outline). The whiskers extend from the hinge to the highest and lowest value that are within 1.5*IQR of the hinge, and the points represent the outliers. The individual p-values of the two-sided Wilcoxon test with the Holm procedure to control the family-wise error rate and of the Kruskal-wallis test are reported in the figure for panels b) and c), where N=1000 independent simulations.

C.10 Statistical results

Table C.4: Characterization of the amount of selling decisions (figure 3A of the main paper) and benefit index.

	Amount of selling decisions	Benefit Index
min	1	0,95
1st Q	9	0,99
median	12	1
mean	11,81	0,9951
3rd Q	14	1
max	22	1
SD	4,213264	0,007416

Table C.5: Results of the two-sided Shapiro–Wilk test for normality performed on different subsets for all figures of the main paper.

Figure	subset	W	p-value
1A	self-consumption maximization strategy: prosumers with PV and battery	0,99741	0,1121
1A	P2P trading strategy: prosumers with PV and battery	0,99845	0,5209
1A	self-consumption maximization strategy: prosumers with PV	0,99881	0,7621
1A	P2P trading strategy: prosumers with PV	0,99867	0,665
1A	self-consumption maximization strategy: traditional consumers	0,99877	0,7321
1A	P2P trading strategy: traditional consumers	0,9987	0,6859
1C	self-consumption maximization strategy	0,99767	0,00018
1C	P2P trading strategy	0,99807	0,001031
2B	self-consumption maximization strategy: Winter	0,96382	<2.2e-16
2B	P2P trading strategy and Winter	0,96365	<2.2e-16
2B	self-consumption maximization strategy: Fall	0,97445	<2.2e-16
2B	P2P trading strategy and Fall	0,97893	<2.2e-16
2B	self-consumption maximization strategy: Summer	0,93737	<2.2e-16
2B	P2P trading strategy and Summer	0,94228	<2.2e-16
2B	self-consumption maximization strategy: Spring	0,92196	<2.2e-16
2B	P2P trading strategy and Spring	0,94301	<2.2e-16
2C	self-consumption maximization strategy	0,94829	<2.2e-16
2C	P2P trading strategy	0,93998	<2.2e-16
2D	self-consumption maximization strategy	0,99788	0,000441
2D	P2P trading strategy	0,99812	0,001287
3B	self-consumption: restrained trading	0,96077	<2.2e-16
3B	self-consumption: moderate trading	0,95488	<2.2e-16
3B	self-consumption: intensive trading	0,93678	<2.2e-16
3B	autarky: restrained trading	0,94145	<2.2e-16
3B	autarky: moderate trading	0,97376	<2.2e-16
3B	autarky: intensive trading	0,98371	<2.2e-16
3B	bill: restrained trading	0,97461	<2.2e-16
3B	bill: moderate trading	0,98259	<2.2e-16
3B	bill: intensive trading	0,98315	<2.2e-16
3C	self-consumption: restrained trading	0,95673	<2.2e-16
3C	self-consumption: moderate trading	0,97253	<2.2e-16
3C	self-consumption: intensive trading	0,95941	<2.2e-16
3C	autarky: restrained trading	0,98927	<2.2e-16
3C	autarky: moderate trading	0,9787	<2.2e-16
3C	autarky: intensive trading	0,98934	<2.2e-16
3C	bill: restrained trading	0,9881	<2.2e-16
3C	bill: moderate trading	0,98847	<2.2e-16
3C	bill: intensive trading	0,98782	<2.2e-16

Table C.6: Results of the two-sided Wilcoxon test with the Holm procedure to control the family-wise error rate performed on different subsets for figures 1 and 2 of the main paper.

Figure	subset A	subset B	W	p-value
1A	self-consumption maximization strategy and prosumers with PV and battery	P2P trading strategy prosumers with PV and battery	867091	<2.2e-16
1A	self-consumption maximization strategy and prosumers with PV	P2P trading strategy prosumers with PV	854860	<2.2e-16
1A	self-consumption maximization strategy and traditional consumers	P2P trading strategy traditional consumers	999817	<2.2e-16
1C	self-consumption maximization strategy	P2P trading strategy	8996625	<2.2e-16
2B	self-consumption maximization strategy and Winter	P2P trading strategy and Winter	1.7494e+10	<2.2e-16
2B	self-consumption maximization strategy and Fall	P2P trading strategy and Fall	3,7E+09	<2.2e-16
2B	self-consumption maximization strategy and Summer	P2P trading strategy and Summer	2E+09	<2.2e-16
2B	self-consumption maximization strategy and Spring	P2P trading strategy and Spring	7,8E+08	<2.2e-16
2C	self-consumption maximization strategy	P2P trading strategy	4029705	<2.3812e-16
2D	self-consumption maximization strategy	P2P trading strategy	5036670	<1.249e-15

Table C.7: Results of the two-sided Kruskal-Wallis test performed on different subsets for figure 3 of the main paper.

Figure	variable	in function of	χ^2	df	p-value
3B	Self-consumption	trading	617,66	2	<2.2e-16
3B	autarky	trading	2012,9	2	<2.2e-16
3B	Bill	trading	19,56	2	5.656e-5
3C	Self-consumption	trading	4349,7	2	<2.2e-16
3C	autarky	trading	12060	2	<2.2e-16
3C	Bill	trading	811,36	2	<2.2e-16

Appendix D

Supplementary Information - National level

D.1 The energy market

D.1.1 The European energy market

Electricity generation and consumption must be equal at all times in order to preserve a balanced grid. When deviations appear, the grid frequency is affected, and large frequency deviations can lead to grid instabilities and blackouts (van der Veen and Hakvoort 2016).

The European wholesale electricity market counts with two features, self-dispatch and balancing responsibility, that help obtain a balanced grid (Lago et al. 2021). The self-dispatch obliges market participants to submit projected generation and consumption schedules ahead of time, while making their own decisions regarding the electricity dispatch, contrary to the case where a system operator makes the dispatch decision in a centralized way (*e.g.*, in the U.S. (Lago et al. 2021)). On the other hand, balancing responsibility puts a financial responsibility to the market participants for deviations from their schedules, to cover the cost of grid imbalances.

To adjust their schedules and avoid the financial responsibility for deviations, market participants can trade in three different markets. The forward market allows to trade electricity from weeks to months in advance. The day-ahead market allows trade of electricity up to 24-h in advance. Finally, the intraday market, the most liquid market, running 24/7, allows electricity trading up to 0-minutes before delivery time and with contracts of 1-h, 30-minute and 15-minute. Due to unplanned outages and the uncertainty of electricity generation and consumption, imbalances are still possible. To ensure real-time balancing, the balancing market was conceived.

The European balancing market

The balancing market is the institutional arrangement that establishes market-based balance management in an unbundled electricity market (van der Veen and Hakvoort 2016). Where balancing is defined as all actions and processes, on all timelines, through which Transmission System Operators (TSOs) ensure, in a continuous way, to maintain the system frequency within a predefined stability range (ENTSO-E 2014).

Each TSO is responsible for the real-time balance in its control area. Balancing markets, separated into balancing capacity markets and balancing energy markets, allow TSOs to procure the resources needed to balance the system. In balancing capacity markets, contracted Balancing Service Providers (BSPs) are paid an availability payment (Meeus 2020). Contracting is done one year ahead up to one day ahead of delivery in order to make sure of real-time balancing energy availability. The BSPs contracted in the balancing capacity market then offer their balancing energy in the balancing energy markets (Meeus 2020). The volume of activated energy depends on real-time imbalances. The capacity markets are mainly national or regional and only some aspects have an European reach.

Europe counts with five synchronous areas, in these areas the use of primary, secondary and tertiary frequency control used to be recurrent, however, the definitions were not aligned. In 2017, the System Operation Guideline and the Electricity Balancing Guideline introduced a new terminology of standard energy balancing products per balancing process to facilitate the sharing of balancing energy across borders at the European level (Meeus 2020).

Real-time imbalances between electricity generation and consumption are measured by the deviation of the nominal system frequency (50 Hz in Europe). To restore the balance in the power system three processes are triggered. However, before giving way to the three processes, the rotational masses of synchronous generators (system inertia) counteract imbalances by repressing the rate of change of frequency. This inertia in future the power system will be smaller due to the increasing amount of (asynchronous) renewable plants, which reduces grid stability (Motte-Cortés and Eising 2019; Bovera et al. 2021).

The first and fastest process is the regulation process, that contains the frequency containment reserves (FCR, equivalent to primary control), that makes part of the frequency containment process (Meeus 2020). A solidarity mechanism is in place to reduce the amount of FCR procurement in each country and the FCR procurement is done per synchronous area (Meeus 2020). The FCR is a service that starts within 30 seconds and spans over 15 minutes, combines upward and downward balancing, and is remunerated only for its capacity availability.

The second process is the frequency restoration process, which is divided into automatic frequency restoration reserves (aFRR, equivalent to secondary control), and manual frequency restoration reserves (mFRR, equivalent to fast tertiary control). This response is organized in the load frequency control (LFC) area. In general, LFC area is the same than the TSOs' control area (Meeus 2020). In the future it is expected that TSO operate jointly across a synchronous area. This process starts after the frequency containment process, to relieve FCR, and is used to restore the frequency within a predefined time. aFRR are usually provided by synchronous units or units with a fast response, to follow TSO's request within one minute. mFRR relieves aFRR, and has two standard products, that differ in the activation mode, a scheduled activation that can only be activated at one point in time, and a direct mFRR that can be activated at any point of time following the point of scheduled activation of the quarter hour for which the bid is submitted and until the point of scheduled activation of the subsequent quarter hour. Both aFRR and mFRR are separated into upward and downward balancing, and are remunerated per available capacity and energy balancing.

The final process is the reserve replacement process, which is the slowest one and can need 30 minutes to be fully activated. The standard product can be activated during periods multiples of a quarter hour and is done manually and according to a

schedule.

D.1.2 Imbalance settlement

Market parties have a balance responsibility. Balance responsible parties (BRPs) are market participants that are financially responsible for keeping supply and demand within their portfolio in balance. In case of imbalances, they have to be settled with the TSO. An imbalance is a deviation between generation, consumption and commercial transactions of a BRP within a given imbalance settlement period. There are two types of imbalance, deterministic and uncertain. The former arises when it is not possible to match the contract length in the energy market with instantaneous changes in demand and supply. Whereas the latter is inherent to the uncertainty of demand and supply forecasting (e.g., errors in forecasting and plant shut downs). Imbalances can be positive and negative. A positive imbalance is a situation in which BRPs demand unexpectedly exceeds electricity generation causing a need for additional supply, and viceversa for the negative imbalance.

The imbalance settlement is the process of allocating cost to market actors that caused the imbalances, and thus, it aims to charge (or pay) BRPs for their imbalances during an imbalance settlement period (from 15-minute to 1-h depending on the country). It aims at recovering the costs of balancing the system and include incentives for the market to reduce imbalances while transferring the financial risk of imbalances to BRPs.

D.2 Models

D.2.1 PV-coupled battery system

We analyze the techno-economic implications of adding a battery system to a new PV system that would otherwise be installed on its own (we hereby disregard all costs related to the PV system). We assume a DC-coupled configuration illustrated in Figure D.1, including an integrated inverter with a buck-boost charge controller (i.e., a step-up and step-down converter combined), a maximum power point tracking system and a bi-directional inverter (required to charge a battery from the main grid). An inverter loading ratio (i.e., the ratio between the inverter rating and the PV rating, referred to as ILR) of 1.2 is considered for this study (Burger and Rüther 2006). We simulate Lithium Nickel Manganese Cobalt Oxide (NMC) batteries since this technology is currently dominating the residential market. Following a conservative approach, we consider relatively high installation costs for the battery and inverter, equal to 2000 USD, regardless their nominal capacity (Baumann and Baumgartner 2017). We assume that NMC batteries can use 100% of depth of discharge (DoD) (ITP Renewables 2016) and can be charged or discharged in 2.5 h (i.e., a C-rate of 0.4*C, where C is the nominal capacity of the battery). Moreover, we consider the battery to reach the end-of-life (EoL) when 30% of the nominal capacity is depleted (Pena-Bello, Barbour, Gonzalez, Patel, et al. 2019). The techno-economic values for the PV-coupled battery system used in this study are displayed in Table D.1.

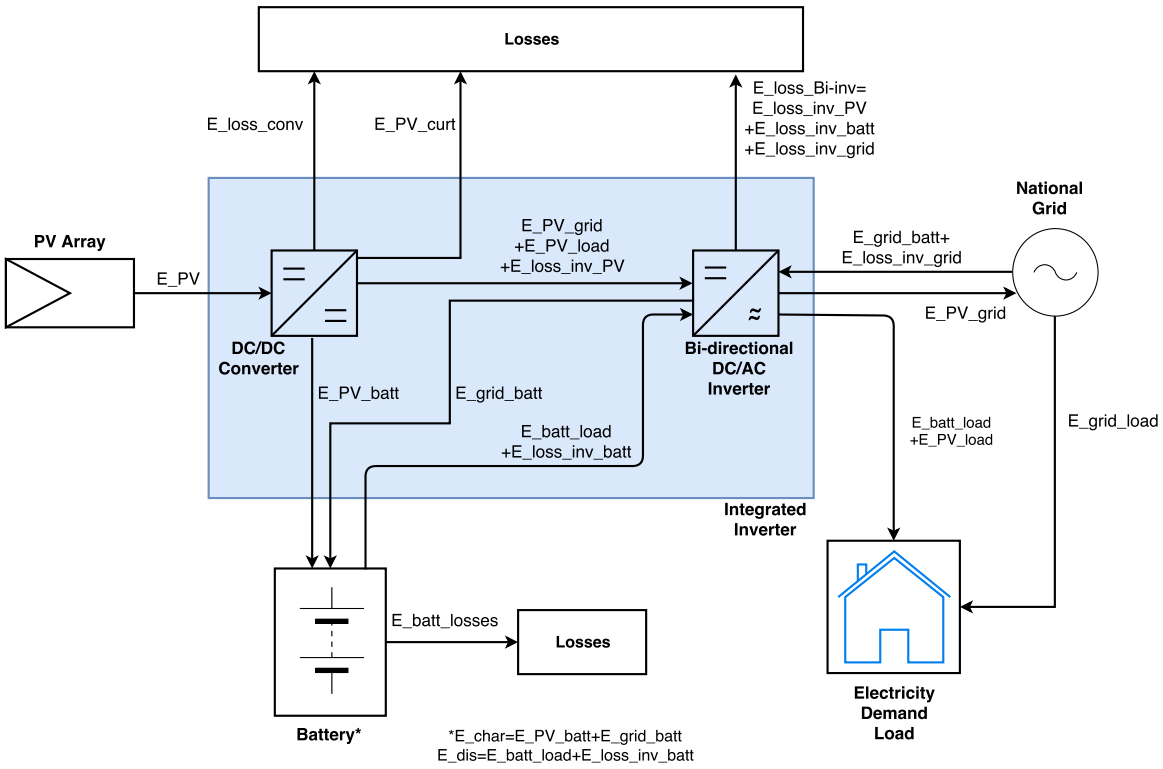

Figure D.1: DC-coupled PV-battery system with integrated inverter used in this study. Arrows indicate the direction of possible energy flows between the individual components.

Table D.1: Values selected for the technical and economic assessment of PV-coupled battery systems. The cycle aging factor is given for a 100% depth-of-discharge.

Component	Units	Value	Reference
Charge controller efficiency	%	98	Energy 2017
Inverter efficiency	%	94	Energy 2017
Bi-directional inverter cost	USD/kW	600	Ardani et al. 2017
Bi-directional inverter lifetime	years	15	Fu et al. 2017
Balance of plant cost	USD/kW	100	Pena-Bello, Burer, et al. 2017
Installation costs	USD	2000	Baumann and Baumgartner 2017
O&M	USD/kW	0	Tesla 2015
Discount factor	% p.a.	4	Stephan et al. 2016
End of life (EoL)	%	70	Käbitz et al. 2013
ILR	p.u.	1.2	Burger and Rüther 2006
Cycles at a given depth of discharge	-	5000 @ 100%	Tesla 2015
Battery lifetime	Years	15	Tesla 2015
Battery roundtrip efficiency	%	91.8	Tesla 2015
Battery Energy costs	USD/nominal kWh	410	Tesla 2015
Maximum charge/discharge rate	kW	0.4*C	Tesla 2015
ΔSOC	%	100	ITP Renewables 2016
Maximum SOC	%	100	ITP Renewables 2016
Minimum SOC	%	0	ITP Renewables 2016
Cycle aging factor	per cycle	0.00042	Based on Truong et al. 2016
Calendar aging factor	per day	0.00038	Based on Truong et al. 2016

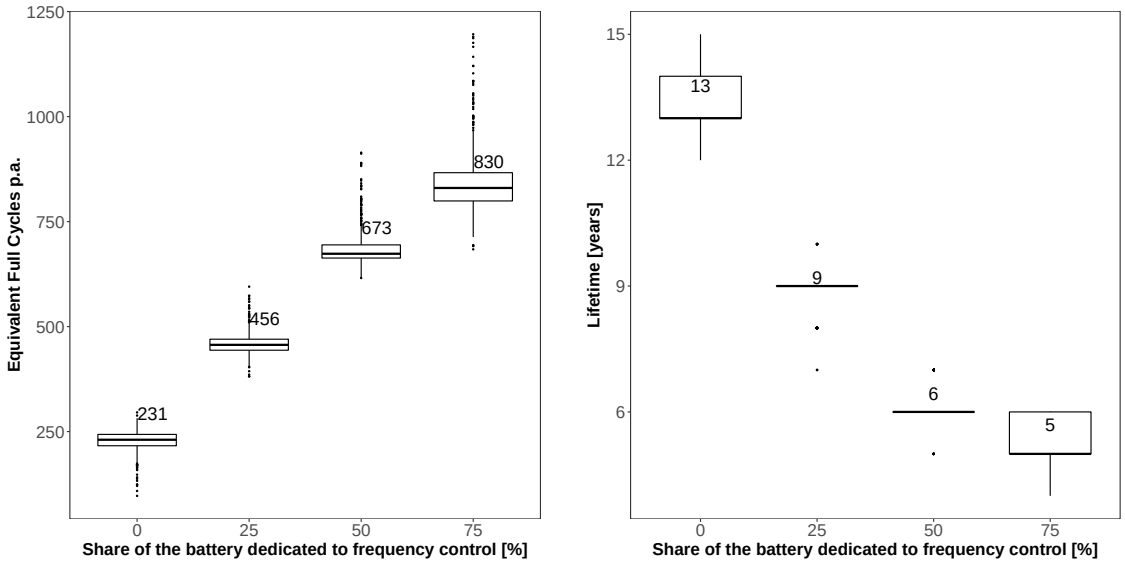

(a) Equivalent full cycles.

(b) Battery lifetime.

Figure D.2: Boxplots (N=636) of EFC and lifetime of residential batteries depending on the share of the battery dedicated to frequency control. The median value for each boxplot is indicated in the figure

D.3 Results

D.3.1 BASOPRA

Figs. D.2a and D.2b show the equivalent full cycles and the battery lifetime depending on the share of the battery capacity dedicated to frequency control. Note that the amount of EFC doubles when going from zero to 25% of the battery capacity is dedicated to frequency control, which reduces the median battery lifetime from 13 years to 9 years.

D.3.2 Monte Carlo simulation

To validate the Monte Carlo simulation, we compare the results for automatic and manual restoration reserve from the model to the real data from 2020 extracted from Swissgrid in Table D.3. The total activated reserves in 2020 were 311.15 GWh upwards and -340.88 GWh downwards according to Swissgrid, whereas for the modeled activated reserves were 307.45 and -356.88 GWh, respectively (average of ten simulations).

D.3.3 Linear Model

To validate the linear model, we compare the results for automatic and manual from the model to the real data from 2020 extracted from Swissgrid in Table D.4. Figure D.4 shows the comparison of the modeled and real data of prices for aFRR and mFRR in each direction.

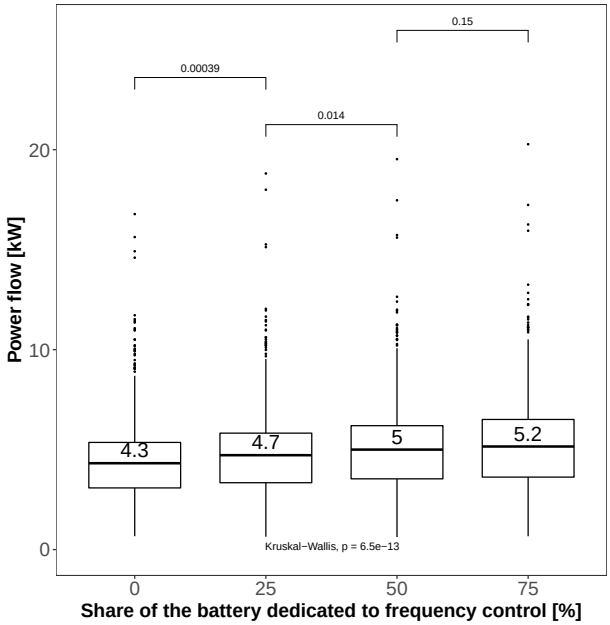

Figure D.3: Boxplots (N=636) of power flow (i.e., the maximum between the import and export power) of PV-coupled battery systems depending on the share of the battery dedicated to frequency control. The median value for each boxplot is indicated in the figure

Table D.2: Descriptive statistics of frequency control associated value per share of dedicated battery and direction

Share of battery	Direction	Min	1Q	Median	Mean	3Q	Max
25%	Upwards	16.2	136.3	191.6	207	258.2	560.7
25%	Downwards	8.81	65.88	91.4	98	122.45	254.8
50%	Upwards	31.79	278.86	390.56	421.93	532.86	1137.7
50%	Downwards	17.98	143.16	200.63	215.24	269.35	560.23
75%	Upwards	48.56	392.54	549.66	591.15	740.13	15558.74
75%	Downwards	27.9	207.6	287.5	307.8	385.9	842.1

Table D.3: Descriptive statistics of the reported and the modeled regulating power price, for the year 2020. Data in MWh except for the column Sum where data is in GWh.

	mean	std	min	25%	50%	75%	max	sum [GWh]
Real aFRR+	16.6	23.7	0.0	1.9	6.8	21.9	256.9	145.7
Modeled aFRR+	17.5	15.5	0.0	9.0	13.5	20.0	156.5	153.7
Real aFRR-	-18.7	23.5	-232.1	-26.4	-9.5	-2.5	0.0	-163.9
Modeled aFRR-	-20.4	19.4	-212.4	-23.0	-15.1	-9.8	0.0	-178.4
Real mFRR+	22.7	57.1	0.0	0.0	0.0	14.3	788.0	198.8
Modeled mFRR+	17.5	15.5	0.0	9.0	13.5	20.0	156.5	153.7
Real aFRR-	-21.0	48.0	-889.8	-16.3	0.0	0.0	0.0	-183.9
Modeled mFRR-	-20.4	19.4	-212.4	-23.0	-15.1	-9.8	0.0	-178.4

Table D.4: Descriptive statistics of the reported and the modeled imbalance prices, for the year 2020. Data in Eur/MWh.

	mean	std	min	25%	50%	75%	max	sum
Real avg price aFRR+	42.6	15.6	13.8	32.6	42.2	51.6	147.0	373.0
Modeled avg price aFRR+	43.9	15.4	-53.5	34.3	44.6	52.9	140.4	384.7
Real avg price aFRR-	26.5	11.2	-68.5	18.5	27.6	33.7	61.4	231.9
Modeled avg price aFRR-	27.1	11.3	-44.2	20.1	27.6	33.7	97.7	237.5
Real avg price mFRR+	16.3	99.2	0.0	0.0	0.0	12.7	5389.3	142.7
Modeled avg price mFRR+	1.4	0.1	0.6	1.3	1.4	1.5	2.1	12.1
Real avg price mFRR-	3.7	14.7	-273.6	0.0	0.0	0.0	56.3	32.8
Modeled avg price mFRR-	2.6	2.7	-14.8	0.9	2.8	4.2	19.8	23.1
Real long	17.4	18.1	-477.6	11.0	19.6	25.9	94.8	152.5
Modeled long	2.4	14.8	-301.5	-0.6	-0.6	-0.6	51.2	21.4
Real short	61.8	94.6	-4.5	46.3	57.1	68.2	4681.1	541.4
Modeled short	54.1	106.2	16.3	37.2	48.2	59.0	5929.3	473.7

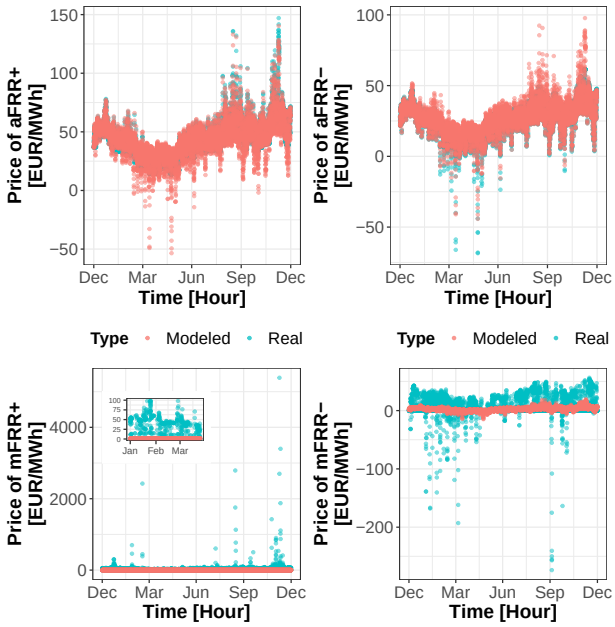

Figure D.4: Comparison of regulating power price reported and modeled for the year 2020

Bibliography

Abdoulaye, M. A. et al. (2020). "Impact of the Intermittency of Photovoltaic Power Plants on the Frequency Management: Case of the Senegalese Electricity Grid". In: *Journal of Power and Energy Engineering* 8.07. [Accessed on 21/03/2022] https://doi.org/10.4236/jpee.2020.87005, p. 55.

Ableitner, L. et al. (2020). "User behavior in a real-world peer-to-peer electricity market". In: *Applied Energy* 270. [Accessed on 21/03/2022] https://doi.org/10.1016/j.apenergy.2020.115061, p. 115061.

ACCC (2018). *Restoring electricity affordability and Australia's competitive advantage Retail Electricity Pricing Inquiry — Final Report*. Tech. rep. [Accessed on 21/03/2022] https://www.accc.gov.au/system/files/Retail%20Electricity%20Pricing%20Inquiry%E2%80%94Final%20Report%20June%202018_0.pdf.

AEMC (Jan. 2014). *2014 Residential Electricity Price Trends*. [Accessed on 21/03/2022] https://www.aemc.gov.au/markets-reviews-advice/2014-residential-electricity-price-trends.

Ahl, A. et al. (2019). "Review of blockchain-based distributed energy: Implications for institutional development". In: *Renewable and Sustainable Energy Reviews* 107. [Accessed on 21/03/2022], https://doi.org/10.1016/j.rser.2019.03.002, pp. 200–211.

Alipour, M. et al. (2020). "Predictors, taxonomy of predictors, and correlations of predictors with the decision behaviour of residential solar photovoltaics adoption: A review". In: *Renewable and Sustainable Energy Reviews* 123. [Accessed on 21/03/2022], https://doi.org/10.1016/j.rser.2020.109749, p. 109749.

Andoni, M. et al. (2019). "Blockchain technology in the energy sector: A systematic review of challenges and opportunities". In: *Renewable and Sustainable Energy Reviews* 100. [Accessed on 21/03/2022], https://doi.org/10.1016/j.rser.2018.10.014, pp. 143–174.

Ardani, K. et al. (2017). *Installed Cost Benchmarks and Deployment Barriers for Residential Solar Photovoltaics with Energy Storage: Q1 2016*. Tech. rep. [Accessed on 21/03/2022] https://www.nrel.gov/docs/fy17osti/67474.pdf. Golden, CO: National Renewable Energy Laboratory (NREL). NREL/TP-7A40-67474.

Arteconi, A., N. J. Hewitt, and F. Polonara (2013). "Domestic demand-side management (DSM): Role of heat pumps and thermal energy storage (TES) systems". In: *Applied thermal engineering* 51.1-2. [Accessed on 21/03/2022], https://doi.org/10.1016/j.applthermaleng.2012.09.023, pp. 155–165.

Attari, S. Z. (2021). "Transforming energy use". In: *Current Opinion in Behavioral Sciences* 42, pp. 104–108. DOI: https://doi.org/10.1016/j.cobeha.2021.04.008.

Azarova, V. et al. (2018). "Exploring the impact of network tariffs on household electricity expenditures using load profiles and socio-economic characteristics".

In: *Nature Energy* 3.4. [Accessed on 21/03/2022], https://doi.org/10.1038/s41560-018-0105-4, pp. 317–325.

Barbour, E. and M. C. González (2018). "Projecting battery adoption in the prosumer era". In: *Appl. Energy* 215. [Accessed on 21/03/2022], https://doi.org/10.1016/j.apenergy.2018.01.056, pp. 356–370.

Barbour, E., D. Parra, et al. (2018). "Community energy storage: A smart choice for the smart grid?" In: *Applied Energy* 212. [Accessed on 21/03/2022], https://doi.org/10.1016/j.apenergy.2017.12.056, pp. 489–497.

Battke, B. et al. (2013). "A review and probabilistic model of lifecycle costs of stationary batteries in multiple applications". In: *Renewable and Sustainable Energy Reviews* 25. [Accessed on 21/03/2022], https://doi.org/10.1016/j.rser.2013.04.023, pp. 240–250.

Bauer, C. et al. (2017). "Potentials, costs and environmental assessment of electricity generation technologies". In: *PSI, WSL, ETHZ, EPFL, Paul Scherrer Institut, Villigen, Switzerland*. [Accessed on 21/03/2022], https://www.psi.ch/sites/default/files/import/ta/HomeEN/Final-Report-BFE-Project.pdf.

Baumann, T. and F. Baumgartner (2017). *Home Batteriespeicher, studie für solarspar*. Tech. rep. [Accessed on 21/03/2022] https://www.solarspar.ch/app/download/12621170687/20170106_Home_Batteriespeicher_solarspar.pdf?t=1569512414. ZHAW / IEFE Winterthur.

Bayer, B. et al. (2018). "The German experience with integrating photovoltaic systems into the low-voltage grids". In: *Renewable energy* 119. [Accessed on 21/03/2022], https://doi.org/10.1016/j.renene.2017.11.045, pp. 129–141.

Beck, T. et al. (2016). "Assessing the influence of the temporal resolution of electrical load and PV generation profiles on self-consumption and sizing of PV-battery systems". In: *Appl. Energy* 173. [Accessed on 21/03/2022], https://doi.org/10.1016/j.apenergy.2016.04.050, pp. 331–342.

Beitollahi, H. and G. Deconinck (2007). "Peer-to-peer networks applied to power grid". In: *Proceedings of the International conference on Risks and Security of Internet and Systems (CRiSIS)'in conjunction with the IEEE GIIS*. Vol. 7. [Accessed on 21/03/2022], https://citeseerx.ist.psu.edu/viewdoc/download?doi=10.1.1.134.7160&rep=rep1&type=pdf, p. 8.

Bellman, R. E. (2015). *Adaptive control processes: a guided tour*. [Accessed on 21/03/2022], https://doi.org/10.2307/j.ctt183ph6v. Princeton university press.

Benıétez, I. et al. (2014). "Dynamic clustering segmentation applied to load profiles of energy consumption from Spanish customers". In: *Int. J. Elec. Power* 55. https://doi.org/10.1016/j.ijepes.2013.09.022, pp. 437–448.

Berger, M. and J. Worlitschek (2018). "A novel approach for estimating residential space heating demand". In: *Energy* 159. [Accessed on 21/03/2022], https://doi.org/10.1016/j.energy.2018.06.138, pp. 294–301.

BFE (2018). *Erneuerbare Energien Einspeisevergütung Berichte*. [Accessed on 21/03/2022] https://www.bfe.admin.ch/bfe/de/home/foerderung/erneuerbare-energien/einspeiseverguetung.html.

Biggins, F. et al. (2022). "To trade or not to trade: Simultaneously optimising battery storage for arbitrage and ancillary services". In: *Journal of Energy Storage* 50. [Accessed on 21/03/2022], https://doi.org/10.1016/j.est.2022.104234, p. 104234.

Blok, K. and E. Nieuwlaar (2016). *Introduction to energy analysis*. Routledge.

Böcker, B. et al. (2017). "Storage valuation in congested grids". In: *IEEE Trans. Smart Grid*. [Accessed on 21/03/2022], https://doi.org/10.1109/TSG.2017.2721982.

Bollen, M. H. and F. Hassan (2011). *Integration of distributed generation in the power system*. Vol. 80. John wiley & sons.

Bovera, F. et al. (2021). "Data-Driven Evaluation of Secondary-and Tertiary-Reserve Needs with High Renewables Penetration: The Italian Case". In: *Energies* 14.8. [Accessed on 21/03/2022], https://doi.org/10.3390/en14082157, p. 2157.

Bozorg, M. et al. (2018). "Influencing the bulk power system reserve by dispatching power distribution networks using local energy storage". In: *Electric Power Systems Research* 163. [Accessed on 21/03/2022], https://doi.org/10.1016/j.epsr.2018.06.017, pp. 270–279.

Bundesnetzagentur (2017). *Zahlen, Daten, Informationen zum EEG*. [Accessed on 21/03/2022] https://www.bundesnetzagentur.de/DE/Sachgebiete/ElektrizitaetundGas/Unternehmen_Institutionen/ErneuerbareEnergien/ZahlenDatenInformationen/zahlenunddaten-node.html.

Bundestag Deutscher (2017). *Gesetz für den Ausbau erneuerbarer Energien*. [Accessed on 21/03/2022] https://www.gesetze-im-internet.de/eeg_2014/.

Burger, B. and R. Rüther (2006). "Inverter sizing of grid-connected photovoltaic systems in the light of local solar resource distribution characteristics and temperature". In: *Solar Energy* 80.1. [Accessed on 21/03/2022], https://doi.org/10.1016/j.solener.2005.08.012, pp. 32–45.

Burmeister, H. and B. Keller (1998). "Climate surfaces: a quantitative building-specific representation of climates". In: *Energy and Buildings* 28.2. [Accessed on 21/03/2022], https://doi.org/10.1016/S0378-7788(98)00012-7, pp. 167–177.

Campana, P. E. et al. (2021). "Li-ion batteries for peak shaving, price arbitrage, and photovoltaic self-consumption in commercial buildings: A Monte Carlo Analysis". In: *Energy Conversion and Management* 234. [Accessed on 21/03/2022], https://doi.org/10.1016/j.enconman.2021.113889, p. 113889.

Carley, S. and D. M. Konisky (2020). "The justice and equity implications of the clean energy transition". In: *Nature Energy* 5.8. [Accessed on 21/03/2022], https://doi.org/10.1038/s41560-020-0641-6, pp. 569–577.

Carlisle, N., J. Elling, and T. Penney (2008). *Renewable Energy Community: Key Elements*. Tech. rep. [Accessed on 21/03/2022], https://www.nrel.gov/docs/fy08osti/42774.pdf. National Renewable Energy Lab.(NREL), Golden, CO (United States).

Castelazzi, L. et al. (2019). "Assessment of second long-term renovation strategies under the Energy Efficiency Directive". In: *JRC Science for Policy Report JRC114200*. [Accessed on 21/03/2022], https://doi.org/10.2760/973672.

Chicco, G. (2012). "Overview and performance assessment of the clustering methods for electrical load pattern grouping". In: *Energy* 42.1. [Accessed on 21/03/2022], https://doi.org/10.1016/j.energy.2011.12.031, pp. 68–80.

Council of European Energy Regulators (2019). *Regulatory Aspects of Self-Consumption and Energy Communities*. Tech. rep. [Accessed on 21/03/2022], https://www.ceer.eu/documents/104400/-/-/8ee38e61-a802-bd6f-db27-4fb61aa6eb6a. Council of European Energy Regulators, Brussels, Belgium.

CPUC (2017). *Self-Generation Incentive Program*. California, U.S. [Accessed on 21/03/2022] https://www.cpuc.ca.gov/sgip/.

Curtius, H. C. et al. (2018). "Shotgun or snowball approach? Accelerating the diffusion of rooftop solar photovoltaics through peer effects and social norms". In: *Energy policy* 118. [Accessed on 21/03/2022], https://doi.org/10.1016/j.enpol.2018.04.005, pp. 596–602.

Denholm, P., R. Margolis, and J. Eichman (2017). *Evaluating the Technical and Economic Performance of PV Plus Storage Power Plants*. Tech. rep. [Accessed on 21/03/2022], https://doi.org/10.2172/1376049. National Renewable Energy Laboratory (NREL), Golden, CO (United States).

Devine-Wright, P. (2019). "Community versus local energy in a context of climate emergency". In: *Nature Energy* 4.11. [Accessed on 21/03/2022], https://doi.org/10.1038/s41560-019-0459-2, pp. 894–896.

do Nascimento, Á. D. J. and R. Rüther (2020). "Evaluating distributed photovoltaic (PV) generation to foster the adoption of energy storage systems (ESS) in time-of-use frameworks". In: *Solar Energy* 208. [Accessed on 21/03/2022], https://doi.org/10.1016/j.solener.2020.08.045, pp. 917–929.

Dong, S. et al. (2021). "Establishing the value of community energy storage: A comparative analysis of the UK and Germany". In: *Journal of Energy Storage* 40. [Accessed on 21/03/2022], https://doi.org/10.1016/j.est.2021.102709, p. 102709.

Dott, R., C. Ackerman, et al. (2019). *Wärmepumpenheizsysteme mit PV und weiteren Komponenten*. [Accessed on 21/03/2022], https://www.fws.ch/wp-content/uploads/2019/05/Ralf_Dott.pdf.

Dott, R., M. Y. Haller, et al. (2013). "The reference framework for system simulations of the IEA SHC Task 44/HPP Annex 38 Part B: buildings and space heat load". In: *International Energy Agency*. [Accessed on 21/03/2022],http://www.taskx.iea-shc.org/data/sites/1/publications/T44A38_Rep_C1_B_ReferenceBuildingDescription_Final_Revised_130906.pdf.

Dudjak, V. et al. (2021). "Impact of local energy markets integration in power systems layer: A comprehensive review". In: *Applied Energy* 301. [Accessed on 21/03/2022], https://doi.org/10.1016/j.apenergy.2021.117434, p. 117434.

Duffie, J. A. and W. A. Beckman (2013). *Solar engineering of thermal processes*. John Wiley & Sons.

Ecker, F., U. J. Hahnel, and H. Spada (2017). "Promoting decentralized sustainable energy systems in different supply scenarios: the role of autarky aspiration". In: *Frontiers in Energy Research* 5. [Accessed on 21/03/2022], https://doi.org/10.3389/fenrg.2017.00014, p. 14.

Ecker, F., H. Spada, and U. J. Hahnel (2018). "Independence without control: Autarky outperforms autonomy benefits in the adoption of private energy storage systems". In: *Energy Policy* 122. [Accessed on 21/03/2022], https://doi.org/10.1016/j.enpol.2018.07.028, pp. 214–228.

Ecoult (2017). *Ultraflex product fact sheet*. [Accessed on 21/03/2022] https://ecosmartsolar.com.au/wp-content/uploads/2017/08/Ecoult_UltraFlex_FS_4pp_1702.pdf.

EMI, A. M. (2015). *Study on tariff design for distribution systems*. Tech. rep. [Accessed on 21/03/2022], https://ec.europa.eu/energy/sites/ener/files/documents/20150313%20Tariff%20report%20fina_revREF-E.PDF. Technical Report.

Energy, V. (2017). *EasySolar 12/1600/70*. [Accessed on 21/03/2022] https://www.victronenergy.no/upload/documents/Datasheet-EasySolar-1600VA-EN.pdf.

Engels, J., B. Claessens, and G. Deconinck (2017). "Combined stochastic optimization of frequency control and self-consumption with a battery". In: *IEEE Transactions on Smart Grid* 10.2. [Accessed on 21/03/2022], https://doi.org/10.1109/TSG.2017.2785040, pp. 1971–1981.

Englberger, S., A. Jossen, and H. Hesse (2020). "Unlocking the potential of battery storage with the dynamic stacking of multiple applications". In: *Cell Reports Physical Science* 1.11. [Accessed on 21/03/2022], https://doi.org/10.1016/j.xcrp.2020.100238, p. 100238.

ENTSO-E, A. (2014). *Entso-e network code on electricity balancing*.

Equipment, V. P. (2018). *International Technology Roadmap for Photovoltaic (ITRPV)*.

EUPD, R. (2020). *89 percent of the solar potential for German single- and two-family houses is still unexploited*. [Accessed on 06/12/2021] https://www.eupd-research.com/en/89-percent-of-the-solar-potential-still-unexploited/.

European Union (2018). "Directive (EU) 2018/2001 of the European Parliament and of the Council of 11 December 2018 on the promotion of the use of energy from renewable sources". In: *Official Journal of the European Union* 5. [Accessed on 21/03/2022], https://eur-lex.europa.eu/eli/dir/2018/2001/oj, pp. 82–209.

Eurostat (2018). *Electricity prices for household consumers - bi-annual data (from 2007 onwards)*. [Accessed on 21/03/2022] http://appsso.eurostat.ec.europa.eu/nui/show.do?dataset=nrg_pc_204&lang=en.

— (2020). "Household energy prices in the EU increased compared with 2018". In: *News release*. [Accessed on 21/03/2022], https://bit.ly/3KR68FH.

Fares, R. L. and M. E. Webber (2017). "The impacts of storing solar energy in the home to reduce reliance on the utility". In: *Nat. Energy* 2. [Accessed on 21/03/2022], https://doi.org/10.1038/nenergy.2017.1.

FCP-1000 Lead Carbon Battery (2018). [Accessed on 21/03/2022] https://res-energy.at/files/res-fcp-1000.pdf. Sun Sacred.

Feldman, D., K. Wu, and R. Margolis (2021). *H1 2021 Solar Industry Update*. Tech. rep. [Accessed on 21/03/2022], https://www.nrel.gov/docs/fy21osti/80427.pdf. National Renewable Energy Lab.(NREL), Golden, CO (United States).

Fell, M. J., A. Schneiders, and D. Shipworth (2019). "Consumer demand for blockchain-enabled peer-to-peer electricity trading in the United Kingdom: An online survey experiment". In: *Energies* 12.20. [Accessed on 21/03/2022], https://doi.org/10.3390/en12203913, p. 3913.

Fidalgo, J. N., M. Couto, and L. Fournie (2016). "The worth of network upgrade deferral in distribution systems–Truism or myth?" In: *Electric Power Systems Research* 137. [Accessed on 21/03/2022], https://doi.org/10.1016/j.epsr.2016.04.001, pp. 96–103.

Figgener, J., D. Habershusz, et al. (2017). *Wissenschaftliches Mess-und Evaluierungsprogramm Solarstromspeicher 2.0*. Tech. rep. [Accessed on 21/03/2022] http://www.speichermonitoring.de/fileadmin/user_upload/Speichermonitoring_Jahresbericht_2017_ISEA_RWTH_Aachen.pdf. ISEA and RWTH Aachen University.

Figgener, J., P. Stenzel, et al. (2021). "The development of stationary battery storage systems in Germany–status 2020". In: *Journal of Energy Storage* 33. [Accessed on 21/03/2022], https://doi.org/10.1016/j.est.2020.101982, p. 101982.

Finance Bloomberg New Energy (2018). *New Energy Outlook 2017. Global overview.* [Accessed on 21/03/2022] https://www.res4med.org/wp-content/uploads/2017/06/BNEF_NEO2017_ExecutiveSummary.pdf.

Fischer, D. et al. (2016). "Impact of PV and variable prices on optimal system sizing for heat pumps and thermal storage". In: *Energy and Buildings* 128. [Accessed on 21/03/2022], https://doi.org/10.1016/j.enbuild.2016.07.008, pp. 723–733.

Franco, A. and F. Fantozzi (Feb. 2016). "Experimental analysis of a self consumption strategy for residential building: The integration of PV system and geothermal heat pump". English. In: *Renewable Energy* 86. [Accessed on 21/03/2022], https://doi.org/10.1016/j.renene.2015.09.030, pp. 1075–1085.

Fridgen, G. et al. (2018). "One rate does not fit all: An empirical analysis of electricity tariffs for residential microgrids". In: *Applied Energy* 210. [Accessed on 21/03/2022], https://doi.org/10.1016/j.apenergy.2017.08.138, pp. 800–814.

Fu, R. et al. (2017). *US solar photovoltaic system cost benchmark: Q1 2017.* Tech. rep. [Accessed on 21/03/2022] https://www.nrel.gov/docs/fy17osti/68925.pdf. Golden, CO: National Renewable Energy Laboratory (NREL). NREL/TP-6A20-68925.

Gardiner, D. et al. (2020). "Quantifying the impact of policy on the investment case for residential electricity storage in the UK". In: *Journal of Energy Storage* 27. [Accessed on 21/03/2022], https://doi.org/10.1016/j.est.2019.101140, p. 101140.

Gigerenzer, G. and W. Gaissmaier (2011). "Heuristic decision making". In: *Annual review of psychology* 62. [Accessed on 21/03/2022], https://doi.org/10.1146/annurev-psych-120709-145346, pp. 451–482.

Guerrero-Mestre, V. et al. (2020). "A probabilistic analysis of power generation adequacy towards a climate-neutral Europe". In: *Energy Reports* 6. [Accessed on 21/03/2022], https://doi.org/10.1016/j.egyr.2020.11.243, pp. 3316–3333.

Gupta, R., F. Sossan, and M. Paolone (2021). "Countrywide PV hosting capacity and energy storage requirements for distribution networks: The case of Switzerland". In: *Applied Energy* 281. [Accessed on 21/03/2022], https://doi.org/10.1016/j.apenergy.2020.116010, p. 116010.

Gupta, R., A. Pena-Bello, et al. (2021). "Spatial analysis of distribution grid capacity and costs to enable massive deployment of PV, electric mobility and electric heating". In: *Applied Energy* 287. [Accessed on 21/03/2022], https://doi.org/10.1016/j.apenergy.2021.116504, p. 116504.

Gupta, R., M. C. Soini, et al. (2020). "Levelized cost of solar photovoltaics and wind supported by storage technologies to supply firm electricity". In: *Journal of Energy Storage* 27. [Accessed on 21/03/2022], https://doi.org/10.1016/j.est.2019.101027, p. 101027.

Gwerder, D. and P. Schuetz (2019). *Machbarkeitsstudie zum Flexibilitätspotential von Wärmepumpen mit Speichern in Smart Grids.* Tech. rep. Bundesamt für Energie.

Haben, S., C. Singleton, and P. Grindrod (2015). "Analysis and clustering of residential customers energy behavioral demand using smart meter data". In: *IEEE transactions on smart grid* 7.1. [Accessed on 21/03/2022], https://doi.org/10.1109/TSG.2015.2409786, pp. 136–144.

Hackbarth, A. and S. Löbbe (2020). "Attitudes, preferences, and intentions of German households concerning participation in peer-to-peer electricity trading". In:

Energy Policy 138. [Accessed on 21/03/2022], https://doi.org/10.1016/j.enpol.2020.111238, p. 111238.

Hahnel, U. J., G. Chatelain, et al. (2020). "Mental accounting mechanisms in energy decision-making and behaviour". In: *Nature Energy*. [Accessed on 21/03/2022], https://doi.org/10.1038/s41560-020-00704-6, pp. 1–7.

Hahnel, U. J., M. Herberz, et al. (2020). "Becoming prosumer: Revealing trading preferences and decision-making strategies in peer-to-peer energy communities". In: *Energy Policy* 137. [Accessed on 21/03/2022], https://doi.org/10.1016/j.enpol.2019.111098, p. 111098.

Hart, W. E. et al. (2012). *Pyomo-optimization modeling in python*. Vol. 67. [Accessed on 21/03/2022], https://doi.org/10.1007/978-3-319-58821-6. Springer.

Hartvigsson, E. et al. (2021a). "Estimating national and local low-voltage grid capacity for residential solar photovoltaic in Sweden, UK and Germany". In: *Renewable Energy* 171. [Accessed on 21/03/2022], https://doi.org/10.1016/j.renene.2021.02.073, pp. 915–926.

— (2021b). "Generating low-voltage grid proxies in order to estimate grid capacity for residential end-use technologies: the case of residential solar PV". In: *MethodsX*. [Accessed on 21/03/2022], https://doi.org/10.1016/j.mex.2021.101431, p. 101431.

He, G. et al. (2018). "An intertemporal decision framework for electrochemical energy storage management". In: *Nature Energy* 3.5. [Accessed on 21/03/2022], https://doi.org/10.1038/s41560-018-0129-9, pp. 404–412.

Heinhold, L. (1965). "Kabel und Leitungen für Starkstrom". In: *Siemens*.

Hennig, R. et al. (2020). "Capacity Subscription Tariffs for Electricity Distribution Networks: Design Choices and Congestion Management". In: *2020 17th International Conference on the European Energy Market (EEM)*. [Accessed on 21/03/2022], https://doi.org/10.1109/EEM49802.2020.9221994. IEEE, pp. 1–6.

Heptonstall, P. J. and R. J. Gross (2020). "A systematic review of the costs and impacts of integrating variable renewables into power grids". In: *Nature Energy*. [Accessed on 21/03/2022], https://doi.org/10.1038/s41560-020-00695-4, pp. 1–12.

Hesse, H., R. Martins, et al. (2017). "Economic Optimization of Component Sizing for Residential Battery Storage Systems". en. In: *Energies* 10.7. [Accessed on 21/03/2022], https://doi.org/10.3390/en10070835, p. 835.

Hesse, H., M. Schimpe, et al. (2017). "Lithium-Ion Battery Storage for the Grid? A Review of Stationary Battery Storage System Design Tailored for Applications in Modern Power Grids". In: *Energies* 10.12. [Accessed on 21/03/2022], https://doi.org/10.3390/en10122107, p. 2107.

Heymann, F. et al. (2019). "Distribution network planning considering technology diffusion dynamics and spatial net-load behavior". In: *International Journal of Electrical Power and Energy Systems* 106. [Accessed on 21/03/2022], https://doi.org/10.1016/j.ijepes.2018.10.006, pp. 254–265.

Hinz, A. and M. Sojer (2012). "Spannungsgeregelte Ortsnetzstationen zur Verbesserung der Netzintegration von erneuerbaren Energien". In: *Tagungsband zum VDE-Kongress*. Vol. 146.

HIT photovoltaic module HIT-N2XXSE10 datasheet (n.d.). [Accessed on 21/03/2022] https://www.evoenergy.co.uk/wp-content/uploads/2012/09/Datasheet-HIT-250W.pdf. Sanyo.

Hollander, M., D. A. Wolfe, and E. Chicken (2013). *Nonparametric statistical methods*. Vol. 751. John Wiley & Sons.

Hollinger, R. et al. (2016). "Distributed solar battery systems providing primary control reserve". In: *IET Renewable Power Generation* 10.1. [Accessed on 21/03/2022], https://doi.org/10.1049/iet-rpg.2015.0147, pp. 63–70.

Holweger, J. et al. (2020). "Mitigating the impact of distributed PV in a low-voltage grid using electricity tariffs". In: *Electric Power Systems Research* 189. [Accessed on 21/03/2022], https://doi.org/10.1016/j.epsr.2020.106763, p. 106763.

Hoppmann, J. et al. (2014). "The economic viability of battery storage for residential solar photovoltaic systems ? A review and a simulation model". In: *Renew. Sust. Energ. Rev.* 39. [Accessed on 21/03/2022], https://doi.org/10.1016/j.rser.2014.07.068, pp. 1101–1118.

Horowitz, K. A. et al. (2018). "Distribution system costs associated with the deployment of photovoltaic systems". In: *Renewable and Sustainable Energy Reviews* 90. [Accessed on 21/03/2022], https://doi.org/10.1016/j.rser.2018.03.080, pp. 420–433.

Hoval (2017). *Dimensionierungshilfe für Wärmepumpenanlagen 2017 Technische*. Tech. rep. Hoval.

Husser, Pius (2017). *National Survey Report of PV Power Applications in Switzerland - 2016*. [Accessed on 21/03/2022] http://iea-pvps.org/index.php?id=93&eID=dam_frontend_push&docID=4055.

Hutty, T. D. et al. (2021). "Peer-to-peer electricity trading as an enabler of increased PV and EV ownership". In: *Energy Conversion and Management* 245. [Accessed on 21/03/2022], https://doi.org/10.1016/j.enconman.2021.114634, p. 114634.

IEA (2019). *Tracking Buildings*. (Accessed on 21/03/2022). URL: https://www.iea.org/reports/tracking-buildings.

— (2020). *REnewables 2020*. (Accessed on 21/03/2022). URL: https://www.iea.org/reports/renewables-2020.

Ineichen, P. (2013). "Solar radiation resource in Geneva: measurements, modeling, data quality control, format and accessibility". In: *Archive ouverte Unige*. [Accessed on 21/03/2022], https://www.unige.ch/sysener/fr/activites/meteo/acces-aux-donnees/.

IRENA (2017a). *Electricity storage and renewables: costs and markets to 2030*. Abu Dhabi.[Accessed on 21/03/2022] https://www.irena.org/-/media/Files/IRENA/Agency/Publication/2017/Oct/IRENA_Electricity_Storage_Costs_2017.pdf.

— (2017b). *REthinking Energy 2017: Accelerating the global energy transformation*. Abu Dhabi. [Accessed on 21/03/2022] https://www.irena.org/-/media/Files/IRENA/Agency/Publication/2017/IRENA_REthinking_Energy_2017.pdf.

— (2019). *Renewable Electricity Capacity and Generation Statistics*. Abu Dhabi. [Accessed on 06/12/2021] https://www.irena.org/Statistics.

— (2020). *Innovation landscape brief: Peer-to-peer electricity trading, IRENA OECD/IEA REN21*. [Accessed on 21/03/2022], https://irena.org/-/media/Files/IRENA/Agency/Publication/2020/Jul/IRENA_Peer-to-peer_trading_2020.pd.

— (2021). *Renewable Power Generation Costs in 2020*. Abu Dhabi. [Accessed on 06/12/2021] https://www.irena.org/publications/2021/Jun/Renewable-Power-Costs-in-2020.

ITP Renewables (2016). *Battery Test Centre - Public Report 1*. Tech. rep. [Accessed on 21/03/2022] http://batterytestcentre.com.au/wp-content/uploads/2017/07/Battery-Testing-Report-1_web.pdf. Lithium Ion Battery Test Centre program.

— (2017). *Battery Test Centre - Public Report 2*. Tech. rep. [Accessed on 21/03/2022] http://batterytestcentre.com.au/wp-content/uploads/2017/07/Battery-Testing-Report-2_web.pdf. Lithium Ion Battery Test Centre program.

Jenkins, K. et al. (2016). "Energy justice: a conceptual review". In: *Energy Research & Social Science* 11. [Accessed on 21/03/2022], https://doi.org/10.1016/j.erss.2015.10.004, pp. 174–182.

Jordan, U. and K. Vajen (2001). "Influence of the DHW load profile on the fractional energy savings:: A case study of A solar combi-system with TRNSYS simulations". In: *Solar energy* 69. [Accessed on 21/03/2022], https://doi.org/10.1016/S0038-092X(00)00154-7, pp. 197–208.

Käbitz, S. et al. (2013). "Cycle and calendar life study of a graphite| LiNi1/3Mn1/3Co1/3O2 Li-ion high energy system. Part A: Full cell characterization". In: *J. Power Sources* 239. [Accessed on 21/03/2022], https://doi.org/10.1016/j.jpowsour.2013.03.045, pp. 572–583.

Kavlak, G., J. McNerney, and J. E. Trancik (2018). "Evaluating the causes of cost reduction in photovoltaic modules". In: *Energy Policy* 123. [Accessed on 21/03/2022], https://doi.org/10.1016/j.enpol.2018.08.015, pp. 700–710.

Kazhamiaka, F. et al. (2017). "On the influence of jurisdiction on the profitability of residential photovoltaic-storage systems: A multi-national case study". In: *Energy Policy* 109. [Accessed on 21/03/2022], https://doi.org/10.1016/j.enpol.2017.07.019, pp. 428–440.

KfW Bank (2016). *Förderprogram Erneuerbare Energien-Speicher*. [Accessed on 21/03/2022] https://www.kfw.de/inlandsfoerderung/Unternehmen/Energie-Umwelt/F%C3%B6rderprodukte/Erneuerbare-Energien-%E2%80%93-Speicher-(275)/.

Koirala, B. P. et al. (2016). "Energetic communities for community energy: A review of key issues and trends shaping integrated community energy systems". In: *Renewable and Sustainable Energy Reviews* 56. [Accessed on 21/03/2022], https://doi.org/10.1016/j.rser.2015.11.080, pp. 722–744.

Korcaj, L., U. J. Hahnel, and H. Spada (2015). "Intentions to adopt photovoltaic systems depend on homeowners' expected personal gains and behavior of peers". In: *Renewable Energy* 75. [Accessed on 21/03/2022], https://doi.org/10.1016/j.renene.2014.10.007, pp. 407–415.

Kosowatz, J. (2018). "Energy Storage Smooths The Duck Curve". In: *Mechanical Engineering* 140.06. [Accessed on 21/03/2022], https://doi.org/10.1115/1.2018-JUN-1, pp. 30–35.

Kwac, J., J. Flora, and R. Rajagopal (2014). "Household energy consumption segmentation using hourly data". In: *IEEE Trans. Smart Grid* 5.1. [Accessed on 21/03/2022], https://doi.org/10.1109/TSG.2013.2278477, pp. 420–430.

Lago, J. et al. (2021). "A market framework for grid balancing support through imbalances trading". In: *Renewable and Sustainable Energy Reviews* 137. [Accessed on 21/03/2022], https://doi.org/10.1016/j.rser.2020.110467, p. 110467.

Leclanche (2015). *TiRack Energy Storage Systems*. [Accessed on 21/03/2022] https://www.leclanche.com/wp-content/uploads/2019/04/LECLANCHE-M2-LTO-moduleWEB.pdf.

Leisen, R., B. Steffen, and C. Weber (2019). "Regulatory risk and the resilience of new sustainable business models in the energy sector". In: *Journal of cleaner production* 219. [Accessed on 21/03/2022], https://doi.org/10.1016/j.jclepro.2019.01.330, pp. 865–878.

Lim, C. S. and A. Yurukoglu (2018). "Dynamic Natural Monopoly Regulation: Time Inconsistency, Moral Hazard, and Political Environments". In: *J. Political Econ.* 126.1. https://doi.org/10.1086/695474, pp. 263–312.

Linssen, J., P. Stenzel, and J. Fleer (2017). "Techno-economic analysis of photovoltaic battery systems and the influence of different consumer load profiles". In: *Applied Energy* 185. [Accessed on 21/03/2022], https://doi.org/10.1016/j.apenergy.2015.11.088, pp. 2019–2025.

Litjens, G. B., E. Worrell, and W. G. van Sark (2018a). "Economic benefits of combining self-consumption enhancement with frequency restoration reserves provision by photovoltaic-battery systems". In: *Applied energy* 223. [Accessed on 21/03/2022], https://doi.org/10.1016/j.apenergy.2018.04.018, pp. 172–187.

Litjens, G. B., E. Worrell, and W. G. van Sark (2018b). "Assessment of forecasting methods on performance of photovoltaic-battery systems". In: *Applied Energy* 221. [Accessed on 21/03/2022], https://doi.org/10.1016/j.apenergy.2018.03.154, pp. 358–373.

Liu, N. et al. (2017). "Energy-sharing model with price-based demand response for microgrids of peer-to-peer prosumers". In: *IEEE Transactions on Power Systems* 32.5. [Accessed on 21/03/2022], https://doi.org/10.1109/TPWRS.2017.2649558, pp. 3569–3583.

Liu, X. et al. (2019). "Optimal design and operation of PV-battery systems considering the interdependency of heat pumps". In: *Journal of Energy Storage* 23. [Accessed on 21/03/2022], https://doi.org/10.1016/j.est.2019.04.026, pp. 526–536.

Lund, P. et al. (2015). "Review of energy system flexibility measures to enable high levels of variable renewable electricity". In: *Renewable and Sustainable Energy Reviews* 45. [Accessed on 21/03/2021], https://doi.org/10.1016/j.rser.2015.01.057, pp. 785–807.

Lüth, A. et al. (2018). "Local electricity market designs for peer-to-peer trading: The role of battery flexibility". In: *Applied energy* 229. [Accessed on 21/03/2021], https://doi.org/10.1016/j.apenergy.2018.08.004, pp. 1233–1243.

Luthander, R., A. M. Nilsson, et al. (2019). "Graphical analysis of photovoltaic generation and load matching in buildings: A novel way of studying self-consumption and self-sufficiency". In: *Applied Energy* 250. [Accessed on 21/03/2022], https://doi.org/10.1016/j.apenergy.2019.05.058, pp. 748–759.

Luthander, R., J. Widén, J. Munkhammar, et al. (Oct. 2016). "Self-consumption enhancement and peak shaving of residential photovoltaics using storage and curtailment". English. In: *Energy* 112. [Accessed on 21/03/2022], https://doi.org/10.1016/j.energy.2016.06.039.

Luthander, R., J. Widén, D. Nilsson, et al. (2015). "Photovoltaic self-consumption in buildings: A review". In: *Appl. Energy* 142. [Accessed on 21/03/2022], https://doi.org/10.1016/j.apenergy.2014.12.028, pp. 80–94.

Magnor, D. and D. U. Sauer (2016). "Optimization of PV battery systems using genetic algorithms". In: *Energy Procedia* 99. [Accessed on 21/03/2022], https://doi.org/10.1016/j.egypro.2016.10.123, pp. 332–340.

Marghetis, T., S. Z. Attari, and D. Landy (2019). "Simple interventions can correct misperceptions of home energy use". In: *Nature Energy* 4.10. [Accessed on 21/03/2022], https://doi.org/10.1038/s41560-019-0467-2, pp. 874–881.

Meeus, L. (2020). *The evolution of electricity markets in Europe*. Edward Elgar Publishing.

Mishra, P. P. et al. (2020). "Analysis of degradation in residential battery energy storage systems for rate-based use-cases". In: *Applied Energy* 264. [Accessed on 21/03/2022], https://doi.org/10.1016/j.apenergy.2020.114632, p. 114632.

Mohamed, A. A. R. et al. (2021). "A Comprehensive Robust Techno-Economic Analysis and Sizing Tool for the Small-Scale PV and BESS". In: *IEEE Transactions on Energy Conversion*. [Accessed on 21/03/2022], https://doi.org/10.1109/TEC.2021.3107103.

Moore, M. et al. (2015). "A Comparison of the Capital Costs of a Vanadium Redox-Flow Battery and a Regenerative Hydrogen- Vanadium Fuel Cell". In: *J. Adv. Chem. Eng.* 5. https://doi.org/10.4172/2090-4568.1000140.

Morstyn, T., I. Savelli, and C. Hepburn (2021). "Multiscale design for system-wide peer-to-peer energy trading". In: *One Earth* 4.5. [Accessed on 21/03/2022], https://doi.org/10.1016/j.oneear.2021.04.018, pp. 629–638.

Moss, R. et al. (2013). *JRC report on Critical Metals in the Energy Sector*. European Commission Joint Research Centre Institute for Energy and Transport. https://doi.org/doi:10.2790/46338r.

Motte-Cortés, A. and M. Eising (2019). "Assessment of balancing market designs in the context of European coordination". In: *2019 16th International Conference on the European Energy Market (EEM)*. [Accessed on 21/03/2022], https://doi.org/10.1109/EEM.2019.8916481. IEEE, pp. 1–7.

Mousavi, O. A., R. Cherkaoui, and M. Bozorg (2012). "Blackouts risk evaluation by Monte Carlo Simulation regarding cascading outages and system frequency deviation". In: *Electric Power Systems Research* 89, pp. 157–164.

Muller, M. et al. (2017). "Evaluation of grid-level adaptability for stationary battery energy storage system applications in Europe". In: *J. Energy Storage* 9. [Accessed on 21/03/2022], https://doi.org/10.1016/j.est.2016.11.005, pp. 1–11.

Mulleriyawage, U. and W. Shen (2020). "Optimally sizing of battery energy storage capacity by operational optimization of residential PV-Battery systems: An Australian household case study". In: *Renewable Energy* 160. [Accessed on 21/03/2022], https://doi.org/10.1016/j.renene.2020.07.022, pp. 852–864.

Narula, K. et al. (2019). "Strategies for decarbonising the Swiss heating system". In: *Energy* 169. [Accessed on 21/03/2022], https://doi.org/10.1016/j.energy.2018.12.082, pp. 1119–1131.

Nousdilis, A. I., G. C. Christoforidis, and G. K. Papagiannis (2018). "Active power management in low voltage networks with high photovoltaics penetration based on prosumers' self-consumption". In: *Applied energy* 229, pp. 614–624.

Nousdilis, A. I., G. C. Kryonidis, et al. (2020). "Impact of policy incentives on the promotion of integrated PV and battery storage systems: a techno-economic assessment". In: *IET Renewable Power Generation* 14.7. [Accessed on 21/03/2022], https://doi.org/10.1016/j.apenergy.2018.08.032, pp. 1174–1183.

NREL (2018). *The Open PV Project*. [Accessed on 21/03/2022] https://openpv.nrel.gov/.

Nyholm, E. et al. (2016). "Solar photovoltaic-battery systems in Swedish households ? Self-consumption and self-sufficiency". In: *Appl. Energy* 183. [Accessed

on 21/03/2022], https://doi.org/10.1016/j.apenergy.2016.08.172, pp. 148–159.
O'Shaughnessy, E. et al. (2018a). "Solar plus: A review of the end-user economics of solar PV integration with storage and load control in residential buildings". In: *Applied energy* 228. [Accessed on 21/03/2022], https://doi.org/10.1016/j.apenergy.2018.07.048, pp. 2165–2175.
— (2018b). "Solar plus: Optimization of distributed solar PV through battery storage and dispatchable load in residential buildings". In: *Appl. Energy* 213. [Accessed on 21/03/2022], https://doi.org/10.1016/j.apenergy.2017.12.118, pp. 11–21.
Obaid, Z. A. et al. (2020). "Control of a population of battery energy storage systems for frequency response". In: *International Journal of Electrical Power & Energy Systems* 115. [Accessed on 21/03/2022], https://doi.org/10.1016/j.ijepes.2019.105463, p. 105463.
Omar, N. et al. (2014). "Lithium iron phosphate based battery ? Assessment of the aging parameters and development of cycle life model". In: *Appl. Energy* 113. [Accessed on 21/03/2022], https://doi.org/10.1016/j.apenergy.2013.09.003, pp. 1575–1585.
Østergaard, D. S. and S. Svendsen (2016a). "Case study of low-temperature heating in an existing single-family house—A test of methods for simulation of heating system temperatures". In: *Energy and Buildings* 126. [Accessed on 21/03/2022], https://doi.org/10.1016/j.enbuild.2016.05.042, pp. 535–544.
— (2016b). "Theoretical overview of heating power and necessary heating supply temperatures in typical Danish single-family houses from the 1900s". In: *Energy and Buildings* 126. [Accessed on 21/03/2022], https://doi.org/10.1016/j.enbuild.2016.05.034, pp. 375–383.
Oualmakran, Y. et al. (2017). "Residential Electricity Tariffs in Europe: Current Situation, Evolution and Impact on Residential Flexibility Markets". In: *Proceedings* 1.7. [Accessed on 21/03/2022], https://doi.org/10.3390/proceedings1071104.
Parag, Y. and B. K. Sovacool (2016). "Electricity market design for the prosumer era". In: *Nature energy* 1.4. [Accessed on 21/03/2022], https://doi.org/10.1038/nenergy.2016.32, pp. 1–6.
Parra, D., S. A. Norman, et al. (2016). "Optimum community energy storage system for demand load shifting". In: *Applied Energy* 174. [Accessed on 21/03/2022], https://doi.org/10.1016/j.apenergy.2014.08.060, pp. 130–143.
Parra, D. and M. K. Patel (2016). "Effect of tariffs on the performance and economic benefits of PV-coupled battery systems". In: *Appl. Energy* 164. [Accessed on 21/03/2022], https://doi.org/10.1016/j.apenergy.2015.11.037, pp. 175–187.
— (2019). "The nature of combining energy storage applications for residential battery technology". In: *Applied energy* 239. [Accessed on 21/03/2022], https://doi.org/10.1016/j.apenergy.2019.01.218, pp. 1343–1355.
Parra, D., M. Swierczynski, et al. (2017). "An interdisciplinary review of energy storage for communities: Challenges and perspectives". In: *Renewable and Sustainable Energy Reviews* 79. [Accessed on 21/03/2022], https://doi.org/10.1016/j.rser.2017.05.003, pp. 730–749.
Parra, D., G. S. Walker, and M. Gillott (2014). "Modeling of PV generation, battery and hydrogen storage to investigate the benefits of energy storage for sin-

gle dwelling". In: *Sustainable Cities and Society* 10. [Accessed on 21/03/2022], https://doi.org/10.1016/j.scs.2013.04.006, pp. 1–10.

— (2016). "Are batteries the optimum PV-coupled energy storage for dwellings? Techno-economic comparison with hot water tanks in the UK". In: *Energy and Buildings* 116. [Accessed on 21/03/2022], https://doi.org/10.1016/j.enbuild.2016.01.039, pp. 614–621.

Patteeuw, D., G. P. Henze, and L. Helsen (Apr. 2016). "Comparison of load shifting incentives for low-energy buildings with heat pumps to attain grid flexibility benefits". In: *Applied Energy* 167. [Accessed on 21/03/2022], https://doi.org/10.1016/j.apenergy.2016.01.036, pp. 80–92. (Visited on 09/11/2018).

Pena-Bello, A., E. Barbour, M. C. Gonzalez, M. K. Patel, et al. (2019). "Optimized PV-coupled battery systems for combining applications: Impact of battery technology and geography". In: *Renewable and Sustainable Energy Reviews* 112. [Accessed on 21/03/2022], https://doi.org/10.1016/j.rser.2019.06.003, pp. 978–990.

Pena-Bello, A., E. Barbour, M. C. Gonzalez, S. Yilmaz, et al. (2020). "How does the electricity demand profile impact the attractiveness of PV-coupled battery systems combining applications?" In: *Energies* 13.15. [Accessed on 21/03/2022], https://doi.org/10.3390/en13154038, p. 4038.

Pena-Bello, A., M. Burer, et al. (2017). "Optimizing PV and grid charging in combined applications to improve the profitability of residential batteries". In: *J. Energy Storage* 13. [Accessed on 21/03/2022], https://doi.org/10.1016/j.est.2017.06.002, pp. 58–72.

Pena-Bello, A., P. Schuetz, et al. (2021). "Decarbonizing heat with PV-coupled heat pumps supported by electricity and heat storage: Impacts and trade-offs for prosumers and the grid". In: *Energy Conversion and Management* 240. [Accessed on 21/03/2022], https://doi.org/10.1016/j.enconman.2021.114220, p. 114220.

Perez, A. et al. (2016). "Effect of battery degradation on multi-service portfolios of energy storage". In: *IEEE Transactions on Sustainable Energy* 7.4. [Accessed on 21/03/2022], https://doi.org/10.1109/TSTE.2016.2589943, pp. 1718–1729.

Perez-Arriaga, I. J., J. D. Jenkins, and C. Batlle (2017). "A regulatory framework for an evolving electricity sector: Highlights of the MIT utility of the future study". In: *Economics of Energy & Environmental Policy* 6.1. [Accessed on 21/03/2022], https://doi.org/10.5547/2160-5890.6.1.iper, pp. 71–92.

Pfenninger, S. (2017). "Energy scientists must show their workings". In: *Nat News* 542.7642. [Accessed on 21/03/2022], https://doi.org/10.1038/542393a, p. 393.

Pfenninger, S., J. DeCarolis, et al. (2017). "The importance of open data and software: Is energy research lagging behind?" In: *Energy Policy* 101. [Accessed on 21/03/2022], https://doi.org/10.1016/j.enpol.2016.11.046, pp. 211–215.

Pfenninger, S. and I. Staffell (2016). "Long-term patterns of European PV output using 30 years of validated hourly reanalysis and satellite data". In: *Energy* 114. [Accessed on 21/03/2022], https://doi.org/10.1016/j.energy.2016.08.060, pp. 1251–1265.

Pimm, A. J., T. T. Cockerill, and P. G. Taylor (2018). "The potential for peak shaving on low voltage distribution networks using electricity storage". In: *Journal of Energy Storage* 16. [Accessed on 21/03/2022], https://doi.org/10.1016/j.est.2018.02.002, pp. 231–242.

Plewnia, F. and E. Guenther (2020). "The transition value of business models for a sustainable energy system: the case of virtual peer-to-peer energy communities". In: *Organization & Environment*. [Accessed on 21/03/2022], https://doi.org/10.1177/1086026620932630, p. 1086026620932630.

Prada, A. et al. (Dec. 2017). "On the optimal mix between lead-acid battery and thermal storage tank for PV and heat pump systems in high performance buildings". In: *Energy Procedia*. Beyond NZEB Buildings (AiCARR 50th International Congress, Matera (I), 10-11 May 2017) 140. [Accessed on 21/03/2022], https://doi.org/10.1016/j.egypro.2017.11.154, pp. 423–433. (Visited on 09/13/2018).

Prettico, G. et al. (2019). "Distribution System Operators Observatory 2018". In: *Publications Office of the European Union*. [Accessed on 21/03/2022], https://publications.jrc.ec.europa.eu/repository/bitstream/JRC113926/jrc113926_kjna29615enn_newer.pdf.

Pyrgou, A., A. Kylili, and P. A. Fokaides (2016). "The future of the Feed-in Tariff (FiT) scheme in Europe: The case of photovoltaics". In: *Energy Policy* 95. [Accessed on 21/03/2022], https://doi.org/10.1016/j.enpol.2016.04.048, pp. 94–102.

Quoilin, S. et al. (2016). "Quantifying self-consumption linked to solar home battery systems: Statistical analysis and economic assessment". In: *Applied Energy* 182. [Accessed on 21/03/2022], https://doi.org/10.1016/j.apenergy.2016.08.077, pp. 58–67.

Rai, V. and S. A. Robinson (2015). "Agent-based modeling of energy technology adoption: Empirical integration of social, behavioral, economic, and environmental factors". In: *Environmental Modelling & Software* 70. [Accessed on 21/03/2022], https://doi.org/10.1016/j.envsoft.2015.04.014, pp. 163–177.

Ransan-Cooper, H. et al. (2021). "Applying responsible algorithm design to neighbourhood-scale batteries in Australia". In: *Nature Energy* 6.8. [Accessed on 21/03/2022], https://doi.org/10.1038/s41560-021-00868-9, pp. 815–823.

Räsänen, T. and M. Kolehmainen (2009). "Feature-based clustering for electricity use time series data". In: *International conference on adaptive and natural computing algorithms*. [Accessed on 21/03/2022], https://doi.org/10.1007/978-3-642-04921-7_41. Springer, pp. 401–412.

Ratnam, E. L., S. R. Weller, and C. M. Kellett (2015). "An optimization-based approach to scheduling residential battery storage with solar PV: Assessing customer benefit". In: *Renewable Energy* 75. [Accessed on 21/03/2022], https://doi.org/10.1016/j.renene.2014.09.008, pp. 123–134.

Reuter, E. and M. Loock (2017). "Empowering local electricity markets: A survey study from Switzerland, Norway, Spain and Germany". In: *Empowerh2020*. [Accessed on 21/03/2022], https://www.alexandria.unisg.ch/252125/.

Rinaldi, A. et al. (2020). "Decarbonising heat with optimal PV and storage investments: A detailed sector coupling modelling framework with flexible heat pump operation". In: *Applied Energy* 282. [Accessed on 21/03/2022], https://doi.org/10.1016/j.apenergy.2020.116110, p. 116110.

Ritchie, H. and M. Roser (2020). "CO_2 and Greenhouse Gas Emissions". In: *Our World in Data*. [Accessed on 21/03/2022], https://ourworldindata.org/co2-and-other-greenhouse-gas-emissions.

Rousseeuw, P. J. (1987). "Silhouettes: a graphical aid to the interpretation and validation of cluster analysis". In: *Journal of computational and applied mathematics* 20. [Accessed on 21/03/2022], https://doi.org/10.1016/0377-0427(87)90125-7, pp. 53–65.

Royston, J. (1982). "Algorithm AS 181: the W test for normality". In: *Applied Statistics*. [Accessed on 21/03/2022], https://doi.org/10.2307/2347986, pp. 176–180.

Ruf, H. (2018). "Limitations for the feed-in power of residential photovoltaic systems in Germany–An overview of the regulatory framework". In: *Solar Energy* 159. [Accessed on 21/03/2022], https://doi.org/10.1016/j.solener.2017.10.072, pp. 588–600.

Salpakari, J. and P. Lund (2016). "Optimal and rule-based control strategies for energy flexibility in buildings with PV". In: *Applied Energy* 161. [Accessed on 21/03/2022], https://doi.org/10.1016/j.apenergy.2015.10.036, pp. 425–436.

Sani Hassan, A., L. Cipcigan, and N. Jenkins (2017). "Optimal battery storage operation for PV systems with tariff incentives". In: *Appl. Energy* 203. [Accessed on 21/03/2022], https://doi.org/10.1016/j.apenergy.2017.06.043, pp. 422–441.

Santos, J. M., P. S. Moura, and A. T. de Almeida (2014). "Technical and economic impact of residential electricity storage at local and grid level for Portugal". In: *Appl. Energy* 128. [Accessed on 21/03/2022], https://doi.org/10.1016/j.apenergy.2014.04.054, pp. 254–264.

Sauer, D. U. et al. (2009). "Concept of a Battery Aging Model for Lithium-Ion Batteries Considering the Lifetime Dependency on the Operation Strategy". In: *24th European Photovoltaic Solar Energy Conference, 21-25 September, Hamburg, Germany*. https://doi.org/10.4229/24thEUPVSEC2009-4BO.11.3, pp. 3128–3134.

Savelli, I. and T. Morstyn (2021a). "Better together: Harnessing social relationships in smart energy communities". In: *Energy Research & Social Science* 78. [Accessed on 21/03/2022], https://doi.org/10.1016/j.erss.2021.102125, p. 102125.

— (2021b). "Electricity prices and tariffs to keep everyone happy: a framework for fixed and nodal prices coexistence in distribution grids with optimal tariffs for investment cost recovery". In: *Omega*. [Accessed on 21/03/2022], https://doi.org/10.1016/j.omega.2021.102450, p. 102450.

Schelly, C. (2014). "Residential solar electricity adoption: What motivates, and what matters? A case study of early adopters". In: *Energy Research & Social Science* 2. [Accessed on 21/03/2022], https://doi.org/10.1016/j.erss.2014.01.001, pp. 183–191.

Schmidt, T. et al. (2019). "Additional emissions and cost from storing electricity in stationary battery systems". In: *Environ. Sci. Technol.* 53.7. [Accessed on 21/03/2022], https://doi.org/10.1021/acs.est.8b05313, pp. 3379–3390.

Schopfer, S., V. Tiefenbeck, E. Fleisch, et al. (2017). "Providing primary frequency control with residential scale photovoltaic-battery systems". In: *Computer science-research and development* 32.1-2. [Accessed on 21/03/2022], https://doi.org/10.1007/s00450-016-0318-3, pp. 105–115.

Schopfer, S., V. Tiefenbeck, and T. Staake (2018). "Economic assessment of photovoltaic battery systems based on household load profiles". In: *Applied Energy*

223. [Accessed on 21/03/2022], https://doi.org/10.1016/j.apenergy.2018.03.185, pp. 229–248.

Schuetz, P., D. Gwerder, et al. (2017). "Thermal storage improves flexibility of residential heating systems for smart grids". In: *Proceedings of the 12th IEA Heat Pump Conference*. [Accessed on 21/03/2022], https://bit.ly/369itGp, pp. 1–9.

Schuetz, P., R. Scoccia, et al. (2018). "Fast Simulation Platform for Retrofitting Measures in Residential Heating". In: *Cold Climate HVAC Conference*. [Accessed on 21/03/2022], https://doi.org/10.1007/978-3-030-00662-4_60. Springer, pp. 713–723.

Schwarz, M. and A. Kollmann (2014). "Wirtschaftliche Betrachtung von Netzausbau und Smart Grid-Lösungen in der Niederspannungsebene". In: *e & i Elektrotechnik und Informationstechnik* 131.3. [Accessed on 21/03/2022], https://doi.org/10.1007/s00502-014-0204-2, pp. 99–104.

Swiss Society of Engineers and Architects (2011). *SIA 382/2 Klimatisierte Gebäude – Leistungs- und Energiebedarf*. Tech. rep.

— (2015). *Raumnutzungsdaten für die Energie-und Gebäudetechnik*. Tech. rep.

Sichilalu, S. M. and X. Xia (2015). "Optimal power dispatch of a grid tied-battery-photovoltaic system supplying heat pump water heaters". In: *Energy conversion and management* 102, pp. 81–91.

Simon, H. A. (1955). "A behavioral model of rational choice". In: *The quarterly journal of economics* 69.1, pp. 99–118.

Sivaraman, P. and C. Sharmeela (2021). "Chapter 2 - Power system harmonics". In: *Power Quality in Modern Power Systems*. Ed. by P. Sanjeevikumar et al. Academic Press, pp. 61–103. ISBN: 978-0-12-823346-7. URL: https://doi.org/10.1016/B978-0-12-823346-7.00002-5.

Skytte, K. (1999). "The regulating power market on the Nordic power exchange Nord Pool: an econometric analysis". In: *Energy Economics* 21.4. [Accessed on 21/03/2022], https://doi.org/10.1016/S0140-9883(99)00016-X, pp. 295–308.

Soini, M. C., D. Parra, and M. K. Patel (2019). "Disaggregation of energy storage operation by timescales". In: *Journal of Energy Storage* 23. [Accessed on 21/03/2022], https://doi.org/10.1016/j.est.2019.04.005, pp. 480–494.

Sonnenschein (2013). *Handbook for Gel-VRLA-Batteries*. [Accessed on 21/03/2022] http://www.sonnenschein.org/PDF%20files/GelHandbookPart2.pdf.

Sony (2017). *Fortelion Energy Storage Module and System*. [Accessed on 21/03/2022] https://zerohomebills.com/wp-content/uploads/SONY-Fortelion.pdf.

Sossan, F. et al. (2016). "Achieving the dispatchability of distribution feeders through prosumers data driven forecasting and model predictive control of electrochemical storage". In: *IEEE Transactions on Sustainable Energy* 7.4. [Accessed on 21/03/2022], https://doi.org/10.1109/TSTE.2016.2600103, pp. 1762–1777.

Staffell, I. et al. (2012). "A review of domestic heat pumps". In: *Energy & Environmental Science* 5.11. [Accessed on 21/03/2022], https://doi.org/10.1039/C2EE22653G, pp. 9291–9306.

Stephan, A. et al. (2016). "Limiting the public cost of stationary battery deployment by combining applications". In: *Nature Energy* 1.7. [Accessed on 21/03/2022], https://doi.org/10.1038/nenergy.2016.79, p. 16079.

Stern, P. C. et al. (2017). "Household production of photovoltaic energy: issues in economic behavior". In: *A. Lewis (2nd ed.), Cambridge handbook of psychology and economic behaviour*, pp. 541–566.

Streicher, K. N., S. Mennel, et al. (2020). "Cost-effectiveness of large-scale deep energy retrofit packages for residential buildings under different economic assessment approaches". In: *Energy and Buildings* 215. [Accessed on 21/03/2022], https://doi.org/10.1016/j.enbuild.2020.109870, p. 109870.

Streicher, K. N., P. Padey, D. Parra, M. C. Bürer, and M. K. Patel (2018). "Assessment of the current thermal performance level of the Swiss residential building stock: Statistical analysis of energy performance certificates". In: *Energy and Buildings* 178. [Accessed on 21/03/2022], https://doi.org/10.1016/j.enbuild.2018.08.032, pp. 360–378.

Streicher, K. N., P. Padey, D. Parra, M. C. Bürer, S. Schneider, et al. (2019). "Analysis of space heating demand in the Swiss residential building stock: Element-based bottom-up model of archetype buildings". In: *Energy and Buildings* 184. [Accessed on 21/03/2022], https://doi.org/10.1016/j.enbuild.2018.12.011, pp. 300–322.

Sweetnam, T. et al. (2019). "Domestic demand-side response with heat pumps: controls and tariffs". In: *Building Research & Information* 47.4. [Accessed on 21/03/2022], https://doi.org/10.1080/09613218.2018.1442775, pp. 344–361.

Swissgrid (2015). *Strategic Grid 2025*. [Accessed on 21/03/2022], https://www.swissgrid.ch/dam/swissgrid/projects/strategic-grid/sg2025-brochure-en.pdf.

— (2018). *BGM Partner Meeting*. [Accessed on 21/03/2022], https://www.swissgrid.ch/en/home/customers/topics/bgm.html.

— (2019). *Balancing Roadmap Switzerland*. [Accessed on 21/03/2022], https://www.swissgrid.ch/dam/swissgrid/about-us/newsroom/publications/balancing-roadmap-ch-en.pdf.

— (2020). *Control Energy Market*. [Accessed on 21/03/2022], https://www.swissgrid.ch/dam/swissgrid/about-us/newsroom/dossiers/control-energy-market-en.pdf.

Tant, J. et al. (2013). "Multiobjective Battery Storage to Improve PV Integration in Residential Distribution Grids". In: *IEEE Trans. Sustain Energy* 4.1. [Accessed on 21/03/2022], https://doi.org/10.1109/TSTE.2012.2211387, pp. 182–191.

Team R Core and others (2013). "R: A language and environment for statistical computing". In.

Terlouw, T. et al. (2019). "Optimal energy management in all-electric residential energy systems with heat and electricity storage". In: *Applied Energy* 254. [Accessed on 21/03/2022], https://doi.org/10.1016/j.apenergy.2019.113580, p. 113580.

Tesla (2015). *Powerwall 2 DC*. [Accessed on 21/03/2022] https://www.solahart.com.au/media/2849/powerwall-2-dc_datasheet_english.pdf.

Thygesen, R. and B. Karlsson (Nov. 2013). "Economic and energy analysis of three solar assisted heat pump systems in near zero energy buildings". In: *Energy and Buildings* 66. [Accessed on 21/03/2022], https://doi.org/10.1016/j.enbuild.2013.07.042, pp. 77–87. (Visited on 03/07/2017).

Tjaden, T., J. Bergner, et al. (2015). "Repräsentative elektrische Lastprofile für Wohngebäude in Deutschland auf 1-sekündiger Datenbasis". In: *Hochschule für*

Technik und Wirtschaft HTW Berlin. [Accessed on 21/03/2022], https://bit.ly/37xaYcJ.

Tjaden, T., F. Schnorr, et al. (2015). "Einsatz von PV-Systemen mit Wärmepumpen und Batteriespeichern zur Erhöhung des Autarkiegrades in Einfamilienhaushalten". In: *30. Symposium Photovoltaische Solarenergie*. [Accessed on 21/03/2022], https://doi.org/10.13140/RG.2.1.4033.9044,

Toradmal, A., T. Kemmler, and B. Thomas (2018). "Boosting the share of onsite PV-electricity utilization by optimized scheduling of a heat pump using buildings thermal inertia". In: *Applied Thermal Engineering* 137. [Accessed on 21/03/2022], https://doi.org/10.1016/j.applthermaleng.2018.03.052, pp. 248–258.

Trina BESS (2017). *S Series NCA type battery*. [Accessed on 21/03/2022] http://www.trinaenergystorage.com/uploads/download/149560986943.pdf.

Truong, C. N. et al. (2016). "Economics of Residential Photovoltaic Battery Systems in Germany: The Case of Tesla's Powerwall". en. In: *Batteries* 2.2. [Accessed on 21/03/2022], https://doi.org/10.3390/batteries2020014, p. 14.

Tureczek, A., P. S. Nielsen, and H. Madsen (2018). "Electricity consumption clustering using smart meter data". In: *Energies* 11.4. [Accessed on 21/03/2022], https://doi.org/10.3390/en11040859, p. 859.

van Amelsvoort, M. (2014). "Spezifische Bewertung unterschiedlicher Lösungsansätze zur Integration erneuerbarer Energien in Mittel-und Niederspannung". In: *VDE-Kongress 2014 - Smart Cities – Intelligente Lösungen für das Leben in der Zukunft*. [Accessed on 21/03/2022], https://www.vde-verlag.de/proceedings-de/453641029.html.

van der Veen, R. A. and R. A. Hakvoort (2016). "The electricity balancing market: Exploring the design challenge". In: *Utilities Policy* 43. [Accessed on 21/03/2022], https://doi.org/10.1016/j.jup.2016.10.008, pp. 186–194.

Varela, J. et al. (2017). "The IGREENGrid project: increasing hosting capacity in distribution grids". In: *IEEE Power and Energy Magazine* 15.3. [Accessed on 21/03/2022], https://doi.org/10.1109/MPE.2017.2662338, pp. 30–40.

Verhelst, C. et al. (Feb. 2012). "Study of the optimal control problem formulation for modulating air-to-water heat pumps connected to a residential floor heating system". In: *Energy and Buildings* 45. [Accessed on 21/03/2022], https://doi.org/10.1016/j.enbuild.2011.10.015, pp. 43–53.

Villalva, M. G., J. R. Gazoli, and E. Ruppert Filho (2009). "Comprehensive approach to modeling and simulation of photovoltaic arrays". In: *IEEE Transactions on power electronics* 24.5. [Accessed on 21/03/2022], https://doi.org/10.1109/TPEL.2009.2013862, pp. 1198–1208.

Vivian, J. et al. (2020). "Demand Side Management of a pool of air source heat pumps for space heating and domestic hot water production in a residential district". In: *Energy Conversion and Management* 225. [Accessed on 21/03/2022], https://doi.org/10.1016/j.enconman.2020.113457, p. 113457.

Vlahinić, S. et al. (2019). "Reactive power compensation with PV inverters for system loss reduction". In: *Energies* 12.21. [Accessed on 21/03/2022], https://doi.org/10.3390/en12214062, p. 4062.

von Appen, J. et al. (2015). "Sizing and grid impact of PV battery systems-a comparative analysis for Australia and Germany". In: *Smart Electric Distribution Systems and Technologies (EDST), 2015 International Symposium on*. [Accessed on 21/03/2022], https://doi.org/10.1109/SEDST.2015.7315280, pp. 612–619.

Al-Wakeel, A., J. Wu, and N. Jenkins (2017). "K-means based load estimation of domestic smart meter measurements". In: *Appl. Energy* 194. [Accessed on 21/03/2022], https://doi.org/10.1016/j.apenergy.2016.06.046, pp. 333–342.

Wang, Z. (Apr. 2018). "Optimizing the Grid Integration of Distributed Solar Energy". [Accessed on 21/03/2022] https://pdfs.semanticscholar.org/9093/69cd437ec5573aed35f956b6fa3f5f8c44cb.pdf. PhD dissertation. Virginia Commonwealth University: Virginia Commonwealth University.

Waser, R. et al. (2019). "Residential-scale demonstrator for seasonal latent thermal energy storage for heating and cooling application with optimized PV self-consumption". In: *2019 IEEE PES Innovative Smart Grid Technologies Europe (ISGT-Europe)*. [Accessed on 21/03/2022], https://doi.org/10.1109/ISGTEurope.2019.8905440. IEEE, pp. 1–5.

Weber, S. et al. (2017). *Swiss household energy demand survey (SHEDS): Objectives, design, and implementation*. Tech. rep. [Accessed on 21/03/2022], https://www.econstor.eu/handle/10419/191509. IRENE Working Paper.

Wen, K. et al. (2021). "Optimal operation framework of customer-premise battery storage for energy charge reduction and primary frequency regulation". In: *Journal of Energy Storage* 43. [Accessed on 21/03/2022], https://doi.org/10.1016/j.est.2021.103147, p. 103147.

Weniger, J., T. Tjaden, and V. Quaschning (2014). "Sizing of Residential PV Battery Systems". In: *Energy Procedia*. 8th International Renewable Energy Storage Conference and Exhibition (IRES 2013) 46. [Accessed on 21/03/2022], https://doi.org/10.1016/j.egypro.2014.01.160, pp. 78–87.

Wilkinson, S. et al. (2020). "Is peer-to-peer electricity trading empowering users? Evidence on motivations and roles in a prosumer business model trial in Australia". In: *Energy Research & Social Science* 66. [Accessed on 21/03/2022], https://doi.org/10.1016/j.erss.2020.101500, p. 101500.

Williams, C. J., J. O. Binder, and T. Kelm (2012). "Demand side management through heat pumps, thermal storage and battery storage to increase local self-consumption and grid compatibility of PV systems". In: *Innovative Smart Grid Technologies (ISGT Europe), 2012 3rd IEEE PES International Conference and Exhibition on*. [Accessed on 21/03/2022], https://doi.org/10.1109/ISGTEurope.2012.6465874. IEEE, pp. 1–6.

Wirth, H. and K. Schneider (2018). "Recent facts about photovoltaics in Germany". In: *Fraunhofer ISE*. [Accessed on 21/03/2022], https://bit.ly/3tkqTU4.

Wörner, A. et al. (2019). "Trading solar energy within the neighborhood: field implementation of a blockchain-based electricity market". In: *Energy Informatics* 2.1. [Accessed on 21/03/2022], https://doi.org/10.1186/s42162-019-0092-0, p. 11.

XALT 60Ah High Power Lithium-Ion LTO Cell (2018). [Accessed on 21/03/2022] https://www.xaltenergy.com/wp-content/uploads/2018/08/60Ah-LTO.pdf. Xalt Energy.

Xu, S., E. Barbour, and M. C. González (2017). "Household segmentation by load shape and daily consumption". In: *Proc. 6th ACM SIGKDD Int. Worksh. Urban Computing Conf. Halifax, Nov. Scotia, Canada, August 2017*. Vol. 2. [Accessed on 21/03/2022] http://urbcomp.ist.psu.edu/2017/papers/Household.pdf.

Yao, S. et al. (2018). "Hybrid timescale dispatch hierarchy for combined heat and power system considering the thermal inertia of heat sector". In: *IEEE Access* 6.

[Accessed on 21/03/2022], https://doi.org/10.1109/ACCESS.2018.2876718, pp. 63033–63044.

Yilmaz, S., J. Chambers, and M. K. Patel (2019). "Comparison of clustering approaches for domestic electricity load profile characterisation-Implications for demand side management". In: *Energy* 180. [Accessed on 21/03/2022], https://doi.org/10.1016/j.energy.2019.05.124, pp. 665–677.

Yilmaz, S., A. Rinaldi, and M. K. Patel (2020). "DSM interactions: What is the impact of appliance energy efficiency measures on the demand response (peak load management)?" In: *Energy Policy* 139. [Accessed on 21/03/2022], https://doi.org/10.1016/j.enpol.2020.111323, p. 111323.

Zhang, Y. et al. (2017). "Battery sizing and rule-based operation of grid-connected photovoltaic-battery system: A case study in Sweden". In: *Energy conversion and management* 133. [Accessed on 21/03/2022], https://doi.org/10.1016/j.enconman.2016.11.060, pp. 249–263.

Zheng, M., C. J. Meinrenken, and K. S. Lackner (2014). "Agent-based model for electricity consumption and storage to evaluate economic viability of tariff arbitrage for residential sector demand response". In: *Appl. Energy* 126. [Accessed on 21/03/2022], https://doi.org/10.1016/j.apenergy.2014.04.022, pp. 297–306.

Zhou, Y., J. Wu, and C. Long (2018). "Evaluation of peer-to-peer energy sharing mechanisms based on a multiagent simulation framework". In: *Applied energy* 222. [Accessed on 21/03/2022], https://doi.org/10.1016/j.apenergy.2018.02.089, pp. 993–1022.

Ziegler, M. S. and J. E. Trancik (2021). "Re-examining rates of lithium-ion battery technology improvement and cost decline". In: *Energy & Environmental Science* 14.4. [Accessed on 21/03/2022], https://doi.org/10.1039/D0EE02681F, pp. 1635–1651.

Alejandro Pena-Bello

Renewable energy · Energy storage · Energy economics
Data analysis · Optimization · Automation

Geneva, Switzerland Alejandro.penabello@unige.ch +41 78 878 48 45
Google scholar @alefunxo Alejandro Pena-Bello @alefunxo

Introduction

Electronic engineer with a strong background in distributed energy resources. Research expertise in energy storage and waste to energy technology, with ten publications (five as first author, *h*-index: 7) in recognized international journals, including one in Nature Energy. Involvement in national and international collaborative research projects. Experience in optimization, techno-economic analysis, and feasibility studies. His multidisciplinary approach allows him to bridge the gap between technical, economic, and environmental aspects.

Education

Ph.D. in Energy Storage — University of Geneva, Switzerland
Mar. 2017 -- Feb. 2022 (expected)
Thesis: "Trade-offs between prosumer benefits and grid impacts in PV systems supported by storage".
Supervisors: Prof. Martin K. Patel. & Dr. David Parra

Visiting Fellow at PV-lab — EPFL, Switzerland
Dec. 2021 -- May. 2022
Supervisor: Dr. Nicolas Wyrsch

Visiting Fellow at Bits to Energy Lab Nuremberg — FAU, Germany
Feb. -- Apr. 2020
Supervisor: Prof. Verena Tiefenbeck

M.Sc. in Environmental Sciences — University of Geneva, Switzerland
2014 -- 2016
Thesis: "Optimization of PV and grid charging for improving the profitability of residential batteries".

M.Sc. in Economics (Meritorious Award) — National University of Colombia, Colombia
2011 -- 2014
Thesis: "Feasibility study WTE plant in Bogotá: Technological diffusion for the country".

B.Eng. Electronic Engineering (Best GPA group) — National University of Colombia, Colombia
2005 -- 2011

DUT Information technology (IT) — IUT2, Université Pierre Mendès-France, France
2009 -- 2010

Publications

1. **Pena-Bello, A.**, Parra, D., Herberz, M., Tiefenbeck, V., Patel, M., & Hahnel, U. (2021). Integration of prosumer peer-to-peer trading decisions into energy community modeling. Nature Energy.
2. Hutty, T. D., **Pena-Bello, A.**, Dong, S., Parra, D., Rothman, R., & Brown, S. (2021). Peer-to-peer electricity trading as an enabler of increased PV and EV ownership. Energy Conversion and Management, 245, 114634.
3. Dudjak, V., Neves, D., Alskaif, T., Khadem, S., **Pena-Bello, A.**, Saggese, P., ... & Papaemmanouil, A. (2021). Impact of local energy markets integration in power systems layer: A comprehensive review. Applied Energy, 301, 117434.
4. **Pena-Bello, A.**; Schuetz, P.; Berger, M.; Worlitschek, J.; Patel, M. K.; Parra, D,. (2021) Decarbonizing heat with PV-coupled heat pumps supported by electricity and heat storage: impacts and trade-offs for prosumers and the grid, Energy conversion and management, 240, 114220, Elsevier
5. Gupta, R., **Pena-Bello, A.**, Streicher, K. N., Roduner, C., Thöni, D., Patel, M. K., & Parra, D. (2021). Spatial analysis of distribution grid capacity and costs to enable massive deployment of PV, electric mobility and electric heating. Applied Energy, 287, 116504.
6. Hahnel, U. J., Herberz, M., **Pena-Bello, A.**, Parra, D., & Brosch, T. (2020). Becoming prosumer: Revealing trading preferences and decision-making strategies in peer-to-peer energy communities. Energy Policy, 137, 111098.
7. **Pena-Bello, A.**, Barbour, E., Gonzalez, M. C., Yilmaz, S., Patel, M. K., & Parra, D. (2020). How does the electricity demand profile impact the attractiveness of PV-coupled battery systems combining applications?. Energies, 13(15), 4038.

8. **Pena-Bello, A.**, Barbour, E., Gonzalez, M. C., Patel, M. K., & Parra, D. (2019). Optimized PV-coupled battery systems for combining applications: Impact of battery technology and geography. Renewable and Sustainable Energy Reviews, 112, 978-990.
9. Schmidt, T. S., Beuse, M., Zhang, X., Steffen, B., Schneider, S. F., **Pena-Bello, A.**, ... & Parra, D. (2019). Additional emissions and cost from storing electricity in stationary battery systems. Environmental Science & Technology, 53(7), 3379-3390.
10. **Pena-Bello, A.**, Burer, M., Patel, M. K., & Parra, D. (2017). Optimizing PV and grid charging in combined applications to improve the profitability of residential batteries. Journal of Energy Storage, 13, 58-72.

Teaching

Teaching Assistant — University of Geneva, Switzerland
2017-present
Research methods & Data analysis (R). Master level.

Instructor — Escuela Colombiana de Carreras Industiales, Colombia
2013-2014
Automation & Dynamic systems. Bachelor level.

Instructor — Universidad Distrital "Francisco José de Caldas", Colombia
2013-2014
Automation & EM Conversion. Bachelor level.

Research

PhD Researcher — University of Geneva, Switzerland
Mar. 2017 -- Feb. 2022 (expected)

- Set up MILP Optimizations for residential batteries, heat pumps, thermal tanks, and EVs.
- Conducted extensive statistical data analysis via python and R.
- Took part of several international research collaborations.
- Presented my results in two international conferences (IRES and Grid integration of peer to peer, community self consumption and transactive energy models), and two international visits (Krakow and Nuremberg).
- Supervised four Master students in final projects.

Master Researcher — University of Geneva, Switzerland
2014 -- 2016

- Set up a Genetic Algorithm Optimization for residential batteries.
- Conducted extensive data analysis via Matlab.

Professional Experience

Associate editor — Innovar Journal, Colombia
2013-2014

- Reviewed, edited and found reviewers for submitted articles.
- Set deadlines, and supervised the production details of the journal.

General manager — Coquelicot, Colombia
2011-2012

- Charged of administration and customer services.
- Supply chain & procurement, accounting & marketing.

Database developer — Same Same, Switzerland
2010

- Designed and implemented the windsurf school database.

Honors

Meritorious award master thesis (1 awardee) — National University of Colombia
2014

Best GPA group — National University of Colombia
2011

yOta, Ecobjeto para la vivienda - 2nd Place — Corona Pro-hábitat Award
2011

Service To The Scientific Community

Reviewer — Applied energy journal
2019-2021

Skills

IT

- Python
- Matlab
- R & Shiny
- LabView
- ArcGIS & QGIS
- Bash

Soft Skills

- Problem-solving
- Critical thinking
- Time management
- Organisation
- Project management
- Teamwork

Languages

- Spanish (Native)
- English (C2)
- French (C2)
- Italian (B2)
- German (B2)
- Portuguese (B1)